

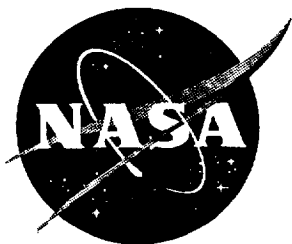
1998 Research Reports

---

# **NASA/ASEE Summer Faculty Fellowship Program**

---

John F. Kennedy Space Center  
and  
University of Central Florida





# **1998 RESEARCH REPORTS**

## **NASA/ASEE SUMMER FACULTY FELLOWSHIP PROGRAM**

**JOHN F. KENNEDY SPACE CENTER**

**UNIVERSITY OF CENTRAL FLORIDA**

### **EDITORS:**

Dr. E. Ramon Hosler, University Program Director  
Department of Mechanical, Materials and Aerospace Engineering  
College of Engineering  
University of Central Florida

Mr. Gregg Buckingham, NASA/KSC Program Director  
University Programs Office  
John F. Kennedy Space Center

NASA Grant No. NAG10-244

Contractor Report No. CR-208546

March 1999



## PREFACE

This document is a collection of technical reports on research conducted by the participants in the 1998 NASA/ASEE Summer Faculty Fellowship Program at the John F. Kennedy Space Center (KSC). This was the fourteenth year that a NASA/ASEE program has been conducted at KSC. The 1998 program was administered by the University of Central Florida (UCF) in cooperation with KSC. The program was operated under the auspices of the American Society for Engineering Education (ASEE) and the Education Division, NASA Headquarters, Washington, D.C. The KSC program was one of nine such Aeronautics and Space Research Programs funded by NASA Headquarters in 1998.

The basic common objectives of the NASA/ASEE Summer Faculty Fellowship Program are:

- a. To further the professional knowledge of qualified engineering and science faculty members;
- b. To stimulate an exchange of ideas between teaching participants and employees of NASA;
- c. To enrich and refresh the research and teaching activities of participants institutions; and,
- d. To contribute to the research objectives of the NASA center.

The KSC Faculty Fellows spent ten weeks (May 26 through July 31, 1998) working with NASA scientists and engineers on research of mutual interest to the university faculty member and the NASA colleague. The editors of this document were responsible for selecting appropriately qualified faculty to address some of the many research areas of current interest to NASA/KSC. A separate document reports on the administrative aspects of the 1998 program. The NASA/ASEE program is intended to be a two-year program to allow in-depth research by the university faculty member. In many cases a faculty member has developed a close working relationship with a particular NASA group that had provided funding beyond the two-year limit.

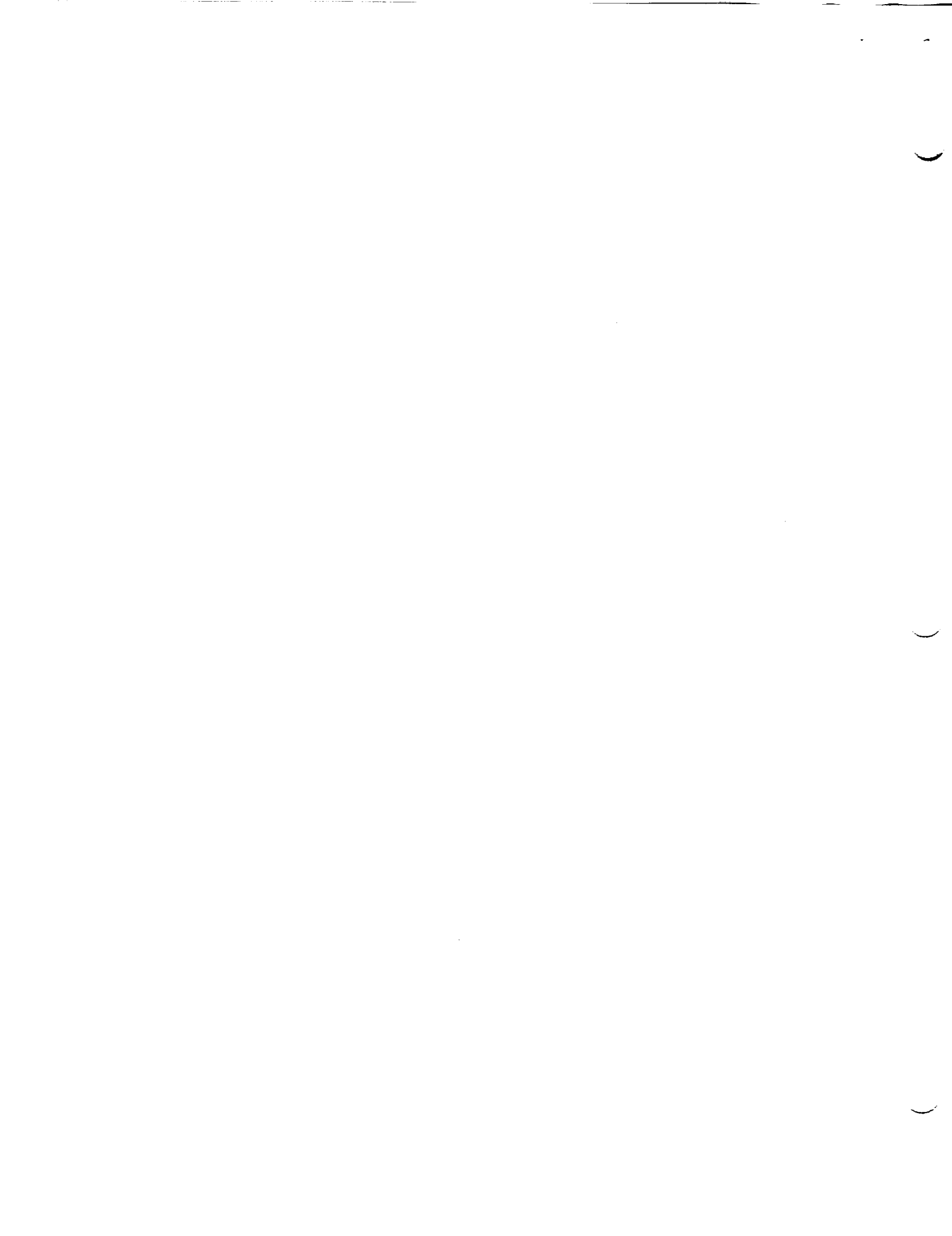
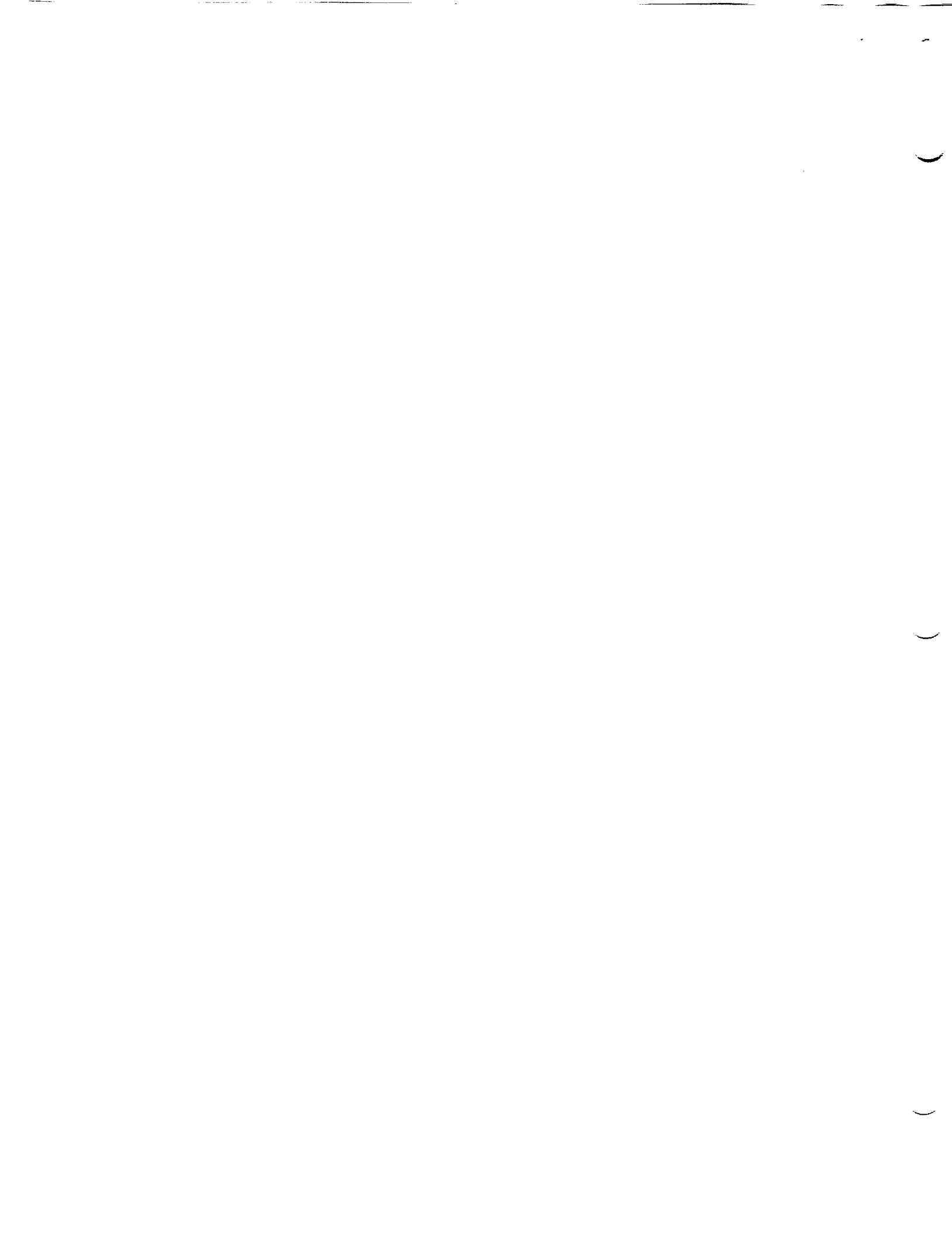


## TABLE OF CONTENTS

	<u>PAGE</u>
1. ANDRAWIS, Alfred S. <i>Digital Television Transmission</i>	1
2. BLUM, Linda K. <i>Characterization of Salt Marsh Impoundment Sediments Under Three Types of Water Management</i>	13
3. CALLE, Carlos I. <i>An Experimental Design to Determine the Electrostatic Properties of Martian Simulant Dust Particles</i>	25
4. CALLE, Luz M. <i>Electrochemical Impedance Spectroscopy of Polyaniline Coated Aluminum Alloys</i>	35
5. CHRISTENSEN, Kenneth J. <i>Capacity Planning for Future NASA-KSC LAN and MAN Networks</i>	45
6. FINSTEIN, Melvin S. <i>Realistic Scale Composting Reactor for a Martian Lunar Habitat: Generations I and II</i>	57
7. HEIDERSBACH, Robert H. <i>Web Pages for the KSC Corrosion Laboratory</i>	71
8. HODGES-TILLER, Brenda <i>Effective Initiatives in Best Leadership Practices</i>	81
9. HOUSHANGI, Nasser <i>Omnibot Mobile Base</i>	93
10. KOZEL, David <i>Noise Characterization and Comparison of Adaptive Noise Suppression Algorithms</i>	103
11. LATINO, Carl D. <i>Using Neural Networks for Evaluating the Health of the Gaseous Hydrogen Flow Control Valve (GH2FCV)</i>	113



12.	MILLS, Aaron L. <i>The Role of Diversity in Conferring Stability and Resistance to Invasion to Microbial Communities: The Use of Dilution to Generate High and Low Diversity Communities</i>	123
13.	MOYNIHAN, Gary P. <i>Workforce Assessment and Validation Exercise</i>	135
14.	MURRAY, Susan L. <i>Human Factors Applications on CLCS</i>	145
15.	OJHA, Anand K. <i>Characterization of Test and Checkout Distributed Data Processing Systems</i>	155
16.	OSBORNE, Deborah M. <i>Application of Statistical Process Control Techniques to Shuttle Processing</i>	165
17.	PATTERSON, Ronald F. <i>Development and Analysis of Acceptance Sampling Plans in Data Validation</i>	175
18.	PEALE, Robert E. <i>Quantitative Infrared Thermography</i>	185
19.	POZO DE FERNANDEZ, Maria E. <i>Examination of PCB Clean Up Technologies in Soil</i>	195
20.	RUIZ-TORRES, Alex J. <i>Modeling Methodologies to Assess Spaceport Operations</i>	205
21.	STANSIFER, Ryan D. <i>A Visual Editor in JAVA for Jview</i>	215
22.	WHITLOW, Jonathan E. <i>Software Development for Autonomous Control of an ISPP Plant on Mars</i>	225



**1998 NASA/ASEE SUMMER FACULTY FELLOWSHIP PROGRAM**

**JOHN F. KENNEDY SPACE CENTER  
UNIVERSITY OF CENTRAL FLORIDA**

**DIGITAL TELEVISION TRANSMISSION**

**Alfred S. Andrawis  
Associate Professor  
Electrical Engineering Department  
South Dakota State University  
Brookings, SD, 57007**

**KSC Colleagues  
Po T. Huang and Larry Hand Jr.  
Communications Division, DL-CMD-V**

**ABSTRACT**

The purpose of this paper is two folds; to investigate effects of timing errors and jitter on digital television signals; and to study error detection and handling in digital television.

Timing errors may result from static phase offset, from alignment jitter or from a combination of both. Timing errors impose a transmission penalty as an extra carrier-to-noise ratio ( $C/N$ ) to achieve certain bit error rate (BER). Penalty due to timing and jitter errors is calculated in the first part of this paper .

The second part of this paper studies error detection and handling (EDH) methods to be used optionally for the transmission of digital television serial interface. Detailed example for error detection method in digital television (*cyclic redundancy check*) is also given.

## ACKNOWLEDGMENTS

I am thankful for the NASA/ASEE Summer Faculty Program and for the opportunity to participate in it. Gregg Buckingham, with his enthusiasm and interest in the program, provided the participants with unique opportunities to learn about the Kennedy Space Center. The program was well organized due to the efforts of Ray Hostler, Kari Stiles, and Stephanie Bealer. They did a great job at assisting, educating, and entertaining the program's participants through the many presentations, tours, and social events.

I would like to extend a special thanks to Po T. Huang, my KSC colleague. He assisted me with his vast experience and knowledge of Digital Television Systems.

I am also very grateful to Larry Hand for the time he spent in discussing with me future network needs for KSC. Larry is always available to answer questions when I needed clarification in any matter of the project.

Also, I would like to thank every one in the Fiber Optics Laboratory for accommodating and tolerating me. Bob Swindle, David Johnson, and Robert Stute were all very friendly and extremely helpful.

Finally, I would like to thank my dear wife Madeleine, who is also my great companion, friend and colleague, and my children (David, Mary, and Danny). They patiently endured long hours alone while I was busy working in this project.

## I. EFFECTS OF TIMING ERRORS ON DIGITAL TELEVISION SIGNALS

### 1. INTRODUCTION

The Kennedy Space Center (KSC) is moving fast towards replacing existing analog NTSC operational television system (OTV) with digital NTSC television. Society of Motion Picture and Television Engineers (SMPTE) 270 Mb/s component video signal standard is adopted to transport digital video signals over KSC networks. On the other hand, an 8-VSB transmission subsystem was approved by the FCC Advisory Committee on Advanced Television Service (ACATS) as a modulation scheme of the compressed digital television system and high definition television (HDTV) intended for terrestrial television broadcasting in North America. Similarly, 16-VSB transmission subsystem was selected for high data rate cable mode [1].

In digital systems, it is essential that the receiver obtains accurate timing information indicating the proper time instants to operate receiver's sampling device. Hence, the timing error must be held to a small fraction of the symbol interval for satisfactory performance.

In an ideal digital system, the symbols (bit in binary systems or M levels symbol in M-VSB) would arrive at times that are integer multiples of the bit interval  $T$ . These received symbols, in turn, are sampled at the receiver side at the point of adjacent symbols zero crossings. This ideal communication system delivers the optimum carrier-to-noise ratio ( $C/N$ ) and no inter-symbol-interference ( $ISI$ ).

In a real system, however, symbols may arrive at times that differ from integer multiples of  $T$  due to timing errors. Furthermore, sampling at the receiver's side may not occur exactly at the zero crossings of adjacent symbols. These timing errors may be due to the transmitter's circuitry, the transmission channel, the front stages of the receiver, inaccuracies in clock recovery, and/or receiver's circuitry. All these different sources of timing errors contribute to jitter. Figure 1a shows a train of unit impulses initially spaced equally in time. Due to jitter, these unit impulses become spaced slightly irregularly in time as shown in Figure 1b. Time deviations from integer multiples of  $T$  from a discrete time  $T_n$  (the time at which the sample is taken), form a continuous amplitude sequence  $J(nT) = nT - T_n$ . This sequence is the fundamental description of jitter [2-4]. Another type of timing error is the static phase offset  $\tau$ . Static phase offset is the static error displacement from the optimum sampling point of the incoming symbol.

The jitter  $J(nT)$  as well as the static phase offset  $\tau$  have dimensions of time in amplitude and is positive for a given pulse that arrives earlier than time  $nT$ .  $J(nT)$  may be converted to units of degrees by setting  $T = 360^\circ$ . Hence, a jitter amplitude of  $T$  seconds is  $360^\circ$ . Jitter amplitude could also be expressed in terms of unit interval (UI), where  $1 \text{ UI} = 360^\circ$ . For example, SMPTE component video signal with 270 Mb/s, has  $T = 3.7 \text{ ns}$  [7]. Then,  $J(nT) = 60^\circ$  is equivalent to, a peak-to-peak jitter of  $0.617 \text{ ns}$  and, a  $0.167 \text{ UI}$ .

Transmission penalty is defined as the extra  $C/N$  needed, for a given bit-error-rate, when compared with the no timing error case. Penalty due to timing jitter depends on both the shape of the data symbols and the particular sequence of symbol amplitudes [3]. In this paper raised cosine shaped symbols are assumed. For the worst case condition, the symbols' polarity is assumed to be alternating (any positive symbol is followed by a negative symbol and visa versa) with an amplitude average value of  $2A/\pi$ , where  $A$  is the maximum symbol magnitude. The alternating sequence tends to give rise to the maximum inter-symbol interference ( $ISI$ ), which in turn results in the worst jitter penalty. Section II outlines the analysis methodology, Section III presents the results of the analysis, and the final section is the conclusion.

### 2. PROCEDURE

This section is to investigate the effects of timing and jitter on signal quality. Definitions, assumptions, and methods of calculation, to be used in the next section, are presented.

The received digital signal can be written as

$$f_i(t) = \sum_{n=-\infty}^{\infty} f(nT) \cdot q(t - nT), \quad (1)$$

where  $f(nT)$  is the received signal amplitude, in volts, at time equals  $nT$ ,  $T$  is the duration between symbols in seconds, and  $q(t)$  is the impulse response of the transmission channel.

Timing error and jitter are due to timing inaccuracies at both the transmitter and the receiver circuitry. If the received signal has a jitter  $J_T(t)$ , which may be due to the transmitter's circuitry, the transmission channel, or the front stages of the receiver, the received signal amplitude, in volts,  $P_r(t)$  may then be written as

$$P_r(t) = \sum_{n=-\infty}^{\infty} \left( f(nT) \cdot q(t - nT - J_T(nT)) \right) + \eta_r(t), \quad (2)$$

where  $\eta_r(t)$  is the total received noise voltage [3]. If the jitter introduced by the timing recovery circuitry is  $J_R(t)$ , then the timing signal  $S_r(t)$  is given by

$$S_r(t) = B \sin \left( \frac{2\pi}{T} (t - J_R(t) - \Delta\tau) \right), \quad (3)$$

where  $\Delta\tau$  is a phase delay, caused by the timing recovery circuitry, in seconds. The sampled received signal (in volts)  $P'_r(t)$  can then be written as

$$P'_r(t) = \left\{ P_r(t) * p(t) \right\} \cdot \sum_{m=-\infty}^{\infty} \delta(t - mT - J_R(mT) - \tau), \quad (4)$$

where  $*$  denotes convolution,  $p(t)$  is the impulse response of receiver's shaping filter,  $\delta(t)$  is the delta function, and  $\tau$  is the total static phase offset in seconds. Static phase offset  $\tau$  is equal to  $\Delta\tau$  plus a time delay due to the physical separation of the time recovery circuitry from the receiver's sampler. By substituting from Equation 2 then moving the quantity  $P_r(t)$  within the summation we obtain

$$P'_r(t) = \left\{ \left[ \sum_n \left( f(nT) \cdot q(t - nT - J_T(nT)) + \eta_r(t) \right) \right] * p(t) \right\} \cdot \sum_m \delta(t - mT - J_R(mT) - \tau), \quad (5)$$

i.e.

$$P'_r(t) = \sum_m \left\{ \left\{ \sum_n \left( f(nT) \cdot q(mT - nT + J_R(mT) - J_T(nT) + \tau) + \eta_r(t_m) \right) * p(t) \right\} \cdot \delta(t - mT - J_R(mT) - \tau) \right\}, \quad (6)$$

where  $t_m = mT + J_R(mT) + \tau$ . Changing indices to  $k=m-n$  and extracting the  $k=0$  term we obtain

$$P'_r(t) = \sum_m \left\{ \left\{ f(mT) \cdot q(J_R(mT) - J_T(mT) + \tau) + \sum_{k \neq 0} \left( f(kT) q(kT + J_R(mT) - J_T((m-k)T) + \tau) + \eta_r(t_m) \right) * p(t) \right\} \cdot \delta(t - mT - J_R(mT) - \tau) \right\}. \quad (7)$$

Since  $J_T(t)$  is a slowly varying low-pass stochastic process, then for small values of  $|k|$  [2]

$$J_T(m-k)T \simeq J_T(mT). \quad (8)$$

We now define the alignment jitter at the receiver's sampling circuit as

$$J_a(mT) = J_R(mT) - J_T(mT). \quad (9)$$

For a raised cosine shaped system, system's impulse response is given by [3]

$$(f(t) \cdot q(t)) * p(t) = \frac{\sin(\pi \nu T)}{\pi \nu T} \cdot \frac{\cos(\pi \nu T)}{1 - 4\nu^2 T^2}. \quad (10)$$

Both the static offset  $\tau$  and the alignment jitter  $J_a(mT)$  affect performance. This is illustrated in Figure 2 where a sequence of raised cosine samples is shown. If both  $\tau$  and  $J_a(mT)$  are equal to zero degrees then the magnitude of the desired sample is maximum while the *ISI* value is zero. If either  $\tau$  or  $J_a(mT)$  (or both) is

unequal to zero, then the received symbol is not sampled at its maximum while the *ISI* magnitude is greater than zero. Therefore, Equation 7 may be rewritten as

$$P'_r(t) = \sum_m \left\{ \left\{ f(mT) \cdot q(J_a(mT) + \tau) + \sum_{k \neq 0} f(kT) \cdot q(kT + J_a(mT) + \tau) + \eta_r(t_m) \right\} * p(t) \cdot \delta(t - mT - J_R(mT) - \tau) \right\}, \quad (11)$$

where  $\eta_r(t_m)$  is the noise voltage at time  $t_m$ , the quantity  $f(mT) \cdot q(J_a(mT) + \tau)$  is the value of the present symbol at a time instant equal to  $J_a(mT) + \tau$  (total timing error), and  $\sum_{k \neq 0} f(kT) \cdot q(kT + J_a(mT) + \tau)$  is the *ISI*. Each term in the summation  $\sum_{k \neq 0} f(kT) \cdot q(kT + J_a(mT) + \tau)$  corresponds to the interference introduced by the  $k^{\text{th}}$  adjacent sample. If the timing error  $(J_a(mT) + \tau) = 0$ , then the value of  $\sum_{k \neq 0} f(kT) \cdot q(kT)$  is equal to zero and no *ISI* exists; otherwise, presence of the *ISI* adds incoherently to the effective overall noise. The combined effect, of decreasing received symbol level and increasing the noise, degrades the overall *C/N*. This overall *C/N* degradation is the *C/N* penalty

### 3. RESULTS

In this section, the transmission penalty (extra *C/N* required to achieve certain BER) is examined as a function of; (a) static phase offset, and (b) static phase offset and jitter.

#### A. Transmission Penalty Due to Static Phase Offset

In this section, the transmission penalty is examined by assuming that the alignment jitter is zero. As a result of the static phase offset  $\tau$ , the desired sample magnitude in volts is  $q(\tau)$  while the *ISI* terms ( $\sum_{k \neq 0} f(kT) q(kT + \tau)$ ) are added to the noise. If these samples are of a pseudorandom, then samples' average power is  $A^2/2$ . Therefore, *C/N*, for samples with absolute average value of  $A/\pi$  and alternating polarities, can be written as

$$\frac{C}{N} = \frac{\frac{1}{2} q^2(\tau)}{\left( \sum_{k \neq 0} \frac{2(-1)^k}{\pi} q(kT + \tau) + \eta_r(t_m) \right)^2}. \quad (12)$$

This relationship is shown in Figure 3 for various values of  $\tau$  (expressed in degrees) and for eight adjacent samples affecting the current sample level ( $k=8$ ). Figure 3 shows that when the static phase offset is  $60^\circ$ , (i.e.  $\frac{1}{6}$  UI), the transmission penalty is less than one dB. Therefore, with no alignment jitter, the effect of static phase on transmission performance is small for reasonable *C/N*. For higher quality transmission, the requirements for static phase offset is more stringent. This may be explained as follows: if the power of the signal at zero offset is  $P$  watts, the reduction due to static offset is  $p$  watts, the IF noise is  $n$  watts, and the additional timing error induced noise is  $n_i$ , then *C/N* can be written as

$$\frac{C}{N} = \frac{(P-p)}{(n+n_i)}. \quad (13)$$

Thus, static offset penalty is more significant when  $n$  is small. Therefore, phase offset penalty is more significant to high quality transmission than to lower quality transmission.

#### B. Transmission Penalty Due to Static Phase Offset and Jitter

In the presence of alignment jitter, the static phase offset is much more serious. This can be shown by assuming that  $J_a(mT)$  has a Gaussian distribution, with zero mean and standard deviation equal to  $\frac{1}{6}$  the peak-to-peak alignment jitter. This distribution approximates the distribution of the alignment jitter in typical transmission links [4].

Similar to the static phase offset, the effects of time jitter are to reduce the desired signal, to increase the magnitude error, and to increase the *ISI*. The dominant distortion in this case is the magnitude error, which

results from the error in the sample value when compared with the zero jitter case. Furthermore, the jitter introduces a distortion as a result of the *ISI*. These two sources of noise and distortion add incoherently reducing the final  $C/N$ . Hence,  $C/N$  can be expressed as

$$\frac{C}{N} = \frac{\langle \frac{1}{2} q^2 (J_a(mT) + \tau) \rangle}{(\mathcal{E}_m + \mathcal{E}_{ISI} + \eta_r(t_m))}, \quad (14)$$

where  $\langle \frac{1}{2} q^2 (J_a(mT) + \tau) \rangle$  is the desired signal average power in watts,  $\mathcal{E}_m = q(J_a(m - 1)T + \tau) - q(J_a(mT) + \tau)$  is the error as a result of the magnitude difference between the previous and present sample values,  $\mathcal{E}_{ISI} = q(\sum_{k \neq 0} \frac{2(-1)^k}{\pi} q(kT + J_a(mT) + \tau))$  is the *ISI*, and  $\eta_r(t_m)$  is the noise.

The Gaussian distributed points  $J_a(mT)$  are generated by converting a set of random numbers by using the following relationship

$$F(x) = \frac{1}{2} + \frac{1}{2} \operatorname{erf}\left(\frac{x-m}{\sqrt{2}\sigma}\right), \quad (15)$$

where  $F(x)$  is the Gaussian cumulative distribution function,  $x$  is the Gaussian distributed random number,  $m$  is the mean,  $\sigma$  is the standard deviation, and  $\operatorname{erf}(x)$  denotes the error function which is defined as

$$\operatorname{erf}(x) = \frac{2}{\sqrt{\pi}} \int_0^x e^{-t^2} dt. \quad (16)$$

By using Monte Carlo techniques, Equation 14 is evaluated. Figure 4 shows the transmission penalty versus  $C/N$  for peak-to-peak alignment jitter of  $60^\circ$  with static phase offset of  $10^\circ$ ,  $30^\circ$  and  $60^\circ$ . In Figure 5 the peak-to-peak alignment jitter is  $120^\circ$ . It is readily seen that the transmission penalty is largest with the largest combination of alignment jitter and static phase offset. This shows that the system is less tolerant to alignment jitter when static phase offset is present. Therefore, static phase offset must be avoided in order to minimize the penalty due to alignment jitter. Also, it is seen that the transmission penalty increases with increasing the  $C/N$ . This may be explained as follows: for a given phase offset and peak-to-peak jitter, the jitter noise is constant regardless of the input  $C/N$ . For high  $C/N$ , the induced *ISI* noise becomes the dominant limiting factor. For low  $C/N$ , the jitter induced *ISI* noise is less dominant than the existing noise which minimizes its penalty. Similar to the previous case, phase offset penalty due to static phase offset and jitter is more significant to high quality transmission than to lower quality transmission.

#### 4. CONCLUSION

SMPTE Component 270 Mb/s digital video requires a minimum  $C/N$  of  $\sim 15$  dB for reasonable BER. Similarly, terrestrial VSB system can operate in a  $C/N$  environment of 14.9 dB (note terrestrial VSB has error correcting codes), while high data cable mode operation needs a  $C/N$  of 28.3 dB [5]. This minimum  $C/N$  of any these three systems should be increased to compensate for any expected timing error penalty. Thus, a margin, to compensate for any anticipated timing errors, should be added to the minimum required  $C/N$ .

We notice from results that the penalty is larger for higher  $C/N$ . Therefore, timing errors has less penalty on 8-VSB than on 16-VSB. We also notice that the penalty due to jitter increases more rapidly in the presence of static phase offset. That is to say, M-VSB system is less tolerant to jitter in the presence of static phase offset. Similarly, M-VSB system is less tolerant to static phase offset in the presence of jitter.

For example, the penalty gap between 8-VSB and 16-VSB increases significantly in the presence of static phase offset.  $C/N$  penalty for  $J_a(mT) = 120^\circ$ ,  $\tau = 10^\circ$  for 8-VSB is  $\sim 3.5$  dB while the penalty for 16-VSB is  $\sim 7$  dB, a gap of  $\sim 3.5$  dB. Meanwhile,  $C/N$  penalty for  $J_a(mT) = 120^\circ$  and  $\tau = 120^\circ$  for 8-VSB is  $\sim 4.4$  dB while the penalty for 16-VSB is  $\sim 10.5$  dB, a gap of  $\sim 6.1$  dB. On the other hand, increasing  $\tau$  from  $10^\circ$  to  $120^\circ$  increased the penalty for 8-VSB by only  $\sim 0.9$  dB, while it increased the penalty for 16-VSB as high as  $\sim 4.5$  dB.

## II. ERROR DETECTION AND HANDLING

Noise, dispersion, and jitter cause errors in digital television transmission. Society of Motion Picture and Television Engineers (SMPTE) Recommendation RP 165-1994 describes the generation for error detection and handling (EDH) checkwords and related status flags to be used optionally for the transmission of digital television serial interface [6]. Two checkwords are defined: one based on a field of active picture samples (AP-CRC) and the other on a full field of samples (FF-CRC). These two checkwords are then placed in the ancillary data block. Vertical and longitudinal redundancy checks are further used to detect and correct single errors in the ancillary data block.

Each checkword consists of 16-bits calculated using the *cyclic redundancy check* polynomial generation method (CRC-CCITT). The generation polynomial is as follows:

$$P(x) = x^{16} + x^{12} + x^5 + 1.$$

Procedure for generating  $n$ -bit CRC is as follows [8]:

### (a) Transmitter Side:

1. The digital stream is multiplied with  $2^n$ , where  $n$  is the highest power of the generating polynomial (i.e. padded at the least significant digit bit side with 16 zeros.)
2. The stream is divided (using modulo 2 arithmetic) with the binary number 10001000000100001 (i.e. divide by  $P(x)$ ).
3. The 16-bit remainder is then transmitted at the beginning of the following field with the ancillary data block.
4. The digital stream is transmitted with the  $n$ -CRC padded to the least significant side of the message (note that the division process does not affect the transmitted stream).

### (b) Receiver Side:

1. The received digital stream is padded at the least significant digit bit side with the received CRC.
2. The received stream is divided (using modulo 2 arithmetic) with the binary number 10001000000100001.
3. Non-zero remainder signifies a transmission error.

### Example

1. Given

Message  $M = 100000\ 0000$  (10-bits)

Generating polynomial  $P(x) = 10001\ 0000\ 0010\ 0001$  (17-bits)

CRC to be calculated (16-bits)

2. The message is multiplied by  $2^{16}$ , yielding 10 0000 0000 0000 0000 0000 0000
3. The product is then divided by  $P(x)$ :

$$\begin{array}{r}
 \phantom{10001\ 0000\ 0010\ 0001} \overline{1000\ 1000\ 1} \\
 10001\ 0000\ 0010\ 0001 \overline{) 10\ 0000\ 0000\ 0000\ 0000\ 0000\ 0000} \\
 \phantom{10001\ 0000\ 0010\ 0001} \underline{10\ 0010\ 0000\ 0100\ 001} \\
 \phantom{10001\ 0000\ 0010\ 0001} 00\ 0010\ 0000\ 0100\ 0010\ 000 \\
 \phantom{10001\ 0000\ 0010\ 0001} \phantom{00\ 0010\ 0000\ 0100\ 0010\ 000} \underline{10\ 0010\ 0000\ 0100\ 001} \\
 \phantom{10001\ 0000\ 0010\ 0001} \phantom{00\ 0010\ 0000\ 0100\ 0010\ 000} 00\ 0010\ 0100\ 0110\ 0010\ 000 \\
 \phantom{10001\ 0000\ 0010\ 0001} \phantom{00\ 0010\ 0000\ 0100\ 0010\ 000} \phantom{00\ 0010\ 0100\ 0110\ 0010\ 000} \underline{10\ 0010\ 0000\ 0100\ 001} \\
 \phantom{10001\ 0000\ 0010\ 0001} \phantom{00\ 0010\ 0000\ 0100\ 0010\ 000} \phantom{00\ 0010\ 0100\ 0110\ 0010\ 000} \phantom{00\ 0010\ 0000\ 0100\ 001} 0110\ 0110\ 0110\ 0010 \leftarrow \text{CRC}
 \end{array}$$

4. The remainder is added to  $2^{16}M$  to give  $T = 10\ 0000\ 0000\ 0110\ 0110\ 0110\ 0010$  which is transmitted.
5. If there is no errors, the receiver receives  $T$  intact. The received message is then divided by  $P(x)$ :

$$\begin{array}{r}
 \phantom{10001\ 0000\ 0010\ 0001} \overline{100010001} \\
 10001\ 0000\ 0010\ 0001 \overline{) 10\ 0000\ 0000\ 0110\ 0110\ 0110\ 0010} \\
 \phantom{10001\ 0000\ 0010\ 0001} \underline{10\ 0010\ 0000\ 0100\ 001} \\
 \phantom{10001\ 0000\ 0010\ 0001} 10\ 0000\ 0010\ 0100\ 011 \\
 \phantom{10001\ 0000\ 0010\ 0001} \phantom{10\ 0000\ 0010\ 0100\ 011} \underline{10\ 0010\ 0000\ 0100\ 001} \\
 \phantom{10001\ 0000\ 0010\ 0001} \phantom{10\ 0000\ 0010\ 0100\ 011} \phantom{10\ 0010\ 0000\ 0100\ 001} 10\ 0010\ 0000\ 0100\ 001 \\
 \phantom{10001\ 0000\ 0010\ 0001} \phantom{10\ 0000\ 0010\ 0100\ 011} \phantom{10\ 0010\ 0000\ 0100\ 001} \phantom{10\ 0010\ 0000\ 0100\ 001} \underline{10\ 0010\ 0000\ 0100\ 001} \\
 \phantom{10001\ 0000\ 0010\ 0001} \phantom{10\ 0000\ 0010\ 0100\ 011} \phantom{10\ 0010\ 0000\ 0100\ 001} \phantom{10\ 0010\ 0000\ 0100\ 001} \phantom{10\ 0010\ 0000\ 0100\ 001} 00\ 0000\ 0000\ 0000 \leftarrow \text{Remainder}
 \end{array}$$

Since there is no remainder, it is assumed that there have been no errors.

From SMPTE RP 165-194 [6] and ANSI/SMPTE 125M- 1992 [7] we can calculate the size of the data block included in active picture CRC for 13.5 MHz component video as follows:

Total number of samples per active line = 1440 samples

First active picture sample to be included in CRC in line 21 (or line 284) = 0

Last active picture sample to be included in CRC in line 262 (or line 525) = 1439

Total number of samples per CRC block =  $((262 - 21) \times 1440) = 347040$  samples

Each sample is represented by 10 bits, then number of bits per block = 3470400 bits/AP-CRC

Similarly, we can calculate the block size for the full-field CRC for 13.5 MHz component video as follows:

Total number of samples per full line = 1716 samples

First full-field sample to be included in CRC in line 12 (or line 275) = 1444

Last full-field sample to be included in CRC in line 8 (or line 271) = 1439

Total number of samples per CRC block =  $(262 - 12 + 8) \times 1716 - 4 = 442724$  samples

Each sample is represented by 10 bits, then number of bits per block = 4427240 bits/FF-CRC

## REFERENCES

- [1] United States Advanced Television Systems Committee, "Digital Television Standard for HDTV Transmission," Doc. A/53, April 1993, Annex D.
- [2] Franks L. and Bubrouski J., "Statistical Properties of Timing Jitter in a PAM Timing Recovery Scheme," *IEEE Trans. on Comm.*, Vol. Com-22, No. 7, July 1974, pp913-920.
- [3] Mengali U. and Pirani G., "Jitter Accumulation in PAM Systems," *IEEE Trans. on Comm.*, Vol. Com-28, No. 8, August 1980, pp1172-1183.
- [4] Patrick T. and Varma E., "Jitter in Digital Transmission Systems," *Artech House, Inc.*, 1989.
- [5] United States Advanced Television Systems Committee, "Guide to the Use of the Digital Television Standard for HDTV Transmission," Doc. A/54, April 1993.
- [6] SMPTE Recommended Practice "Error Detection Ceckwords and Status Flags for Use in Bit-Serial Digital Interfaces for television" RP 165-1994.
- [7] SMPTE Standard, "Component Video Signal 4:2:2 Bit parallel Digital Interface," ANSI/SMPTE 125M-1992.
- [8] Stallings W., "data and Computer Communications," Fourth Edition, MacMillan Publishing Company, 1994.

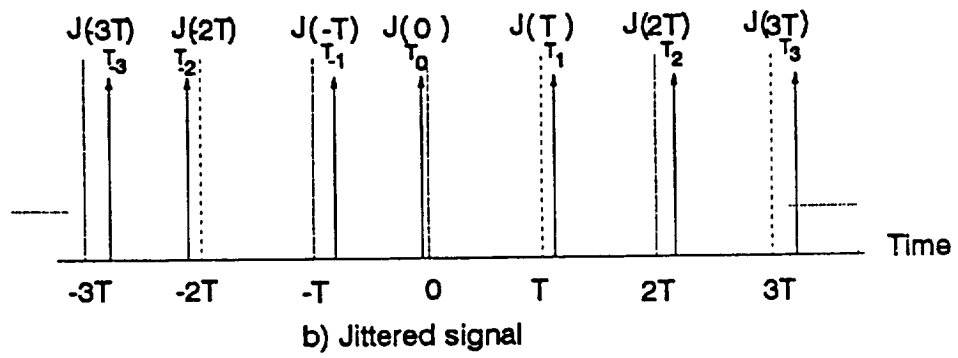
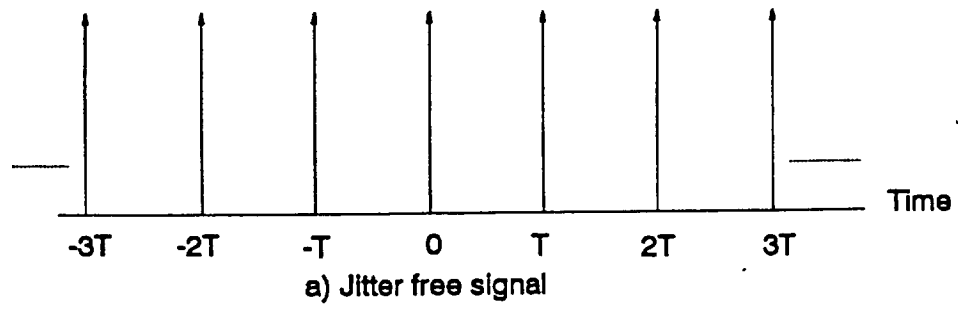


Figure 1 : Illustration of jitter (a) Jitter free signal, (b) Jittered signal.

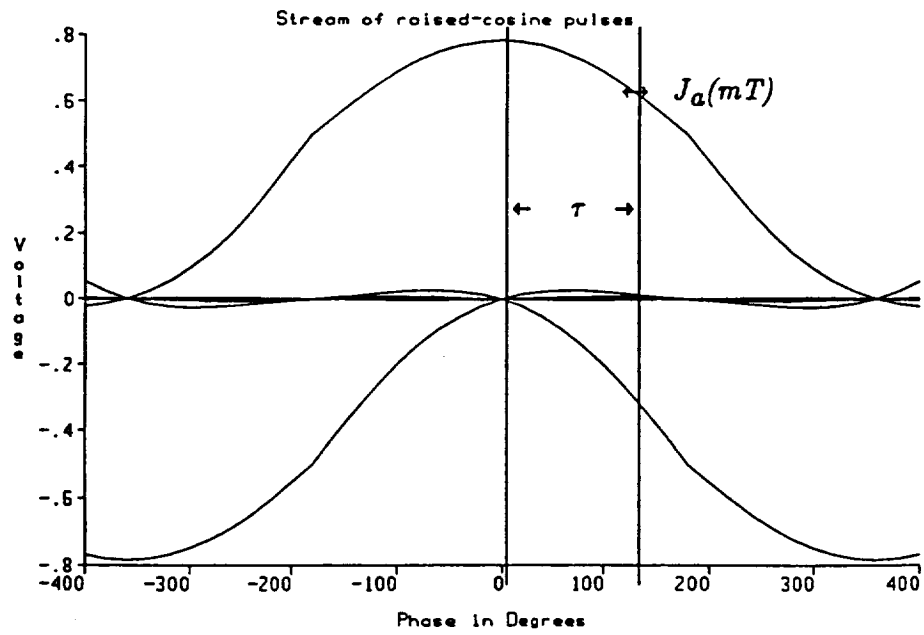


Figure 2 : Sequence of raised cosine samples sampled with static offset  $\tau$  and alignment jitter  $J_a(mT)$ .

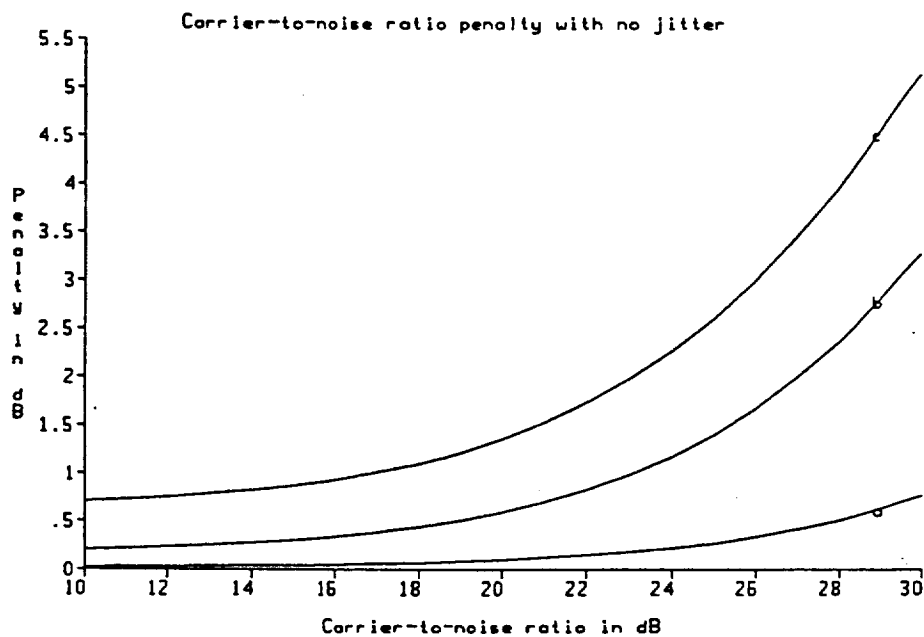


Figure 3 : Transmission penalty in dB versus carrier-to-noise in dB, the alignment jitter  $J_a(mT) = 0^\circ$  (a)  $\tau = 10^\circ$ , (b)  $\tau = 30^\circ$  & (c)  $\tau = 60^\circ$

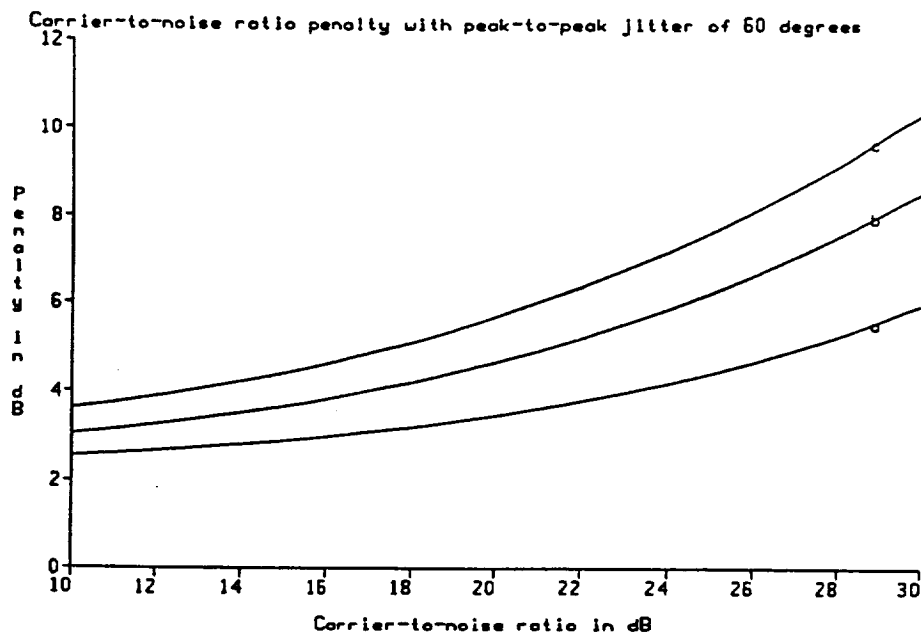


Figure 4 : Transmission penalty in dB versus carrier-to-noise in dB, the alignment jitter  $J_a(mT) = 60^\circ$  (a)  $\tau = 10^\circ$ , (b)  $\tau = 30^\circ$  & (c)  $\tau = 60^\circ$

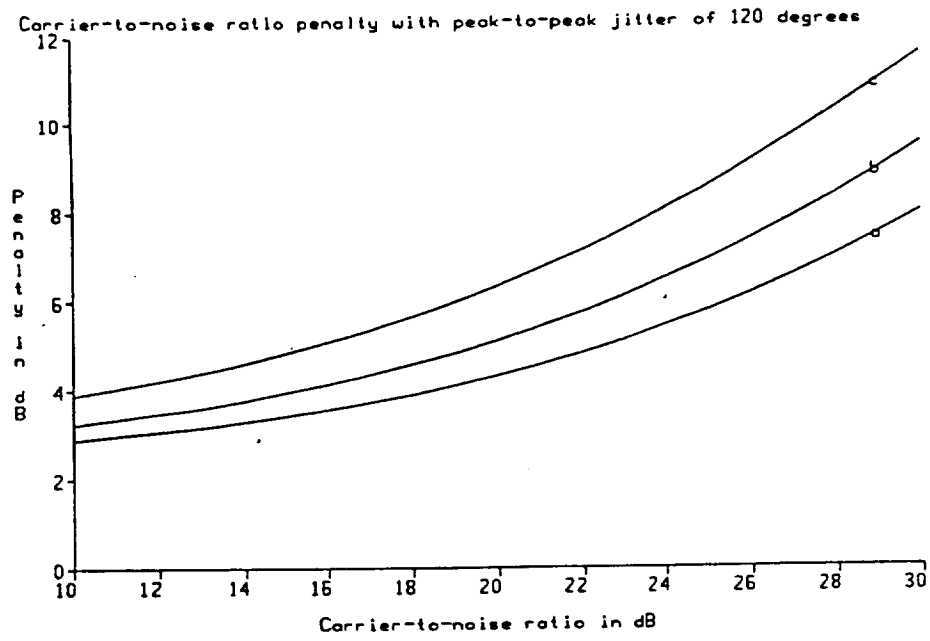


Figure 5 : Transmission penalty in dB versus carrier-to-noise in dB, the alignment jitter  $J_a(mT) = 120^\circ$  (a)  $\tau = 10^\circ$ , (b)  $\tau = 30^\circ$  & (c)  $\tau = 60^\circ$



## 1998 NASA/ASEE SUMMER FACULTY FELLOWSHIP PROGRAM

JOHN F. KENNEDY SPACE CENTER  
UNIVERSITY OF CENTRAL FLORIDA

### CHARACTERIZATION OF SALT MARSH IMPOUNDMENT SEDIMENTS UNDER THREE TYPES OF WATER MANAGEMENT

Linda K. Blum, PhD  
Research Associate Professor  
Department of Environmental Sciences  
University of Virginia

KSC Colleague: Kelly Gorman

Dynamac Colleagues: Ross Hinkle & Jay Garland

#### ABSTRACT

Sediments were characterized from samples collected in salt marsh impoundments located at Black Point on Kennedy Space Center's Merritt Island National Wildlife Refuge. The impoundments selected for study were exposed to a variety of water management strategies. Some are flooded for as long as 8-10 months (WAM) of the year and favor the growth of submerged aquatic vegetation (SAV), while others are open to the lagoon, flooded infrequently (2 months) during the winter, and colonized by emergent vegetation. Sediment samples were collected at two depths; 0-10 cm and 10-20 cm below the surface in open, restored, and WAM impoundments as well as native marshes. Samples were analyzed for moisture content, bulk density, and organic matter (OM) content. The infrequently flooded, open impoundments and native marshes had a tendency to have high OM content while the nearly continuously flooded impoundments (WAM) had lower OM contents. Although these results were not statistically significant, these findings do suggest several testable hypotheses. First is that open and restored impoundments accumulate sediment organic matter, while WAM impoundments accumulate organic materials at a slower rate. Secondly, the flux of dissolved organic matter and nutrients to the Indian River Lagoon is enhanced for WAM impoundments, and the flux of particulate materials to the Lagoon will be greater from open and restored marshes. The consequences of dissolved vs. particulate organic matter and nutrient flux on the lagoon ecosystem water quality are largely unknown. Tests of these hypotheses are planned for subsequent years as part of an ongoing joint environmental monitoring program between NASA, St. John's River Water Management District, and the U.S. Fish and Wildlife Service.

# CHARACTERIZATION OF SALT MARSH IMPOUNDMENT SEDIMENTS UNDER THREE TYPES OF WATER MANAGEMENT

Linda K. Blum

## 1. INTRODUCTION.

The National Aeronautics and Space Administration (NASA) is the landholder of 140,000 acres at Kennedy Space Center (KSC) of which, only 6,700 acres are directly used for launch operations or in support of launch operations. The remaining area is comprised of highly diverse habitats including 50,000 acres of oak-palmetto scrub and pine flatwoods uplands, 35,500 acres of impounded high salt marsh and wetlands, and 54,500 acres of open estuarine lagoons with extensive seagrass beds. Despite the relative pristine nature of much of the KSC property, over 75% the historical wetlands (26,000 acres) were impounded 20 to 30 years ago for control of salt marsh mosquitoes. Many of the KSC impoundments have been recently reconnected to the estuary as recommended by the US EPA (1998) in order to return to a more natural hydroperiod, and, thus exchange of materials between the wetlands and the adjacent estuarine water column. Currently, over 18,000 acres of wetland have been reconnected to the lagoon and are managed by the U.S. Fish and Wildlife Service.

At KSC a combination of marsh impoundment management techniques (Table 1) are used to attain the multiple goals of optimizing wildlife habitat, mosquito control, and restoration of natural wetland processes in re-connected impoundments. However, the effects of the various marsh management techniques on marsh surface elevation, marsh plant distribution, nutrient cycling, and the adjacent estuary are largely unknown. Yet, these are important issues from both the management and theoretical viewpoints.

Alteration in the depth of water, period of flooding, and the source of the flooding water have the potential to alter the types of vegetation capable of growing in wetlands (Johnson & York 1915; Adams 1963; King et al. 1982; Odum et al. 1984). For example, under the nearly continuous flooded conditions of wildlife aquatic management (WAM), submerged aquatic vegetation (SAV) will replace emergent marsh plants. Re-establishment of the hydrologic connection and natural hydroperiod will result in replacement of SAVs with emergent macrophytes that typically resemble native plant communities. Plant community composition and distribution has the potential to affect organic matter accumulation and nutrient mineralization. Although SAV plant production may be equal to that of emergent plants, the organic matter of SAV is soft tissue that decomposes quickly (Lagera 1988; Blum & Mills 1991) and will have different N and P mineralization dynamics than emergent plants (Lagera 1988). In contrast to WAM impoundments, in impoundments which are only seasonally flooded for mosquito control (RIM), emergent plants are not replaced by SAV (Rey et al. 1990a.) Rey et al. (1990b) found that plant litter had a longer residence time in impoundments than in near by unimpounded marshes. Brockmeyer et al. (1997) suggest that this difference would result in the accumulation of litter

(and thus sediment organic matter) which would function as a nutrient reservoir in RIM managed marshes. Consequently, impoundments with different water management histories will result in differences in sediment organic matter accumulation and the potential for transfer of organic materials and nutrients to the adjacent estuarine waters. Thus, it seems reasonable to hypothesize that organic matter accumulation in nearly continuously flooded impoundments will occur more slowly than in impoundments where emergent plants grow. A corollary of this hypothesis is that nutrient regeneration (e.g., N & P) as a result of mineralization would be much greater in impoundments dominated by SAV.

## 2. GOAL

The goal of this NASA faculty fellowship was characterization of impoundment sediments under three types of water regimes. The information collected as a result of this work provides the baseline observations necessary to establish a long-term monitoring program of water management effects on the impoundments and on water quality in the adjacent lagoon. It accomplishes this by identifying impoundments where water management has the potential to have the greatest effect on the land surface elevation and on nutrient transport between the lagoon and impoundments using sediment organic matter content as an integrated measure of plant production and microbial decomposition/mineralization processes.

## 3. DESCRIPTION OF IMPOUNDMENT WATER MANAGEMENT

A variety of water management schemes are currently used in Merritt Island National Wildlife Refuge (MINWR) impoundments: rotational impoundment management (RIM), wildlife/aquatic (WAM); and open marsh management (Table 1). Several impoundments have been restored to a native condition: the dikes have been removed and the perimeter ditches have been filled. Flooding of these restored marshes is not manipulated and is similar to that of marshes that were never impounded (i.e., native marshes). The approximate length of time the impoundments are flooded during the year varies. WAM marshes are flooded nearly continuously while open, restored, and native marshes are flooded primarily in the winter for approximately two months. In addition, the timing of the flooding and the depth of the flood water also vary among impoundment management types.

## 4. METHODS

4 a. Sampling Design. Five representative impoundments, one restored impoundment, and two "native" salt marshes were selected for examination (Fig. 1). Five of the impoundments studied represent a temporal gradient or chronosequence of exposure to the WAM treatment from T-10-D and T-10-J which have been selected to continue under WAM treatment, T-10-C which was exposed to WAM treatment until spring 1998 when it was converted to open management, T-10-H which was converted to open management approximately 10 years ago, and T-10-K which was

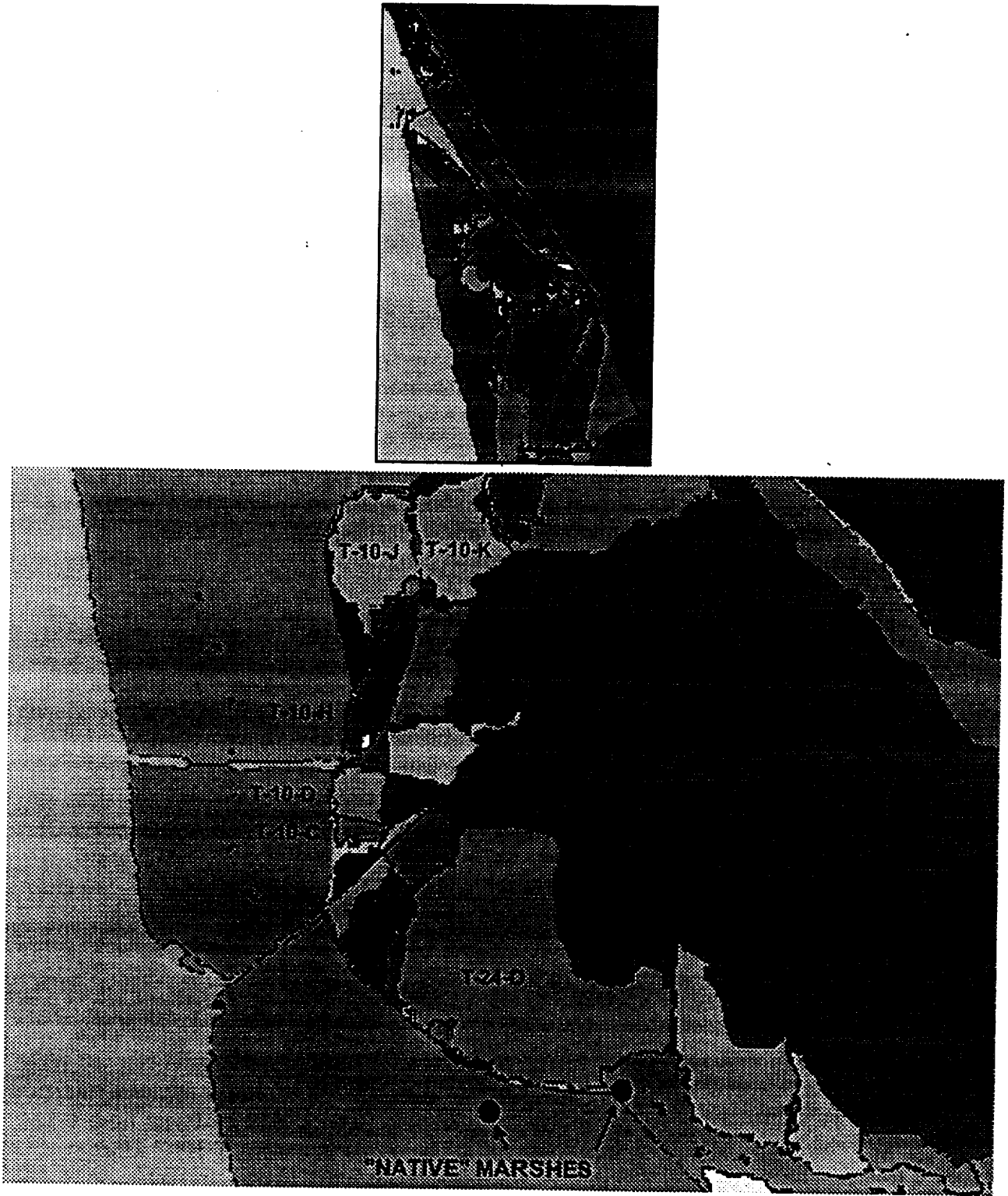


**Fig. 1.** Location of the several impoundments at the Merritt Island Wildlife Reserve, Kennedy Space Center, FL.

converted from WAM treatment to a restored condition nearly 20 years ago. In addition to the water management history of the impoundments as criterion for inclusion in the survey, the marshes selected for study are all located in a similar position within the landscape. The marshes are all located directly adjacent to the IRL to maximize the probability that the pre-impoundment history of the marshes was similar. As a result, no suitable RIM-managed impoundments were included in this study. Within each of the 7 impoundments, transects parallel to the flow of flooding water were established. The number of transects was dependent on the size of the individual impoundment. At a minimum, 3 transects at 3 stations (total of 9 cores) were sampled within each impoundment with the exception of the two “native” marshes. “Native” marsh islands were so small that only 3 cores were taken in each marsh. A total of 102 cores were collected for analysis (Table 1). At each position, the GPS coordinates (+/- 10 m resolution) and plant cover were recorded.

Table 1. Marsh water management schemes at MINWR result in different hydroperiods that are dependent on the management type. Examples of marshes impoundments exposed to each of the management schemes are shown. The number of cores collected in each impoundment/marsh sampled is indicated. Location of these impoundments is shown in Fig. 1.

Management Type	Months Flooded per Year	Marsh Impoundment	Number of Cores Collected
Restored - 20yrs	2-3	T-10-K	18
Open - 10 yrs	2	T-10-H	15
Open - 0.1 yrs	2	T-10-C	9
Moist Soil	4	T-24-D	24
RIM (mosquito)	4-6		
WAM (wildlife)	8-10	T-10-D, T-10-J	9, 18
Native	2-3	marsh islands	9

4 b. Sample Collection and Analysis. Sediment samples were collected in core tubing (6.35 cm diameter × 30 cm long, electrical conduit). Sediment cores were extruded in the field and cut into 2 10-cm sections. The samples were wrapped in pre-weighed, labeled, pieces of aluminum foil and then sealed in ziplock bags for return to the laboratory. Samples were held for no more than one day before analysis. In the lab, the wet weight of each sample was determined including any water that leaked from the foil into the ziplock bag. Next, the samples were dried at 70° C to a constant weight (approximately 5 days). Once the dried samples were re-weighed, they were homogenized using a 5-lb drill hammer. A sub-sample (approximately 5 cm<sup>3</sup>) of the homogenized material was removed for estimation of organic matter by mass-loss-on-ignition at 500° C for 8 h. Moisture content (% H<sub>2</sub>O per g dry mass sediment), bulk density (g dry mass per cm<sup>3</sup>), and organic matter content (% mass loss per g dry mass sediment) were calculated.

4 c. Statistical Analysis. Samples were analyzed using a multivariate model (SPSS-PC) to determine if statistically significant differences could be attributed to the treatments of depth (top 10-cm and 10-20 cm), location (i.e., impoundment type), and/or plant cover. Variables included moisture content, bulk density, and organic matter content. The hypotheses were tested at  $\alpha = 0.05$ .

4 d. Sample Archival. After organic matter determination, any remaining oven-dried sediment was placed in a labeled ziplock bag and shipped to the Department of Environmental Sciences at the University of Virginia where the samples will be analyzed for pH and salinity (10 g required). If sufficient sample remains (10 - 20 g required), the sediments will be extracted for nutrients ( $\text{NH}_4^+$ ,  $\text{NO}_3^-$ ,  $\text{NO}_2^-$ , and  $\text{PO}_4^{3-}$ ). For those samples with organic matter contents less than 20% (i.e., organic soils) and sufficient sample remaining (50 - 60 g required), sediment texture will also be determined. All data collected during summer 1998 have been archived with Dynamac and will be included in their impoundment data base that is currently under development. Any additional information (textural data, nutrient content, pH, and/or salinity) will be submitted to Dynamac for archival as the data are obtained.

## 5. RESULTS AND DISCUSSION

### 5 a. General Observations.

It is important to note that May and June of 1998 were the driest on record in over 100 years. Sediment samples were collected at the end of June and in early July during the most extreme part of the 1998 dry spell. Impoundments T-10-C, T-10-D, and T-10-H were sampled prior to any significant rain during these months. Between sampling these impoundments and impoundments T-24-D, T-10-J, and the native marshes a brief afternoon thunderstorm occurred. Another afternoon thunderstorm occurred prior to sampling T-10-K. Insufficient rain fell during these events to saturate the sediments. Regardless of when the impoundments were sampled, the depth to the water table in impoundment/marsh sediments during June and July 1998 remained relatively constant and was never more than 30 cm below the sediment surface except those in areas of T-10-C and T-10-D where submerged mudflats were sampled.

There was a very noticeable absence of animals in the sediment samples collected. This may be typical of sediments from this region of Florida, but in comparison with native marshes in Virginia, North Carolina, and South Carolina the lack of invertebrates is quite distinctive (personal observation).

The typical rooting depth of emergent plants in native and impounded marshes was between 5 and 10 cm regardless of the flooding history. This is shallow in comparison with rooting depths reported in the literature for Massachusetts (Valiela et al. 1976), Mississippi (de la Cruz and Hackney 1977), Georgia (Schubauer and Hopkinson 1984), South Carolina (Morris and Bowden

1986), North Carolina (Yelverton and Hackney 1986), and Virginia (Blum 1993) marshes where roots are typically reported to range between 20-30 cm deep in the sediment.

In contrast to Virginia salt marshes, there appears to be a significant contribution of aboveground plant materials to the sediment organic matter pool in MINWR impoundments and “native” marshes. This difference is likely due to differences in the lunar tides experienced by Virginia (100 - 150 cm) vs. Northern Indian River Lagoon (< 0.5 cm) marshes.

#### 5 b. Specific Observations.

Statistically significant differences ( $p = 0.0007$ ) in moisture content, bulk density, and organic matter content were evident among surface sediments and sediments collected from the 10-20 cm depth (Fig. 2, 3, 4). Organic matter content was greatest in surface sediments (Fig. 4) and can probably be attributed to above- and below ground organic matter inputs from plants. Although 1998 was an exceptionally dry year, the surface layers in all impoundments contained a greater percentage of water than deeper sediments except in impoundment T-10-D (WAM) where the sediments were dominated by exposed, “dry” mudflats.

In contrast to organic matter and moisture content, sediment bulk density was greater at depth than in the surface layers of all impoundments (Fig. 3). The bulk density of organic materials is much lower than that of mineral particles (Buckman and Brady 1969). As the amount of organic matter in a given volume of sediment increases, the space available for mineral particles decreases, thus lowering the samples bulk density. This interpretation is supported by the statistically significant, negative correlation between organic matter and bulk density (Fig. 5). The statistically significant, negative correlation between moisture content and bulk density (Fig. 6) is predictable (Buckman and Brady 1969). As bulk density decreases, the pore space available

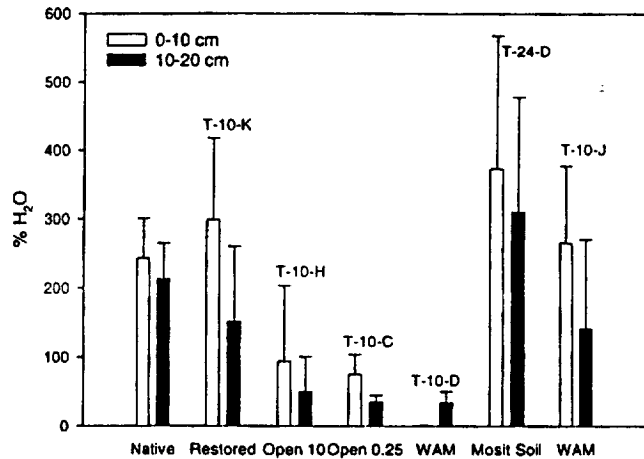


Fig. 2. Moisture content (% water per g dry weight sediment) at two depths (0 - 10 cm and 10 - 20 cm) in impoundment sediments. Error bars are one standard deviation of the mean.

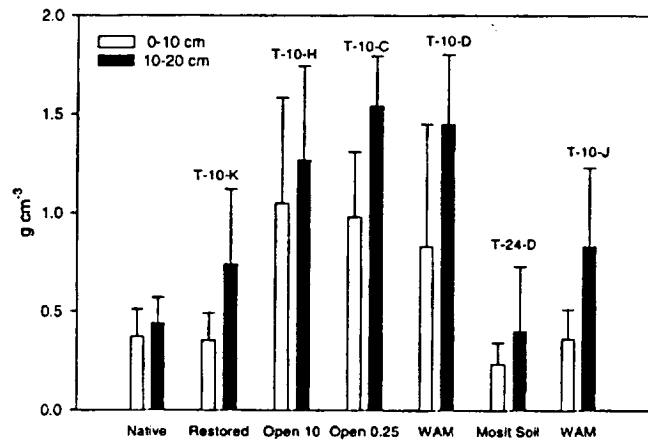


Fig. 3. Bulk density ( $\text{g cm}^{-3}$ ) at two depths (0 - 10 cm and 10 - 20 cm) in impoundment sediments. Error bars are one standard deviation of the mean.

to contain water increases. Additionally, the water-holding capacity of organic matter is widely recognized (Buckman and Brady 1969) and is illustrated by the statistically significant, positive relationship between organic matter and moisture content (Fig. 7). The extensive cracking of the dried surface sediments that occurred during early summer 1998 suggests that the bulk densities measured for exposed mudflats may be overestimates in comparison with similar measurements made during a year with more typical rainfall. However, the relationship between bulk density and depth would probably show a similar pattern even in a very wet year.

No significant differences were observed for moisture content, bulk density, or organic matter based on the location sampled (i.e., impoundment) or the plant cover. This is not surprising given that only one impoundment of each water management type was sampled and that the heterogeneity within each impoundment was high. Demonstration of statistically significant differences in sediment characteristics that are only suggested by trends in figures 2, 3, and 4 would require a more intensive sampling effort than this summer's field campaign.

The impoundments can be arbitrarily divided into two groups based on sediment characteristics. Impoundments T-10-K (restored) and T-24-D (moist soil), and the native marshes had higher concentrations of organic materials and greater amounts of water in the surface sediments (Fig. 2,3, & 4) than impoundments T-10-D (WAM), T-10-C (open 0.1 years), and T-10-H (open 10

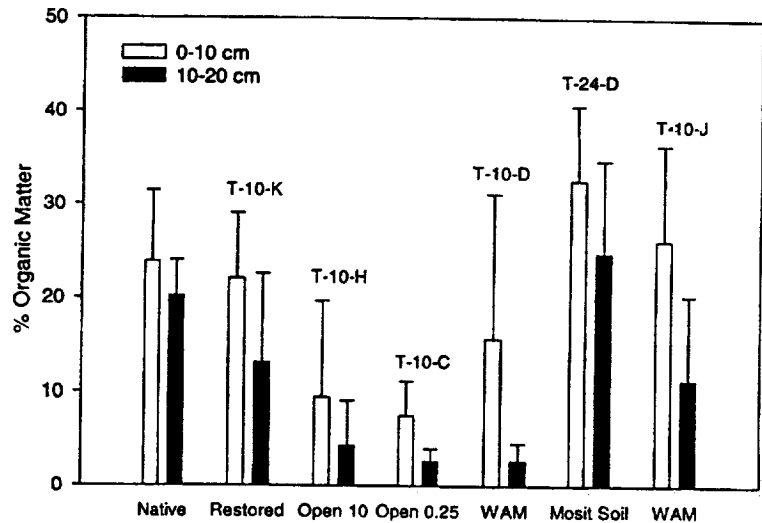


Fig. 4. Organic matter content (weight loss on ignition per g dry weight sediment) at two depths (0 - 10 cm and 10 - 20 cm) in impoundment sediments. Error bars are one standard deviation of the mean.

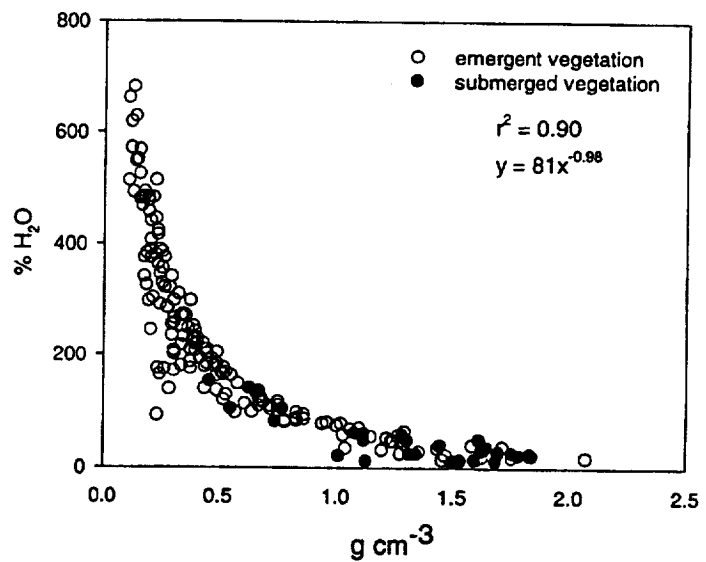


Fig. 5. Relationship between organic matter content and bulk density. Two categories of sediments (under submerged vegetation or emergent vegetation) were established based on the type of plants normally found at the sampling location.

years). Bulk density values were lower for the restored-moist soil-native marsh group than for the WAM chronosequence group of impoundments T-10-D, T-10-C, and T-10-H. Plant growth form is an important difference between these two groups.

Sediment characteristics of impoundment T-10-J (under WAM) is more similar to the restored and native marshes than T-10-D, T-10-C, and T-10-H (also under WAM). This difference is probably related to very high degree of heterogeneity of habitat in T-10-J and the limited number of samples collected in this very large impoundment. Examination of the aerial photos taken in 199X suggests that large areas of T-10-J are ponded during much of the year in comparison to T-10-K. If sediment samples had been collected in the ponded areas of T-10-J it is likely that these sediments would have been more similar to the other WAM impoundments. Samples from all other impoundments appear to have been collected from representative areas of the impoundments based on qualitative interpretation of sampling locations relative to habitat distribution as observed from the aerial photos.

Emergent grasses and rushes dominate the restored, native and moist soil marshes plant communities. Impoundments T-10-D, T-10-C, T-10-H plant communities are dominated by submerged aquatic vegetation or have only recently come to be dominated by emergent plants (e.g., T-10-H). The organic

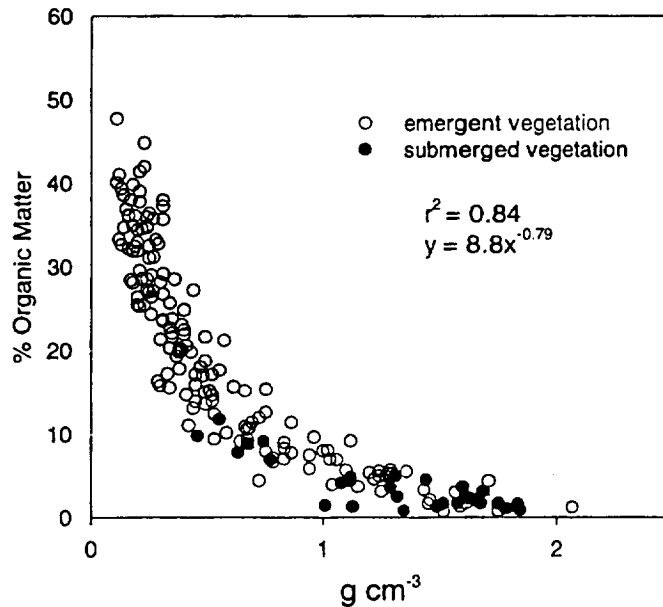


Fig. 6. Relationship between moisture content and bulk density. Two categories of sediments (under submerged vegetation or emergent vegetation) were established based on the type of plants normally found at the sampling location.

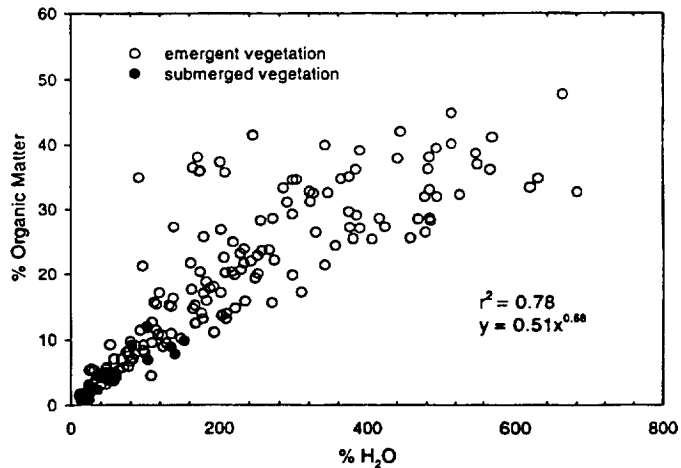


Fig. 7. Relationship between moisture content and organic matter content. Two categories of sediments (under submerged vegetation or emergent vegetation) were established based on the type of plants normally found at the sampling location.

matter of SAVs is soft tissue and has a relatively low N to P ratio so that it decomposes more rapidly than emergent plant tissues (Blum and Mills 1991; Lagera 1988). Furthermore, SAVs do not have an extensive below ground component. Emergent marsh grasses, especially those in high marsh regions allocate large proportions of their total production to the growth of below ground plant structures (e.g., roots, rhizomes, etc.) (Blum 1993). Therefore, it is reasonable to hypothesize that organic matter accumulation in nearly continuously flooded, WAM, impoundments will occur more slowly than in impoundments where emergent plants dominate. A corollary of this hypothesis is that nutrient regeneration (e.g., N & P) as a result of mineralization would be much greater in impoundments dominated by SAV. Rapid nutrient mineralization rates of SAV tissues relative to emergent vegetation forms the basis for an additional hypothesis - in WAM impoundments surface flood water concentrations of N & P are elevated relative to Indian River Lagoon water. If this proves to be the case, then the potential for nutrient enrichment of the lagoon exists when WAM impoundments water is drawn down and released to the estuary. In contrast, open, restored, and native marshes where high C:N ratio plants dominate will slowly release mineralized N & P to flooding water or may actually immobilize or reduce N & P concentrations in tidal water.

## 6. CONCLUSIONS

Linkages between estuarine wetlands and the estuarine water column have the potential to impact estuarine water quality. In the Indian River Lagoon (IRL), good water quality is critical to maintenance of the productivity of the IRL ecosystem. The role of impounded wetlands in processing of organic matter, nutrients, and suspended particulates is not well known and could be of critical importance to IRL water quality. Differences in sediment characteristics among impoundments subjected to different management schemes at Merritt Island National Wildlife Refuge suggest that the potential for impoundment management to impact IRL water quality exists. The potential effects are stated as above as hypotheses that should be tested at MINWR.

## 7. LITERATURE CITED

- Blum, L. K. 1993. *Spartina alterniflora* root dynamics in a Virginia salt marsh. Marine Ecology Progress Series. 102:169-178.
- Blum, L. K. and A. L. Mills. 1991. Microbial growth and activity during the initial stages of seagrass decomposition. Marine Ecology Progress Series. 70:73-83.
- Buckman, H. O. and N. C. Brady. 1969. The nature and properties of soils, 7 ed. Macmillan Company, London.
- de la Cruz, A. A. and C. T. Hackney. 1977. Energy value, elemental composition, and productivity of belowground biomass of a *Juncus* tidal marsh. Ecology. 58:1165-1170.
- Lagera, J., L. M. 1988. The role of macrophyte decomposition in the depletion of oxygen and sequestering of nutrients in the lower Chesapeake Bay. Ph.D. Dissertation. University of Virginia, Charlottesville, Virginia.

- Morris, J. T. and W. B. Bowden. 1986. A mechanistic, numerical model of sedimentation, mineralization, and decomposition for marsh sediments. Soil Science Society of America Journal. 50:96-105.
- Schubauer, J. P. and C. S. Hopkins. 1984. Above- and belowground emergent macrophyte production and turnover in a coastal marsh ecosystem, Georgia. Limnology and Oceanography. 29:1052-1065.
- Valiela, I., J. M. Teal, and N. Y. Persson. 1976. Production and dynamics of experimentally enriched salt marsh vegetation: Belowground biomass. Limnology and Oceanography. 21(2):245-252.
- Yelverton, G. F. and C. T. Hackney. 1986. Flux of dissolved organic carbon and pore water through the substrate of a *Spartina alterniflora* marsh in North Carolina. Estuarine and Coastal Shelf Science. 22:255-267.



**1998 NASA/ASEE SUMMER FACULTY FELLOWSHIP PROGRAM**

**JOHN F. KENNEDY SPACE CENTER  
UNIVERSITY OF CENTRAL FLORIDA**

**AN EXPERIMENTAL DESIGN TO DETERMINE THE ELECTROSTATIC PROPERTIES OF  
MARTIAN SIMULANT DUST PARTICLES**

Carlos I. Calle  
Professor and Chair  
Physics Department  
Sweet Briar College  
Sweet Briar, Virginia

NASA Colleague: Hae Soo Kim

**ABSTRACT**

The Viking mission and, more recently, the Hubble Space Telescope, provided evidence for the existence of global dust storms on Mars. Several of these dust storms were observed to last for several months. Dust particles striking the surfaces of any equipment used in future Mars missions may create potentials that may compromise the safety of astronauts and equipment in future Mars missions. Experiments that yield information on the electrostatic properties of the Martian soil and its effects on common space materials are needed before any such missions are undertaken.

In this project, experimental designs were constructed and setup to measure the electrostatic properties of small particles derived from Andesitic rocks and to determine the charging characteristics of common space materials exposed to these particles. Andesitic rock was identified by Pathfinder to be the primary type of rock on Mars. These experimental designs should serve as the basis for experiments to be performed in a simulated Mars environment (SME).

MARS-1, a simulant prepared from Andesitic rocks by NASA Johnson Space Center was used in this project. Characterization of this simulant was made using using a Scanning Electron Microscopy (SEM) and Inductively Coupled Argon Plasma Spectroscopy (ICAP) coupled with a carbon-sulfur detector. These results were compared to the Alpha Proton X-Ray Spectrometer analysis on the Sojourner rover. The simulant was found to be a suitable substitute for Martian soil. Experimental designs to determine the polarization of this simulant were set up. The simulant was observed to acquire a polarization in the presence of electric fields of the order of 2.9 N/C. Initial measurements yielded values of charge polarization densities of the order of 30 nC/g.

Two experimental designs and methods to simulate the exposure of different materials to wind-blown dust were made. These designs permit dust particle delivery to samples at different speeds. Initial rough experiments made with these designs to determine their viability were promising. These initial experiments indicated the need for several minor modifications in the designs and in the methods.

## ACKNOWLEDGEMENT

I would like to express my deepest appreciation to NASA/ASEE and in particular to Mr. Gregg Buckingham, Dr. E. Ramon Hosler, and Kari L. Stiles for providing me with the opportunity to participate in the 1998 Summer Faculty fellowship program.

I would also like to thank the people in the Materials Science Division for their kind help during the many hours of research. I am especially grateful to my NASA colleague, Dr. Hae Soo Kim, for his helpful insights and his tireless, patient, and enthusiastic collaboration in this project. My student Anne J. Lombardi worked very diligently on this project.

Dr. Ray Gompf provided helpful insights and ideas for this project. I am indebted to him. Discussions with Cole Bryan, Tim Bollo, John Bayliss, Dr. Rupert Lee, and Mica Parenti were very fruitful in the experimental designs and in the development of the methods. Stan Young and Dionne Jackson worked with Anne Lombardi on the characterization of the simulant. Sandy Locks provided the SEM photographs of the simulant that were used in the determination of the polarization density. Bill Dearing, Andy Finchum, Steve Huff, Larry Ludwig, Peter Marciniak, Lou MacDowell, James Martin, Steve McDanel, and Mike Spates were very generous with their time and provided their expertise when needed. I am grateful for their help and collaboration. I would also like to express my gratitude to Lee Underhill, my section lead, for making me feel welcomed.

Finally, I would like to thank my wife, Dr. Luz Marina Calle, professor and fellow NASA scientist, for her encouragement and guidance during our work here and for putting up with my deep immersion in the project and the unending daily reports on its status.

## AN EXPERIMENTAL DESIGN TO DETERMINE THE ELECTROSTATIC PROPERTIES OF MARTIAN SIMULANT DUST PARTICLES

Carlos I. Calle, Ph.D.

Sweet Briar College, Sweet Briar, VA 24595

### 1. INTRODUCTION

The existence of global dust storms on Mars has been well documented. The Viking mission provided evidence for the existence of planet-wide winds that may last for months and that are strong enough to pick up dust particles from the surface. The extremely dry surface conditions and the fine clays which compose the Martian soil are conducive to charge buildup. Dust particles striking metallic and nonmetallic surfaces of any equipment used in future Mars missions may create electrostatic charges large enough to produce electrical discharges in the Martian atmosphere. These electrical discharges may compromise the safety of astronauts and equipment in future Mars missions.

Experimental designs were constructed and setup to measure the electrostatic properties of small particles derived from Andesitic rocks and to determine the charging characteristics of common space materials exposed to these particles. Andesitic rock was identified by Pathfinder to be the primary type of rock on Mars. These experimental designs should serve as the basis for experiments to be performed in a simulated Mars environment (SME).

### 2. EXPERIMENTAL DESIGNS IN TERRESTRIAL ATMOSPHERIC CONDITIONS

An Ambient Atmosphere Chamber (AAC) was designed and constructed to design and test our experimental set up in ambient atmosphere. Martian Regolith Simulant (MARS-1) was acquired from NASA-Johnson Space Center.<sup>1</sup> To simulate the atmospheric conditions on Mars in future experiments, a vacuum system with a 41" x 62" chamber was acquired. This chamber is currently being installed.

To determine the electric polarization of MARS-1, that is, the effect that electric fields have on the dipole moments of its atoms and molecules, a parallel-plate capacitor was set up and connected to a variable power supply (0-40 kV). A Hipotronics AC-DC Hipot Tester Model HC3-AT-DT was connected across two aluminum plates of area 70 cm<sup>2</sup>. A Keithley Model 2501 detector and Keithley 610C Electrometer were connected to a Nicolet model 310 digital storage oscilloscope to measure the electric potential of MARS-1 after being exposed to strong electric fields (figure 1).

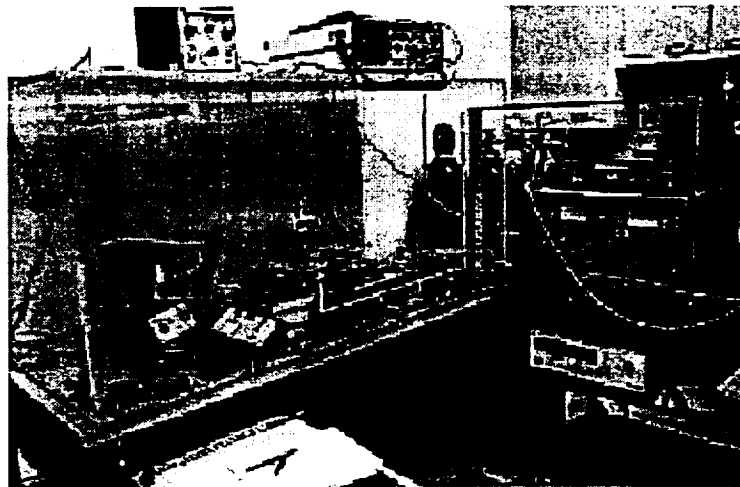


**Figure 1.** Experimental set-up to measure MARS-1 electric polarization.

To simulate the wind-blown sand striking on different surfaces, two different sand delivery mechanisms were designed. A sand blasting attachment (SBA) connected to a pressurized bottle of CO<sub>2</sub> was obtained commercially and set-up to deliver MARS-1 at different velocities to our samples. A small (8" x 4" x 12") Plexiglass box was constructed to contain the simulant particles after they strike the sample (figure 2).

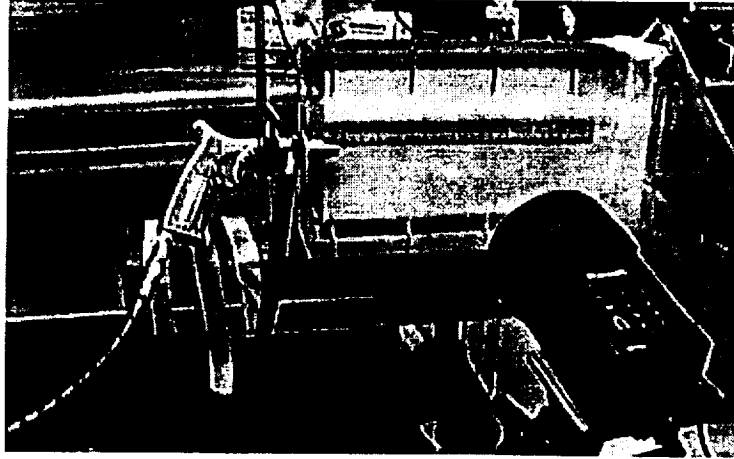


Figure 2. Sand Blasting Attachment (SBA) and Plexiglass box to contain the simulant after it strikes the sample.

A mechanical sand delivery mechanism (MSD) has also been designed and constructed to propel MARS-1 at different speeds toward the sample without the additional introduction of CO<sub>2</sub> into the chamber (figure 2). MARS-1, stored in a hopper with a narrow neck, is allowed to fall into chamber containing a motorized stainless-steel paddle wheel of moment of inertia  $5.1 \times 10^{-4} \text{ kg-m}^2$ . A Variac supplies 0-115 V to a 1/15 hp electrical motor. The motor spins the paddle wheel at frequencies ranging from 0 to 1725 RPM. MARS-1 is delivered to the sample with speeds ranging from 0 to 12 m/s. Since Viking recorded winds reaching 30 m/s, a faster motor will be installed later. A motorized, rotating multiple sample holder was also designed and constructed (figure 3).

A Sample Holder Carousel (SHC) was designed to hold and test 12 samples simultaneously with the SBA or the MSD (figure 4). After the sample is tested, the carousel is rotated an angle of 30° to be measured by the electrometer detector head.

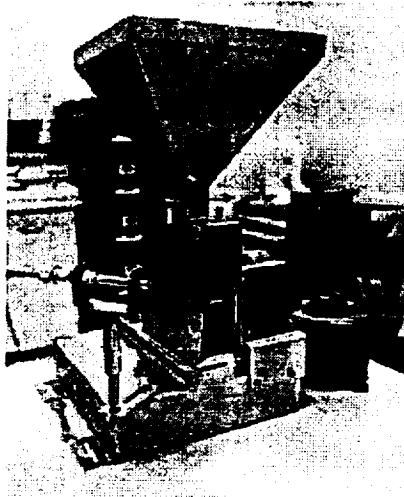


Figure 3. Mechanical Sand Delivery (MSD) apparatus.

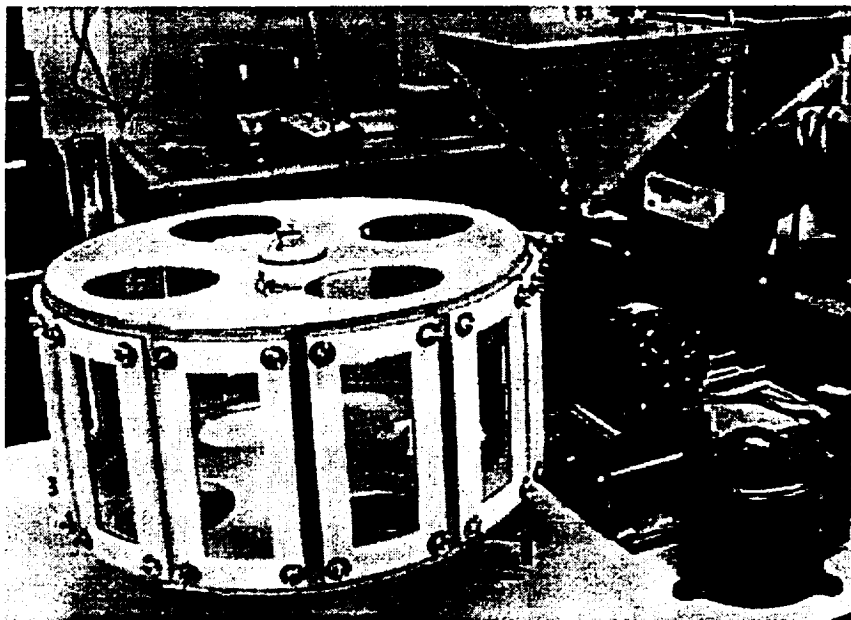


Figure 4. Sample holder carousel (SHC).

### 3. INITIAL EXPERIMENTS

Simple initial experiments were performed to test the experimental designs, our main objective in the first phase of this investigation.

**Electrical Conductivity:** The electrical conductivity  $\sigma$ , of MARS-1 was measured to be of the order of  $10^{-4} \Omega^{-1} \text{ m}^{-1}$ , intermediate between a good conductor ( $\sigma \sim 10^8 \Omega^{-1} \text{ m}^{-1}$ ) and a good insulator ( $\sigma \sim 10^{-10} - 10^{-16} \Omega^{-1} \text{ m}^{-1}$ ). For comparison,  $\sigma$  for a semiconductor is about  $10^3 \Omega^{-1} \text{ m}^{-1}$ , while that of pure silicon is  $4 \times 10^{-4} \Omega^{-1} \text{ m}^{-1}$ .

**Characterization of MARS-1:** MARS-1, the Martian Regolith Simulant, obtained from NASA Johnson Space Center, is volcanic ash from the Pu'u Nene cinder cone on the Island of Hawaii chosen for its spectral similarity to Martian soil. Although extensive characterization of this material is available, a characterization was performed using a Scanning Electron Microscopy (SEM) and Inductively Coupled Argon Plasma Spectroscopy (ICAP) coupled with a carbon-sulfur detector. These results are compared to the Alpha Proton X-Ray Spectrometer analysis on the Sojourner rover (Table 1).<sup>2</sup> Figure 5 shows a SEM photograph of the simulant particles.

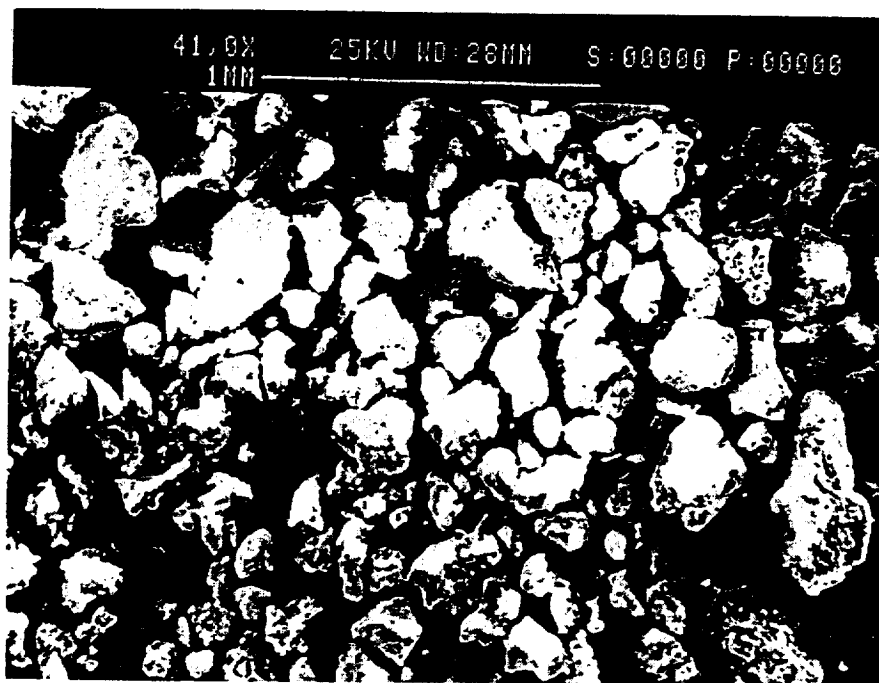


Figure 5. SEM photograph of fine MARS-1 particles.

Table 1. Elemental and Oxide Analyses in Weight %

Element	APXS	SEM	ICAP	Oxide	APXS	SEM
C	n.o.	n.o.	n.a.	Na <sub>2</sub> O	4.3	1.79
O	42.5	59.05	n.a.	MgO	8.7	1.14
Na	3.2	0.36	0.2	Al <sub>2</sub> O <sub>3</sub>	8.0	25.08
Mg	5.3	0.52	1.53	SiO <sub>2</sub>	46.1	40.22
Al	4.2	10.21	5.66	SO <sub>3</sub>	4.3	0.86
Si	21.6	13.76	n.a.	K <sub>2</sub> O	0.6	n.o.
P	n.o.	0.34	n.a.	CaO	6.3	4.08
S	1.7	0.24	n.a.	TiO <sub>2</sub>	1.1	3.53
Cl	n.o.	n.o.	n.a.	MnO	0.5	0.65
K	0.5	n.o.	n.a.	FeO	19.5	21.52
Ca	4.5	2.16	1.28	Total	99.4	100
Ti	0.6	1.58	1.37	n.o.	not observed	
Cr	0.2	n.o.	0.02	n.a.	not analyzed	
Mn	0.4	0.38	0.15			
Fe	15.2	11.4	7.83			
Ni	n.o.	n.o.	0.04			
Total	100	100	18.08			

**Electrostatic Properties of MARS-1:** To determine the electrostatic properties of MARS-1, two different methods were developed. The first method involved placing different amounts of MARS-1 under the constant electric field,  $E$ , of magnitude 200 kV/m, of a parallel-plate capacitor (figure 6).

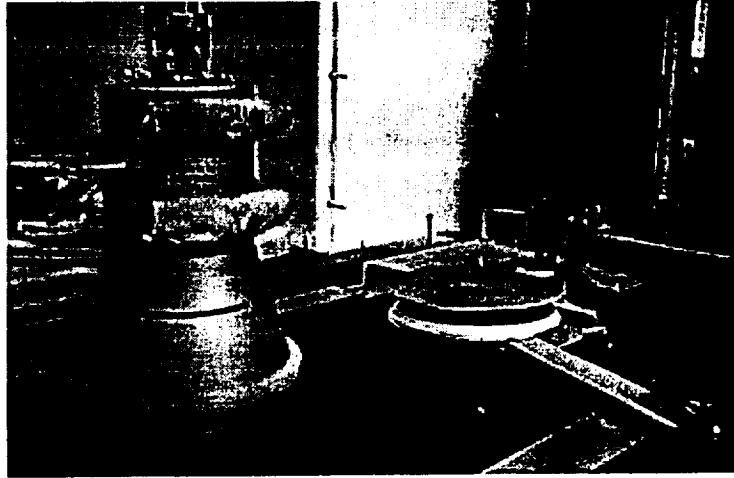


Figure 6. MARS-1 under a constant electric field.

To isolate the potential generated by MARS-1 from that of its container, materials of known (preferably low) relative electric permittivity were used. The electrical permittivity,  $\kappa$ , is related to the electric susceptibility  $\chi$ , by

$$\kappa = 1 + \chi,$$

For most dielectrics, the polarization is

$$\mathbf{P} = \epsilon_0 \chi \mathbf{E} = \epsilon_0 (\kappa - 1) \mathbf{E}$$

where  $\epsilon_0$  is the electric permittivity of free space.

The Keithley detector, the MARS-1 sample, and its container can be modeled as three parallel-plate capacitors in series (figure 6). Capacitor  $C_1$  consists of the detector's target electrode and the MARS-1 charged surface, when placed at a distance  $d_0$  from the detector. The electric potential  $\phi_0$  across this capacitor gives the charge on the polarized MARS-1. The second capacitor consists of the charged surface and the bottom of the container. This capacitor has a dielectric constant  $\kappa_M$ , which is that of MARS-1. The final capacitor consists of the two surfaces of the container, with a relative permittivity  $\kappa_c$ . The electric potential  $\phi_0$  of the charged surface can be obtained with the following expression,

$$\phi_0 = \frac{d_0 \phi}{d_0 + \frac{d_M}{\kappa_M} + \frac{d_c}{\kappa_c}}$$

Since the permittivity,  $\kappa_c$ , of the material used as container is known, the electric permittivity  $\kappa_M$  of MARS-1 needs to be measured to obtain the potential  $\phi_0$ . Since the electric conductivity of MARS-1 lies between that of a good conductor and a good insulator, its conduction current should be of the same order of magnitude as its polarization current and a measurement of its permittivity should be possible.

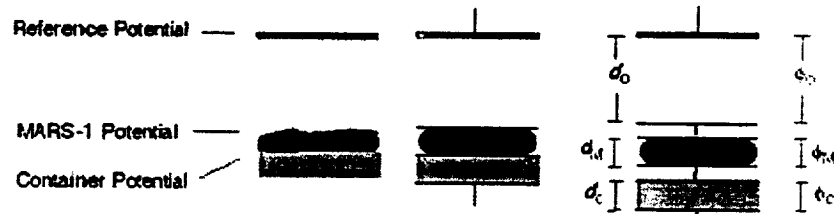


Figure 6. The detector head with its container holding MARS-1 sample can be modeled as three parallel-plate capacitors in series.

The second method involves a direct determination of the electrostatic charge on MARS-1 when placed under a constant electric field. A grain of sand of mass  $m$  and net surface charge  $q$  exposed to an electric field  $E$  between the two horizontal plates of the parallel-plate capacitor is also subject to gravitational attraction from the earth. A grain of sand accelerating across the plates due to the net force acting on it is also subject to an air resistance force and to a buoyant force. The air resistance force will retard the motion of the grain until it reaches terminal velocity,  $v$ . The equation of motion for this grain of sand is

$$qE - mg = C \eta v + B$$

where  $\eta$  is the coefficient of viscosity of the air,  $C$  is a proportionality constant that depends on the shape and size of the grain, and  $B$  is the buoyant force. The coefficient of viscosity of air is  $1.819 \times 10^{-5}$  N sec/m<sup>2</sup>. For a first approximation, the small buoyant force can be neglected and the grain of sand can be assumed to be nearly spherical. In this case,  $C$  is equal to  $6\pi r$ , where  $r$  is the radius of the grain. The equation of motion for a grain of MARS-1 under a constant electric field  $E$  is

$$qE - mg = 6\pi r \eta v$$

In this expression, all the quantities except  $q$  are known or can be measured.

The masses of twelve particles that were observed moving across a  $2.9 \times 10^5$  N/C electric field were measured. Magnifications under a scanning tunneling microscope provided the dimensions of these particles. An approximate calculation gives the value of MARS-1 charge to be of the order of 30 nC/g.

**Charging Characteristics of Materials Exposed to MARS-1:** MARS-1 was delivered to samples of different materials with the MSD and SHC set up (figure 7). A constant mass of MARS-1 was placed in the MSD and delivered to the samples with the same linear velocity. For a given RPM of the paddle wheel, the linear speed of the sample as it comes out of the MSD can be calculated with the simple expression

$$v = \pi f R / 30$$

where  $R$  is the radius of the paddle wheel and  $f$  is the RPM.



Figure 7. MSD and SHC set up with electrometer and oscilloscope in the background.

MARS-1 grains with a constant total mass of 3.0 g were launched at 2.5 m/s toward 10 different samples. The total mass was chosen to correspond to measurements of dust settling rates on Mars as measured by the Materials Adherence Experiment on the Sojourner Rover.<sup>3</sup> Table 2 shows the electrostatic potentials detected on the different samples. For comparison, we show the result of electrostatic charge and discharge (ESD) tests performed at NASA KSC on plastic films.<sup>4</sup> These tests evaluate the material's capability to develop a charge and its ability to discharge it to a grounded frame. If the electrostatic potential decays below 350 V in 5 seconds, the ESD test is said to pass.

Table 2. Electrostatic Potentials Generated on Samples

Material	$\phi$ (V)	ESD	Material	$\phi$ (V)	ESD
Teflon	-385	Fail	RCAS 2400	0	Fail
Velostat	0	Pass	Carbon Steel with Zn Primer	0	
Llualloy HST	0	Pass	Aluminum	-30	
Aclar 22A	-520	Fail	Stainless Steel	0	
FDX-2707	0	n.a.	Carbon Steel	+20	

#### 4. CONCLUSIONS

The initial tests performed indicate that the experimental designs described in this paper should provide good experimental methods to determine the electrostatic properties of the Martian Regolith Simulant and its ability to produce electrostatic charge on different surfaces. These designs still require some modifications even for experiments performed in ambient atmosphere. Much work remains to be done both in the designs themselves and in the experimental methods before these designs are ready to be used in a simulated Martian environment.

MARS-1 was found to have the same basic chemical composition as Martian soil. The SEM tests revealed that MARS-1 contained the same elements and oxides as the Martian soil samples and in very similar quantities. These results were reinforced by the ICAP tests. Although the SEM and ICAP results differ for certain elements, this difference appears to be due to the tendency of the SEM to overcorrect the amounts of lighter elements.

Electric fields appear to polarize the simulant. In addition, preliminary measurements yielded electrostatic charge densities on the simulant of the order of 30 nC/g. The source of this charge is not known at this time. More accurate measurements should be performed using the methods suggested here to determine the electric potential of MARS-1 after its exposure to electric fields and by direct determination of its electric charge. Measurements in vacuum should provide information as to the source of this charge. Once these methods are refined, experiments should be performed in low humidity, in a CO<sub>2</sub> atmosphere, and in a SME. Since the permittivity of air differs from that of empty space by 0.5% (with similar values for CO<sub>2</sub>), and this difference becomes smaller at low pressures, we expect the equipment to work without any modifications in the SME.

In our initial tests, the MSD was found to work well up to delivery speeds of 12 m/s (the maximum speed with our current system). No potentials were detected either on the paddle wheel itself or on MARS-1. The electrometer and digital oscilloscope were able to detect the rapid potential changes on a charged Styrofoam wheel on which a notch was made, when this wheel was spun with an electric drill in front of the detector. This system was determined to be able to register any electric potentials on the sand after being struck by the paddle wheel at maximum speed. However, these conclusions should not be taken as final. More careful measurements of any possible electrostatic potentials generated on the simulant by the collision with the paddle wheel are needed (using perhaps a Faraday cup to measure the charge) before more tests are run with MSD.

Once further tests determine that the MSD works as expected, some modifications are needed on the design. A better valve system is needed to start and stop the delivery of simulant to the samples. The steel paddle wheel should be replaced with one with a smaller moment of inertia to allow for smaller rotational speeds without increasing substantially the power of the motor. In addition, a motor capable of delivering simulant at 30 m/s is needed. When the system is ready to be assembled in the SME, a special motor capable of operating at low pressures will be needed.

Measurements with the Sand Blasting Attachment design were not made. The particle speed at different delivery pressures should be measured using the available strobe light at 17,000 RPM and a still digital camera at 1/30 s. This set up should provide nine exposures on a single frame. Using different color dyes on the simulant might make the grains distinguishable on the photographs.

If the simulant delivery speeds of the SBA are found to be suitable at low delivery pressures, tests should be conducted in the SME chamber at 5-9 mbar to determine the pressure variation. These tests can be made with air and without the simulant.

We expect that for small amounts of the simulant at low wind speeds, the MSD will be the preferred method. At higher simulant velocities, the SBA might perform better, provided that the pressure variation remains within tolerable limits, that is, those similar to atmospheric pressure changes on Mars during dust storms.

Once a selection of the best method of MRS delivery is made, an attempt to determine the average threshold particle speed that will cause a given sample to develop an electrostatic charge should be made. Higher particle velocities will then be used up to the maximum velocity expected on Mars. Martian wind speeds range from 2-7 m/s in the summer, 5-10 m/s in the fall, to 17-30 m/s during a wind storm (Viking Lander data). Taking into account the different molecular composition and density of the Martian atmosphere (Mars: 95% CO<sub>2</sub>,  $\rho = 0.020 \text{ kg/m}^3$ ; Earth:  $\rho_{\text{air}} = 1.21 \text{ kg/m}^3$ ) a simple kinetic theory calculation shows that the dynamic pressure of a 30 m/s (108 km/hr) wind on Mars corresponds to that of a 3.9 m/s (13.9 km/hr) wind on Earth. Since the acceleration due to gravity on Mars is  $3.69 \text{ m/s}^2$  (compared to Earth's  $9.8 \text{ m/s}^2$ ), wind speeds on Earth need to carry 2.7 times more momentum to be as effective at picking up sand from the ground as those on Mars. Thus, a 30 m/s wind will deliver as much sand as a 15.2 m/s (55 km/hr) wind on Mars.

#### REFERENCES

- [1] C.C. Allen *et al*, "Martian Regolith Simulant JSC MARS-1," Lunar and Planetary Science Conference XXX, Houston, TX, 1998.
- [2] D.R. Williams, "Preliminary Mars Pathfinder APXS Results, [http://nssdc.gsfc.nasa.gov/planetary/marspath/apxs\\_table1.html](http://nssdc.gsfc.nasa.gov/planetary/marspath/apxs_table1.html), 1998.
- [3] P.P. Jenkins, G.A. Landin, and L.G. Oberle, "Materials Adherence Experiment: Technology," 32<sup>nd</sup> Intersociety Energy Conversion Technology Conference, Honolulu, HI, 1997.
- [4] R.H. Gompf, "Physical And Chemical Test Results Of Plastic Films," NASA Technical Memorandum 103500, Kennedy Space Center, September 1988.

**1998 NASA/ASEE SUMMER FACULTY FELLOWSHIP PROGRAM**

**JOHN F. KENNEDY SPACE CENTER  
UNIVERSITY OF CENTRAL FLORIDA**

**ELCTROCHEMICAL IMPEDANCE SPECTROSCOPY OF POLYANILINE COATED  
ALUMINUM ALLOYS**

Luz Marina Calle  
Professor  
Chemistry Department  
Randolph-Macon Woman's College  
Louis G. MacDowell

**ABSTRACT**

Chromate coatings have been used for the protection of aluminum alloys for over 70 years. Interest in new protective coatings for aluminum alloys has been motivated by concern for improved protection and the environment. In the present investigation, electrochemical impedance spectroscopy (EIS) was used to investigate the corrosion inhibiting properties of a polyaniline (PANI)-based coating on aluminum alloys under immersion in aerated 3.55% NaCl. The coating was prepared by mixing a water soluble lignosulfonic acid doped polyaniline with a high solids methoxymethylated melamine resin in a 1:2 ratio. The alloys used were aluminum 2024, 6061 and 7075. Corrosion potential as well as EIS measurements were gathered at several immersion times for one week. Nyquist as well as Bode plots of the data were obtained. The PANI-coated alloys showed large fluctuations in the corrosion potential during the first 24 hours of immersion that later subsided and approached a more steady change. The EIS spectra of the PANI-coated alloys were characterized by an impedance that is higher than the impedance of the bare alloy. Changes in the EIS spectra were similar for PANI-coated aluminum alloys 2024 and 7075. There was a decrease in the rate of corrosion of these alloys during the first 24 hours of immersion followed by an increase. The rate of corrosion of PANI-coated aluminum 6061 did not show the initial decrease. The rate of corrosion of bare aluminum 2024 decreased with time of immersion. The low frequency impedance (at 0.05 Hz),  $Z_{lf}$ , for the PANI-coated alloys decreased with immersion time. Visible signs of coating failure (in the form of blisters) developed in aluminum alloys 2024 and 7075.

## AKNOWLEDGEMENT

I would like to express my deepest appreciation to Cole Bryan of the Materials Science Division and to NASA/ASEE for providing me with the opportunity to participate in the 1998 Summer Faculty Fellowship Program. My professional development and my appreciation for the space program have been enhanced considerably during the ten weeks of the fellowship. Gregg Buckingham, Dr. E. Ramon Hosler, Dr. Jane Hodges, Kari L. Stiles, and Stephanie Bealer provided the leadership that makes this program such a wonderful experience for the faculty fellows. Gregg, with his enthusiasm and interest in the program, provided us with unique opportunities to learn about NASA and the Kennedy Space Center. Ray, Kari, and Stephanie were always there for us when we needed them. I would also like to thank Dr. Robert Heidersbach for sharing his knowledge of corrosion with me. His student, James Martin, provided valuable help with computer related issues.

Scott Murray, Jennie Cummings, Peter Marciniak, Patrick Faughnan, and Steve McDanel in the Materials Engineering Section of the Materials Science Division were always there to help and provided me with a warm and friendly environment during long hours of research. Jennie and Peter contributed with their photographic skills to the project. Jennie and contributed her expertise in SEM photography. Dr. Ray Gompf, in the Physical Test Section, provided assistance with the conductivity measurements. I am specially grateful to my NASA colleague, Louis MacDowell, for introducing me to the field of corrosion research. I treasure my collaboration with him.

## ELCTROCHEMICAL IMPEDANCE SPECTROSCOPY OF POLYANILINE-COATED ALUMINUM ALLOYS

Luz Marina Calle

### 1. INTRODUCTION

Electrically conductive polymers have attracted a great deal of interest since their discovery about two decades ago. Soon after their discovery, it became clear that their unique properties could be used in several technological applications, such as the development of a new class of superconductors, light emitting plastics, polymer-based switching devices, and sensing devices. The sheer volume of fundamental and applied research in this field makes it inevitable that conductive polymers will find an increasing range of applications.<sup>1</sup>

Polyaniline (PANI) has attracted much attention as a unique electrically conductive polymer.<sup>2</sup> There have been many publications revealing the unusual electrical and optical properties of this material. The reversibility of these properties combined with its good environmental stability and its low cost of production makes this polymer suitable for the development of the aforementioned technological applications.<sup>3</sup> Another possible application of PANI involves its use in protecting metals and semiconductors from corrosion.<sup>4,5</sup> Investigations aimed at following the development of this application are justified.

Research has been ongoing for over 20 years at the Kennedy Space Center (KSC) to find coating materials to protect launch site structures and equipment from the extremely corrosive conditions present at the launch complexes. The combination of proximity to the Atlantic ocean and acidic combustion products from solid rocket boosters results in corrosive stresses unique to KSC. In the mid 1980s, researchers at KSC in Florida became interested in PANIs as protective coatings for metallic surfaces.

Several proprietary PANI-based coatings have been tested at KSC as possible coatings for the protection of steel from corrosion. Exposure of PANI-coated steel panels at the KSC corrosion test site and evaluation by electrochemical impedance spectroscopy led to the conclusion that the PANI-based coatings are not suitable as corrosion inhibitors of stainless steel.<sup>6</sup> This conclusion is supported by the work of other investigators.<sup>7</sup>

The PANI-based coatings previously tested for the corrosion protection of steel were not water soluble. Water soluble PANIs have been synthesized recently.<sup>8</sup> Water solubility has favorable economic and environmental advantages in terms of ease of processing and of reduced toxicity. Interest in new protective coatings for aluminum alloys has been motivated by concern for improved protection and the environment. The availability of the water-soluble PANI coatings lead to the idea of testing them as possible replacements for chromate coatings on aluminum alloys.

## 2. EXPERIMENTAL PROCEDURE

### Test Samples

The test samples were supplied by Dr. Tito Viswanathan from the University of Arkansas at Little Rock. Specimens were PANI-based coatings on Aluminum alloy flat panels 0.16 cm (1/16 in) x 5.0 cm (2 in) x 7.6 cm (3 in), with a mill finish, spin coated on one side. The PANI-based coating was prepared by dissolving lignosulfonic acid doped polyaniline in a high solids methoxymethylated melamine resin (Resimine 735<sup>®</sup> made by Monsanto) in a 1:2 ratio. Table 1 shows the composition and temper of the alloys used.

Table 1. Aluminum alloys

AA Designation	Composition % <sup>a</sup>							Temper
	UNS	Cr	Cu	Mg	Mn	Si	Other	
2024	A92024	0.1	3.8-4.9	1.2-1.8	0.3-0.9	0.5		T6
6061	A96061	0.04-0.35	0.15-4	0.8-1.2	0.15	0.4-0.8		T6
7075	A97075	0.18-0.28	1.2-2.0	2.1-2.9	0.3	0.40	5.1-6.1Zn	T73

<sup>a</sup> Single values are maximum values

The panels were photographed for documentation purposes prior to any testing or exposure. Coating thickness measurements were performed using a Positector<sup>®</sup> 6000 coating thickness gauge and found to be in the range between 0.3 and 1 mils (8  $\mu$ m and 30  $\mu$ m). The conductivity of the coatings was measured with a 500 V megohmmeter with cylindrical 5 pound (454 g) weights, 2.5 in (6.4 cm) in diameter, according to NFPA-99 (National Fire Protection Association floor test) and found to be in the range between 180-250 kohms.

### Corrosion Potential Measurements

Corrosion potential measurements were performed using a system manufactured by EG&G Princeton Applied Research Corporation. The system used includes: (1) the Model 273 Computer-Controlled Potentiostat/Galvanostat, (2) the Model 5210 Computer-Controlled Lock-In Amplifier, and (3) the Model 352/342 SoftCorr<sup>™</sup> II Corrosion Measurement Software. The electrochemical cell included a Ag/AgCl (silver/silver chloride) electrode, a platinum counter electrode, the sample working electrode, and a bubbler/vent tube. The flat specimen holder in the electrochemical cell is designed such that the exposed surface area is 1 cm<sup>2</sup>. Corrosion potential values were gathered for one hour in aerated 3.55% NaCl before the first set of EIS measurements was obtained. Subsequent corrosion potential values were collected before each set of EIS measurements. All solutions were prepared using deionized water. Aeration with dry air was maintained throughout the tests.

## Electrochemical Impedance Measurements

A Model 378 Electrochemical Impedance system manufactured by EG&G Princeton Applied Research Corporation was used for all EIS measurements. The system includes: (1) the Model 273 Computer-Controlled Potentiostat/Galvanostat, (2) the Model 5210 Computer-Controlled Lock-In Amplifier, and (3) the Model M388 Electrochemical Impedance Software including circuit modeling routines. Data were gathered in the frequency range from 100 kHz to 0.01 Hz. The AC amplitude used for the experiments was 10 mV. Each sample was studied at various immersion times in aerated 3.55% NaCl for one week.

Bode magnitude plots of the data (showing the logarithm of the modulus of the impedance,  $\log |Z|$ , as a function of the logarithm of frequency and phase angle, alpha in degrees, as a function of the logarithm of frequency) as well as Nyquist plots (showing the negative of the imaginary component of impedance as a function of the real component of the impedance) were obtained for each coating.

## 3. RESULTS AND DISCUSSION

### Corrosion Potential Measurements

Corrosion potential values gathered during the hour immediately preceding the first set of EIS measurements for each PANI-coated alloy indicated that an hour was sufficient to allow the potential to equilibrate. Subsequent values of the corrosion potential were obtained immediately before each set of EIS measurements was obtained. Figure 1 shows the change in corrosion potential with immersion time for all PANI-coated alloys, identified as (c), and for bare aluminum 2024 alloy, identified as (u). Due to time limitations, corrosion potential measurements were not collected on the other bare alloys but they were assumed to follow similar trends based on the fact that their corrosion potentials are similar ( $-0.77V_{Ag/AgCl}$ ,  $-0.79V_{Ag/AgCl}$ , and  $-0.80V_{Ag/AgCl}$  for aluminum 2024, 6061, and 7075 respectively).<sup>9</sup> The PANI-coated alloys showed large fluctuations in the corrosion potential during the first 24 hours of immersion that later subsided and approached a more steady change. Large fluctuations in the corrosion potential may be indicative of electrochemical processes that result in a more stable configuration of the corroding specimen. A gradual increase in corrosion potential with immersion time was expected if the coating encouraged slow but uniform (i.e., pit free) growth of the aluminum oxide. This behavior was observed for PANI-coated Al 6061 and Al 2024.

### Electrochemical Impedance Spectra

Figure 2 shows representative impedance spectra (Bode format: The phase angles have been omitted for clarity) for the coated alloys (c) and bare (u) aluminum 2024 alloy after 24 hours of immersion in 3.55% NaCl. The impedance of the coated alloys is greater than the impedance of the bare alloy. The low frequency impedance values for aluminum 6061, 2024, and 7074 are in the order of  $10^8$ ,  $10^5$ , and  $10^5 \Omega\text{cm}^2$  respectively. Low frequency impedance for chromate

conversion coatings on aluminum alloys 6061, 2024, and 7075 after 3 hours of immersion in aerated 0.5 M (3%) NaCl have been reported as being in the order of,  $10^7$ , and  $10^4, 10^4 \Omega\text{cm}^2$  respectively.<sup>11</sup> These values are lower than  $10^{10} \Omega\text{cm}^2$  which is the value expected of an excellent barrier coating.<sup>12</sup> It can be seen on Figure 2 that PANI coated aluminum alloy 6061 has a higher impedance than the other two alloys. This is consistent with the fact that the intrinsic corrosion resistance of the alloy substrate is in the order: 6061>7075>2024.<sup>13</sup>

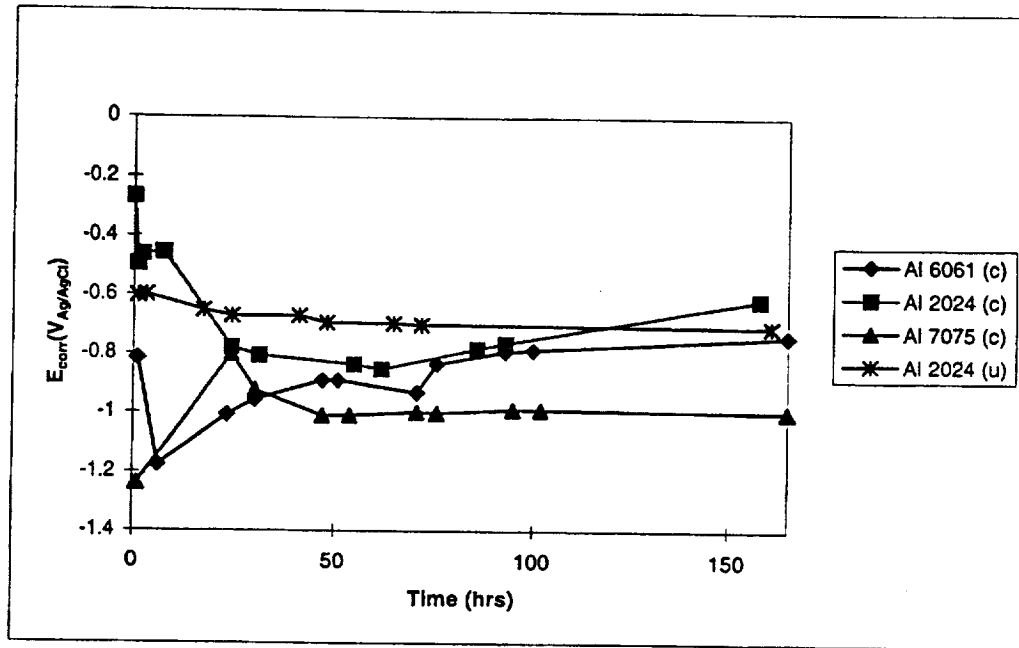


Figure 1. Corrosion potential as a function of immersion time in 3.55% NaCl

Figure 3 shows impedance spectra (Nyquist plot) for bare aluminum 2024 as a function of immersion time in 3.55% NaCl. Although the high frequency semicircle is not complete, it can be concluded that an extrapolation of the curves to obtain the diameter of the semicircles would yield values that increase with immersion time. The diameter of the semicircle represents the charge transfer resistance which is inversely related to the rate of corrosion. The Nyquist plots indicate that the rate of corrosion of the bare alloy decreases as the time of immersion increases.

EIS spectra revealed that PANI-coated aluminum 2024 and PANI-coated aluminum 7075 had a rate of corrosion that decreased during the first 24 hours of immersion. This initial trend was reversed to an increase in the rate of corrosion for subsequent immersion times. It can be hypothesized that the initial decrease is due to the formation of a protective layer of aluminum oxide that breaks down after 24 hours of immersion. The rate of corrosion of PANI-coated aluminum 6061 increased with immersion time.

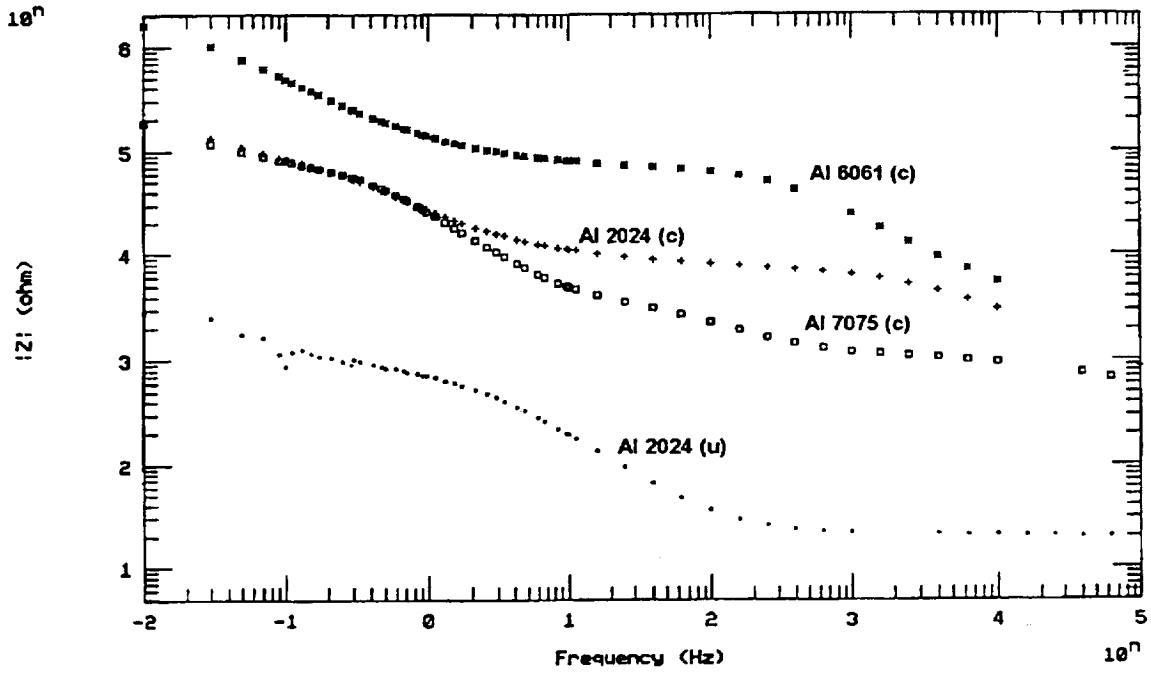


Figure 2. Bode plots of PANI-coated aluminum alloys and of bare aluminum 2024 alloy.

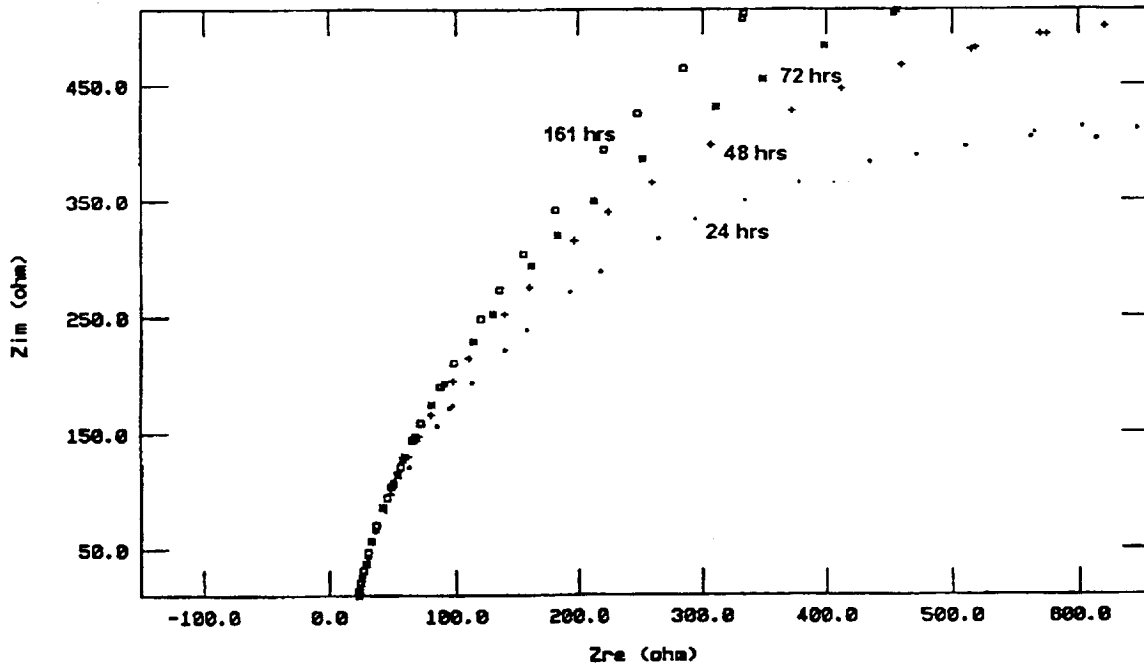


Figure 3. Nyquist plots for aluminum 2024 at different immersion times in 3.55% NaCl

## Electrochemical Impedance Measurements

The low-frequency impedance,  $Z_{lf}$  (determined from data at 0.05 Hz), has been proposed as the optimal EIS parameter to evaluate the performance of corrosion inhibiting coatings on aluminum.<sup>14</sup> The impedance at this frequency includes the response of the coating as well as part of the response of the oxide and/or corrosion product in the pores at the metal interface.  $Z_{lf}$  reflects the condition of the substrate as well as that of the coating. Although the  $Z_{lf}$  values do not give information about how a coating degrades (i.e., water uptake, blistering, etc.), they correlate with coating performance. Figure 4 shows the variation of  $Z_{lf}$  with immersion time for the PANI-coated (c) as well as the bare (u) aluminum alloys. PANI-coated aluminum 6061 and aluminum 2024 showed a large decrease in  $Z_{lf}$  while PANI-coated aluminum 7075 exhibited values that were slightly higher, by an order of magnitude, than those of the bare aluminum alloy. It should be noticed that the initial values of  $Z_{lf}$  follow the trends in coating thickness which decreased from 30  $\mu\text{m}$  for PANI-coated aluminum 6061 to 9  $\mu\text{m}$  for PANI-coated aluminum 2024 to 7  $\mu\text{m}$  for PANI-coated aluminum 7075. For a coating to be an effective inhibitor of corrosion in aluminum, its  $Z_{lf}$  value should increase with immersion time. None of the PANI-coated aluminum alloys included in this investigation exhibited this behavior. Visual signs of coating failure in the form of blisters were more pronounced for PANI-coated aluminum 7075 than for PANI-coated aluminum 2024. No visual evidence of blistering was observed for PANI-coated aluminum 6061.

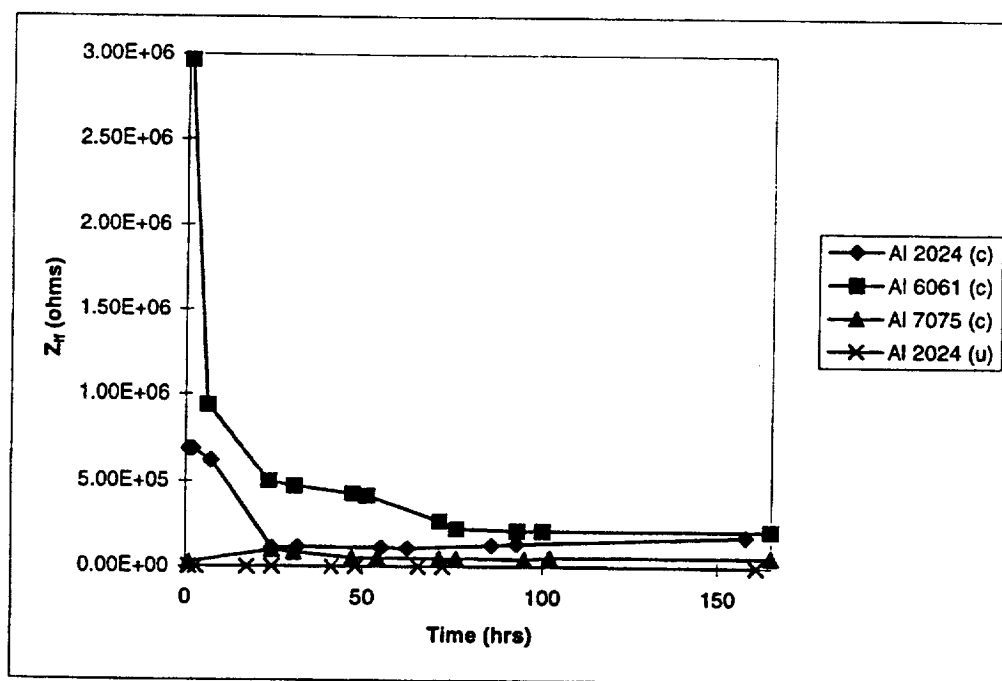


Figure 4. Low frequency impedance,  $Z_{lf}$ , as a function of immersion time in 3.55% NaCl

#### 4. CONCLUSIONS

PANI-coated aluminum alloys 2024, 6061, and 7075 exhibit a variation in the corrosion potential with immersion time that is different from what is obtained for the bare alloy. The PANI-coated alloys exhibit large fluctuations in the corrosion potential during the first 24 hours of immersion. After 24 hours, PANI-coated aluminum 2024 and 6061 exhibited the gradual increase in corrosion potential expected of a coating that encourages the formation of a defect free aluminum oxide layer.

The low frequency impedance values for the PANI-coated aluminum alloys were lower than what is expected for an excellent barrier coating but consistent with what other researchers have reported for chromium conversion coatings on the same alloys under somewhat similar conditions.

Different trends in the variation of the rate of corrosion with immersion time were observed for the PANI-coated alloys. EIS revealed a decrease in the rate of corrosion during the first 24 hours of immersion followed by an increase for PANI-coated aluminum 2024 and 7075. The rate of corrosion of PANI-coated aluminum 6061 increased with immersion in the electrolyte. This behavior is in contrast to the decrease in the rate of corrosion with immersion time observed for the bare aluminum 2024 alloy.

Bode plots of the EIS data revealed that as the time of immersion increased, the low frequency impedance for the PANI-coated aluminum alloys decreased. The magnitude of the decrease was correlated to the thickness of the coating. None of the PANI-coated alloys exhibited the increase in  $Z_{if}$  expected of a coating that is effective as a corrosion inhibitor.

Additional experiments including exposure at the beach corrosion test site and EIS measurements using multiple samples of each coating prepared in such a way that all panels have the same thickness are needed in order to confirm the above conclusions. Analysis of the metal substrate using metalography is suggested in order to look for the presence of pitting.

#### REFERENCES

- [1] S. Haddlington, *Chemistry and Industry* 1 (1995): p. 11.
- [2] M. Morita, *Journal of Applied Polymer Science* 52 (1994): p. 711.
- [3] G. D'Aprano, M. Leclerc, G. Zotti, G. Schiavon, *Chem. Mater.* 7 (1995): p. 33.
- [4] G. Mengoli, M.M. Musiani, B. Pelli, E. Vecchi, *J. Appl. Polym. Sci.* 28 (1983): p. 1125.

- [5] R. Noufi, A. J. Nozik, J. White, L.F. Warren, *J. Electrochem. Soc.* 129 (1982): p. 2261.
- [6] L.M. Calle, *Accelerated Testing of Coatings Containing Polyaniline by Electrochemical Impedance Spectroscopy*, 1997 NASA/ASEE Research Reports NASACR-207197, E.R. Hosler and G. Buckingham editors, January, 1998.
- [7] M.M. Attar, J.D. Scantlebury, *Corrosion science*, (submitted for publication).
- [8] M. Sudhakar, "Synthesis and Characterization of Lignosulfonic Acid Doped Polyaniline" (Master's Thesis, University of Arkansas at Little Rock, 1998).
- [9] *ASM Metals Handbook*, volume13, p.584, 1987.
- [10] P.C. Su and O.F. Devereux, *Corrosion*, 54 (1998): p. 419.
- [11] J.E.O. Mayne, and D.J. Mills, *J. Oil & Colour Chemists Assoc.*, 58 (1975) p. 155.
- [12] R. G. Buchheit, M.D. Bode, and G.E. Stoner, *Corrosion*, 50 (1994): p. 205.
- [13] J.E. Hatch, ed., *Aluminum Properties and Physical Metallurgy* (Metals Park, OH: ASM International (1986), p. 301.
- [14] J.A. Grandle and R.S. Taylor, *Corrosion*, 50 (1994): p. 792.

# 1998 NASA/ASEE SUMMER FACULTY FELLOWSHIP PROGRAM

JOHN F. KENNEDY SPACE CENTER  
UNIVERSITY OF CENTRAL FLORIDA

## *Capacity Planning for Future NASA-KSC LAN and MAN Networks*

Kenneth J. Christensen  
Assistant Professor  
Department of Computer Science and Engineering  
University of South Florida

KSC Colleagues: John Schnitzius (NASA) and Chris Kerios (Dynacs Engineering)

### ABSTRACT

NASA-KSC is in the middle of a transition to a consolidated networking infrastructure based on Asynchronous Transfer Mode (ATM) switching with a Synchronous Optical Network (SONET) Physical Layer. Other technologies, including Gigabit Ethernet and Internet Protocol (IP) switching, are also being studied. Capacity planning is necessary to design cost-effective networks and predict their future performance. Commercial tools for capacity planning are expensive (\$30K to \$100K) to purchase and require trained personnel to operate. This paper describes research conducted during the summer of 1998 at NASA-KSC in the Advanced Networks Development (AND) group within the Development Engineering (DE) Directorate to develop capacity planning requirements, evaluate tools, and develop a strategy. The requirements for capacity planning were developed and documented in a formal requirements document to be used for procurement of tools. Several commercial tools were evaluated via software trial programs and on-site vendor demonstrations. Direct assistance was given to AND engineers to develop an overall strategy presented to NASA technical contacts. This work will enable the AND group to procure capacity planning tools and begin modeling and baselining the current network. The final result of a consolidated networking infrastructure will be cost savings by 1) increased efficiency in the use of the existing in-ground cabling plant, and 2) reduced operations and maintenance requirements. The resulting networking infrastructure will be state-of-the-art and will be able to support future applications, including real-time voice and video distribution.

# Capacity Planning for Future NASA-KSC LAN and MAN Networks

Kenneth J. Christensen

## 1. Introduction

NASA-KSC is in the middle of developing a consolidated networking infrastructure based on Asynchronous Transfer Mode (ATM) and other networking technologies. The KSC Development Engineering (DE) directorate is accountable for this project which is described in [6]. Within the DE directorate, the Advanced Networks Development (AND) group is examining new networking technologies and developing the design specification. The goal of the consolidated networking infrastructure is to reduce the number of disparate networks at KSC and thus achieve cost savings by 1) increased efficiency in the use of the existing in-ground cabling plant, and 2) reduced operations and maintenance requirements. In addition, a state-of-the-art networking infrastructure will be able to support future requirements such as combined data, video, and voice. A key component in the planning, design, and deployment of any large network is capacity planning. The goal of capacity planning is to deliver the most cost-effective network designs while ensuring that performance levels will meet specified service requirements. While very valuable, building experimental test networks in a laboratory setting is expensive and limited in size and scope. For example, the entire KSC transmission system cannot be duplicated in a laboratory. Thus, a capacity planning tool for modeling of existing and future networks is needed to validate proposed designs and design-changes.

The goals of this research, funded by the NASA/ASEE Summer Faculty Fellowship program and conducted between May 27 and July 31, 1998, were:

1. Develop requirements for capacity planning at NASA-KSC
2. Evaluate vendor capacity planning tools
3. Educate Dynacs Engineering communications engineers in the area of capacity planning
4. Assist in preparing a strategy for capacity planning at NASA-KSC
5. Develop a long-term research relationship with NASA-KSC

The key research deliverable was a formal requirements document, see [14]. Research activities included information gathering, evaluation of vendor tools, initial modeling of the proposed ATM Transmission System (ATXS) network design with these tools, and many focused discussions with key AND development engineers.

The remainder of this paper is organized as follow. Section 2 is a brief overview of capacity planning. Section 3 is an overview of the AND proposed ATXS network design. Section 4 describes the steps in the capacity planning process and KSC requirements for a capacity planning tool. In Section 5 the evaluation results for three key vendor tools are described. Section 6 is a summary and describes future work.

## 2. Overview of Capacity Planning

Planning is the process of defining methods to achieve a goal. Capacity planning of computer systems is the process of predicting the future performance of a system. Specifically, capacity planning intends to predict when performance will drop below a desired level of service. Key service level measurements for computer networks include packet delay, packet loss, and the reliability of connections. Typically, service levels are specified in bounds, for example, 95% of all packets must be delivered in less than 2 milliseconds. Other measures include mean (average) and variance of delays. Inputs to the capacity planning process are the *workload* of the system and its expected evolution over time, the *system parameters*, and the desired *service levels*. In a computer network, the workload is the traffic carried by the network generated by network applications such as WWW, FTP, and email. The system parameters are the design of the network including its links and components. The output of the capacity planning process is a *prediction* of when saturation will occur and *cost-effective alternatives*. Saturation is defined as the system performance falling below a formally specified Service Level Agreement (SLA). Figure 1 shows the capacity planning process (reference [9] describes the capacity planning process in detail).

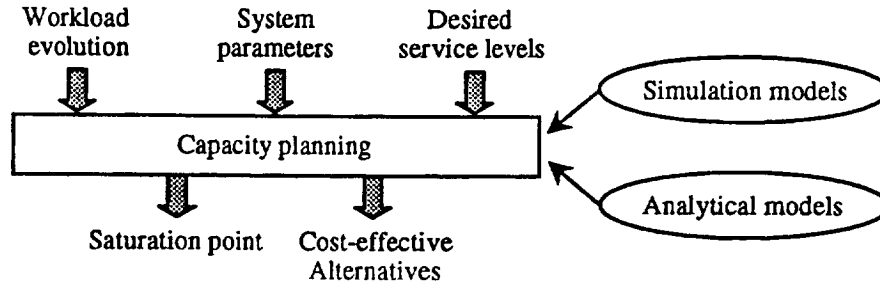


**Figure 1** - The capacity planning process (from [9])

For any moderately large or complex system it is not possible to physically build and test design options, hence modeling is required. Capacity planning uses both simulation and analytical modeling methods. Analytical methods use “math formulas” to model and solve for the performance measures of a system. For computer networks, analytical methods are rooted in queueing theory and require simplifying assumptions to build tractable models. Reference [5] is the classic reference on queueing theory. Simulation methods use discrete event simulation programs executed on a computer to find statistical approximations for the performance measures of a system. Reference [7] is the classic reference on discrete event simulation. One trade-off between analytical and simulation methods is speed versus accuracy. Simulation models require much longer execution time than analytical models. However, simulation models do not require many of the simplifying assumptions of analytical models. Another trade-off is correctness, given that the underlying assumptions are accepted, an analytical model can be formally proved correct. However, a simulation model consist of thousands to millions of lines of code and is hence almost certain to contains “bugs”, some of which may affect the accuracy of the output. Table 1 shows the “pluses” and “minuses” of simulation and analytical modeling.

Criterion	Analytical modeling	Simulation modeling
Time to build model	Usually very quick	Can take a long time to program
Time to execute model	Very fast (seconds or minutes)	Slow (hours or days)
Correctness of model	Can be proven	Cannot be proven
Accuracy of results	Low given need for assumptions	High if model and input is correct

**Table 1** - Trade-offs between analytical and simulation modeling

The accuracy of results for any model is no better than the accuracy of the input. Given first order approximations for input, the output of both an analytical and simulation model will be poor. This last fact is very important, if many assumptions must be made on the input to a model then faster analytical modeling may be better than simulation modeling since one can study many design options with an analytical model in the same amount of time that only one option can be studied with simulation methods.

Computer networks are modeled as queueing systems. The buffers in network components such as routers and switches are packet (or cell for ATM) queues. Delay in a network occurs when packets are forced to wait for service in these buffers. Packet loss occurs when these buffers overflow due to packet arrival rates temporarily exceeding the service rate. Packets arrive with probabilistically distributed interarrival times, often in bursts. A packet is serviced when it is transmitted on an outgoing link. Packet service time is a function of the packet size and the data rate of the outgoing link. For example, a 1500 byte packet has a 1.2 millisecond service time on a 10-Mbps Ethernet. Both packet interarrival times and packet sizes can be modeled with probability distributions. Figure 2(a) shows job (e.g., packet) arrivals over time and Figure 2(b) a single server queue.

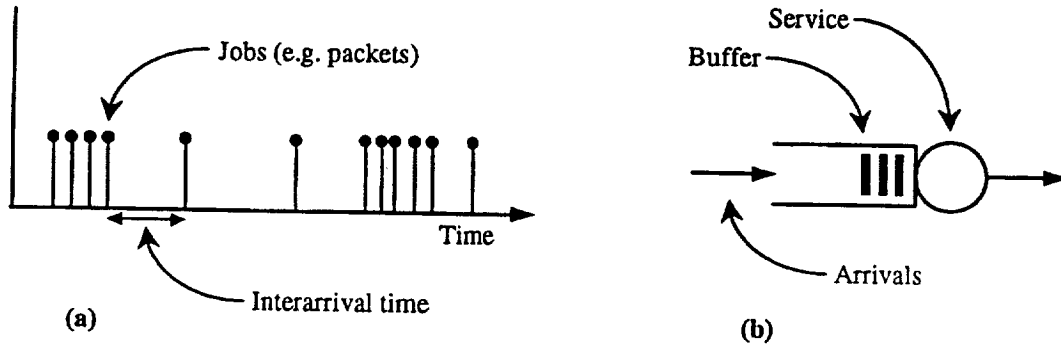


Figure 2 - (a) Job arrivals over time and (b) a single server queue

Figure 3 shows the behavior of a single server queue given random and bursty packet arrival streams and deterministic service times. The results of Figure 3 were generated using a simulation model. Burstiness can be informally defined as how much the arriving packets are clumped together. A more formal definition of the burstiness of a packet arrival stream is the coefficient of variation ( $CoV$ ),

$$CoV = \frac{\sqrt{\text{Variance of packet interarrival times}}}{\text{Mean of packet interarrival times}}, \quad (1)$$

where the mean of packet interarrival times is simply the reciprocal of the packet arrival rate. Determining the variance of packet interarrival times requires analyzing packet traces of network traffic. Packet traces contain time-stamps for received packets. It is from these time-stamps that the variance of packet interarrival times is determined. Tools to determine the  $CoV$  of filtered packet traces can be found at [16]. For deterministic traffic the  $CoV = 0$ , for random (or Poisson) traffic the  $CoV = 1$ , and an increasing burstiness is indicated with a higher value of the  $CoV$ . Note that as the arrival process increases in burstiness, the saturation knee occurs at lower utilization levels. The knee effect is common to all queueing systems. The challenge of capacity planning is to determine at what utilization level this knee will occur. For the queue of Figure 3, given an SLA corresponding to a delay of 10 jobs in system, the queueing system with random arrivals saturates at about 95% utilization, the extremely bursty system at about 70%. This example shows that knowledge of only means (utilization equals the mean arrival rate divided by the mean service rate) is not sufficient, knowledge of the variability of the packet arrival and service processes is also needed to predict where the saturation knee will occur.

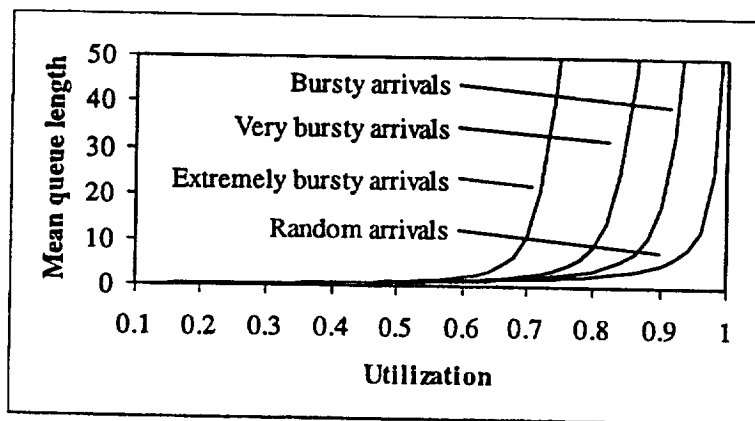


Figure 3 - Behavior of a single server queue showing the knee effect and the significance of variability

### 3. Overview of the AND Proposed ATXS Design

The AND project has been organized to examine new technologies that could strategically benefit both present and future missions at NASA-KSC. Benefits are to include both cost reduction of existing networks and the provisioning of new services such as voice and video. A key technology expected to enable these benefits is Asynchronous Transfer Mode (ATM). ATM is a packet switched technology based on fixed-size packets called cells and is covered in [4]. All major networking vendors, including Cisco, 3COM, and IBM, support ATM. Emerging technologies that may supplement and/or replace ATM include Gigabit Ethernet and switched Internet Protocol (IP). Being able to accommodate changes in both requirements and technologies is a key need for future network designs. Figure 4 shows a top-level view of the AND proposed KSC ATXS network. The key components for this network include the ATM enterprise switches at an approximate cost of \$220K each and the facility and edge switches at a lower cost. Within a typical facility, there may be several networking technologies, including Ethernet and Token Ring, that will need to be connected to the ATXS.

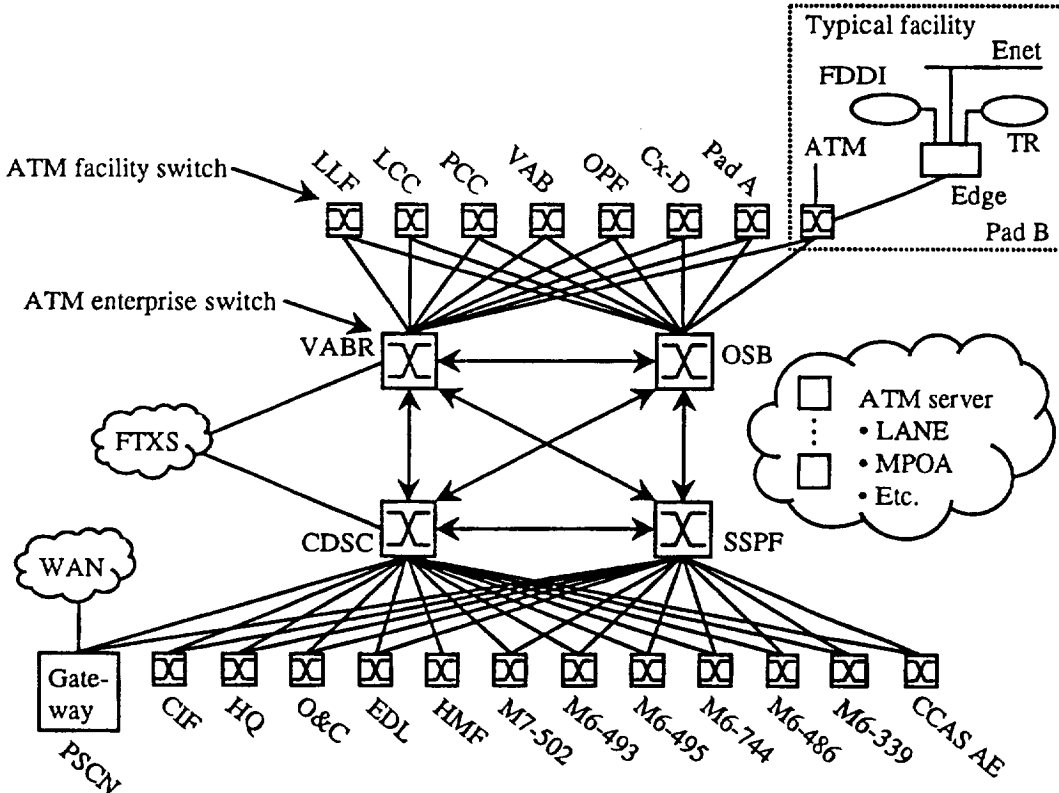


Figure 4 - Proposed ATXS network

The current networks at NASA-KSC include many 10 and 100-Mbps Ethernets, a few 16-Mbps Token Ring networks, and a 100-Mbps Fiber Distributed Data Interface (FDDI) backbone - the FDDI Transmission System (FTXS). The FTXS is well suited to carrying traditional data traffic, but not future voice and video traffic. In addition, the FTXS is limited to 100-Mbps. The proposed ATXS would initially parallel the FTXS and then in the near future replace it. The parallel FTXS is shown in Figure 4. Key to ATXS succeeding as a replacement to FTXS, and also being able to provision new services, is the correct operation of ATM traffic management (see [17]) features in the ATM switches and ATM-attached hosts.

## 4. Capacity Planning at NASA/KSC

Capacity planning is a process that is followed as part of the overall design and deployment of high-performance networks. A capacity planning tool for modeling of existing and future networks is needed to validate proposed AND network designs and design changes. This section describes the capacity planning process and the requirements for a tool.

### 4.1 Steps in capacity planning for NASA-KSC networks

The key steps in the capacity planning of a high-performance network involve automatically discovering the topology of the existing network, discovering the traffic flows, and then modeling the network topology and traffic flows. For a new network design, the topology and traffic flows are manually constructed and/or added to a model of an existing network. More formally, the steps are:

1. Discover the existing network topology and components
2. Collect traffic traces and characterize the existing traffic flows on all subnetworks
3. Build model of network and its traffic from (1) and (2) above
4. Project changes in network topology, protocols, components, and traffic
5. Execute the model, collect results, and derive insights
6. Repeat (4) and (5) for design iterations and "what if" scenarios

The network topology can be derived from a network management tool such as HP OpenView (see [3]). The traffic flows can be derived from traffic trace files collected from tools such as the Network Associates Sniffer (see [12]) and standard RMON probes (see [18]). The traffic flows are the streams of packets generated by network applications including email, WWW, and FTP. Traffic flows must be collected systematically on all subnets and across different times of the day. The packet streams are "characterized" by packet size and interarrival times. This characterization process is very important to the capacity planning process. As demonstrated in Section 2, an incorrect characterization of an input process will result in an incorrect determination of the saturation point.

### 4.2 Requirements for a capacity planning tool for NASA-KSC

The following list summarizes the full set of requirements listed in [14]. These requirements pertain to a capacity planning tool to be used by AND to validate the ATXS design.

- a. Modeling of networks based on existing and future ANSI, ATM Forum, Bellcore, IEEE, ITU, IETF, ISO, and vendor protocols, standards, and specifications.
- b. Inclusion of typical components (e.g., ATM switches and IP routers) with custom and vendor specific performance and reliability characteristics, and applications (e.g., Web, FTP, telnet, email, database transactions, voice, and video).
- c. Selective output of throughput and response time at the application layer, throughput, delay, and loss at the packet and cell levels, and utilization and uptime at the component and link levels. This is to include validation of compliance to Quality of Service (QoS) and SLA specifications.
- d. Model building by automatic discovery of topology, components, and traffic flows. Also, manual model building using "drag-and-drop" GUI-based methods using standard components with vendor-specific performance characteristics and customized generic components. Figure 5 shows the GUI interface of the tool.
- e. Simulation and analysis output generated quickly, repeatably, and with high accuracy.
- f. Model verification and validation based on calibration with real network data collected with NMP-included and/or HP OpenView, Cisco NetFlow, Network Associates Sniffer, and RMON probe performance monitoring tools.
- g. Training for an expected user population of network engineers and not specifically "performance modeling experts".
- h. Execution on readily available Sun Solaris and/or Windows 95/98/NT platforms.

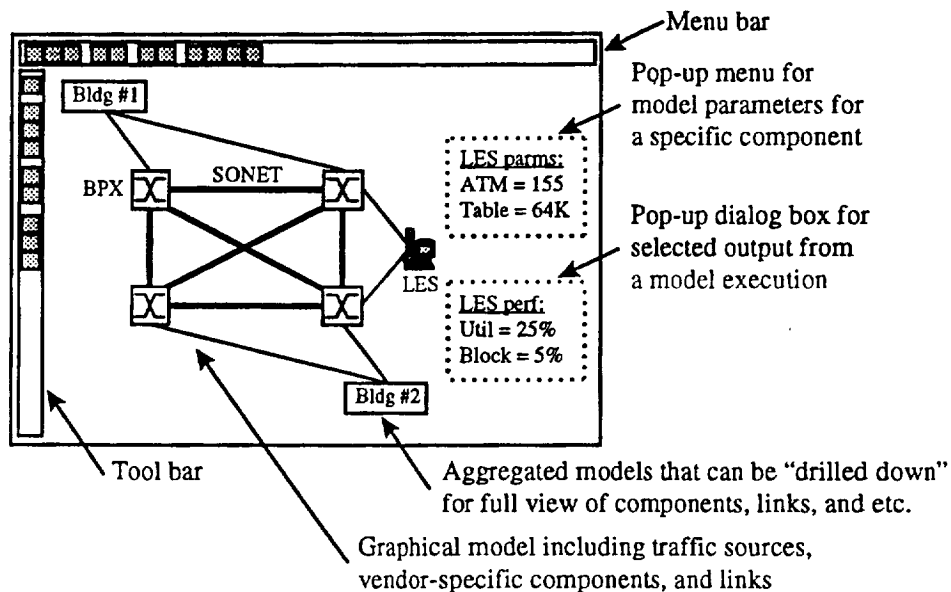


Figure 5 - Graphical User Interface (GUI) for a capacity planning tool

## 5. Evaluation of Vendor Capacity Planning Tools

This section contains evaluations of network capacity planning tools from three major vendors. The tools are, CACI COMNET and Predictor (see [1]), MIL3 Modeler and Planner (see [10]), and Make Systems NetMaker (see [8]). Each of these vendors were invited to KSC to present and demonstrate their modeling products. In the case of CACI COMNET and Predictor and MIL3 Modeler and Planner, trial versions of the software were installed and tested. MakeSystems did not offer a copy of their NetMaker product for testing. In addition to direct evaluation of vendor products, trade press evaluations were studied (see [15]) and an informal survey of other NASA sites and their use of modeling tools was made. NASA/GSFC had formally evaluated modeling tools in 1991 and 1994, a copy of their evaluation document was obtained (see [13]). Previous to summer 1998, Cadence Bones, Stanford Telecom NetCoach, and Cisco NetSys were evaluated by Dynacs Engineering. Their functionality was found to be limited and no further evaluations of these products were deemed necessary.

### 5.1 Evaluation of CACI COMNET III 2.0 and Predictor 1.1

CACI Products Company was founded in 1962 with strong associations with the RAND corporation. CACI International, the parent company of CACI Product Company, is a government contractor in a wide range of software related projects. CACI Products Company offers a range of modeling products including COMNET III for simulation modeling, Predictor for analytical modeling, and Profiler for characterizing network usage by applications and users. The COMNET III and Predictor products include a tool called the Baseline used to import topology and traffic data from a wide range of vendor products (including HP OpenView and Network Associates Sniffer). CACI promotes the use of the Predictor tool for an overall view of network performance, and then the use of COMNET III for detailed simulation of specific areas of greater interest. The Predictor tool solves for network utilization and delay based on projected increases and decreases in application or protocol usage on a daily, weekly, or monthly basis. Due to the limitation of analytical modeling, detailed analysis of ATM QoS cannot be done with Predictor. However, COMNET III supports ATM traffic management features and validation of QoS. Figure 6 shows a model of the proposed ATXS built with Predictor. COMNET III and Predictor were demonstrated to Chris Kerios and Ken Christensen on July 24, 1998 by Eric Chapman and John Marciniak (both from CACI Products Company).

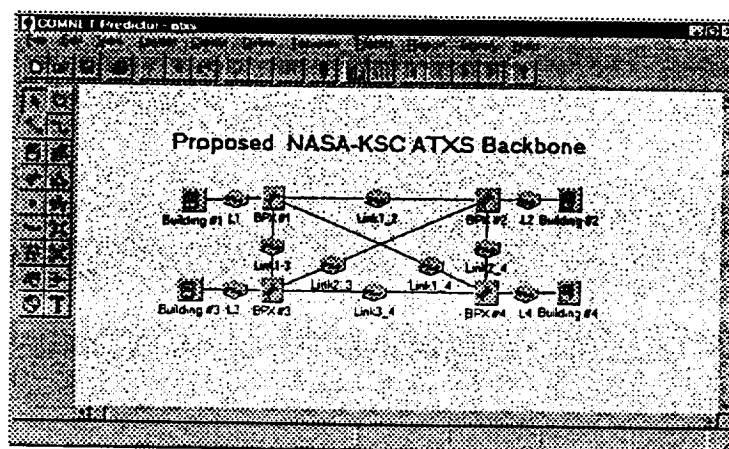


Figure 6 - A first-pass model of the proposed ATXS built with CACI Predictor

### 5.2 Evaluation of MIL3 Modeler 4.0 and Planner 5.0

MIL 3, Inc. was founded in 1987 as a spin-off from a Massachusetts Institute of Technology (MIT) project that pioneered the use of object oriented simulation modeling. MIL 3 has two products for modeling of networks - OPNET Modeler and Planner. Modeler claims to be the first tool to focus on network simulation. Modeler is a programming-oriented tool that allows the user to create new protocols or modify existing protocols (e.g., the packet bursting changes to IEEE 802.3 CSMA/CD for Gigabit Ethernet were originally modeled with OPNET, see [11]). Planner is a front-end to Modeler than eliminates the need for programming and otherwise simplifies modeling. For capacity planning of networks based on standard protocols and vendor components, the ability to modify protocols is not necessary. The Planner product is a recent addition to the MIL 3, Inc. product set and, it appears, does not have the strong user base as does Modeler. The MIL 3 company has established strong ties with Hewlett Packard and supports topology import from OpenView and traffic import from NetMetrix probes. Traffic import from Network Associates Sniffer and RMON probes is not easily possible. No analytical modeling capability is offered in any of the MIL 3 products. Overall, Modeler is best suited to component and protocol researchers and designers. The applicability of Planner to capacity planning for large networks is not yet established. The forte of MIL 3 products is in very detailed modeling of network protocols. Modeler 4.0 was demonstrated to Chris Kerios, Ken Christensen, and Kumar Singh on July 6, 1998 by Eric Martin (from MIL 3, Inc.). Planner was not demonstrated during the July 6, 1998 meeting, but was made available for trial evaluation on July 27, 1998.

### 5.3 Evaluation of Make Systems NetMaker 2.7

MakeSystems was founded in 1987 and has been supported by the Defense Information Systems Agency (DISA). DISA has funded MakeSystems \$13.0 million for development of capacity planning tools for the worldwide Defense Information System Network (DISN) (see [2]). MakeSystems has developed a suite of tools, called NetMaker 2.7, to support Network Resource Planning (NRP). NRP is a cyclical process of discovering network components and topologies, baselining network usage, profiling application use of network resources, simulating to predict network behavior, analyzing network responses to failures or traffic fluctuations, and designing cost effective and reliable network topologies. This includes tools for topology design and evaluation of tariffing options. NetMaker 2.7 uses analytical methods to solve for utilization and delays in a network. Simulation methods are used to determine the routes within a network for individual source-destination traffic flows. Without simulation capabilities for determining network delays, detailed analysis of network behaviors cannot be done. For example, determining the time required for a network to recover from a failure cannot be determined with the NetMaker 2.7. NetMaker98, scheduled for release in October 1998, will emphasize modeling for SLA conformance and includes support for ATM QoS measures. NetMaker 2.7 was demonstrated to Chris Kerios and Ken Christensen on July 7, 1998 by Don Feld and Larry Hallman (both from Make Systems).

### 5.4 Summary of Evaluations

Table 2 contains a summary of the evaluation of the CACI COMNET III 2.0, CACI Predictor 1.1, MIL 3 Planner 5.0, and MakeSystems NetMaker 2.7 capacity planning tools. The MIL 3 Modeler is covered by the Planner, as discussed in Section 5.2 of this paper. The identified features in the criterion column are those features necessary to meet the requirements specified in [14] and summarized in Section 4 of this paper. Support for a criterion are graded as “(-)” for poor and “(+)” for excellent.

Criterion	CACI COMNET	CACI Predictor	MIL 3 Planner	MakeSys NetMaker
Topology and traffic import				
Topology import from OpenView	Yes	Yes	Yes	Yes
Traffic import from Sniffer and RMON	Yes	Yes	No	Yes
Library of common network protocols				
ATM CBR, VBR, ABR, and UBR	Yes	No	Yes (-)	No
ATM TM 4.0 QoS metrics	Yes	No	Yes (-)	No
ATM LANE	No	No	Yes	No
ATM MPOA	No	No	No	No
Gigabit Ethernet	No	No	Yes	No
IEEE 802.1P and 802.1Q	No	No	No	No
RIP, OSPF, and IGRP routing	Yes	Yes	Yes	Yes
TCP/IP	Yes	No	Yes	No
Library of vendor components				
Cisco routers and switches	Yes	Yes	Yes (-)	Yes (-)
Fore switches	Yes	Yes	Yes (-)	No
Traffic sources				
Library of applications	Yes	No	Yes	Yes (+)
Support for theoretical sources	Yes	Yes (-)	Yes	Yes (-)
Output of results				
Output of utilization, throughput, and delay	Yes	Yes	Yes	Yes
Output of packet or cell loss	Yes	No	Yes	No
Modeling methods and execution				
GUI drag-and-drop model building	Yes	Yes	Yes	Yes
Simulation modeling	Yes	No	Yes	No
Analytical modeling	No	Yes	No	Yes
Batch runs with different configurations	Yes	Yes	Yes	Yes
Study of recovery from failure is possible	Yes	No	Yes (-)	No
Training and support of users				
Free vendor training classes	Yes	Yes	Yes	Yes
On-line tutorials	Yes	Yes	Yes (+)	No
User community	Yes (-)	Yes (-)	Yes (+)	No
Availability of references and white papers	Yes	Yes	Yes	Yes
Learning curve for product	Medium	Easy	Difficult	Difficult
Platforms supported				
UNIX	Yes	Yes	Yes	Yes
Windows 95/98/NT	Yes	Yes	Yes	No
Product cost				
Purchase	\$44,000	\$28,500	\$17,000	\$80,000
Yearly maintenance fee	15% of cost	15% of cost	15% of cost	\$15,000

Table 2 - Feature summary of CACI, MIL 3, and MakeSystems capacity planning tools

In summary, CACI is the only vendor to offer both simulation and analytical modeling capabilities and also traffic import from Sniffer and RMON trace files. MIL 3 offers only simulation (no analytical modeling or traffic import from other than NetMetrix probes). MakeSystems offers only analytical modeling (no true simulation modeling capability, but import from Sniffer and RMON trace files is supported). All three vendors support topology import from HP OpenView. The MIL 3 Planner, while easier to use than the MIL 3 Modeler, is still difficult and (subjectively) less intuitive than the CACI COMMNET and Predictor tools.

## 6. Summary and Future Work

Capacity planing is an important component of designing high-performance computer networks. The research conducted in the summer of 1998 developed the requirements for capacity planning of future KSC networks as being designed by the AND group in the NASA-KSC DE directorate. The key deliverable to NASA-KSC was a formal requirements document for a capacity planning tool (see [14]). This requirements document will be used as a procurement vehicle for open procurement of a capacity planning tool. Additional contributions have included the direct evaluation of the tools from three major vendors (CACI Products Company, MIL 3, Inc., and MakeSystems), educating Dynacs Engineering network engineers in capacity planning, and contributing to strategic planning. This paper contains the vendor tool evaluation results including a summary comparison table. To quote Chris Kerios (Team Lead, Dynacs Engineering), "The old rules of thumb don't apply anymore when designing for the next generation of telecommunication systems. The work done here this summer by Dr. Christensen begins a new way for us to design the communication systems required to support the space programs of tomorrow." Future work will include the development of traffic models for proposed voice and video services. Specifically, this will entail characterizing the proposed voice and video sources and then building models that will be directly used by the modeling tools procured by AND. This work is necessary to enable AND to predict the performance of proposed ATXS designs for future voice and video requirements.

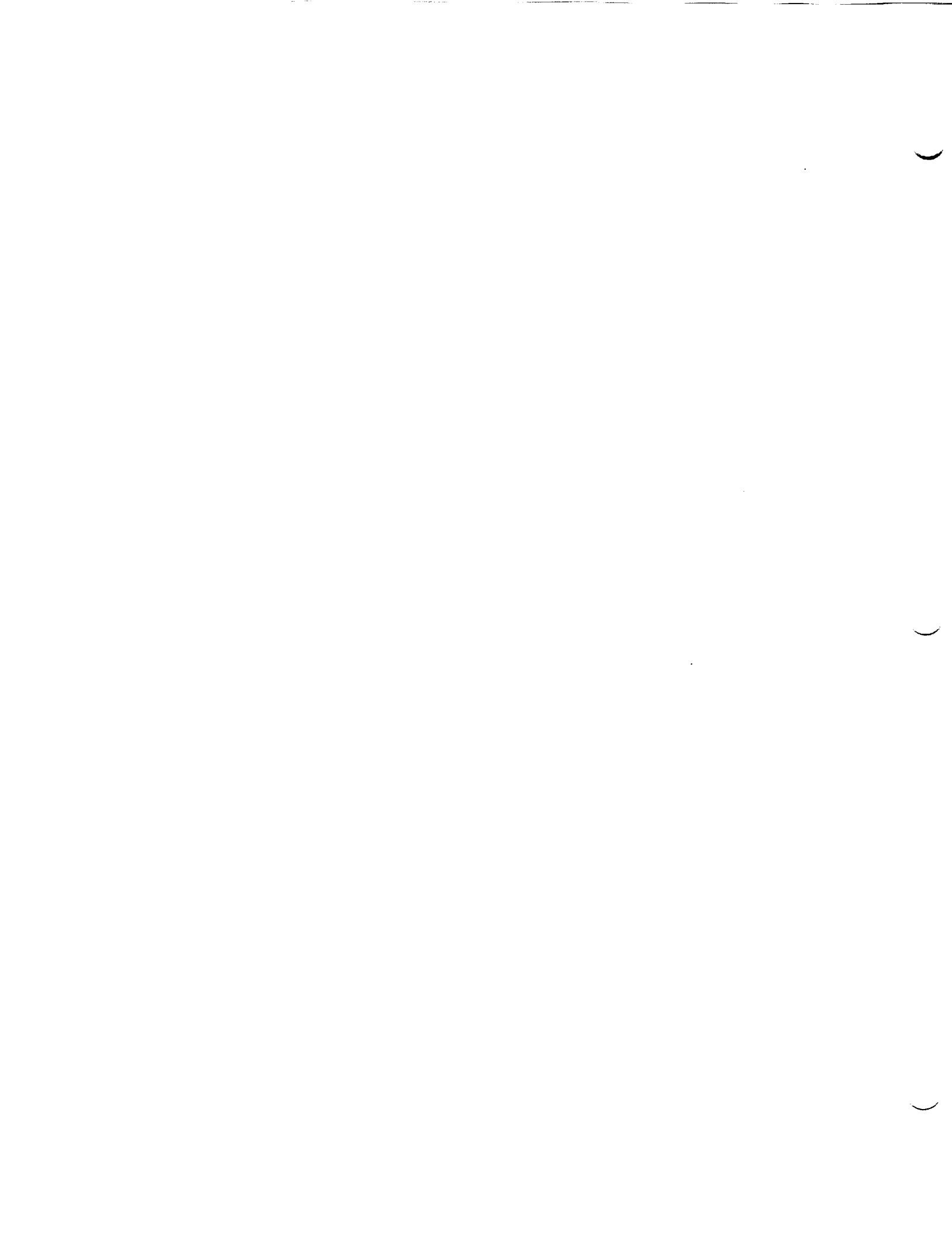
## Acknowledgments

The author would like to acknowledge Gregg Buckingham, Ray Hosler, and Kari Stiles of the NASA-KSC University Programs Office, John Schnitzius and Bryan Boatright of NASA-KSC Development Engineering, and Chris Kerios, R.J. Edwards, Cindy Johnson, Dave Johnson, Paul Kaun, Dave Miller, Greg Nelson, Don Philp, Steve Schaefer, Kumar Singh, Bruce Winters, and Henry Yu of Dynacs Engineering. These people made this work possible. Apologies to anyone inadvertently omitted from this list.

## References

- [1] CACI Products Company, Simulation Products, 1998. URL: <http://www.caciasl.com/>.
- [2] J. Duffy, "Defense Organization Funds Vendor Work on Network Design Pack," *NetworkWorld*, Vol. 14, No 34, August 25, 1997.
- [3] HP OpenView, 1998. URL: <http://www.openview.hp.com/>.
- [4] S. Kesahv, An Engineering Approach to Computer Networking : ATM Networks, the Internet, and the Telephone Network. Addison-Wesley Publishing Company, Reading, MA, 1997.
- [5] L. Kleinrock, Queueing Systems, Volume 1: Theory. John Wiley and Sons, New York, 1975.
- [6] KSC Communications Systems Upgrade Preliminary Engineering Report (PER). *KSC-DL-3700*, September 1996.
- [7] A. Law and D. Kelton, Simulation Modeling and Analysis. McGraw-Hill, New York, 1982

- [8] Make Systems, The Network Resource Planning Company, 1998. URL: <http://www.makesystems.com/>.
- [9] D. Menasce, V. Almeida, and L. Dowdy, Capacity Planning and Performance Modeling. Prentice Hall, Englewood Cliffs, New Jersey, 1994.
- [10] MIL 3, Inc. Simulation Products, 1998. URL: <http://www.mil3.com/>.
- [11] M. Molle, M. Kalkunte, and J. Kadambi, "Frame Bursting: A Technique for Scaling CSMA/CD to Gigabit Speeds," *IEEE Network*, Vol. 11, No. 4, pp. 6 - 15, July-August 1997.
- [12] Network Associates, Sniffer Network Analyzer, Ethernet, 1998. URL: [http://www.networkassociates.com/products/network\\_visibility/sniffer\\_lan/s\\_nae.asp](http://www.networkassociates.com/products/network_visibility/sniffer_lan/s_nae.asp).
- [13] Network Modeling Tool Survey. *Prepared under contract NAS5-31500, Task Assignment 44317*, Goddard Space Flight Center, September 1994.
- [14] Requirements for a Network Modeling and Planning Tool for NASA-KSC Development Engineering. *KSC-xxxx (draft)*, 1998.
- [15] T. Stearns, "Buyer's Guide - Mastering Modeling," *NetworkWorld*, Vol. 15, No. 6, February 23, 1998.
- [16] Tools Page for Kenneth J. Christensen, 1998. URL: <http://www.csee.usf.edu/~christen/toolpage.html>.
- [17] Traffic Management Specification, Version 4.0. The ATM Forum Technical Committee, *af-tm-0056.000*, April 1996.
- [18] S. Waldbusser, Remote Network Monitoring Management Information Base, *Request For Comments 1757*, February 1995. URL: <http://www.cis.ohio-state.edu/htbin/rfc/rfc1757.html>.



**1998 NASA/ASEE SUMMER FACULTY FELLOWSHIP PROGRAM****JOHN F. KENNEDY SPACE CENTER  
UNIVERSITY OF CENTRAL FLORIDA****REALISTIC SCALE COMPOSTING REACTOR****FOR A MARTIAN OR LUNAR HABITAT: GENERATIONS I AND II**

Melvin S. Finstein

Professor

Department of Environmental Sciences  
Cook College, NJ-NSCORT, Rutgers University  
New Brunswick, New Jersey

KSC Colleague: John C. Sager

**ABSTRACT**

Well understood principles governing the behavior of the composting microbial ecosystem were applied to the development of a realistic scale reactor for a Martian or Lunar habitat. Reactor Generation I proved unworkable, but instructive. Generation II was based on a 5.3 ft<sup>3</sup> polypropylene cylinder standing on the frame of a rotatable grate. Material to be removed from the system (wasted), or to be recycled, was unloaded at the bottom through the grate. A mixture of surrogate waste (field grown wheat straw and corn silage in equal amounts on dry matter basis) and recycle were loaded at the top. Air was forced in at the top as demanded via temperature feedback control, or according to a baseline schedule, for a single pass through the composting matrix. Unloading and loading was at 2 or 3 day intervals (M-W-F). Addition of straw and silage combined was equivalent to 2 kg dry matter per day. The average material retention time was 7 days. Over the course of 35 days routine operation, dry matter disappearance per interval averaged 25% (range, 10-42%). The amount that disappeared and that which was wasted were inversely related. Performance was consistent with respect to temperature (nominal peak, 53-57°C), O<sub>2</sub> (9-14%), moisture (no drainage), air usage (~ 3,500 ft<sup>3</sup> per 2-day interval), and pressure head loss (0.2-0.5" water head). The exhaust gas was virtually odorless. This design approach would accommodate a toilet seat integral to a Generation III reactor, as indicated for a bioregenerative ecological life support system.

# REALISTIC SCALE COMPOSTING REACTOR

## FOR A MARTIAN OR LUNAR HABITAT: GENERATIONS I AND II

Melvin S. Finstein

### 1. INTRODUCTION

Distance precludes resupply of a manned expedition to Mars, hence much of the food must be grown on the planet's surface in a Controlled Ecological Life Support System. Nutrients would have to be recovered from such wastes as wheat straw, soybean leaves, and feces, for reuse in succeeding crop cycles. The need to keep nutrients in circulation for maximal self-sufficiency is similarly compelling for prolonged stays on the moon.

Composting is a candidate resource recovery technology because it potentially offers such advantages as compactness, low mass, near ambient reactor temperatures and pressures, and operational reliability and simplicity. Importantly, the scientific principles governing the behavior of the composting microbial ecosystem, involving interactions among metabolic heat generation, temperature, vaporization of water, and oxygenation, are well understood<sup>1,2,3</sup>. This underlies rational design for high rates of waste decomposition, as needed to minimize reactor mass and volume. This general understanding must be applied to the particular problem of developing a reactor integral to an extraterrestrial CELLS.

These general principles were applied in two successive composting reactor designs. Generation I proved unworkable, but instructive. It is outlined briefly to benefit 'institutional memory,' so that repetition of non-successful approaches may be avoided. The emphasis is on Generation II.

Process control for both generations was predicated on ventilative heat removal in reference to a microbially favorable temperature ceiling (~ 55°C), as implemented via temperature feedback control of a forced air source in a single pass through the composting matrix. This approach ensures thorough oxygenation in that oxygen consumption and temperature are linked via heat generation. Given adequate moisture levels, among other factors, decomposition is thereby speeded. Both generations were bottom-unloaded/top loaded, to accommodate discontinuous and non-uniform loading (e.g., surge at harvest time) in a single reactor vessel. This materials flow pattern would permit the incorporation of a toilet seat in a Generation III reactor for the direct deposition of feces onto the composting mass. Other similarities between Generations I and II, and crucial differences, are outlined below.

## 2. MATERIALS AND METHODS

### Reactors

*Common Features:* A single polypropylene tube (18" ID x 36" H x 1/8" thick) served as the body of both reactor generations (Fig. 1)<sup>4</sup>. (English units are used for consistency with supplier specifications.) Spring clips pressed a lid (3/4" thick) against an O-ring seated in a circular grooved ledge (21/16" W) integral to the tube. Control/monitoring probes were fashioned from type T thermocouple wire housed in rigid phenolic tubing (0.5" OD). Each of four probes housed three couples along its length, though ultimately only one per probe was used (see later). Compression fittings held the probes at right angles to the wall of the reactor tube, in an in-line vertical series. The distances were (inches): bottom of ledge to probe #1, 6-1/4; between probes, 8-1/2; probe #4 to bottom end of reactor tube, 3.

Compressed air from a central supply passed sequentially through a pressure regulator, solenoid valve, flow meter, and a port in the lid (6/16" orifice D) into the reactor head space, which was connected pneumatically to a pressure transducer (1/8" orifice). After passing through the composting matrix, the air exited from the reactor through loose fitting panels of insulation.

*Features specific to Generation I.* The upper portion of the reactor tube was grasped by two purpose-fabricated polypropylene C-clamps attached to legs straddling a tub (Fig. 1a). This served to suspend the open end of the tube above the floor of the tub. The lower portion of the tube was encircled by a tight-fitting outer sleeve which could be slid to vary the distance to the floor. The control/monitoring probes extended to the center of the circle described by the tube.

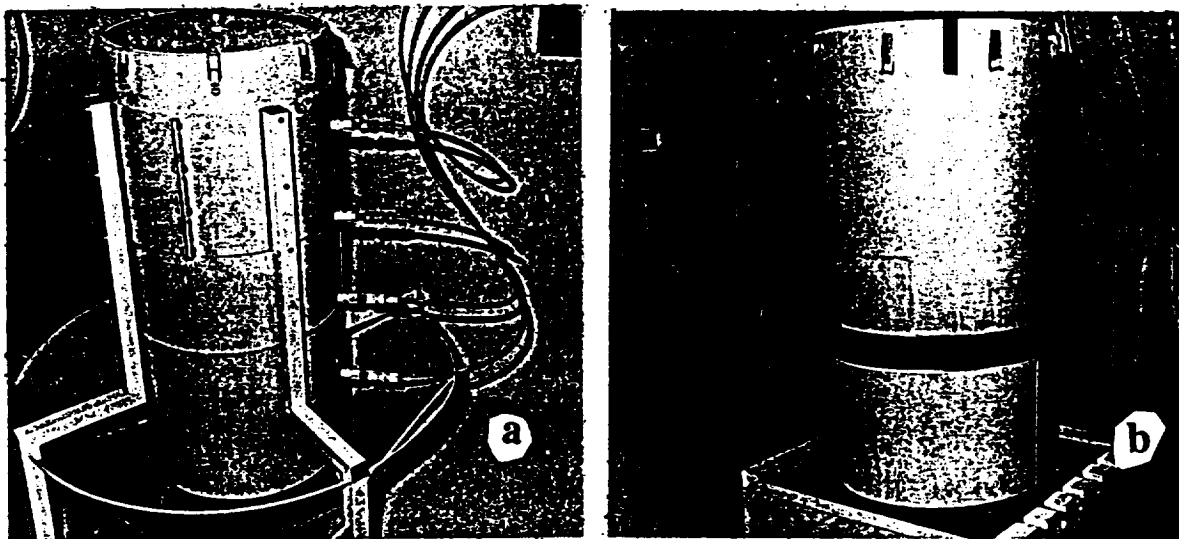


Fig. 1. Reactor Generations I and II. a: I, without insulation; b: II, bottom plenum insulated.

*Features specific to Generation II.* For rigidity, the outer sleeve was positioned so that its bottom end and that of the main tube were adjacent. The assembly stood on a wooden frame at four points (Fig. 1b). The end was open, except where blinded by the frame and the members of a grate. The grate, which could be rotated, was made from five lengths of stainless steel tubing (3/4" OD), their ends seated in notches in the wooden frame, and nuts and bolts (Fig. 2a). Early on, the control/monitoring probes were repositioned so their distal ends were flush with the inside of the wall, leaving the interior of the tube unobstructed (Fig. 2b). Material was extracted by rotating the grate (Fig. 2c), abetted by use of a hand tool to bring compacted material within range of the grate's rotation (Fig. 2d). The upper part of the reactor was insulated with blown polyurethane foam (thickness, 3") surrounded by an aluminized metal sheath, and the lower part, including projecting grate ends, with polystyrene sheets (minimum 2" thick) (Figs. 2e and 2f).

## Materials and Procedures

*Feedstock.* In lieu of sufficient inedible crop residue grown under CELLS-like conditions, wheat straw and corn silage (fermented chopped whole corn plants, pH ~ 4.0), obtained from a dairy farm was used as surrogate wastes. The straw was chopped by four passes through a shredder/mulcher and stored dry. The silage was stored in airtight 55 gallon drums. As the drum was emptied, inert objects were placed inside to occupy space and exclude air. Fresh inputs to the composting reactor were equal dry weights of straw and silage, adjusted with lime to pH ~ 6.5.

*Inoculum.* The straw and silage was initially inoculated with a sprinkling of several soils, commercial peat moss, and mulch. Thereafter, in routine operation, a portion of freshly extracted material (recycle) was mixed with the feedstock.

*Dry weight.* One to two kg representative samples of silage, waste (first fraction removed through grate), and recycle (second fraction), or ~ 200 g straw, were placed in paper bags and dried for at least eight days at 70°C in a forced-convection oven. Crusts forming at the bottom of the bag were broken up by hand early in the drying cycle.

*Ash weight.* Portions of dried material were put into tared porcelain crucibles, re-dried in a vacuum oven at 70°C, weighed, and ashed in a muffle furnace at 600°C for six hours.

*Unloading and loading the reactor:* On Mondays, Wednesdays, and Fridays the procedure was as follows: 1) 2.33 kg (oven dry weight) of straw, wetted with 12-14 L water, 2.33 kg silage (oven dry weight), and 160 g lime, were mixed and put aside<sup>5</sup>. Mixing was by shovel in two cement mixing basins. 2) Ventilation was deactivated and the reactor lid removed. 3) By rotating the grate and use of the hand tool, 11-17 kg of material (wet weight) was extracted and removed from the system (wasted). 4) A further 12-19 kg (wet weight) was extracted for recycling within the system. 5) The materials denoted by 1) and 4) were mixed and placed on top of that remaining in the reactor (not extracted). 5) The lid was replaced and ventilation reactivated.

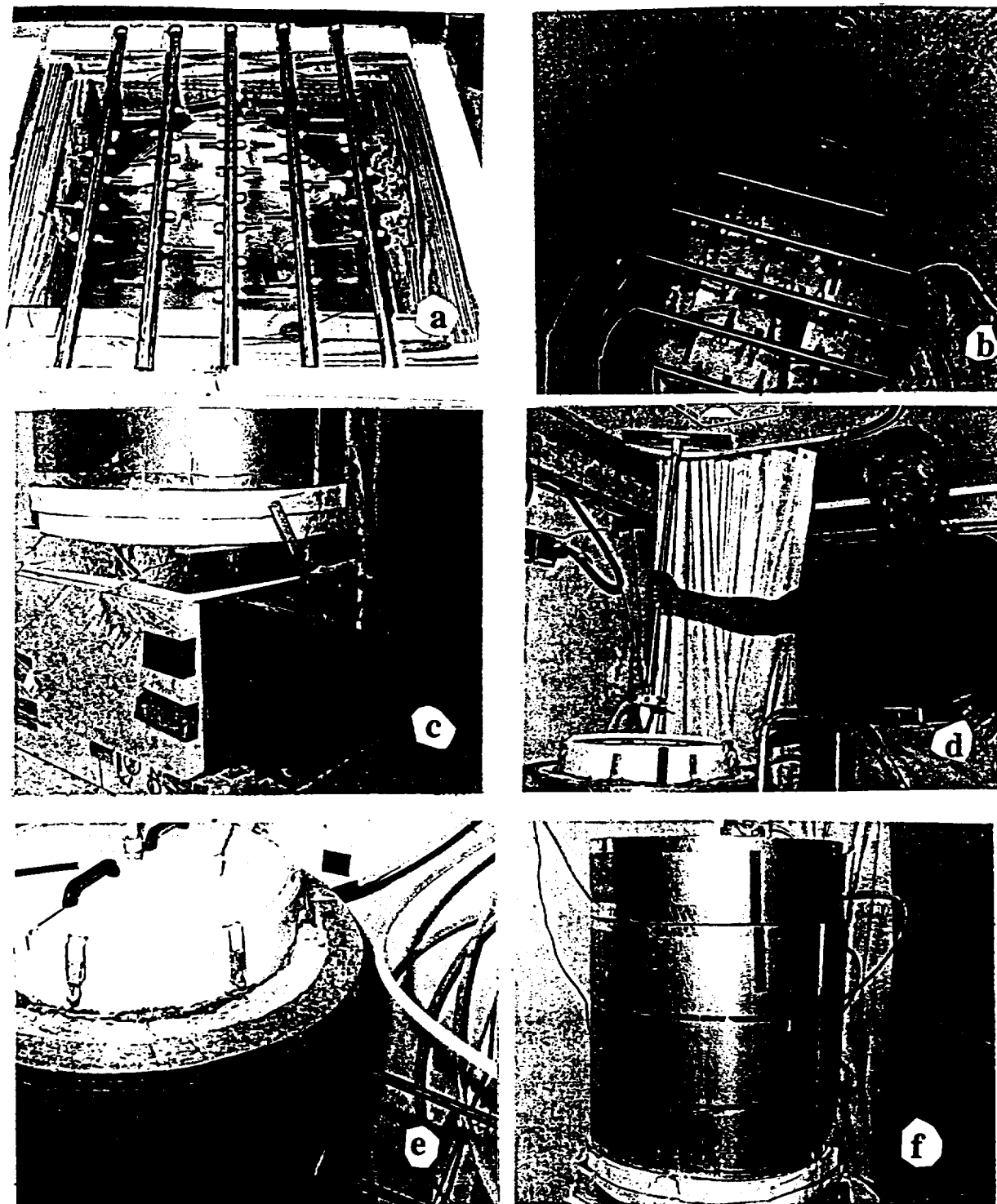


**Fig. 2 (Generation II).** a, wooden frame and rotatable grate; b, view through body tube - note ports for control/monitoring probes; c, means of rotating grate - extracted material in bin; d, tool with retractable prongs used to loosen compacted material; e, lid assembly showing air (larger) and pressure transducer (smaller) conduits - compare probe positions with Fig. 1a; f, reactor fully assembled and insulated.

*Temperature feedback control and monitoring, and oxygen determination.* Temperature data were logged automatically every five minutes. When a set point temperature was exceeded by 0.1°C, ventilation was demanded and the solenoid valve opened. It closed when the temperature declined below this value. Occasionally, temperatures in the composting material were observed manually by inserting a special probe (1/8" D) downward from the top. Oxygen was determined by inserting a probe (circular porous surface, 22/16" D) into a vertical shaft excavated in the material by hand, backfilling, and recording the minimum value.

*Ventilation events.* At the termination of each ventilation event, whether demanded via temperature feedback or baseline-scheduled, the event's duration was logged cumulatively. The event ledger was reset to zero every day at midnight.

### 3. RESULTS AND DISCUSSION

#### Reactor Generation I - Instructive Failure

With respect to materials movement, the initial design was predicated on the idea that the material, after descending into the tub, would 'flow' up and around the outer perimeter of the tube. This proved unfounded. Rather, the material had to be dug out from under the tube, and a cone-shaped mass of dry crusted material formed on the floor of the tub. This restricted airflow, aggravating air short-circuiting. Generation I was unworkable, but highly instructive.

#### Reactor Generation II - Modifications and Familiarization

*Physical modifications.* A hold-over from the above reactor was a holed baffle plate ('Swiss cheese') suspended from the lid, intended to intersect and disperse the entering air stream. The idea was to prevent direct impingement of the airstream on the material, and to combat short-circuiting along the reactor wall. However the baffle, modified numerous times, came to be recognized as causing problems rather than solving them, and was abandoned. Thereafter, air entered the headspace without deliberate dispersal.

Another hold-over was that the control/monitoring probes extended to the center of the reactor tube, so that they would be surrounded by composting material. So positioned, however, the probes induced severe air short-circuiting in that the affected material was comparatively cool and dry, interfered with downward movement, and conducted considerable heat to the outside. The probes were therefore repositioned to be flush with the wall, and only the end-most thermocouples kept operational.

*Operational familiarization.* The supportive computer infrastructure allowed any of the probes, or all of them, to serve both control and monitoring functions. The assignment of multiple, sequential, set points was tried but proved problematic (e.g., probes #2, #3, #4 assigned set points of 45°C, 50°C, 55°C, respectively). With this arrangement, probe #2 was the first to reach its set

point and exert demand for ventilation. But the downward, cumulative, transfer of heat soon shifted control to probe #3, and then to #4. The result was that the most active material, in the upper part of the reactor, became stranded. That is, judging from temperature, oxygen, and odor observations, the amount of air demanded downstream was not sufficient to keep the upstream material thoroughly oxygenated. This pattern of behavior is intrinsic to the reactor's physical and operational configuration -- that of periodic bottom-unloading/top-loading, and single pass, forced-pressure, downward ventilation

It was concluded that there should be only one control point, sited near the bottom of the column of the freshly added material. This corresponds to probe #2. At the loading rate adopted (equivalent to 2 kg dry matter per day), a set point of 35°C, and baseline ventilation (independent of demand) of 1 minute out of 10 proved satisfactory. Thus probe #2 served both control and monitoring functions, while the others served only as monitors.

The air delivery rate that proved satisfactory was 7 CFM. In the empty reactor this would correspond to one air exchange per 46 seconds. Assuming 50% pore space in the composting material, it would correspond to two exchanges per 1.5 minute.

### **Routine Reactor Performance -- Temperature, Ventilation, Oxygen, Odor**

*Temperature and Ventilation.* Familiarization was complete by 12 June. Thereafter, till 18 July, the above physical and operational features were used routinely. The period from 14 through 21 June illustrates routine system behavior in terms of temperature and ventilation (Fig. 3a).

The previous unloading/loading operation was on Friday 12 June, between approximately 0800 and 1100 hours. By midnight Sunday demand for ventilation had ceased, as indicated by the temperature at the control probe (#2) being <35°C (set point) and declining (Fig. 3a, upper panel). The abrupt temperature declines on Monday morning signifies the first unloading/loading operation of the week. The erratic temperatures at probe #1 (near surface of material) may reflect the expansion of compressed air immediately on entering the reactor. The ambient temperature was around 33°C, except during the unloading/loading operation when the setting of the room's air conditioner was lowered for personal comfort. Similar declines in the composting material and ambient air occurred on Wednesday and Friday.

Within a few hours of loading and restoring process control, the temperature at probe #2 reached 35°C, initiating on-demand ventilation. A transient temperature override typically occurred at this point. Thereafter, the set point temperature was maintained precisely until a decline set in. The 'squiggles' on 16 and 18 June (Tuesday and Thursday) signify the manual stirring of the top few inches of material with addition of ~ 0.5 L of water. At probe #4, the lowest one, temperature peaked at <55°C. Deeper in the column (distance between probe #4 and grate = 3"), measurement with the hand held probe inserted from underneath showed slightly higher temperatures. The highest temperature observed throughout routine operation was 60°C .

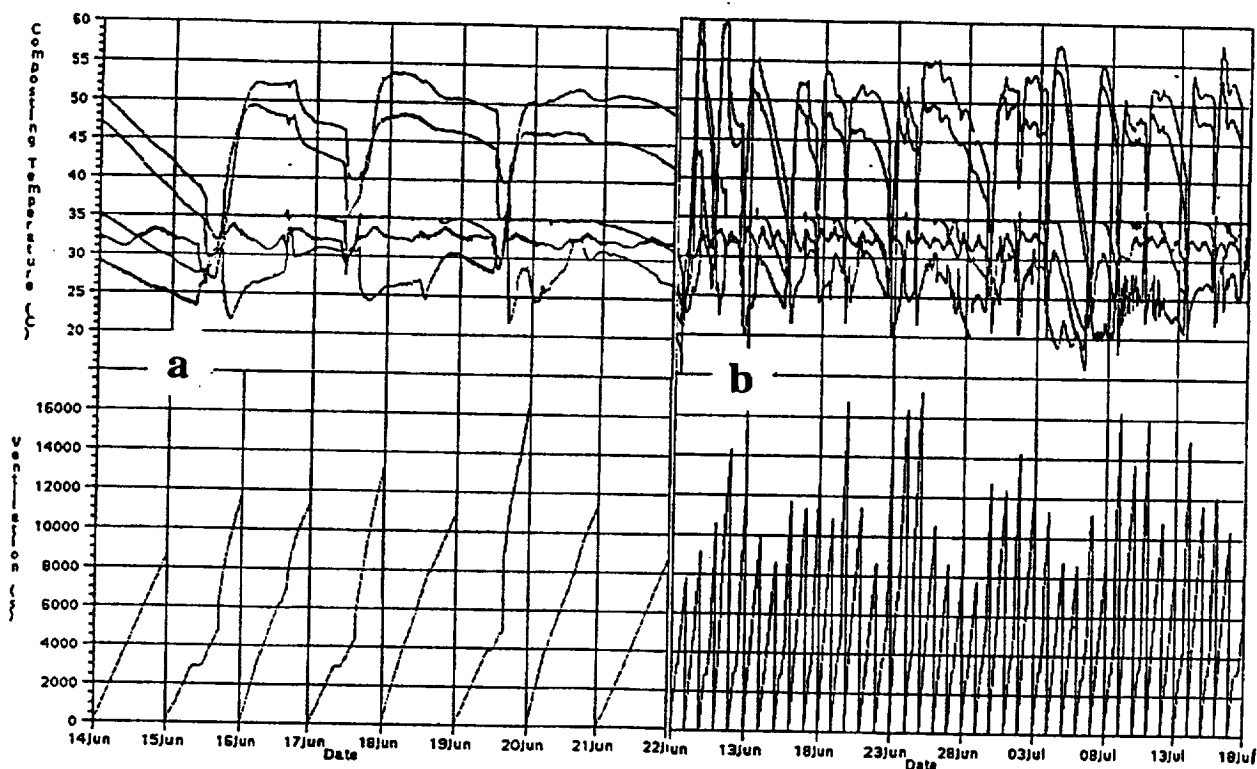


Fig. 3. Temperature and ventilation events (ledger reset at midnight).

Over the course of the Sunday under review, 8,640 seconds accumulated (0.1 day), exclusively from scheduled baseline events (Fig. 3a, lower panel). Baseline events continued to accumulate on Monday, until ventilation was deactivated for the unloading/loading operation. The signature of this hiatus is the horizontal segment of the trace. Baseline accumulation resumed after restoration of process control. A few hours later demanded ventilation commenced, as exerted via temperature feedback, signified by a vertical segment. Accumulation for Monday totaled nearly 12,000 seconds. On Tuesday morning ventilation was briefly inactivated to stir the surface material, signified by another, brief, vertical segment. That day's accumulation was similar.

A lengthier segment of temperature and ventilation data, from shortly before the beginning of routine operation to its termination, indicates consistent behavior throughout (Fig. 3b). Because of a scheduled power outage on 27-28 June, the 26 June unloading/loading for 26 was canceled. The material was not disturbed over this period. Over the period between the unloading/loading operations of 3 and 8 July the air conditioner in the room was left on the high setting, decreasing ambient temperature from the usual level of  $\sim 33^{\circ}\text{C}$  to  $\sim 20^{\circ}\text{C}$ . This resulted in unusually smooth traces and high temperature peaks, explicable in terms of greater conductive heat loss resulting in less demand for ventilation.

Occasionally, on intervening days (e.g., Tuesdays), or immediately before unloading (Wednesdays), temperature at different levels within the composting matrix was determined manually (Fig. 4). The four values at the right, (30.0°C, 35.2°C, 44.8°C, 48°C) were sensed by the permanently in-place probes, and the others by the hand-held probe inserted into the composting material. That probe #2 was 0.2°C higher than its assigned set point reflects the inactivation of ventilation during the measurement period. The other values were probably similarly affected. Probe #1 aside, on this occasion and others the permanently in-place probes (flush to wall) adequately represented the bulk of the material in the reactor. This refers to both the control and monitoring functions.

*Oxygen.* On intervening days, oxygen was occasionally measured (Table 1). The pattern of increasing oxygen content at lower depths is explicable in terms of the introduction of both air and material at the top of the reactor. With the more active material on top, upon termination of a ventilation event the non-flowing air would be depleted of oxygen faster.

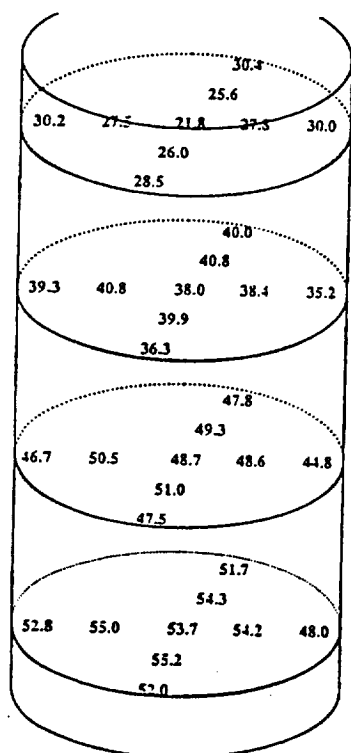


Fig. 4. Composting matrix temperature at different levels

**Table 1. Oxygen in the composting matrix\***

Approx. depth** (inches)	Position in horizontal plane		
	Center	Midway	Wall
5	8.6	8.8	8.4
10	9.6	9.0	9.7
15	10.4	10.4	11.6
20	12.6	11.4	--
25	13.6	--	--

\* Values for % O<sub>2</sub> (v/v) on 16 June 1998.

\*\* Distance from the surface.

The oxygen observations may not be representative of other stages of the unloading/loading cycle (e.g., at the onset of demand for ventilation).

*Odor.* During familiarization, Prior to 12 June, malodors were generated on several occasions. This is attributed variously to severe air short-circuiting, inappropriate set points, inadequate air delivery rate, and overloading of the reactor. In routine operation (12 June-18 July), the exhaust air was essentially odorless.

### **Routine Reactor Performance – Other Aspects**

*Drying at the surface.* Inspection on intervening days revealed surface dryness to a depth of ~ 0.5" directly below the air inlet orifice and in a narrow band (~ 1/8" wide) next to the wall. Otherwise, dryness was shallower. The top few inches of material was usually stirred by hand and moistened. The signature of this procedure, noted before in connection with Fig. 3a, may be seen in the lengthier representation of Fig. 3b.

Based on these visual observations, and multiple manual temperature observations, it was concluded that air short-circuiting was not a significant problem.

*Drainage.* Drops of water could be squeezed from the material extracted on first rotating the grate. Water could not be easily squeezed from overlying material. Throughout the period of routine operation, no liquid drainage was observed.

*pH.* The pH of the lime-amended silage and straw was ~ 6.5. That of the material extracted through the grate was 8.6.

*Material movement pattern.* Bottom unloading/top loading would, by itself, result in the plug flow movement of material. This pattern is compromised by two other aspects, however. One is that use of the hand tool to counteract compaction intermingled newer and older material. The other is that the second fraction extracted (recycle) was brought back into the system in admixture with fresh straw and silage. Thus, materials flow was neither plug flow nor completely mixed, but some combination of these patterns.

*Material pass through time.* Because of the above, a small amount of material could pass through the system in as little as 2 days. Similarly, a small amount of material would have a very long, indeterminate, pass-through time.

*Retention time.* Over the course of a week the oven dry weight of straw and silage added, in three installments, was 14 kg. In a non-routine procedure, the addition of this amount of fresh material plus about 40 L water to the empty reactor exactly filled it. In routine operation, therefore, the average retention time was approximately 7 days.

*Pressure head loss.* At the beginning of an interval, head loss was relatively slight. It then increased, presumably reflecting gravity-induced compaction. About midpoint in an interval (e.g., Tuesday), head loss started to decrease. This would reflect an increase in porosity stemming

from the vaporization of water. The mean *peak* value and range representing the thirteen unloading/loading operations were (inch of water head): 0.37 (0.24-0.54).

*Head space.* At the end of an interval, the distance from the ledge of the reactor to the surface of the material was 3-6 inches. On unloading both the waste and recycle fractions, and packing the material remaining in the reactor with moderate pressure to partially reverse the effect of using the hand tool, the distance was 16-22 inches. Addition of fresh material, with moderate packing, brought the distance to the ledge to 1-4 inches.

### Routine Reactor Performance – Materials Accounting

*Dry Weights.* Work done in composting is best judged in terms of such direct manifestations of microbial decomposition as metabolic heat generation or carbon dioxide evolution. These measurements were not accessible, however. What was accessible was an accounting of the dry weights of the straw and silage additions, and the fraction removed from the system (wasted). The fraction recycled was also known, though this does not enter into the accounting. Equal amounts of straw and silage were added each time, totaling 4.66 kg, while the amount wasted was variable (Fig. 5a). Because the calculation involved subtraction of the wasted value from that of the added straw and silage, the estimate of the proportion disappeared varied from interval to interval (5b). This would be independent of any variability caused by differences in the actual extent of microbial decomposition. On average 25% of the dry matter disappeared, while the range was 10-42%. Similarly, because of the subtraction, the proportion that disappeared and the amount wasted are inversely related.

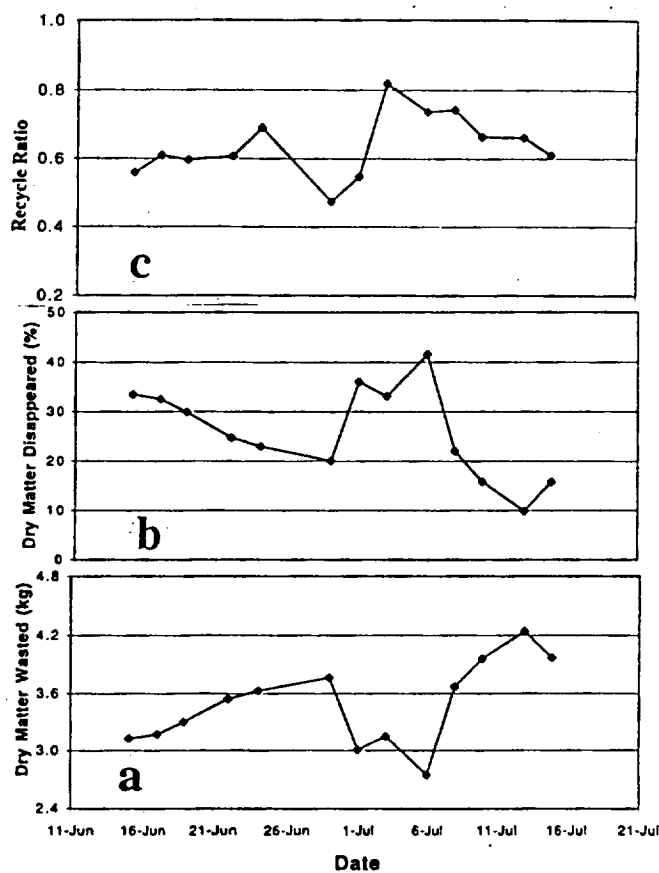


Fig. 5. Materials Accounting.

There was no consistent relationship between recycle ratio and extent of disappearance (Fig. 5c). Given sufficient recycle to ensure thorough inoculation of fresh inputs, no such relationship would be expected.

*Percent ash.* The data for straw, silage, and equal dry weights of straw and silage were combined, giving an average ash content of 8.41 % (7.06-9.16, n = 5). Similarly, the data for both fractions extracted through the grate (waste and recycle) were combined, giving an average

ash content of 12.57 % (11.99-13.74, n = 6). Thus, composting these materials in this fashion increased the ash content 1.5-fold.

## **CONCLUDING REMARKS**

In an Earth-orbiting space station, and during the transit to Mars, little food is likely to be grown. As such, it is difficult to imagine an essential role for composting or other means of recovering resources from solid waste. Moreover, designing and operating a composting reactor to function in weightlessness poses major difficulties yet to be addressed.

In contrast, a habitat on the surface of Mars or the Moon would necessarily have a large bioregenerative component. Resource recovery, for which composting is well suited, would clearly have a role in that setting.

A novel composting reactor and operational configuration, that of bottom unloading/top loading in conjunction with forced pressure, single pass, temperature feedback controlled ventilation, was proved in the present study. This refers to prototype reactor Generation II. This design approach is compatible with the incorporation of a commode.

Numerous design and performance details would have to be worked out to realize a flight-ready reactor. Some aspects needing consideration are as follows: reactor shape (rectangle with smooth corners?) with corresponding grate redesign; flared reactor skirt to promote downward movement of material (but air short-circuiting?); effect of input particle size; fate of pathogenic microbes; advantages/disadvantages of air recirculation, multiple pass, ventilation.

Regardless of the particular unit processes employed in a bioregenerative habitat, all must function harmoniously in a mutually supportive manner.<sup>6</sup> Thus, all candidate components need to be tested in an integrated Earth-based, realistic, simulated extraterrestrial habitat.

## **ACKNOWLEDGEMENTS**

The straw and silage was kindly donated by Norm Watts of Swiss Haven Dairy, Paisley FL. I thank John A. Hogan and John C. Sager for their in-depth involvement, Jay Garland for his help and encouragement, Scott Young and Morgan Simpson for setting up and maintaining the computer infrastructure, and others in the Life Science Support Group at KSC (Hanger L) too numerous to mention for their varied assistance. I thank Jeanne Gasiorowski (NASA Classroom of the Future) for preparing some of the illustrations and helping set up a data management scheme. This work was performed while on sabbatical leave from Rutgers University, and as a NASA Summer Faculty Fellow. I am grateful to both organizations for the opportunity extended.

## REFERENCES AND NOTES

---

<sup>1</sup> Finstein, M.S., F.C. Miller, P.F. Strom. 1986. Waste Treatment Composting as a Controlled System. *In Biotechnology*, Vol. 8, Rehm and Reed, eds., VCH Publ. Inc., NY, NY, p. 363-398.

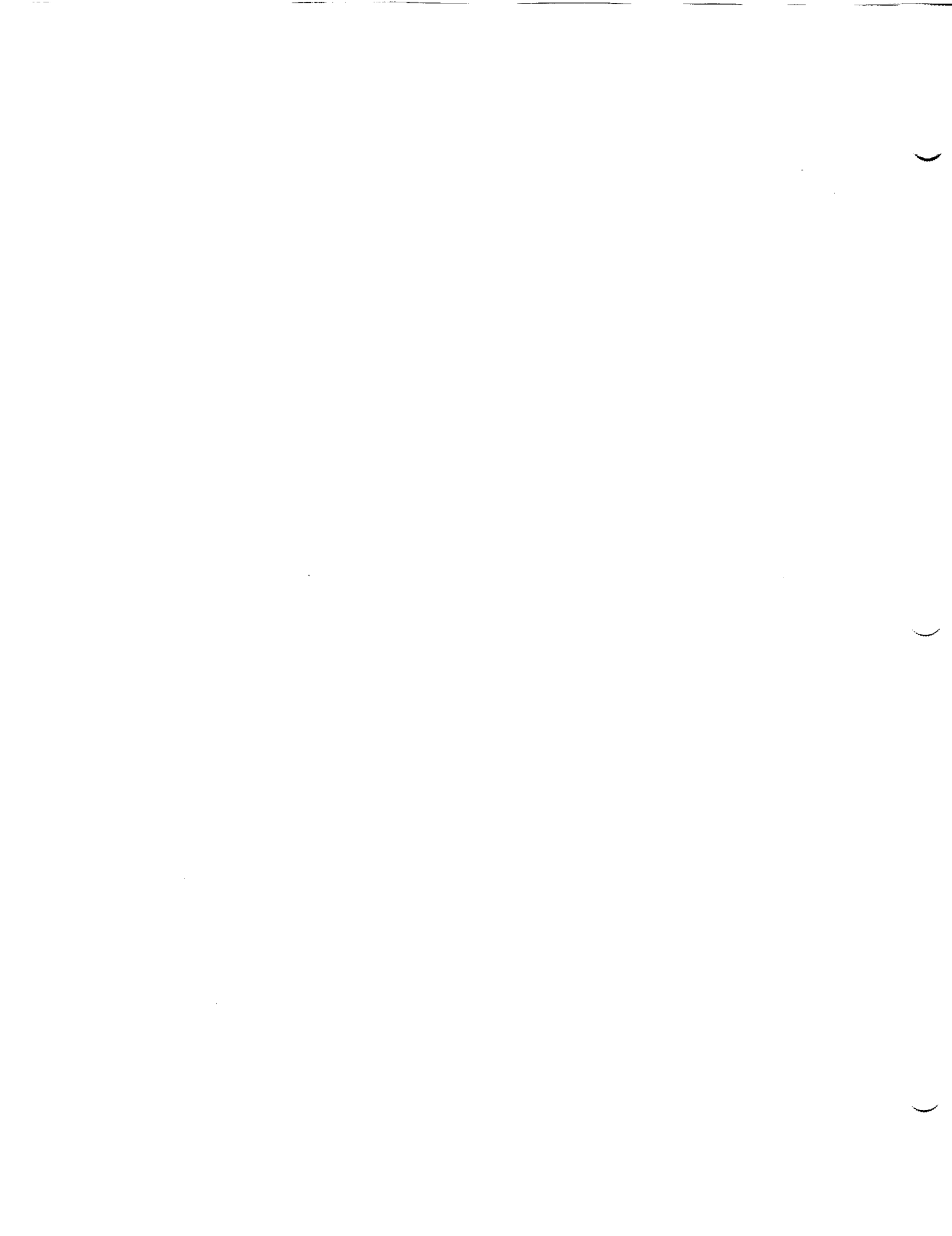
<sup>2</sup> Hogan, J.A., F.C. Miller, M.S. Finstein. 1989. Physical Modeling of the Composting Ecosystem. *Appl. Environ. Microbiol.* 55: 1082-1092.

<sup>3</sup> Hogan, J.A., M.S. Finstein. 1991. Composting of Solid Waste During Extended Human Travel and Habitation in Space. *Waste Management and Research* 9: 453-463.

<sup>4</sup> Fabricated by Plastics Concepts Inc., Billerica, MA.

<sup>5</sup> The target was 2.33 kg each (equivalent to a total of 2.00 kg per day). The actual average dry weights were: straw, 2.36 kg; silage, 2.35 kg. The actual average value was used in calculating materials disappearance.

<sup>6</sup> Hogan, J.A., et. al. 1998. On the Development of Advanced Life Support Systems Maximally Reliant on Biological Systems. SAE Tech. Paper Series 981535. 28<sup>th</sup> Intern. Conf. Environ. Systems. Danvers, MA.



**1998 NASA/ASEE SUMMER FACULTY FELLOWSHIP PROGRAM**

**JOHN F. KENNEDY SPACE CENTER  
UNIVERSITY OF CENTRAL FLORIDA**

**WEB PAGES FOR THE KSC CORROSION LABORATORY**

Robert H. Heidersbach  
Professor and Department Head  
Materials Engineering  
California Polytechnic State University  
KSC Colleague: Louis MacDowell

**ABSTRACT**

This report discusses the development of a revised World Wide Web site for the corrosion activities at NASA-Kennedy Space Center. The report reviews the existing site, discusses reasons for the new site, and explains the features of the new site. A discussion is provided on web site development including authoring software, marketing/visibility of web sites, and the characteristics of a good web site. While the topic of the web site is corrosion, most of the information in this report would be relevant to any web site development project.

# WEB PAGES FOR THE KSC CORROSION LABORATORY

Robert H. Heidersbach

## 1. INTRODUCTION

The purpose of this project was to develop a new web site for the corrosion activities at the NASA Kennedy Space Center. The current KSC corrosion web site was developed in 1996 and, while it was adequate at the time, it has not been developed to serve its primary objectives:

- Inform KSC personnel about corrosion control information and expertise at KSC
- Inform the general public about corrosion control information with emphasis on activities unique to KSC
- Inform potential users of the KSC corrosion laboratory facilities and expertise of the methods available for cooperative efforts

The current project was intended to redesign the KSC corrosion web pages to make the new web pages more compatible with the above objectives.

## 2. WEB SITE INFORMATION

All efforts on web site development should consider the following subjects:

- The purpose of the web site
- Characteristics of a good web site
- The intended audience
- Software necessary to develop and/or update the site
- Marketing and promoting the visibility of the web site to potential readers

The purpose of a web site: Web sites are developed for a number of purposes. Marketing and distribution of information are common to almost all web sites. If marketing is a primary goal of a web site, then access and visibility through search engines and browsers becomes a major consideration. If all users of the web site will be within an given audience and know of the site's existence and address, then access and visibility become less of a concern.

The current KSC corrosion web site has multiple purposes, which include presenting information to people who are not familiar with KSC. The limited visibility of the current site, caused in part by the linking within the KSC web structure, has substantially reduced the traffic on the corrosion site during recent months.

Characteristics of a good web site:

Many experts agree that the following characteristics are found in most good web sites<sup>[1]</sup>.

- They must be useful
- They should be designed with a real purpose in mind
- They should work quickly
- They should be easily understood and navigated

There are many ways of developing web sites, but most authorities recommend that a survey of similar sites to determine the useful characteristics and features to be incorporated into the proposed site is an excellent way to start. Another useful technique is to review successful commercial sites selected by authorities and decide which of these sites should be emulated and why<sup>[2]</sup>.

It is easy to be carried away by the innovations in computer technology that allow for many different multimedia techniques to be incorporated into a site. Unfortunately, many of these techniques require special software that not all users of a potential site have available to them. Thus it is generally advisable to limit the multimedia displays to following pages and have main pages which are quick to load, easy to understand, and can be seen by a majority of browsers likely to be used by people seeking access to a given site<sup>[3]</sup>.

Additional characteristics which should be considered are the amount of text versus white space and graphics on a given page<sup>[4]</sup>. Too much text makes a page hard to read and boring to many readers. A rough rule of thumb of limiting any line to no more than 60 characters increases readability. Headings and subheadings should also be used so that the reader can quickly scan the page and concentrate on the portion of the text of interest.

#### Intended audience:

The primary intended audience for this web site is technical personnel and managers at government agencies who could use the corrosion capabilities available at the KSC corrosion laboratories.

#### Software used on this project:

World wide web sites require conversion of computer code to HTML (hypertext markup language). At one time this meant that all developers of web sites needed to be conversant in HTML. This is no longer the case, and many commercial software packages are now available that will convert standard text or presentation files into HTML.

A review of the source code used on successful corrosion-related web sites showed that a number of proprietary software packages were used to develop the sites. The corrosion web site developed for this project used FrontPage, a commercial software package. This was chosen because it is in wide use at KSC and elsewhere. Updated versions of the

corrosion site will become necessary, and having software that is easily used will facilitate changes as they become necessary for various reasons.

There are many advantages and tradeoffs associated with developing frames and nonframes web sites. The decision to avoid frames was made to allow for the largest number of viewers and for easy bookmarking of individual pages within the site.

#### Site marketing:

"Remember, if no one can find your web site, it doesn't matter what's on it [3]."

Guidance on how the various web search engines work and the systems they use for placing a given site within a category are available. This is very important, because if the site is not one of the first sites listed by a given search engine, then the number of people who find the site will be very limited.

It is not necessary to have an elaborate web page in order for the site to be listed high in a given category. Most of the browsers rank the sites using software which searches the "home" page and ranks the site according to proprietary algorithms. Guidance on how to make web pages more visible is available [3]. Unfortunately, the logic behind different browser "spiders" is different, and it is virtually impossible to have a web page that ranks equally high with all browsers. In late August 1998, the most important browsers for the United States market were:

- Yahoo!
- Excite/Webcrawler
- Infoseek
- Hotbot

The corrosion web site has been designed with information that is intended to increase its ranking with the top four search engines listed above. (NOTE: Yahoo! is a Search or Web Directory, not a search engine, and the system for listing with Yahoo! is different than for the other listing services). A complete set of instructions on how to list with each of the top four browser systems was submitted to the KSC colleague along with a copy of this report.

### 3. CORROSION ACTIVITIES AT KENNEDY SPACE CENTER

#### History:

Corrosion research has been conducted at KSC since the 1960's and the Center has a nationwide reputation for expertise on corrosion control of structures to include

protective coatings for steel and aluminum, cathodic protection of underground utility systems, and corrosion of reinforced concrete structures. The current web site was developed in 1996.

A sample web page from the 1996 corrosion web site is shown below:



## Corrosion Research and Engineering

### Introduction

The Space Shuttle Launch Pad is only 1000 feet from the Atlantic Ocean. Salt from the ocean, combined with corrosive rocket exhaust, make corrosion protection a high priority at Kennedy Space Center. KSC's Materials Science Division has conducted research in the field of corrosion prevention since 1968.

### Facilities

This facility is staffed full-time and is composed of a corrosion laboratory, accelerated corrosion laboratory, coatings application laboratory, and a beach corrosion exposure site.

### On-line KSC Corrosion Control Documents

-   KSC-STD-C-0001D: KSC Protective Coating Standard with Approved Products List
-   TM-584C: KSC Corrosion Control and Treatment Manual

### Coatings Evaluation and Corrosion Research Reports 1968

Over the years, KSC has been active in the area of coatings evaluation and corrosion research. These reports contain information about the performance of brand name coatings and alloys subjected to the severe environment at the Kennedy Space Center Beach Corrosion Test Site. [Click here to view a list of available reports with associated abstracts, photos, and information on how to obtain copies of the documents.](#)

### Images

-   Aerial view of KSC beach corrosion test site
-   Ground view of beach corrosion site with Shuttle in background

### Anonymous FTP Site

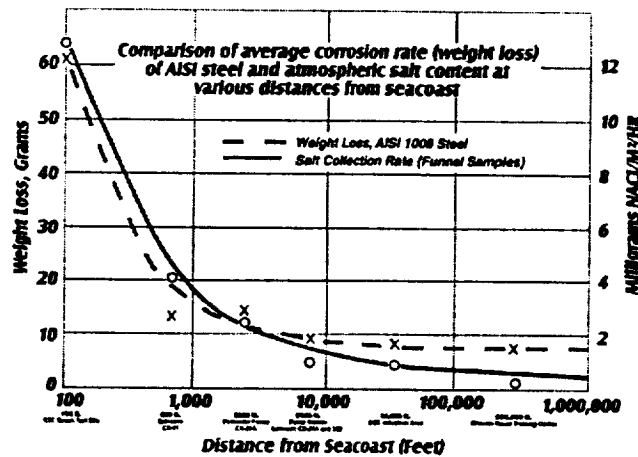
[Misc corrosion related files.](#)

These pages were technically correct and consistent with other KSC Material Science Division pages. Unfortunately, this 1996 version of the web site was not very visual,

which reduced reader interest. It also didn't mention the availability of the labs for use by outside parties. Equally important, but not apparent on the pages, is the fact that these pages were difficult to find if someone was not aware of the fact that KSC had a corrosion web site and knew the KSC organizational structure.

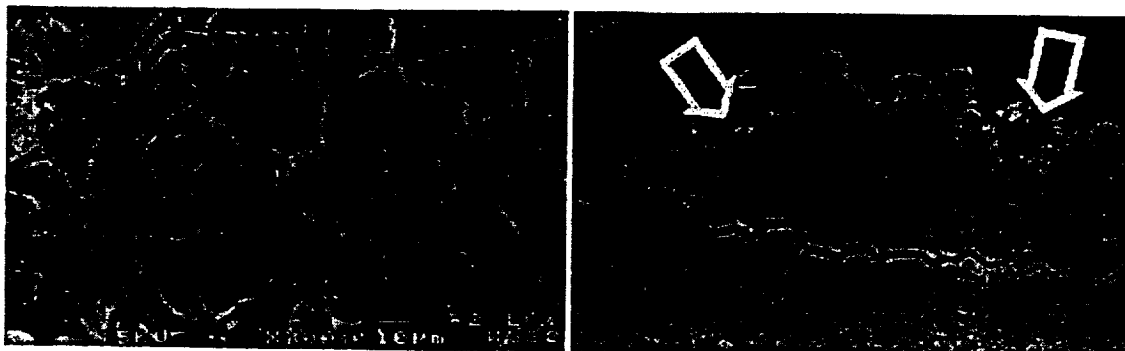
Corrosion information available at KSC:

Existing corrosion information at KSC included extensive photo archives with photos of corrosion on test samples and actual hardware, failure analysis reports of corroded hardware submitted to the KSC Material Science Division for analysis, actual hardware for examination and photodocumentation, and extensive reports on corrosion research and testing. KSC has conducted corrosion research and testing for over 30 years, and the complete archives were made available for this project.



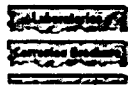
The chart above shows some of the corrosion information that has been collected over the years to explain why corrosion rates are so high at KSC and why corrosion control is so important to NASA. Visual data such as this was incorporated into the new web site.

The next two photos show intergranular SCC of an aluminum aerospace part. The intergranular nature of the corrosion can be seen in the scanning electron microscope image on the left and in the microscopic cross section on the right. The arrows indicate the primary crack shown in both pictures. Note that secondary crack are also apparent. These secondary cracks are common in stress corrosion cracking.





### Purpose



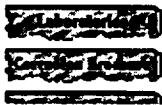
This corrosion web site was developed to inform and educate on issues involving environmental deterioration of materials. The site includes information and pictures of the corrosion engineering, research, and testing capabilities at the Kennedy Space Center (KSC). This virtual tour includes information about our [Corrosion Laboratories](#) detailing efforts at the [Beach Corrosion Test Site](#) and the [Coatings Applications Laboratory](#). A [brochure](#) about our KSC Beach Corrosion Test Site

## 4. RESULTS

The home page of the corrosion site has been changed to make it more visual. The screen capture below shows part of the new home page with pictures of the Space Shuttle during launch along with photos showing how close the test site is to the launching pads and a close-up image of a corrosion coupon. These photos, which are thumbnails so that they will load quickly, are an important part of the new look on the web site.



### Purpose



This corrosion web site was developed to inform and educate on issues involving environmental deterioration of materials. The site includes information and pictures of the corrosion engineering, research, and testing capabilities at the Kennedy Space Center (KSC). This virtual tour includes information about our [Corrosion Laboratories](#) detailing efforts at the [Beach Corrosion Test Site](#) and the [Coatings Applications Laboratory](#). A [brochure](#) about our KSC Beach Corrosion Test Site

This home page and the pages that introduce main topics on the site also have buttons on the left for easy navigation among the various sections of the site. Links at the bottom of these pages also have e-mail connections to "corrosion@ksc.nasa.gov" for easy communications with KSC staff and links to the Materials Science Division, Logistic Operations, and KSC home sites.

Deeper into the site are sections discussing:

- Laboratories
- Corrosion Brochure
- Forms of Corrosion
- Protective Coatings
- Publications

Additional sections provide information under the following categories:

- Photo Archive
- Search
- Links
- Table of Contents
- Doing Business

The screen capture below shows a portion of one page with information on stress corrosion cracking. Similar discussions are available on all forms of corrosion and serve to both educate the public and highlight the KSC Materials Division corrosion capabilities.

The next two photos show intergranular SCC of an aluminum aerospace part. The intergranular nature of the corrosion can be seen in the scanning electron microscope image on the left and in the microscopic cross section on the right. The arrows indicate the primary crack shown in both pictures. Note that secondary cracks are also apparent. These secondary cracks are common in stress corrosion cracking.



## 5. RECOMMENDATIONS

- The revised KSC corrosion page should be placed on the web as soon as possible.
- Revisions should be incorporated into this web site whenever new corrosion information is made available.
- The recommended listings with Yahoo, Excite, and Webcrawler should be submitted to insure the new site increased visibility.

## 6. ACKNOWLEDGEMENTS

The author gratefully thanks James Martin, the Cal Poly student assistant who turned all of the ideas about these pages into computer code, and Louis MacDowell, the NASA-KSC colleague whose vision and foresight made this project possible.

Billy Deering provided invaluable assistance on all aspects of computer usage and made contacts with important KSC computer personnel possible. Peter Marciniak, Virginia Cummings, and Steve McDanel provided photographs which were used throughout the web site. Other Material Science Division Personnel who provided help include Tim Bollo, Cole Bryan, Luz Calle, Rupert Lee, Scott Murray, and Stan Young.

Ramon Hosler and Kari Stiles from the University of Central Florida ran the KSC NASA Summer Faculty Fellows program under the guidance of Gregg Buckingham and Jane Hodges from NASA-KSC. Their help and guidance made this project possible.

## REFERENCES

- [1] Peter Kent, Poor Richard's Web Site, Top Floor Publishing, Boulder, Colorado, 1998.
- [2] Molly Holzschlag, Sizzling Web Site Design, Sams.net Publishing, Indianapolis, Indiana, 1997.
- [3] John DeUlloa, The Step by Step Guide to Successfully Promoting a Web Site, Promote One, San Diego, 1997.
- [4] Crystal Waters, Universal Web Design, New Riders Publishing, Indianapolis, Indiana, 1997.



***EFFECTIVE INITIATIVES IN BEST LEADERSHIP PRACTICES***

**NASA/ASEE Summer Faculty Fellowship Program**

***Final Report***

**Brenda Hodges-Tiller, Ed.D  
Assistant Vice President for Academic Affairs  
Albany State University**

***NASA COLLEAGUES***

**Mr. James Jennings, Deputy Director of Business Operations  
Mr. Patrick Simpkins, Acting Personnel Officer  
Human Resources Policy, Development and Operations  
Mr. James H Norman, Employee Development Specialist**

**Kennedy Space Center, NASA  
University of Central Florida  
September 11, 1998**

## ABSTRACT

Winning organizations win because they have good leaders who nurture the development of other leaders at all levels of the organization. The ultimate test will be the degree of continued success the organization experiences as it moves into the next millennium. The major ingredient in the formula for winning organizations and winning leaders is the ability to develop leaders who exemplify proven best leadership practices. It is essential that changing organizational behaviors in the federal sector remain viable to be successful in a competitive society. NASA issued an agency-wide mandate to seek cutting edge strategies for smarter and better ways of doing business. The purpose of this activity is to identify best leadership practices of senior executive personnel at selected NASA Centers and corporate organizations of similar structure.

The primary objective of the project focused on a comparison of the best leadership practices of the executive teams of NASA Centers (KSC, Ames Research Center), executive teams of selected Fortune 500 corporations and other organizations exemplifying world class intelligence needed to maintain a competitive edge. The process focused on the utilization of an instrument specifically designed for interviews and forum groups to gather information from participants regarding critical knowledge, skills, experiences and personal characteristics necessary for success now and in the future.

The methodology included the following:

1. Review of the literature
2. Review of past activities
3. Acquisition of knowledge of interview instruments
4. Interviews with selected senior executives
5. Qualitative analysis of the data and the formulation of conclusions

The expected outcomes and formulation of conclusions will address:

6. The identification of critical knowledge, skills, best practices at KSC and selected corporations and other organizations.
7. Cross-referencing critical knowledge, skills, etc. with other known practices;
8. Identification of appropriate learning experiences and leadership training options for the target populace; and
9. Development of appropriate learning experiences and training modules specifically designed to address identified skills.

The outcomes are expected to complement and/or modify current and future leadership and management practices to enhance and ensure effective leadership for optimum success in a world class corporate environment where competition will be prevalent and ever increasing.

## ACKNOWLEDGEMENTS

I am most appreciative to The John F. Kennedy Space Center for the opportunity to explore the impact of best leadership practices on effective leadership. Many thanks to my NASA Colleagues, Deputy Director James Jennings, Mr. Patrick Simpkins and Mr. Jim Norman and the assistance of Ms. Shannon Roberts, Mr. Frank Nesbitt and Ms. Loretta Drier and Ms. Kim Cochrane, Ms. Evelyn Johnson and Ms. Helen Kane. Their direction and insightful assistance served to provide the support, information and resources necessary to complete this project. I am especially appreciative to Mr. James Jennings for the opportunity to interface with KSC, the administration and professional staff. I would be remiss if I didn't also extend my appreciation to Mr. Michael Hill, Ms. Marie Donat, Ms. Lorene Williams, Ms. Kathleen Ellis, and Ms. Shondrae Bain. The interaction and assistance of the entire Human Resources Development and Operations team have made my short tenure positive and rewarding added a dimension that has made the work on this project a smooth process and adventuresome.

Thanks to Lynn Diesel for her software support at KSC, Terry Teplitz at Ames Research Center and Jan Moore and Debbie Duarte from NASA Headquarters for their support throughout this project.

My special thanks to J. Albert Diggs for his support and assistance. While his retirement is an official status, his dedication and commitment to excellence for KSC remains a constant.

Finally, my appreciation to Dr. Ray Hosler, Mr. Gregg Buckingham and Ms. Kari Stiles and Dr. Jane Hodges for a positive experience and the opportunity to work with such a professional team.

## 1.0 INTRODUCTION

Today's leaders face many issues in the corporate world. Staying abreast of the accelerating rate of change, motivating employees, obtaining reliable information, competing internationally are constants. The rate of technological change alone exceeds the comprehension of any concept possible a decade ago. Employees are more educated and demand greater empowerment. Customers' product and service expectations are higher and thus, no organization can afford to overlook quality.

Few CEOs and managers have cause to doubt that the American business scene is undergoing vast changes. To meet the challenges of the future, now as never before, there is a growing awareness that the success of any organization is directly dependent upon the effective use of human resources. As one considers the challenging problems in the management of organization-business (profit and nonprofit), government, educational agencies, military, and family, the real test of ability for future leaders is how effectively they can establish and manage human organizations.

The executive team for NASA embarked upon a NASA Initiative to create an agency wide leadership and management development to compliment the NASA Strategic Plan and Strategic Management System. The Model is also intended to ensure that:

- a. The learning strategy for leadership and management development is integrated across The Agency.
- b. There is a broadening of learning modalities that go beyond traditional classroom techniques and include learning from experience, peers and managers.
- c. There is a method that will allow ongoing measurement and evaluation of the effectiveness of leadership development activities at the individual and organizational levels.

One of the cornerstones of NASA's Initiative is the development of a set of Performance Dimensions designed to be applicable across the NASA Agency and across all functional and leadership roles. Performance Dimensions, as defined by NASA, are measurable skills, knowledge, and personal characteristics that can best demonstrate the delivery of higher performance based on a comprehensive plan to include assessment, development and coaching applications.

Performance Dimensions are designed to be applicable across The NASA agency and across all functional and leadership roles including: Senior Executives, Managers or leaders of others such as managers or supervisors, Team Leaders, and Individuals in technical leadership positions such as SES Technical or Professional, R & D and Program and Project Managers.

A critical challenge facing all senior executives is how to exercise effective managerial leadership throughout their organizations. In organizations with four or more strata, it is not physically possible for the CEO to build and sustain an effective interpersonal relationship with all employees. Senior executives will need to seek ways to continue to communicate across the strata to maintain interpersonal relationships with all employees.

There is a specific set of practices that must be carried out if senior executives in any organization hope to lay a strong foundation for everybody moving in the same direction in an enthusiastic and innovative manner. Actions are not a matter of choice as to whether or not the choices will or will not be made. These are executive imperatives.<sup>1</sup>

---

<sup>1</sup> Jaques, Elliott and Clement, Stephen. *Executive Leadership*. Cason Hall & Co. Publishers. Falls Church, VA. 1994.

To meet these challenges, leaders must prepare and groom future leaders to ensure that they possess the appropriate core knowledge, business skills and personal attributes necessary to effectively lead in the world class business environment of the next millennium. Today's leaders are compelled to prepare their organizations for future success. This is only possible by creating environments now which support and nurture change for the future.

An antecedent to The NASA Initiative was The KSC Initiative. A special team was established and charged to define the essential skills required to facilitate leaders in creating an environment conducive for change. The team's activities addressed the following goals:

1. Define the skills necessary for supervisor/team leaders to perform effectively at KSC.
2. Define a set of training modules that will provide these skills.
3. Define requirements for maintaining and reinforcing supervisory leadership critical success factors.
4. Define performance measures to evaluate the effectiveness of the training.

The team, termed "The LEAP team", formulated a list of skills needed for senior executives, supervisors and team leaders of the future based on the goals and external surveys sent to selected industries and government. The surveyed participants served as benchmarks and the data served to assist in designing a tool for identifying skills and behaviors (critical success factors) of the best leadership practices in the participating agencies. These data were used to formulate objectives for training modules, alternatives, resources and methods.

This initial process, and the subsequent design of The Leadership Excellence Achievement Program, called LEAP, is considered tantamount to The NASA Initiative. The LEAP is designed to facilitate The Center's leaders in the creation of an environment that supports and nurtures a transition to the future.

The LEAP, which addresses knowledge, skills, critical success factors and behaviors that are considered essential to best leadership practices for KSC, is recommended as required training for new and existing leaders including executive staff, senior management staff, directors, deputy directors, comparable offices, division Chiefs, branch chiefs and functional leaders.

This project's foundation is based on the historical perspectives of the NASA Initiative and The KSC LEAP.

## 2.0 REVIEW OF THE LITERATURE

Leadership has been defined by many from many different perspectives. Most definitions reflect the assumption that leadership involves a social influence process whereby one person exerts intentional influence over other people to structure the activities and relationships in a group or an organization. Otherwise, the definitions differ in many respects, including who exerts influence, the intended purpose of the influence, the manner in which influence is exerted, and the outcome of the influence attempt.

Jaques defines leadership as "... that process in which one person sets the purpose or direction for one or more other persons, and gets them to move along together with him or her and with each other in that direction with competence and full commitment."<sup>2</sup> This definition is not intended to describe how one goes about the process of achieving it, or the mental characteristics and organizational conditions necessary for doing so. Leadership is not an isolated activity; it is one function, among many, that occurs in some but not all roles.

Some theorists have advocated treating the acts of leading and managing as separate processes. This distinction is considered by some to be an arbitrary one that seems simplistic and unnecessary. In leadership, it is important to interpret events, chart a course for the organization, and build commitment for shared objectives. It is equally important to help followers organize themselves in an efficient way and maintain cooperative interpersonal relationships as they work together to accomplish the objectives. If many leaders are ineffective due to omitting or

---

<sup>2</sup> Jaques, Elliott and Stephen D. Clement. *Executive Leadership*. Cason Hall & Co. Cambridge, Mass. 1994.

neglecting to address these functions, somehow this oversight should be addressed to ensure a wholistic approach to leading and managing.

Doug Snetsinger, Executive Director of The Institute of Market Driven Quality, a division of the Faculty of Management at the University of Toronto surveyed 326 Canadian CEOs to determine the relationship between the senior executive's personal development and the organization's performance. Data revealed that regardless of the size of the business or the industry in which it competes, organizations headed by nurturing leaders are far more likely to be achieve their operational goals.<sup>3</sup>

Edgar Schein indicates that leaders of the future will need to be perpetual learners and teachers. This will require (1) new levels of perception and insight into the realities of the world and also into themselves, (2) extraordinary levels of motivation to go through the inevitable pain of learning and change, (3) the emotional strength to manage their own and others' anxiety as learning and change become more and more a way of life; (4) new skills in analyzing and changing cultural assumptions; (5) the willingness and ability to involve others and elicit their participation; and (6) the ability to learn the assumption of a whole new organizational culture.<sup>4</sup>

Empowerment has been defined as "the creation of an environment which employees at all levels feel that they have real influence over standards of quality, service, and business effectiveness within their areas of responsibility."<sup>5</sup>

The ability of leaders to ensure empowerment as a reality is important. Empowered employees make more decisions and have more accountability. This may differ in large, expansive, successful organizations where there are more decisions to make. In growing organizations where the executive leadership has created an empowered culture of empowered employees, executives learn to move flexibly from one group to another to solve problems, examine opportunities, and provide encouragement and/or moral support.

We measure what we treasure. Today, managerial accounting omits from its accounts and accountability, large portions of behaviors and outcomes that are associated with leading people and consequently, organizations end up measuring some the costs of mismanaging people on the negative side of balance sheets. Other organizational debits are exemplified below:

- \* Under-informed employees
- \* Lack of urgency and initiative
- \* Limited new ideas and innovations
- \* Excessive absenteeism and accidents
- \* Costly disputes and grievances
- \* Tampering and sabotage
- \* Angry, alienated customers<sup>6</sup>
- \* Negative public image
- \* Under-performing technologies
- \* Underdeveloped products and markets
- \* Lack of employee commitment and goodwill
- \* Conformity and over-compliance
- \* Stress-related work compensation claims

Leaders with proven track records of success take direct responsibility for the development of other leaders. Leaders who develop other leaders have teachable points of view in the specific areas of ideas, values, emotional energy and edge. Tichy advocates the concept of the teaching organization rather than the learning organization and theorizes that, to be an effective teacher, one needs to be a world-class learner. He further indicates that winning leaders'-teachers' ideas are articulated and taught to others regarding how to make the

---

<sup>3</sup> Snetsinger, Doug. *Learning Leaders: Perspectives From Canadian CEOs*, Institute of Market Driven Quality, Faculty of Management, University of Toronto, pp. v, 9.

<sup>4</sup> Schein, Edgar. *Organizational Culture and Leadership*, pp. 391-392.

<sup>5</sup> The Price Waterhouse Change Integration® Team. *Better Change: Best Practices for Transforming Your Organization*. Irwin Professional Publishing, pp. 95.

<sup>6</sup> Rosen, Robert H. *Leading People*, Viking Penguin. Ontario, Canada. 1996.

organization successful in the marketplace and how to develop other leaders.<sup>7</sup>

Many evaluate leadership effectiveness in terms of the consequences of the leader's actions for followers and other organization stakeholders. Criteria will vary as leaders move their organizations into the next millennium. Transitional change will become a major factor. Kouzes claims that future leaders must be change agents as well as innovative in their strategizing.<sup>8</sup> The leader of the future will forge change for new practices, pioneer innovative practices and navigate change processes to remain continuously effective. Carrigan purports that change will mandate leaders to take risk, accept responsibility, and be accountable for their actions. He also advocates that effective leaders, to be future change agents, must:

- Respect all people; promote unity, trust, pride and dedication to the stated mission.
- Strive to achieve a high quality of work life through involvement of all our people in an environment of openness and fairness in which everyone is treated with dignity, honesty, and respect.
- Promote good communication among all employees by operating in an open atmosphere with freedom to share ideas and speak one's mind without fear of reprisal.<sup>9</sup>

Today, the function of leadership continues to be a primary concern of every major organization. Senior executive teams recognize the importance of strategic planning, the preparation and retention of a competent workforce for the next millennium. This is only possible when a dynamic leadership team is in place to support and nurture a positive cultural change.

### 3.0 METHODOLOGY

Interviews were conducted with seven (7) CEOs and Executive Officers of Fortune 500 companies and other organizations and agencies. Participation selections were made because of their notable contributions to their various professions and businesses (Please refer to the comprehensive report for complete descriptions).

Interviewed CEOs and Executive Officers included the following corporations and organizations:

Proctor and Gamble Paper Products  
Delta Air Lines, Inc.  
Synovus Financial Corporation  
Georgia Department of Human Resources  
Miller Brewing Company  
NationsBank Corporation  
Albany State University

*Synovus Financial Corporation* is a multi-billion dollar, multi-financial services company that traces its roots back to 1888 with the founding of CB&T in Columbus, Georgia. It is composed of 34 banks, operating in the states of Georgia, Alabama, Florida, and South Carolina. Synovus, as a subsidiary of Total Systems, for the 15<sup>th</sup> consecutive year of increased revenues, net income and new accounts, experienced a 20.4 percent increase for 1997. A component of the S&P 500 Index, Synovus was named 11<sup>th</sup> on FORTUNE Magazine's inaugural list of "The 100 Best Companies to Work For in America."

*Delta Airlines, Inc.* recorded \$886 million in net income and \$1.6 billion in operating income in 1997. It is one of the largest U.S. airlines based on aircraft departures and passenger enplaned, and the third largest U.S. airline as measured by operating revenues and revenue passenger miles flown. Internationally, Delta is the leader across the North Atlantic with more than 67,000 employees. The Airline's international route network covers 68 cities in 38 foreign countries and provides air freight, mail and other related aviation services.<sup>10</sup>

<sup>7</sup> Tichy, Noel. Eli Cohen. *The Leadership Engine*. Harper Business. New York, New York. 1997.

<sup>8</sup> Kouzes, James. Barry Z. Posner. *The Leadership Challenge*. Jossey-Bass Publishers. San Francisco.

<sup>9</sup> Carrigan, P.M. "Up from the Ashes". *OD Practitioners*, 1986, 18 (1). pp.2-3.

<sup>10</sup> *Delta Air Lines 1997 Annual Report*. Delta Air Lines, Inc. Atlanta, Georgia

*The Georgia Department of Human Resources (Georgia DHR)* operates with a budget of more than \$2 billion. The Department responsibilities, with more than 24,000 employees, are vast and touch the lives of every of Georgia citizen in some respect. The five divisions of The Georgia DHR which include:

- \* Division of Family and Children Services
- \* Division of Aging Services
- \* Division of Public Health
- \* Division of Mental Health/Mental Retardation/Substance Abuse
- \* Division of Rehabilitation Services<sup>11</sup>

*Miller Brewing Company*, a subsidiary of The Phillip Morris Companies, Inc., operates plants in six (6) states and distributes throughout the U.S, Puerto Rico and twenty-three (23) foreign countries. Miller Brewing reported \$4,201 million in operating revenues and \$459 million in operating companies income.<sup>12</sup> The Albany Brewery, one of the largest plants, is staffed with eleven (11) managers, twenty-seven (27) team managers, thirty-two (32) reliability engineers six (6) systems engineers, twenty-three (23) QS engineers and seven (7) administrative assistants.

*NationsBank Corporation*, soon to complete a merger with Barnett Banks, held approximately \$310 million (January 1, 1998) in assets and ranks as one of the three largest banking companies in the nation. This corporation is noted as one of America's largest and most diverse banking companies.<sup>13</sup> NationsBank operates in more than 26 states and provides services to more than 20 million customers throughout the country.

*Procter and Gamble Paper Products (P&G)*, with more than \$35.7 billion in net sales and over \$3.4 billion in 1998, operates 300 plants in more than (70) countries to include the US, Europe, the Middle East and Africa, Asia and Latin America. P&G markets more than three hundred (300) brands to nearly five billion consumers worldwide. This company employs more than 106,000 persons globally.<sup>14</sup>

*Albany State University*, located in the Southwest corner of Georgia, is a regional university serving with one of the most diverse student clientele in The University System of Georgia. This institution suffered major losses in The Flood of 1994 and 1998 and has successfully reclaimed many of the flooded structures as well as built new structures with more than \$22 million in state funds. Over the past 5 years, The University's enrollment has increased and remained constant; even during the major recovery period in 1994.<sup>15</sup>

### 3.1 THE INTERVIEW INSTRUMENT

The interview instrument contained ten (10) major questions with several sub-questions for most questions. The content of the survey instrument was developed by utilizing questions from The Individual and Focus Group Questions of The NASA Initiative and The KSC Supervisor/Team Leader Training Evaluation Team Local Survey (See Appendix B).

### 3.2 DATA GATHERING SESSIONS

Interviews were conducted with each selected CEO and Senior Executive Officer to garner their perceptions of the core knowledge, interpersonal skills and other critical success factors that have attributed to their effective leadership. Prior to the scheduled interaction, each interviewee was provided the ten (10) questions to ensure that the responses genuinely reflected their perspectives on best leadership practices.

Responses were recorded, edited and returned to each participant for review, corrections, and modifications necessary to crystallize or reinforce a particular given response. A database was developed from the information gathering sessions for quantitative data analysis purposes. A frequency analysis of the interviewees'

<sup>11</sup> *Georgia Department of Human Resources 1997 Annual Report*. Atlanta, Georgia.

<sup>12</sup> *The Phillip Morris Companies, Inc. 1997 Annual Report*. New York, NY.

<sup>13</sup> *NationsBank Corporation 1997 Summary Annual Report*. NationsBank Corporate Center, Charlotte, North Carolina.

<sup>14</sup> *Procter&Gamble Annual Report 1997*. Cincinnati, Ohio.

<sup>15</sup> *Albany State University Archives*. Albany, Georgia.

perceptions of the knowledge, skills and other characteristics was performed to determine the essential skills that existing and prospective leaders should possess to ensure effective leadership in the competitive world class environment of the next millennium.

#### **4.0 RESULTS**

The survey instrument yielded a total of more than 950 responses from the ten (10) questions and sub-questions for data review. The qualitative data analysis revealed the most frequently identified key indicators in each section of the questions posed (See Appendix B). For this report, because of the requirement for brevity, statements have been abbreviated where possible. Responses for each question and sub-questions are indicated in each section of the comprehensive report.

The quantitative data analysis of the participants' perceptions of critical skills and success factors revealed a set of knowledge, skills, behaviors and personal characteristics exemplary of best principles essential to effective world-class leadership in the next millennium. When characteristics for leaders at all levels were compared to those identified for The LEAP, the comparisons in Exhibit 1.1 were noted. Participants' perceptions of the importance of leaders' knowledge, skills and behavior categories identified as essential for best leadership practices are summarized in Exhibit 1.2 while Exhibit 1.7 shows the frequency of the identified key indicators provided among the CEOs and executive officers.

#### ***Experiential Leadership Development Modules***

The development of a series of Leadership Development modules was initiated to address the identified essential skills and other related characteristics. The modules are designed to provide the participants with opportunities to first introspectively reflect on their feelings, attitudes and aspirations and subsequently evaluate them as well as their motives. Sessions are designed for 1-2 days and focus on group discussions, simulated exercises, role playing, experiential learning activities and other problem solving ventures (See Appendix C for a complete description).

### **LEADERSHIP, CHANGE AND DIVERSITY SERIES\*\***

#### **Welcome – Orientation Get Acquainted Session**

This session is important to provide participants with a brief overview of the Leadership, Change and Diversity program. Sessions will provide an opportunity to learn about each other from another perspective.

#### **Understanding Leadership**

The hallmark of an effective leader is clear focus and direction. Successful leaders operate with a vision of where they are going and they inspire others in the organization to "buy in". People are most productive when they have a clear understanding of "the big picture, their role and what is expected of them. Effective leaders understand this to be a key factor in successful leadership.

#### **Self-Assessment: What Kind of Leader Am I?**

Effective leaders first understand and feel good about themselves. Subsequently, they find it easier to demonstrate principled leadership and sound business ethics. They show consistency among principles, values and behavior and build trust with others through their own authenticity and follow-through on commitments. Sessions will provide opportunities for participants to identify and assess their own leadership styles.

#### **Exercising Collective Wisdom**

Leaders who tap into collective wisdom will first nurture a positive team environment. Leaders, by selectively sharing power, inspire their people to share, take responsibility and make commitments. In futuristic organizations, leaders will often find it necessary to share power, trust their people's competence and judgement, and thereby create leaders at all levels of the organization.

#### **Coaching and Developing**

Good coaches often make the difference between effective leaders and just leaders. Coaching requires skill communication, the ability to evaluate employees, articulate performance feedback and facilitate professional growth. Coaching a peer who is weak in an area which you have strengths is also a beneficial concept.

### **Capitalizing On Strengths in Diversity**

Leaders of the next millennium know that diversity will be a major source of organizational strength. Today, as well as in the future, maximizing diversity is a critical business issue. Creating a culture of respect is very important. This usually begins with leaders looking introspectively at their own passions and self-esteem to discover what makes them feel inspired and respected. Sessions will provide participants opportunities to reflect upon their own and others' perspectives and values to arrive at a better understanding and appreciation of differences, perceived or otherwise.

### **Effective Communications**

Effective communication skills form the foundation for successful management and leaders are not able to energize their people to follow unless they are able to communicate and demonstrate the ability to lead. Sessions are designed to assist participants in recognizing that effective leaders are effective communicators and to enhance participants' communication skills.

### **Adaptability to Change**

Effective leaders not only address day-to-day issues confidently, but are also able to adjust to multiple demands, shifting priorities, ambiguity, and rapid change. They learn from their experiences, opportunities and challenges and show resilience in the face of constraints, frustrations or adversity. Through it all, effective leaders demonstrate flexibility. Sessions will provide opportunities for participants to experience activities to fine-tune their ability to react proactively to rapid change and related issues.

**\*\*Due to the required brevity of this report, please refer to the comprehensive report for recommended module content and related references.**

## ***REFERENCES***

- Agor, W.H. "The Logic of Intuition: How Top Executives Make Important Decisions." *Organizational Dynamics*, 14 (3).
- Albany State University Archives*. Albany, Georgia. Albany State University.
- Argyris, C. "Teaching Smart People How To Learn." *Harvard Business Review*. 69 (3) 1991.
- Bennis, Warren. "Learning to Lead." *Executive Excellence*, January, 1996.
- Blanchard, Kenneth and Michael O'Connor with Jim Ballard. *Managing By Values*. San Francisco, CA. Berrett-Koshler Publishers, Inc. 1997.
- Blanchard, Kenneth and Sheldon M. Bowles. *Gung Ho!: Turn On The People in Any Organization*. New York, NY. William Morrow and Company, Inc. 1998.
- Carrigan, P.M. "Up from the Ashes". *OD Practitioners*, 1986.
- Delta Air Lines 1997 Annual Report*. Atlanta, Georgia. Delta Air Lines, Inc.
- Georgia Department of Human Resources 1997 Annual Report*. Atlanta, Georgia. Georgia Department of Human Resources.
- Jaques, Elliott and Clement, Stephen. *Executive Leadership*. Falls Church, VA. Cason Hall & Co. Publishers. 1994.
- Hahn, Robert. "How Tough Is It To Be A College President?" *The Chronicle of Higher Education*, Jan.6, 1995.
- Kouzes, James. Barry Z. Posner. *The Leadership Challenge*. San Francisco, CA. Jossey-Bass Publishers. 1996.

*The Philip Morris Companies, Inc. 1997 Annual Report.* New York, NY. The Philip Morris Companies, Inc.

The Price Waterhouse Change Integration® Team. *Better Change: Best Practices for Transforming Your Organization.* Irwin Professional Publishing. 1997.

Tichy, Noel and Eli Cohen. *The Leadership Engine.* New York, NY. Harper Business. 1997.

Yukl, Gary A. *Leadership in Organizations.* Englewood Cliffs, NJ. Prentice Hall. 1994.

**EXHIBITS**

**Exhibit 1.2: CEOs' and Executive Officers' Perceptions of The Critical Level of Leaders' Knowledge, Skills and Behavior Categories. (N=8)**

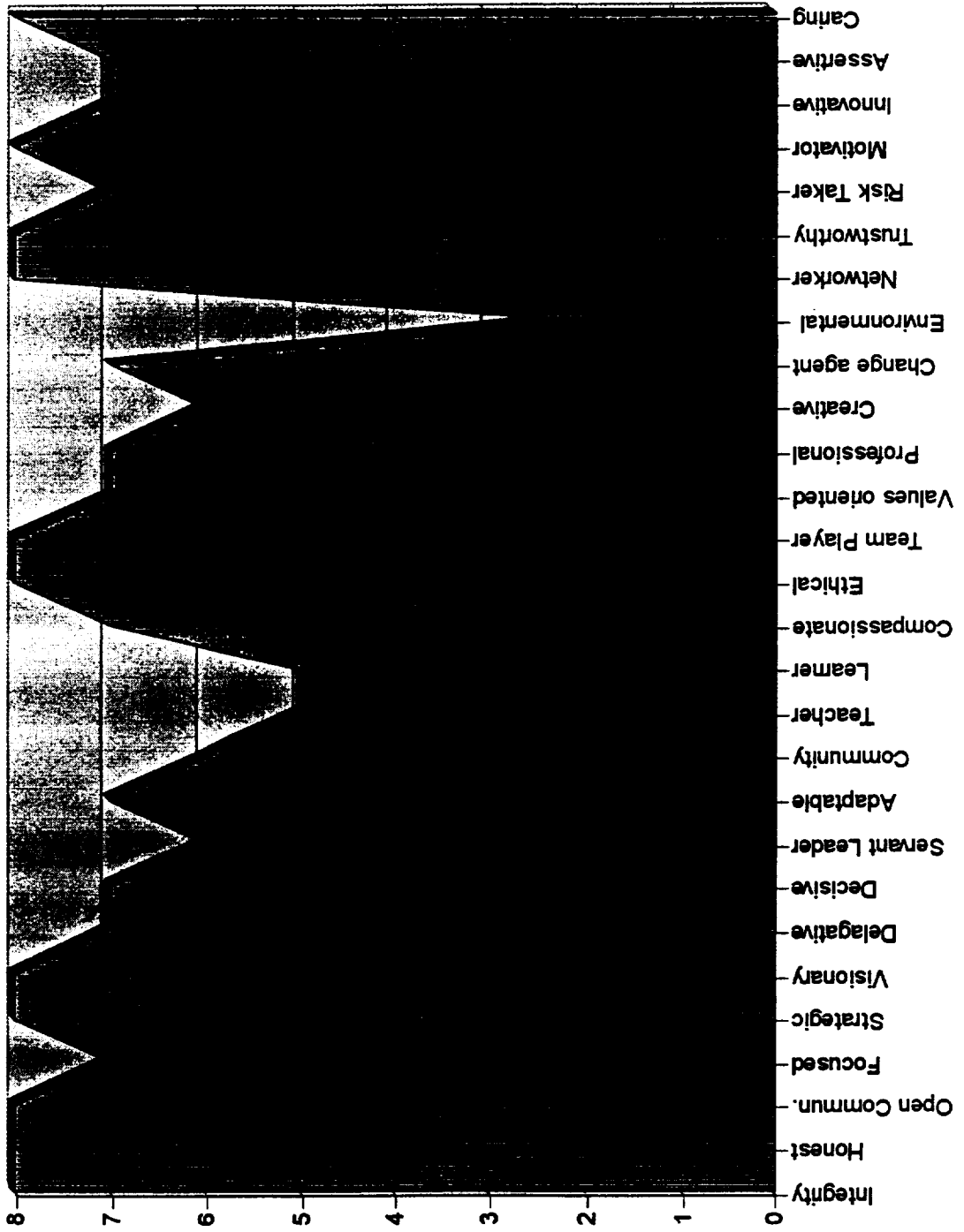
Overall Critical Rating (1-7)	1	2	3	4	5	6	7
Organizational Knowledge Skills							
Interpersonal Knowledge Skills							
Business Management Knowledge Skills							
Strategic Planning Knowledge Skills							
Technical Knowledge Skills							

**Exhibit 1.1: A Comparison of Characteristics for Leaders At All Levels**

Characteristics	CEOs	The LEAP
1. Self-Confidence	X	
2. Change Agent	X	
3. Visionary	X	
4. Communicator	X	
5. Collaborative	X	
6. Visionary	X	
7. Strategic	X	
8. Analytical	X	
9. Detail Oriented	X	
10. Risk Taker	X	
11. Empathetic	X	
12. Broad Based	X	
13. Knowledgeable	X	
14. Business	X	
15. Fair	X	
16. Pragmatic	X	
17. Direct	X	
18. Humble	X	
19. Humble	X	
20. Analytical	X	
21. Analytical	X	
22. Analytical	X	
23. Analytical	X	
24. Analytical	X	
25. Analytical	X	
26. Analytical	X	
27. Analytical	X	
28. Analytical	X	
29. Analytical	X	
30. Analytical	X	
31. Analytical	X	
32. Analytical	X	
33. Analytical	X	
34. Analytical	X	
35. Analytical	X	
36. Analytical	X	
37. Analytical	X	
38. Analytical	X	
39. Analytical	X	
40. Analytical	X	
41. Analytical	X	
42. Analytical	X	
43. Analytical	X	
44. Analytical	X	
45. Analytical	X	
46. Analytical	X	
47. Analytical	X	
48. Analytical	X	
49. Analytical	X	
50. Analytical	X	
51. Analytical	X	
52. Analytical	X	
53. Analytical	X	
54. Analytical	X	
55. Analytical	X	
56. Analytical	X	
57. Analytical	X	
58. Analytical	X	
59. Analytical	X	
60. Analytical	X	
61. Analytical	X	
62. Analytical	X	
63. Analytical	X	
64. Analytical	X	
65. Analytical	X	
66. Analytical	X	
67. Analytical	X	
68. Analytical	X	
69. Analytical	X	
70. Analytical	X	
71. Analytical	X	
72. Analytical	X	
73. Analytical	X	
74. Analytical	X	
75. Analytical	X	
76. Analytical	X	
77. Analytical	X	
78. Analytical	X	
79. Analytical	X	
80. Analytical	X	
81. Analytical	X	
82. Analytical	X	
83. Analytical	X	
84. Analytical	X	
85. Analytical	X	
86. Analytical	X	
87. Analytical	X	
88. Analytical	X	
89. Analytical	X	
90. Analytical	X	
91. Analytical	X	
92. Analytical	X	
93. Analytical	X	
94. Analytical	X	
95. Analytical	X	
96. Analytical	X	
97. Analytical	X	
98. Analytical	X	
99. Analytical	X	
100. Analytical	X	

Exhibit 1.7

Frequency of Identified Key Indicators



# **1998 NASA/ASEE SUMMER FACULTY FELLOWSHIP PROGRAM**

**JOHN F. KENNEDY SPACE CENTER  
UNIVERSITY OF CENTRAL FLORIDA**

## **OMNIBOT MOBILE BASE**

**Nasser Houshangi, Ph.D., P.E.  
Associate Professor of Electrical Engineering  
Department of Engineering  
Purdue University Calumet**

**NASA/KSC Colleague: Tom Lippitt  
Lead/ Automated Ground Support Systems Lab  
Robotics and Automation**

### **ABSTRACT**

The objective of this project is to develop a highly maneuverable mobile base suitable for operation in a hazardous environment. The base utilizes Omni wheels whose unique motion properties allow for complete three degrees of freedom: two translation degrees and one rotational. The phase I of the project, construction of the Omnibot mobile base is already complete. The mobile base provided the testbed going into the phase II of the project. Our main emphasis is to incorporate a vision system, and hazardous gas detectors to the mobile base. The Omnibot mobile system consist of two main components, the mobile base and the command base. The issues concerning the mobile base and the command base design and implementation for phase II is detailed in this report.

## 1.0 INTRODUCTION

Mobile robots provide a suitable alternative for many hazardous environment applications [1,2,3]. Responding to incidents involving hazardous materials can be extremely dangerous and requires specially trained personnel. A remotely controlled Omnibot mobile base equipped with sensors like vision system, gas detectors, and a robotic arm is an effective tool. At Kennedy Space Center, there are number of applications which may be desirable to use the Omnibot. Possible applications are in the Hypergol Test Facility, fire and rescue, and the Shuttle Landing Facility (performing initial sweep around the shuttle).

Instead of personnel approaching hazardous or unknown environment, the Omnibot mobile base is send first to the site to insure that the location is safe. In case hazardous materials are detected, the Omnibot is to Investigate the source of the problem and alert the operator. The tasks Omnibot mobile base may be required to perform:

- Traveling on various surfaces at different speed ranges
- Maneuvering in confined spaces
- Providing visual feedback
- Detecting remote hazardous gas detection
- Manipulating and moving objects at the incident site

Steps taken to be able to use the mobile vehicle in hazardous environments are: (i) The mobile base is sealed so all areas of the robot that contain electrical components can be pressurized; (ii) Solid state devices are used to eliminate electrical arcs and sparks where ever possible and the wheels are derived with brushless DC motors.

The Omnibot project is divided to three phases. Phase I dealt with the mobile base construction. The base utilizes Omni wheels whose unique motion properties allow for the mobile base complete three degrees of freedom: translation in the x and y directions and rotation in the z direction. The hazard proofed mobile base will provide the testbed for sensors, and a robotic arm with an end-effector. This phase is already complete.

Phase II objectives are to incorporate vision systems, hazardous gas detectors, and command and mobile base design and implementation. The command base is responsible for issuing the desired action for the mobile base, the robotic manipulator, and the vision system. In the phase III, a robotic manipulator with an end-effector and a wrist mounted camera will be developed on the mobile base.

This report summarizes the work completed during the summer of 1998 on the phase II of the Omnibot project. In section 2, the aspects relating to the mobile base will be discussed. The command base issues are detailed in Section 3. The discussions and conclusions are presented in sections 4 and 5, respectively.

## 2.0 MOBILE BASE ISSUES

At the end of phase I , the constructed mobile base shown in figure 1 is controlled remotely by an operator using a control box. A joystick, an RF transmitter, and number of switches (power, low/high speed, E-stop, and a deadman) make up the control box. The communication between the control box and the mobile base computer is established using an RF modem. Single board Intel 486 based microcomputer is used to control the wheels of the mobile base in conjunction with motion controllers. The software program is written using C language on a DOS operating system platform.

The work done on the mobile base to integrate sensors to the Omnibot is described next. In Section 2.1, the hardware and software requirement of the mobile base to support the phase II and III of the project is discussed. The vision system is detailed in Section 2.2.

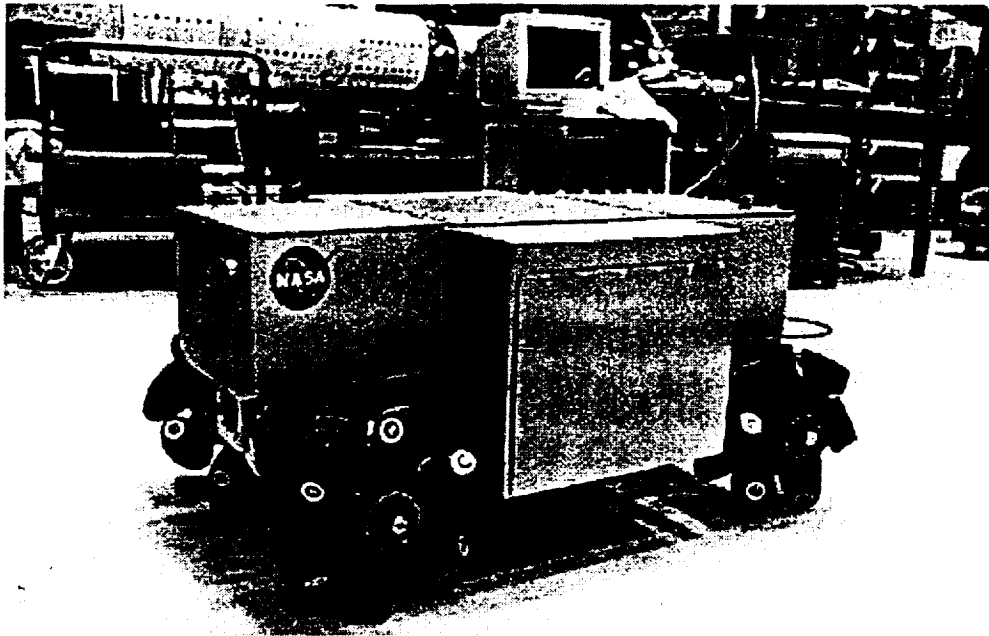


Figure 1. Omnibot Mobile Base

### 2.1 Mobile Base Software and Hardware

In order to decide on the proper platform, one should consider the required tasks needed to be performed by the mobile base computer. The tasks are : (i) control the mobile base independent four wheel drive; (ii) control the cameras; (iii) control the robotic arm and the end-effector; (iv) monitor the gas detectors; (v) communicate with the command base; and (vi) provide flexibility to add other sensors as needed in the future. The different tasks mentioned above are performed simultaneously in real-time. A real-time

system is characterized by the need to respond rapidly to events occurring asynchronously in time. The computational load for performing the mentioned real-time tasks will be demanding on a single processor.

For the phase I, a single STD-32 Ziatech processor with DOS operating system is used. STD-32 bus supports 32-bit data transfers across the backplane, without multiplexing of the signals. The STD-32 bus can run at 32 M byte per second. STD-32 performance characteristic are multiprocessing, with centralized arbitration logic; 32 bit addressing and pipelining, high speed DMA; and slot specific interrupts. A standard for interprocessor communication (IPC) software incorporates a NetBIOS layer to simplify communication between multiple processors in a single system.

To select a proper platform, different operating systems were considered. From the considered list two options appeared promising. First option was to use QNX real-time operating system. QNX provides multitasking, priority-driven preemptive scheduling, and fast context switching - all essential ingredients of a real-time system. The STAR-QNX from Ziatech offers the multitasking QNX operating system on the multiprocessing STD-32 Star System.

DOS operating system with STD-32 Star multiprocessing computer system was considered as a second option. In this configuration each CPU has its own local memory and DOS operating system, but shares backplane memory, DOS disks, and video with other CPUs in the system. This platform works very effectively if the tasks every processor performs real-time are independent for each processor. DOS is non intrusive and can be used as a real-time operating system but it is not multitasking. Operating systems like AMX from Kadak company can work with DOS to provide a multitasking real time operating system if the need exist.

The second option was selected as a software platform. One advantage of second option is that the code written to control the mobile base for the phase I can be used without any changes. The other feature of using DOS in control system is familiarity and the wealth of software available to help get the job done. The first option would have been a overkill for this project and would have cost significantly more.

As far as mobile base hardware, two processors will be used with a arbiter card. The arbiter provides STD-32 bus master arbitration to facilitate up to seven processors in an STD-32 system. The fact that more processors up to seven can be added, provide the flexibility for future development of the system. For now, the plan is to use an existing single board 486 based computer to control the mobile base or the robotic arm and monitor the gas detectors. Another single board Pentium based processor will serve as master in the multiprocessing system. The master processor will control the cameras and communicate with the command base. The hardware and software ordered for the system are included in the report submitted to the KSC colleague [4].

## 2.2 Vision System

Control of mobile robots with vision in the feedback loop has a long history both in robotics and machine vision feedback. The vision system plays an important role for the Omnibot mobile system by providing visual feedback to the operator. The feedback is used by the operator to guide the mobile base remotely.

Two cameras will provide the feedback. One CCD camera with a wide angle lens will be placed in a fixed position in front of Omnibot to provide a road side view to the operator. The other one will be a motorized camera (auto focus, zoom control) placed on a pan/tilt unit as shown in figure 2. The pan/tilt unit will sit on the middle right hand side on a platform raised from the top surface of the mobile base by 20 inches. This way the camera will provide a better viewing angles to the operator. As far as mechanical structure, the range for the eye pan is -159 to 159 degrees and the range for the eye tilt is -46 to 31 degrees .

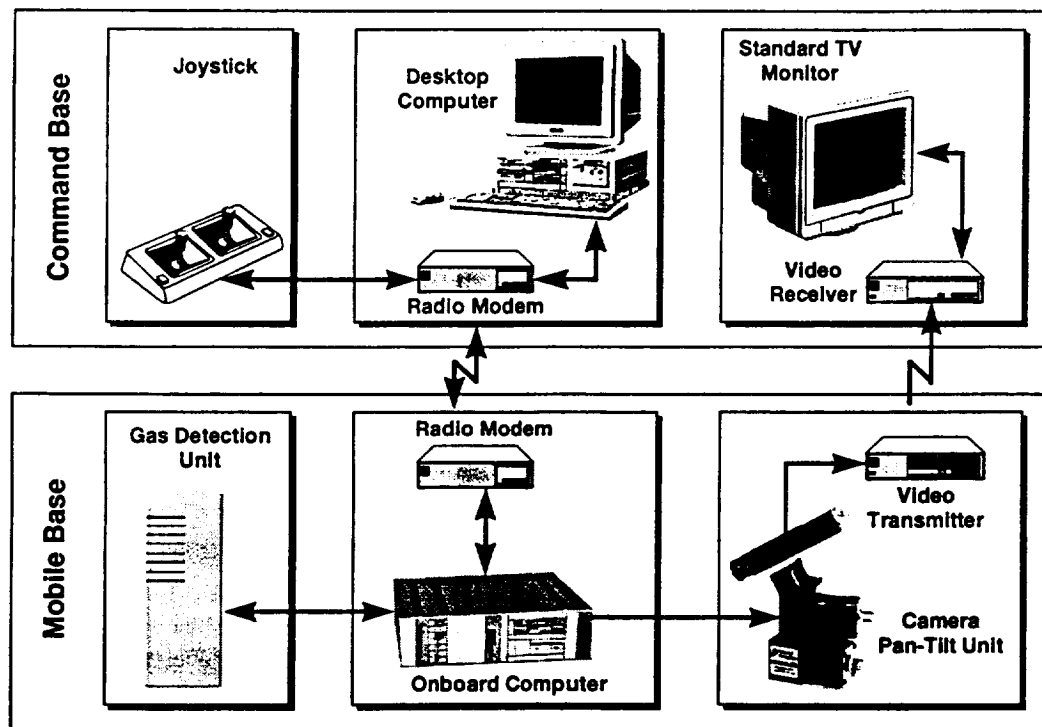


Figure 2. Teleoperated Omnibot Mobile System

A software program is written to control the pan/tilt unit in the vision system. The operator controls the pan right and left turns and tilt up and down movements using a joystick. A RS-232 interface for higher bandwidth binary serial communication is established between mobile base computer and the pan-tilt controller unit.

The motion of the pan/tilt unit is controlled with two levels of speed control based on the joystick position. At low speed, the operator will be able to zoom on a particular object, while high speed, will be used to change the camera view quickly (e.g. look behind). The pan/tilt joystick control program is written in the C language and successfully tested. The developed control software with documentation is given to my KSC colleague [4] which will be used to actively control the CCD camera on the pan/tilt unit.

As shown in figure 2, the signal from the camera is transmitted to a monitor at the command base using a wireless video transmitter/receiver. Number of commercial video transmitter/receiver were tested. As was indicated by the experiments, the transmitter and the receiver need to be in line of sight in order to receive an acceptable video signal. Finally, one providing a best range (close to a mile) with a solid video signal is selected and ordered.

### **3.0 COMMAND BASE ISSUES**

The command base specifies the desired trajectory for the mobile base, the robotic arm, and the camera pan/tilt unit, and monitors the gas detectors. The intend of the project is to make the command base a small portable unit which supports one operator. In section 3.1, the hardware and software platform used for the command base is discussed. The preliminary design work for the operator console is specified in section 3.2.

#### **3.1 Command Base Hardware and Software**

The command base is responsible for: i) issuing desired actions for the mobile base, camera's, and the robotic arm; ii) receive the status of the gas detectors; iii) provide the user interface; and iv) communicate with mobile base. A single board 200 MHZ Pentium processor with 4M byte flash PROM, 32 M byte RAM will provide the computing power needed for the command base. The command base is powered using a battery.

The operating system used for the command base is the Microsoft windows NT. This software platform will enable a graphical user interface to be developed for the system. A sun readable flat panel monitor will provide the desired display for the operator. The operator receives the visual feedback by looking at a TV monitor as shown in figure 2. The joysticks at the command base also shown in figure 2 will control the mobile base and the camera pan/tilt unit movements.

### 3.2 Operator Console

The operator console graphical display is the user interface between the operator and the command system. The operator will select from the screen the mode of operation which is explained in the next paragraph. The operator's monitor should indicate the status of (i) gas detectors; (ii) mobile and command base batteries; (iii) Omnibot wheels and brakes; and (iv) the temperature. The operator selects the Omnibot speed ( low or high ) from the screen and will be provided with the capability to select the camera for visual feedback, or stop the Omnibot in case of emergency.

Currently, the Omnibot mobile base is controlled only in a manual teleoperated mode. To provide flexibility and reduce operator load, three modes of autonomy in remote will be supported. The modes are manual teleoperated, telepresence, and supervisory control.

Manual teleoperation operating mode, defines all the situation in which the human operator is constrained to remain continuously in the control loop. If human operator stops controlling, the loop is opened, and the Omnibot is stopped .

The telepresence mode supports actions like Go-straight( ), Turn-left( ), Turn-right( ), and Go-back( ). An action finishes when the goal is reached, responding with a message of successful completion; one example of such a action is Go-straight (20ft, low speed), which will terminate when a distance of 20 ft. covered.

Supervisory control mode describes a wide range of options, according to which the human operator can take a variety of supervisory roles. As an example, the path the mobile robot needs to travel can be taught in advance. Then, in the supervisory mode the operator monitors the Omnibot mobile base. The human operator can take the Omnibot to the manual teleoperated mode if it chooses. The supervisory mode will be used in a structured environment to reduce the load on the human operator.

A software modular approach to a operator interface design is shown in figure 3. The interpretation module responsibility is to take the plan from the operator and issue actions to the command module and update the knowledge database. Knowledge database has all the data concerning the status of the sensors, actuators, Omnibot mobile base, and the robotic arm.

Both command and interpretation module could access information in the knowledge database and updates its contents. The command module executes the desired actions and issues the desired information for the control module. The information is send through an RF link using an RF modem to the Omnibot master processor. The control module responsibility is to control the actuators in the robotic arm, vision system, mobile base, and monitor the gas detectors based on the information received. This architecture will be more useful for the telepresence and supervisory control modes.

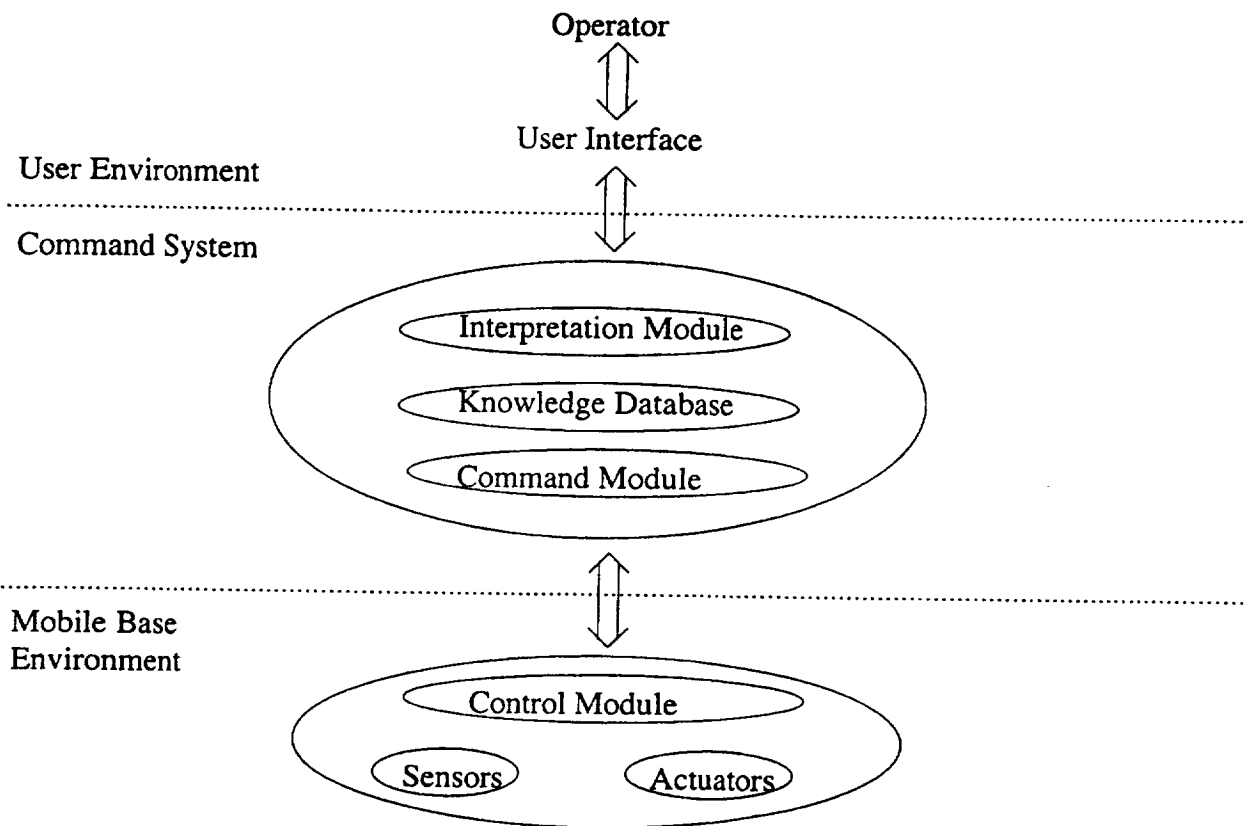


Figure 3 . Operator Interface Modular Architecture

#### 4.0 DISCUSSIONS

Currently, the Omnibot lacks the automatic collision avoidance capability. The operator need to use a deadman or a emergency switch to stop the mobile base. It is recommended that this capability be added to the Omnibot using ultrasonic sensors in a ring configuration.

Sonar sensing for collision avoidance, is cost effective, relatively quick in response, processing is not time consuming, and can cover wide horizontal range depending on the number of ultrasonic sensors attached. Although, once the height of sonar sensors fixed, the vertical readable range is very restrictive.

It may be desirable to provide feedback to the operator on three possible situations, no-treat, future-treat, or immediate-treat situation. In case of immediate-treat, immediate

action is taken by the Omnibot processor to stop the mobile base, independent of the operator. The operator using the visual feedback will then evaluate the situation and will provide the mobile robot with the desired action.

Another feature of the Omnibot is the gas detection capability. The gases like Oxygen, Combustible, Hydrogen, Ammonia, and Hypergol is of interest to sense. The challenge is to come up with a small multi-sensor gas detection unit capable of communicating with the Omnibot processors. For Hypergol testing a unit is already identified at the toxic vapor laboratory for possible use. It is realized that Hypergol detection needs to be a separate unit. For other gases, number of commercial products were considered and the information is passed to my KSC colleague for selection.

## 5.0 CONCLUSIONS

As was mentioned earlier, my main emphasis was the phase II of the Omnibot project. There are number of contributions made to the project during the summer of 1998. The proper hardware and software platform for the mobile base was selected and all the components identified and ordered. The software to control the pan/tilt unit using a joystick, which is an important part of the Omnibot vision system, was written and successfully tested. The pan/tilt motion with low and high speed control is very responsive to the joystick commands. The control software will be used to enable the operator to effectively point the camera to different locations. Number of wireless video transmitter/receiver were tested and one selected for the project. The use of proper gas detector was investigated. Also, the preliminary design work for the operator console was accomplished.

For future work, the following tasks are to be completed for the phase II of this project: (i) further design and develop software for a user friendly operator interface; (ii) develop software to monitor the gas detectors; (iii) control the mobile base in the telepresence and supervisory control modes; (iv) design and implement automatic mobile base collision avoidance.

## ACKNOWLEDGEMENTS

I like to express my sincere appreciation to my NASA-KSC colleague Tom Lippitt for his help and useful suggestions during this summer. I also like to thank Greg Buckingham, Ramon Hosler, Kari Stiles, and Jane Hodges for their contributions to a successful Summer Faculty Program. I learned a lot about Kennedy Space center facilities, operations, and goals. The people in automated ground system Bill Jones, Kim Ballard, Andy Bradley, Mike Hogue, Robert Morrison, and Flix Soto-Toro provided many helps when it was needed. Many thanks to all of you for helping to make this summer both enjoyable and professionally interesting.

**REFERENCES**

- [1] R.V. Welch, "A Mobile Robot for Reconnaissance of HAZMAT Incident Sites", Proceedings of the ASCE Specialty Conference on Robotics for challenging environments, Albuquerque, New Mexico, pp. 269-277, February, 1994.
- [2] J.S. Byrd, and R.O. Pettus, "A Robotic Inspector for Low-Level Radioactive Waste", Proceedings of the ASCE Specialty Conference on Robotics for challenging environments, Albuquerque, New Mexico, pp. 276-282, June, 1996.
- [3] H. Schempf, "Houdini: In-Tank Mobile Cleanup Robot", Proceedings of the ASCE Specialty Conference on Robotics for challenging environments, Albuquerque, New Mexico, pp. 286-295, February, 1994.
- [4] N. Houshangi, "Omnibot Mobile Base", Final report delivered to Tom Lippitt, 1988 NASA/ASEE Summer Faculty Fellowship Program, NASA Kennedy Space Center, 1998.

**1998 NASA/ASEE SUMMER FACULTY FELLOWSHIP PROGRAM**

**JOHN F. KENNEDY SPACE CENTER  
UNIVERSITY OF CENTRAL FLORIDA**

**NOISE CHARACTERIZATION AND COMPARISON OF ADAPTIVE NOISE  
SUPPRESSION ALGORITHMS**

**Dr. David Kozel  
Associate Professor of Electrical Engineering  
Purdue University Calumet  
Department of Engineering  
Hammond, IN**

**NASA/KSC  
NASA Colleagues: Frederick McKenzie and Richard Nelson  
Communications/RF and Audio**

**Abstract**

The noise characteristics of the emergency egress vehicle are determined. The noise reduction and intelligibility retaining capability of three different algorithms are compared: signal to noise ratio adaptive spectral subtraction using no reference microphone, signal to noise ratio adaptive spectral subtraction using a reference microphone, and adaptive noise cancellation using least mean square estimation.

## 1. Introduction

In an effort to reduce noise and improve the intelligibility of speech, it is desired to incorporate adaptive noise suppression into the communications equipment on the emergency egress vehicle and the crawler-transporter. An adaptive algorithm is necessary for both applications due to the varying nature of the noise. Furthermore, the noise frequencies produced by both applications are in the voice band range so standard filtering techniques will not work. In the following sections, the noise in the emergency egress vehicle is characterized, the spectral subtraction algorithm with and without a reference microphone and the least mean square algorithm are described, and results from these techniques are compared.

## 2. Characterization of the Noise

The noise level inside the emergency egress vehicle was measured using a decibel meter. The noise level is 90 decibels (dB) with the engine idling and 120-125 dB once the vehicle starts moving. As a result, it is impossible to understand what the crew is saying during a rescue operation. The noise inside the engine rooms of the crawler-transporter are also in the 120 dB range causing the same difficulty with communication. The headsets used by both crews have OIS-RF microphones, which have noise suppression of a mechanical nature and provide 15 decibels of noise suppression. Furthermore, the frequency response of the microphone and communication system attenuates frequencies outside of the voice band range of 300 Hz to 3 kHz. Since data from two microphones in close proximity was not obtained for the crawler-transporter, this report will consider only the case of the emergency egress vehicle. Due to the similarities of both applications, results should apply to the crawler-transporter.

The noise in the emergency egress vehicle was measured using a data acquisition circuit. For each microphone, data was sampled at 12.05 kHz using a 12-bit A/D converter. For signal conditioning, a high gain amplifier and anti aliasing filter with a 300 Hz to 3 kHz passband and minimum 30db attenuation at 100 Hz and 7.9 kHz was used. The combination of filter and signal power rolloff at higher frequencies proved sufficient to prevent aliasing. Three locations were tested for the reference microphone. They are shown in Figure 1.

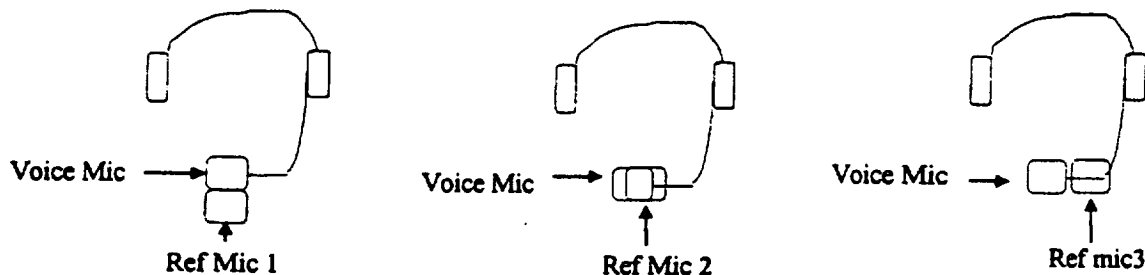


Figure 1. Relative Position of Voice and Reference Microphone

The reference microphone below the voice microphone is denoted as Ref Mic 1. The reference microphone behind and slightly to the side of the voice microphone is denoted as Ref Mic 2. The reference microphone to the side of the voice microphone is denoted as Ref Mic 3. For all three locations the reference microphone is facing opposite the direction of the voice microphone (i.e., away from the speaker).

Using 12,050 samples of noise data from each microphone, crosscorrelation and autocorrelation functions were estimated using the MATLAB function, `xcorr`. The normalized crosscorrelation between the voice microphones and each of the reference microphones was determined using:

$$\text{Normalized}(R_{xm}(\tau)) = R_{xm}(\tau) / \text{Sqrt}(R_{xx}(0) R_{mm}(0)) \quad (1)$$

where:

$R_{xm}(\tau)$  = crosscorrelation between the voice microphone and reference microphone signals with a time shift of  $\tau$  samples

$R_{xx}(0)$  = autocorrelation of the voice microphone signal with no time shift

$R_{mm}(0)$  = autocorrelation of the reference microphone signal with no time shift

$\text{Sqrt}()$  is the square root of the value in parentheses

The normalized crosscorrelations are shown in Figure 2. It can be seen that Ref Mic 1 and Ref Mic 2 are more highly correlated with the voice microphone. Furthermore, Ref Mic 1 correlates the best with a strong periodic component of the noise in the voice microphone. The autocorrelations of the voice microphone and Ref Mic 1 are shown in Figure 3. The average power difference between the microphones is seen from Figure 3 by comparing the autocorrelations with zero time shift. The quick reduction in the main lobe of the autocorrelation functions shows that except for the strong period component, the noise at any microphone becomes uncorrelated with itself within 10 samples (i.e., less than a millisecond).

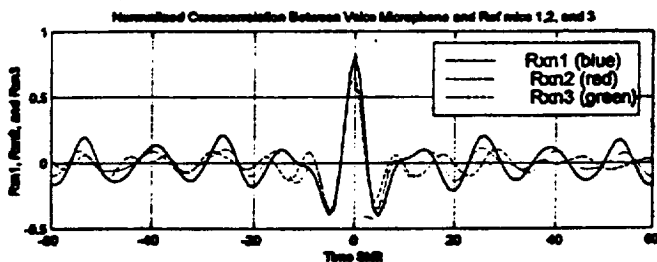


Figure 2. Normalized Crosscorrelation Between Microphones

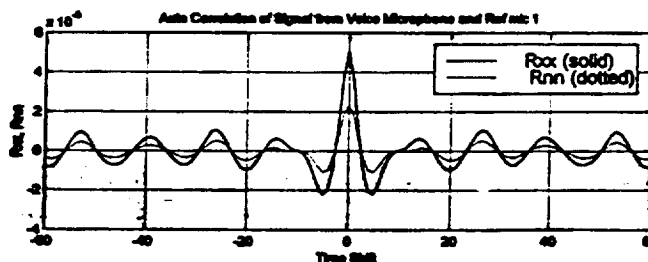


Figure 3. Autocorrelation of the Voice Microphone and Reference Microphone 1

A time segment containing only noise and the corresponding frequency response are displayed in Figure 4 for the voice microphone and Ref Mic 1. A second time segment and frequency response containing the onset of speech are displayed in Figure 5. From Figure 4 it is seen that Ref Mic 1 tracks the voice microphone fairly well in the time and frequency domains. The

differences in the response are due to microphone, amplifier, and anti aliasing filter characteristics and differences in the sound waves at each microphone. From Figures 4 and 5 it is seen that the noise characteristics change with time and thus need to be updated during speech. From Figure 5 it can be seen that the phase of the noise is independent of the phase of the speech.

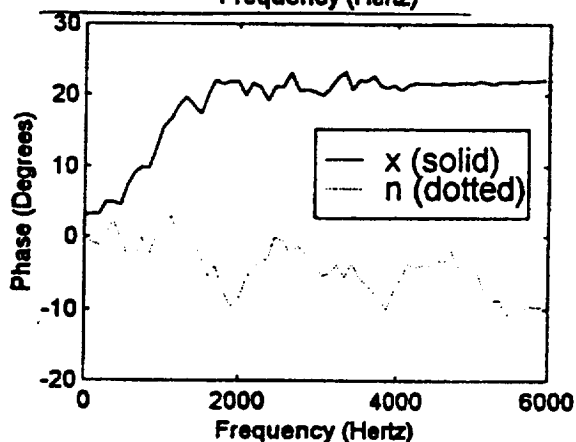
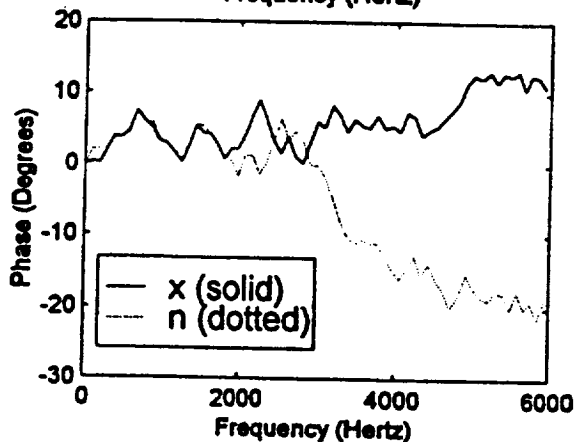
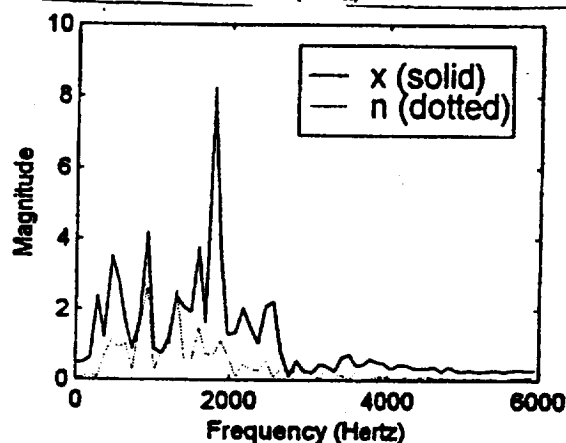
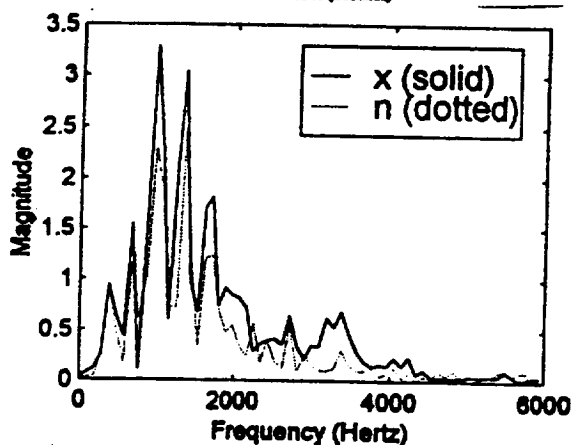
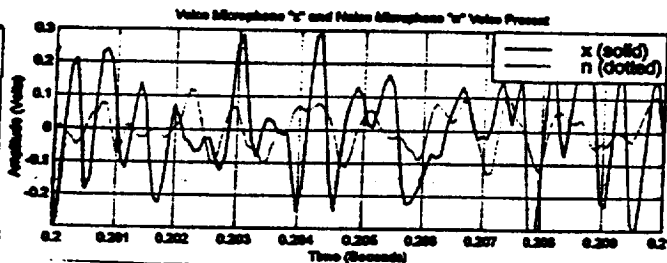
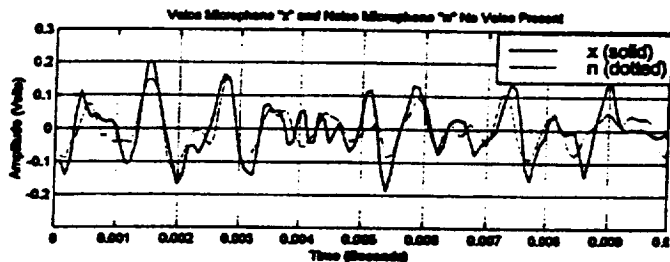


Figure 4 Time and Frequency Comparison for Noise Segment

Figure 5. Time and Frequency Comparison for Speech Segment

### 3. Spectral Subtraction Algorithm

A signal to noise ratio dependent adaptive spectral subtraction algorithm to remove the noise from a noise-corrupted speech signal was developed in [1] and was improved in [2] by adding prefiltering. Following is a description of the spectral subtraction algorithm.

The additive noise model used for spectral subtraction assumes that noise-corrupted speech is composed of speech plus additive noise.

$$x(t) = s(t) + n'(t) \quad (2)$$

where:

$x(t)$  = noise-corrupted speech

$s(t)$  = speech

$n'(t)$  = noise at the voice microphone

Taking the Fourier Transform of equation (2)

$$X(f) = S(f) + N'(f) \quad (3)$$

$X(f)$ ,  $S(f)$ , and  $N'(f)$  are complex so they can be represented in polar form.

$$|X(f)|e^{j\theta_x} = |S(f)|e^{j\theta_s} + |N'(f)|e^{j\theta_n} \quad (4)$$

Solving for the speech,

$$|S(f)|e^{j\theta_s} = |X(f)|e^{j\theta_x} - |N'(f)|e^{j\theta_n} \quad (5)$$

When a reference microphone is used, the differences in the microphones, amplifiers, and anti-aliasing filters,  $D(f)$ , are accounted for.

$$|S(f)|e^{j\theta_s} = |X(f)|e^{j\theta_x} - D(f)|N(f)|e^{j\theta_n} \quad (6)$$

Where,  $N(f)$ , is the frequency response of the noise at the reference microphone. When using a single microphone, no information about the noise is present during speech. The average noise when no speech is present is used in place of the noise during speech. Thus, no relative phase information is available for the noise estimate. For this reason, the phase of the noise-corrupted speech is commonly used to approximate the phase of the speech.

$$\hat{S}(f) = \left| \hat{S}(f) \right| e^{j\theta_x} = \left\{ |X(f)| - \sqrt{|N'(f)|} \right\} e^{j\theta_x} \quad (7)$$

This is equivalent to assuming the noise-corrupted speech and the noise are in phase. Since the algorithm is implemented on a digital signal processor (DSP) using an FFT, the signal is processed using frames of the input data. If a frame does not contain speech, the average noise estimate, for the single microphone case, or the difference between microphones, for the reference microphone case, are updated. For the algorithm developed in [1], the proportion of noise subtracted,  $\alpha$ , is variable and signal to noise ratio dependent.

$$\hat{S}(f) = \left\{ |X(f)| - \alpha(SNR(f))\sqrt{|N'(f)|} \right\} e^{j\theta_x} \quad (8)$$

For magnitude spectral subtraction using a reference microphone:

$$\hat{S}(f) = \left\{ |X(f)| - \alpha(SNR(f))D(f)\sqrt{|N(f)|} \right\} e^{j\theta_x} \quad (9)$$

An artifact of spectral subtraction is “musical noise”, random spectral components, which result from incomplete subtraction of spectral peaks that are much larger than the average for any given frequency. To reduce “musical noise”, the proportion,  $\alpha$ , is greater than one when speech is not present. This is termed over subtraction. Over subtraction reduces the musical noise at the expense of reducing the intelligibility of the speech. To reduce the loss in intelligibility,  $\alpha$  is proportional to the reciprocal of the noise-corrupted speech to noise energy and is thus reduced when speech is present. If for any particular frequency the subtraction results in a negative magnitude, the magnitude is set to zero. The inverse Fourier Transform yields the estimate of the speech.

$$\hat{s}(t) = F^{-1} \left\{ \hat{S}(f) \right\} \quad (10)$$

Using Figure 5, it was demonstrated in Section 2 that the assumption of the noise and speech being in phase has no basis. Since the two signals have no physical dependence, the phase difference between them has an equal probability of being any value between  $-\pi$  and  $\pi$  radians. This implies that the magnitude of the noise-corrupted speech can be larger or smaller than the magnitude of the speech with equal probability. Furthermore, the noise-corrupted speech should not be in phase with the noise or the speech. Thus, subtracting an in-phase noise signal from the noise-corrupted speech has the same probability of distorting the speech further as it does of reducing the noise. The error produced as a result of the assumption in equation (7) depends on the relative amplitudes of the vectors representing each spectral component of the speech and noise. As noted in [1], if the spectral components of the speech are much larger than the corresponding spectral components of the noise, the error is negligible. For the consonant sounds at the onset and ending of words, this is the case only for a large speech to noise ratio or the consonant information and intelligibility is lost.

#### 4. Least Mean Square Algorithm

The least mean square noise cancellation algorithm is described in [3]. Figure 6 shows a block diagram of the process.

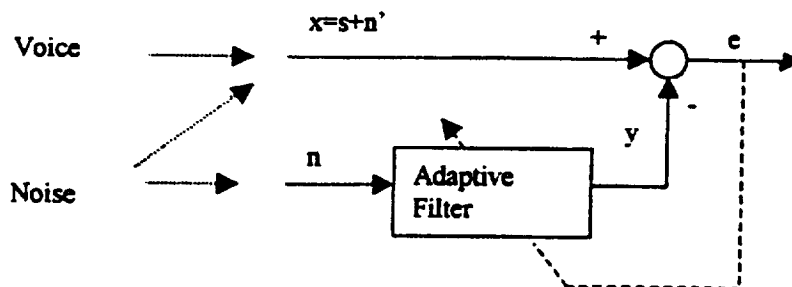


Figure 6. Block Diagram of Adaptive Noise Cancellation Using Least Mean Square Algorithm

The least mean square noise cancellation technique assumes the additive noise model given in equation (2). The algorithm uses an adaptive filter, equation (11), to make the noise at the reference microphone match the noise at the voice microphone.

$$y(k) = \sum_{m=0}^{L-1} w_m(k) n(k-m) \quad (11)$$

where:

$w_m(k)$  = filter weight  $m$  at sample  $k$

$y(k)$  = filter output at sample  $k$

$n(k)$  = input to reference microphone at sample ( $k$ )

$L$  = filter length

If the filter output does not exactly match the signal in the voice microphone, an error is generated.

$$e(k) = x(k) - y(k) \quad (12)$$

The error and the noise from the reference microphone are used to update the adaptive filter weights.

$$w_m(k+1) = w_m(k) + \mu n(k-m) e(k) \quad \text{for } m = 0, 1, \dots, L-1 \quad (13)$$

Initial filter weights were set to

$$w_m(k) = [\text{Sqrt}( P_x(\text{initial}) / P_n(\text{initial}) ) 0, \dots, 0 ] \quad (14)$$

where:

$P_x(\text{initial})$  = average power of the voice microphone over the initial length of the filter

$P_n(\text{initial})$  = average power of the reference microphone over the initial length of the filter

The filter weight update factor,  $\mu$ , determines the proportion used for updating.

$$\mu = \beta / (L P_x(k)) \quad (15)$$

Where  $\beta$  is a scale factor (initially chosen to be 2). If the error signal increases during iterations the scale factor  $\beta$  is reduced using

$$\beta = 0.5 \beta \quad (16)$$

The correlation coefficient,  $\rho$ , between the voice microphone and reference microphone were determined at each sample using

$$\rho = R_{xm}(0) / (\text{Sqrt}( R_{xx}(0) R_{mm}(0) )) \quad (17)$$

The auto and crosscorrelation are determined using 500 points. Speech is considered present during sample  $k$  if the correlation coefficient,  $\rho$ , is less than a specified amount (0.72).

## 5. Results and Discussion

The noise reduction techniques described in Sections 3 and 4 were tested. Spectrograms of the signals from the voice microphone and Ref Mic 1 are shown in Figures 7 and 8 respectively. Spectrograms of results obtained from magnitude spectral subtraction using one microphone are

shown in Figure 9. Spectrograms of results obtained from magnitude and complex (magnitude and phase) spectral subtraction using a reference microphone are shown in Figures 10 and 11 respectively. Comparing Figures 7 through 11, it can be seen that using a reference microphone provides a better estimate of the noise than using an average of the noise. By comparing the speech segments of Figures 9 through 11, it can be seen that the complex spectral subtraction does not remove as much noise, but it does keep the speech in tact. Thus, it does not decrease intelligibility like the magnitude spectral subtraction. The reduction of noise using complex spectral subtraction should be able to be increased with an improvement in the modeling of the relationship between the microphones, associated circuitry, and sound at each microphone. The adaptive filter in the least mean square technique provides a way to model this relationship. Its tracking capability can follow changes in the noise. Unfortunately, when speech is present, the algorithm produces a filter that tries to relate the reference microphone to the noise-corrupted speech. As a first estimate, the algorithm was turned off during speech. Two simple possibilities were considered: freezing the filter weights to final pre-speech values, and setting filter weights to initial values (square root of power difference between microphone signals over the length of the filter during the initial noise sequence). Spectrograms of results obtained from least mean square noise cancellation using frozen weights and initial weights during speech samples are shown in Figures 12 and 13 respectively. Use of the correlation coefficient, equation (13), to determine the presence of speech is shown in Figure 14.

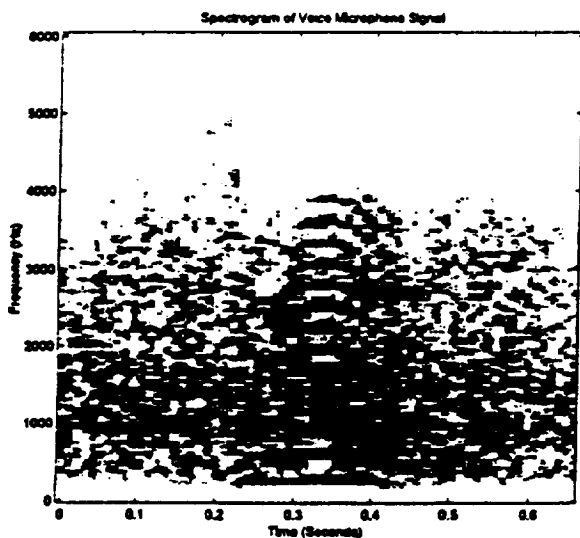


Figure 7. Spectrogram of Voice Microphone

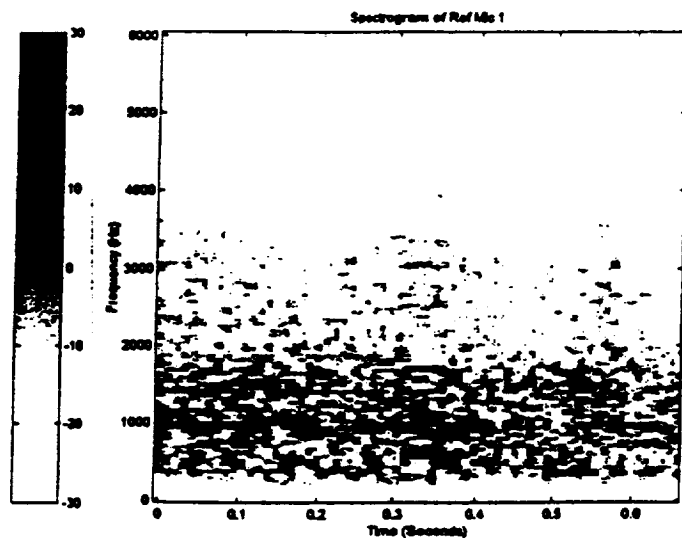


Figure 8. Spectrogram of Reference Microphone 1

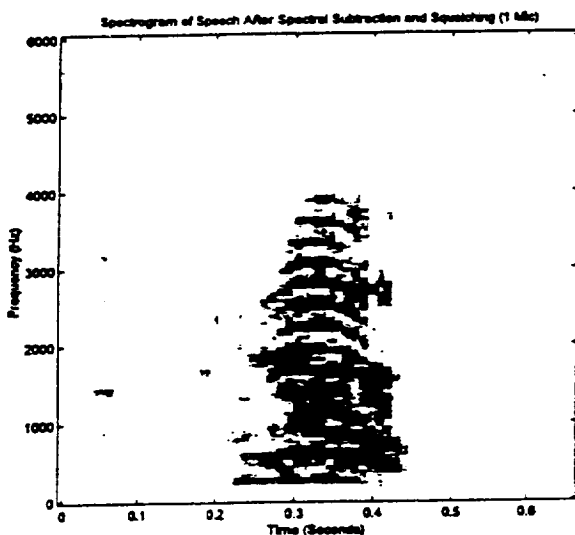


Figure 9. Spectrogram of Speech After Magnitude Spectral Subtraction Using No Reference Microphone

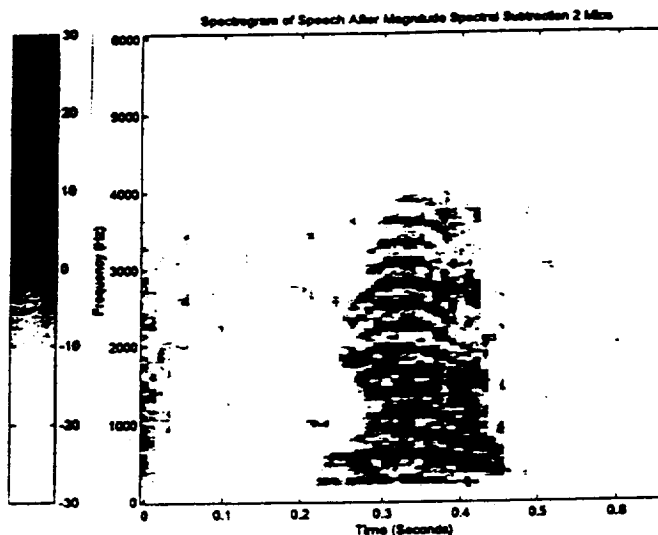


Figure 10. Spectrogram of Speech After Magnitude Spectral Subtraction Using Reference Microphone 1

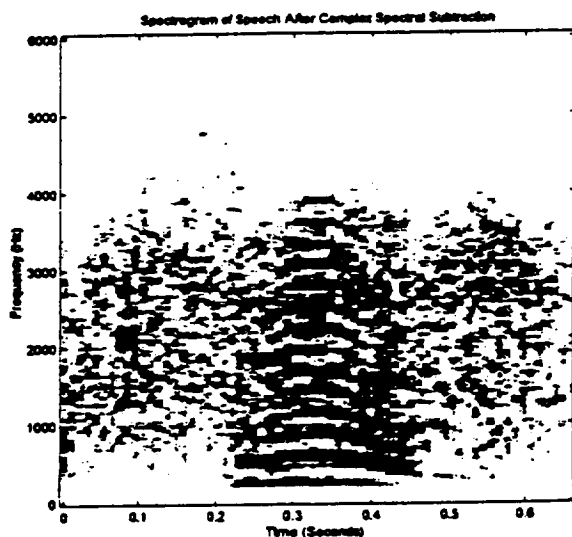


Figure 11. Spectrogram of Speech After Complex Spectral Subtraction Using Reference Microphone 1

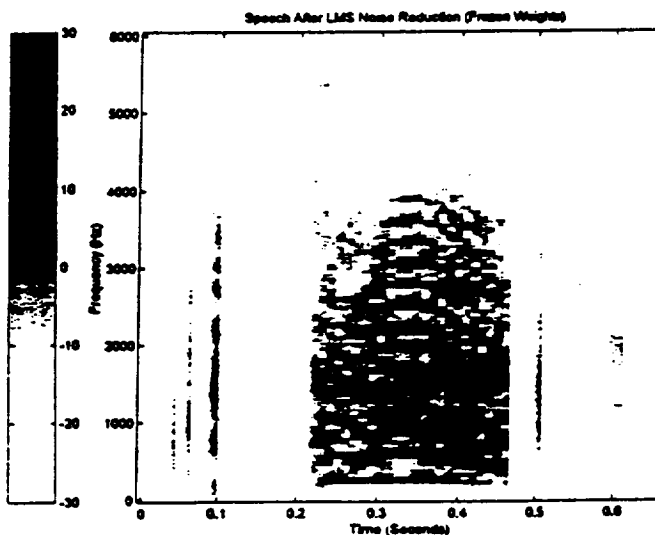


Figure 12. Spectrogram of Speech After Least Mean Square Noise Cancellation Using Frozen Weights

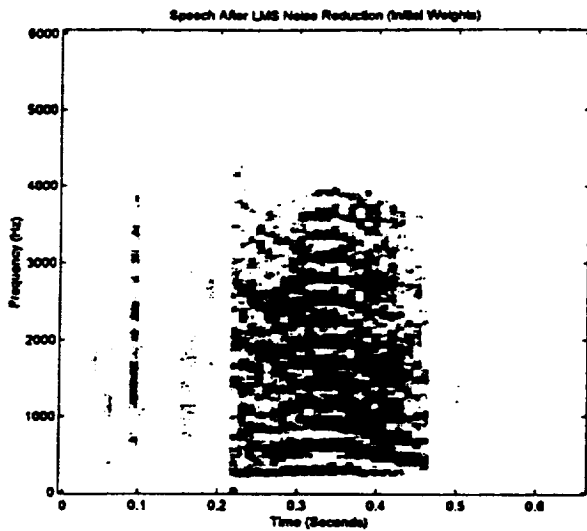


Figure 13. Spectrogram of Speech After Least Mean Square Noise Cancellation Using Initial Weights

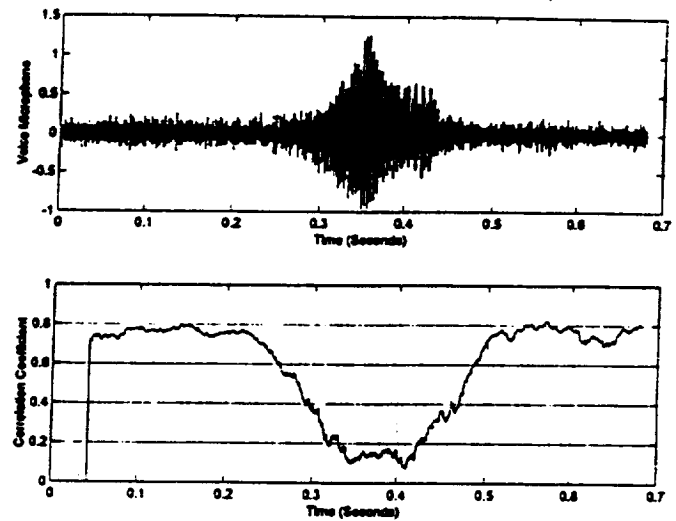


Figure 14. Use of Correlation Coefficient to Determine the Presence of Speech

## 6. Conclusions

There is a great deal of difference between eliminating noise and improving intelligibility. For the magnitude subtraction schemes eliminating noise also means eliminating speech. When speech is present, a reference microphone provides a better estimate of the noise than using an average of the noise. This is particularly true since the noise is highly uncorrelated with itself. The phase information present in the reference microphone has not yet been utilized to its fullest extent. Furthermore, the use of adaptive time domain filters such as the least mean square algorithm has not yet been fully explored. The work on both of these topics is ongoing.

## References

- [1] Kozel, David, NASA/ASEE Summer Faculty Fellowship Program Research Reports: NASA CR-202756; 1996, p143-157.
- [2] Kozel, David, NASA/ASEE Summer Faculty Fellowship Program Research Reports: NASA CR-207197; 1997, p113-122.
- [3] Kuo, Sen M., and Morgan, Dennis R., Active Noise Control Systems Algorithms and DSP Implementations, John Wiley & Sons, Inc., New York, NY, 1996.

1998 NASA/ASEE SUMMER FACULTY FELLOWSHIP PROGRAM

JOHN F. KENNEDY SPACE CENTER  
UNIVERSITY OF CENTRAL FLORIDA

USING NEURAL NETWORKS FOR EVALUATING THE HEALTH OF THE  
GASEOUS HYDROGEN FLOW CONTROL VALVE (GH2FCV)

Carl D. Latino, Associate Professor  
Electrical and Computer Engineering  
Oklahoma State University  
Stillwater, Oklahoma  
KSC Colleague - Hector Delgado  
Advanced Developments and Shuttle Upgrades

ABSTRACT

This project is the continuation of work begun during the summer of 1997. The theoretical groundwork of the summer of 1997 led to the design and construction of hardware capable of learning and reporting on the characteristics of the Gaseous Hydrogen Flow Control Valve (GH2FCV). The FCV is a critical flight component of the space shuttle system. It is constructed under very tight tolerances and its purpose is to use gaseous hydrogen to control the pressure in the liquid hydrogen external tank. In spite of the tight tolerances each valve is different and has unique characteristics. This makes ordinary testing methods difficult to employ especially if quantifying the health of the valve is desired. The system we designed can be trained to monitor and to quantify the valve's performance as defined by an experienced user. Gauging the health of the GH2FCV is accomplished by monitoring the current flowing through the valve during activation. The time function of this curve contains information regarding the performance of the valve. Presently, testing requires considerable human intervention and is consequently inefficient and time consuming. The system we developed was designed to speed up testing, increase accuracy and reduce cost. The objective was to both demonstrate a proof of concept and construct a ground test system. With a suitable sensor installed on the orbiter, a version of the system could be used in flight to report real time information on the health of the valve. The system was designed to be simple in design and operation and, if considered for flight, makes very modest demands on orbiter system resources. By using neural networks the system can learn valve characteristics making valve testing more accurate and less expensive. This report describes some of the system features and advantages of neural networks over currently used and more conventional means.

# USING NEURAL NETWORKS TO EVALUATE THE HEALTH OF THE GH2 FLOW CONTROL VALVE

Carl D. Latino Ph.D.

## 1. INTRODUCTION

The GH2FCV is used to regulate the pressure in the external hydrogen tank. The valve controls gas flow by operating in two flow modes, low and high. When energized it is in low flow and when de-energized it goes to high flow. The operation of the valve is monitored by observing the current through the coil in response to the actuating voltage. To energize the valve a 28 volt signal is applied to a solenoid which, acting against a spring force, moves the poppet to the low flow position. When voltage is removed, the return spring takes the valve back to its original position. The current flowing through the solenoid is a function of the applied voltage, electromechanical characteristics of the valve, the motion of the poppet as well as other factors. The current versus time gives a characteristic curve unique to each individual valve. Changes to the valve parameters such as friction, spring constants, and electrical values cause the current signature trace to change. Detecting these subtle, almost imperceptible changes allows a trained evaluator to make determinations about the health of the valve. Making these determinations is difficult, it takes time and requires knowledge, experience and a certain amount of subjectivity. A properly trained neural network, on the other hand, can make rapid and accurate determinations without the subjectivity.

## 2. THE NEED FOR NEURAL NETWORK MONITORING

In spite of careful manufacturing techniques and tight tolerances, every valve has its own unique signature. Since each flow control valve is unique, a system for testing must be capable of learning subtle differences between similar valves. This seemed an ideal application for neural networks because the networks can be trained to learn the individual features of the valve in question. Training requires that knowledge be imparted to the network to discriminate between good and bad or to quantify degrading conditions. Once trained, the network monitors the valve and produces outputs relating the condition of the valve.

Training is accomplished by showing the network a finite number of conditions and what each target should be. The network, when properly trained, uses this information to "fill in the gaps" for the conditions not specifically addressed. This information must be extracted from a single input provided to the monitoring system, this being the solenoid current versus time. From this single input, many characteristics can be extracted such as valve response time, rise times, fall times etc. Extracting this information requires some pre-processing of the raw data. The pre-processed data and other information is used as inputs for training the neural network and monitoring the system. Once trained, monitoring is accomplished by observing the current trace and (almost) immediately getting the desired output(s). The outputs could indicate "good", "bad" or can isolate

and quantify particular conditions of the valve. This immediate response makes the system a useful ground support test tool as well as a tool for monitoring the valve in flight.

### 3. THE NEURAL NETWORK MONITORING SYSTEM

In order to monitor the valve using neural networks, a system had to be designed and assembled. The system was conceived during the summer of 1997 and designed and built by The Oklahoma State University Systems Prototyping Laboratory during the Spring '98 semester. The laboratory is part of the OSU ECEN undergraduate program and combines students and faculty talent to produce a wide variety of systems at modest cost. The system, designed specifically for NASA/KSC, requires a sensor for detecting the current, data acquisition system for collecting the data, algorithms for user interface, pre-processing of the data and software for training the neural network.

Once pre-processed, this information is part of the data used for training a neural network. If actual failure modes cannot be simulated with the valve they may be inferred by the user's knowledge of the valve. The neural network structure chosen for this effort is a multiple input, multiple output, two layer feed forward network. The specific network complexity is user defined and the weights and biases of the network are determined by training. Once fully defined and trained, the neural network is a computer program that runs internal to the monitoring system hardware. The network structure chosen has multiple inputs, one hidden layer, one output layer and the neurons use the tansig transfer function. Training is accomplished using Matlab and the Neural Network Toolbox. These are powerful, commercially available software packages. The valve solenoid current is converted to digital information, stored and pre-processed. This, and possibly other pertinent data, is used to train the neural network. Training requires input data and corresponding user defined targets. Training defines the value of the weights and biases of the neural network. Once trained, the resultant weights and biases are sent to the monitoring system and communications between the PC and monitoring system is no longer needed. At this point the user toggles the switch on the hardware to Monitor mode and the system can now operate stand alone. To monitor the valve, the sensor and monitoring unit are all that are needed. In monitor mode, the coil current data is collected and pre-processed. The pre-processed data is used as input to the neural network. The neural network is not an actual piece of hardware but exists in the system as a flexible computer program. The neural network is automatically invoked each time the valve is activated. The output(s) of the network then report on the status of the valve as defined by the user training. In short, the neural network reads the current signature trace, analyzes it and reports the findings in user friendly format. As designed, the output is a liquid crystal display. Other display modes are also possible to suit the preferences and needs of the user. For demonstration purposes, an animated graphic program using colors to depict good, questionable and bad valve characteristics was designed by Gerald Stahl of CLCS.

#### 4. THE NEURAL NETWORK MONITORING SYSTEM

Color graphics of the system demonstration are included without explanation at the conclusion of the report. Detailed description of the system hardware and software are included in the project report generated by the Systems Prototyping Laboratory. That information will not be repeated here.

A block diagram of the training system consists of the valve under test, the current sensor, which is currently being designed by NASA, the data collection/monitoring system and a PC with Matlab and Neural Network Toolbox. Once the neural network is trained the PC is no longer needed. The data collection/monitoring system has an internal microprocessor and is equipped with a 2 line by 16 character display for user feedback. When energized the display shows each of the output in sequence. Sequencing to the next output is accomplished by the push of a button. When all outputs have been displayed the system is ready to monitor the next energize cycle.

#### 5. THEORY OF OPERATION

In order to know if the valve is operating nominally, its characteristic curve must be known by the neural network. Good data for the valve is the easy part to obtain and this is used to partly train the network. The problem occurs when anomalies are to be considered. Some anomalies are possible to simulate whereas others must be known. In any event, if the proper information is provided and the network is adequately trained, every time the valve is activated the system returns outputs commensurate with the inputs. As an illustrative example, assume the network has two inputs and two outputs. If the inputs form the x-y plane and the output is in the z axis, the inputs are the x-y values and the corresponding z value would be the output. Training constitutes generating a surface using a finite number of points on this surface. Table 1 shows what the training data is and Figures 1 and 2 show what the corresponding surfaces might be. Knowledge of the valve is essential to determine if the surfaces accurately depict the operation of the valve.

The neural network fills in the spaces between the training points and gives values to the outputs at locations where training did not take place. The danger here is that the problem must be well understood in order to be solved properly. It should be mentioned that a two input two output network was used for demonstration purposes only. The actual network may have as many inputs and outputs that are germane to the problem. Insufficient number of neurons and/or insufficient training might result in unacceptable performance surfaces. Excessive neural network complexity and/or training on the other hand can result in over fitting. Over fitting is the condition where the surface accurately depicts the values where it was trained, but is inaccurate in places where training did not take place. In this case the network has not accurately generalized the problem. Using a small number of neurons, the complexity of the surface is limited. Properly defining network complexity and training are part of the design problem and are the responsibility of the designer. There are numerous ways of addressing these well known problems.

These are beyond the scope of this report. Once this part of the problem has been resolved, testing can be performed by technical personnel with a very limited knowledge of the valve.

## 6. CONCLUSIONS

The purpose of the work conducted this summer was to demonstrate that neural networks could in fact be used to quickly and passively monitor and accurately evaluate the performance of the GH2FCV. The method used is unobtrusive and user friendly. The system designed was primarily a demonstrator unit, but in its current state it can be used to ground test valves. To determine the feasibility of such a system in flight, more data is needed. The system was designed to show that by monitoring the current signature trace of the flow control valve, many different anomalies could be automatically identified without the need of an experienced evaluator. The system is flexible in that, with some software changes, can be used to test many shuttle valves, motors and other systems. Incorporating such a system in the shuttle would require a small amount of memory for data storage, some processing capabilities (the orbiter on board IVHM computer can be used for this) and the addition of a sensor for detecting current. The hardware constructed for this application clearly demonstrates that this is a real application of neural networks in automating valve testing and health monitoring.

## 7. REFERENCES

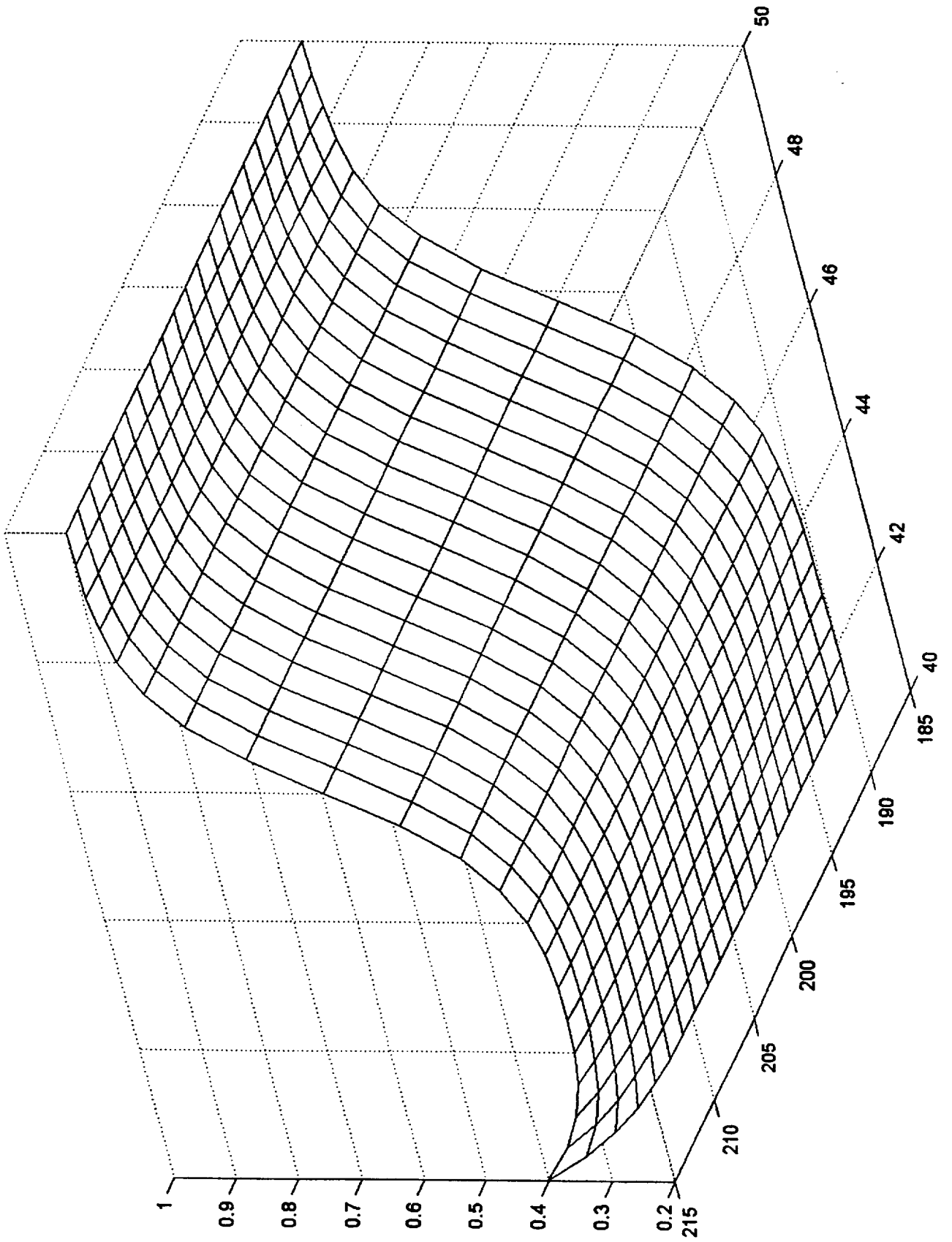
- [1] M. Hagan, H. Demuth and M. Beale, *Neural Network Design*, Boston, MA: PWS Publishing Company, 1996
- [2] Final Report for IVHM System

## 8. ACKNOWLEDGMENTS

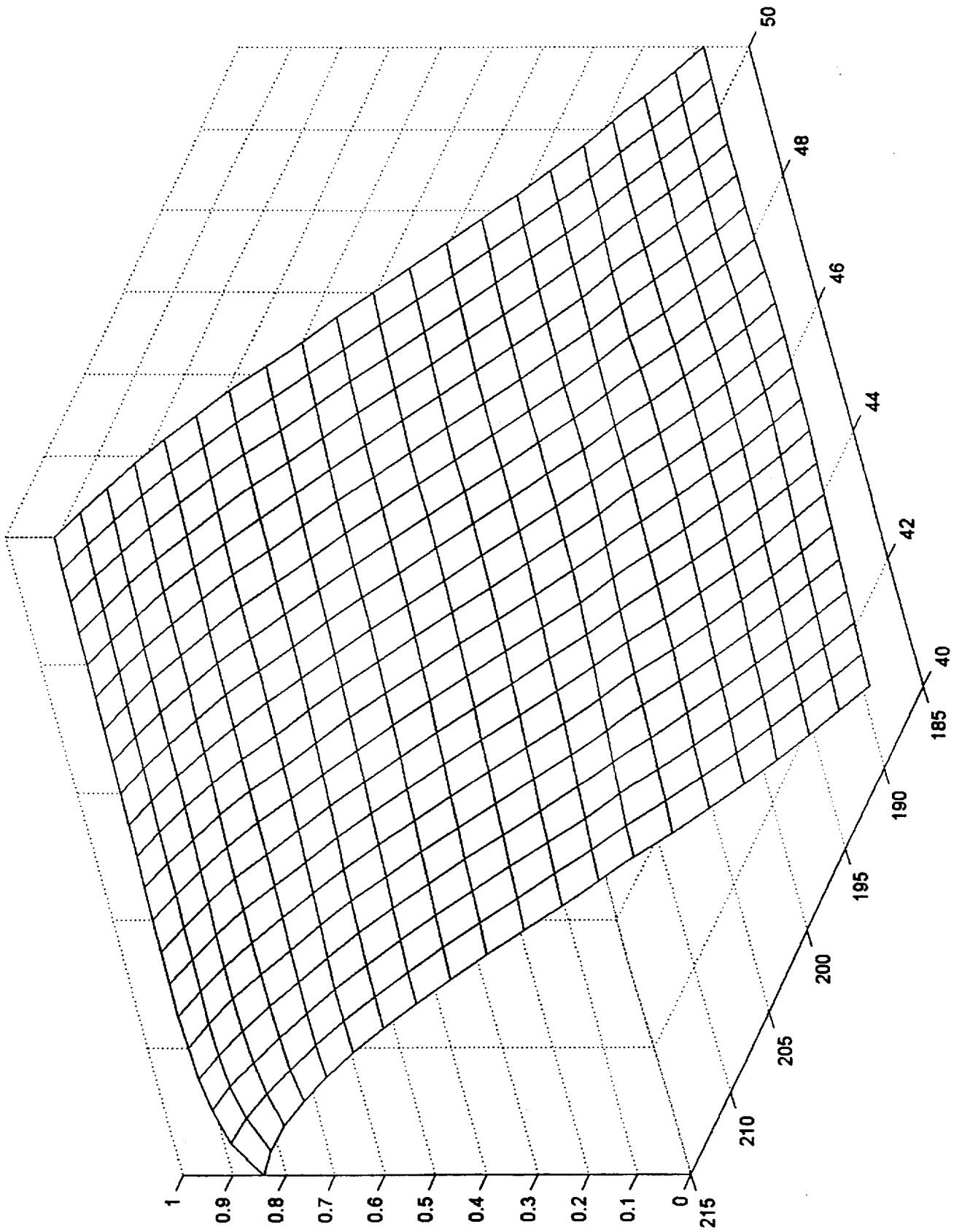
Identifying all who helped made this project possible is impossible. The time, talent and sincere effort put into this important endeavor by the many contributors is greatly appreciated. With apologies to those not identified by name, there are a few that require special recognition. The hardware construction and much of the software was designed and developed by the OSU Systems Prototyping Laboratory. Building the system and writing the necessary software in the limited time of one summer would have been impossible. We acknowledge the student team members and faculty mentors who assisted in this effort. The concept of using NN to monitor the GH2FCV was conceived by Hugo Delgado. This application may bring great returns in terms of cost savings and improved health monitoring. Hector Delgado made it possible for me to come here to work on the project. Jack Fox and the entire IVHM team provided valuable input and support during the summer. Mario Bassignani was invaluable as he worked very closely with me with hardware construction and software refinements to the system. Geral Stahl of CLCS provided his talents to interfacing to our system and making the graphics for the system demonstration. The graphics make explaining the operation of the system easy, even for a non technical audience. There are many more who helped with acquisition of equipment, system installations, solving network problems etc., etc., etc.. Not to be forgotten are Dr. Ramon Hosler, Gregg Buckingham, Kari and Stephanie who handled many of the difficult administrative duties. We sincerely appreciate all that you have done.

	Network Targets		
	4 out	3 out	2 out
0 Ohm	0.9/0.9	0.6/0.9	0.3/0.9
1 Ohm	0.9/0.5	0.6/0.5	0.3/0.5
2 Ohm	0.9/0.1	0.6/0.1	0.3/0.1
	Network Outputs		
	4 out	3 out	2 out
0 Ohm	.901/.885	.598/.899	.300/.920
1 Ohm	.900/.470	.598/.518	.298/.507
2 Ohm	.900/.086	.598/.108	.298/.124
	Peak/Final		
	4 out	3 out	2 out
0 Ohm	50/215	46/214	42/214
1 Ohm	50/200	46/200	42/199
2 Ohm	50/186	46/186	41/186

(z1) GH2FCV Preload Related Output

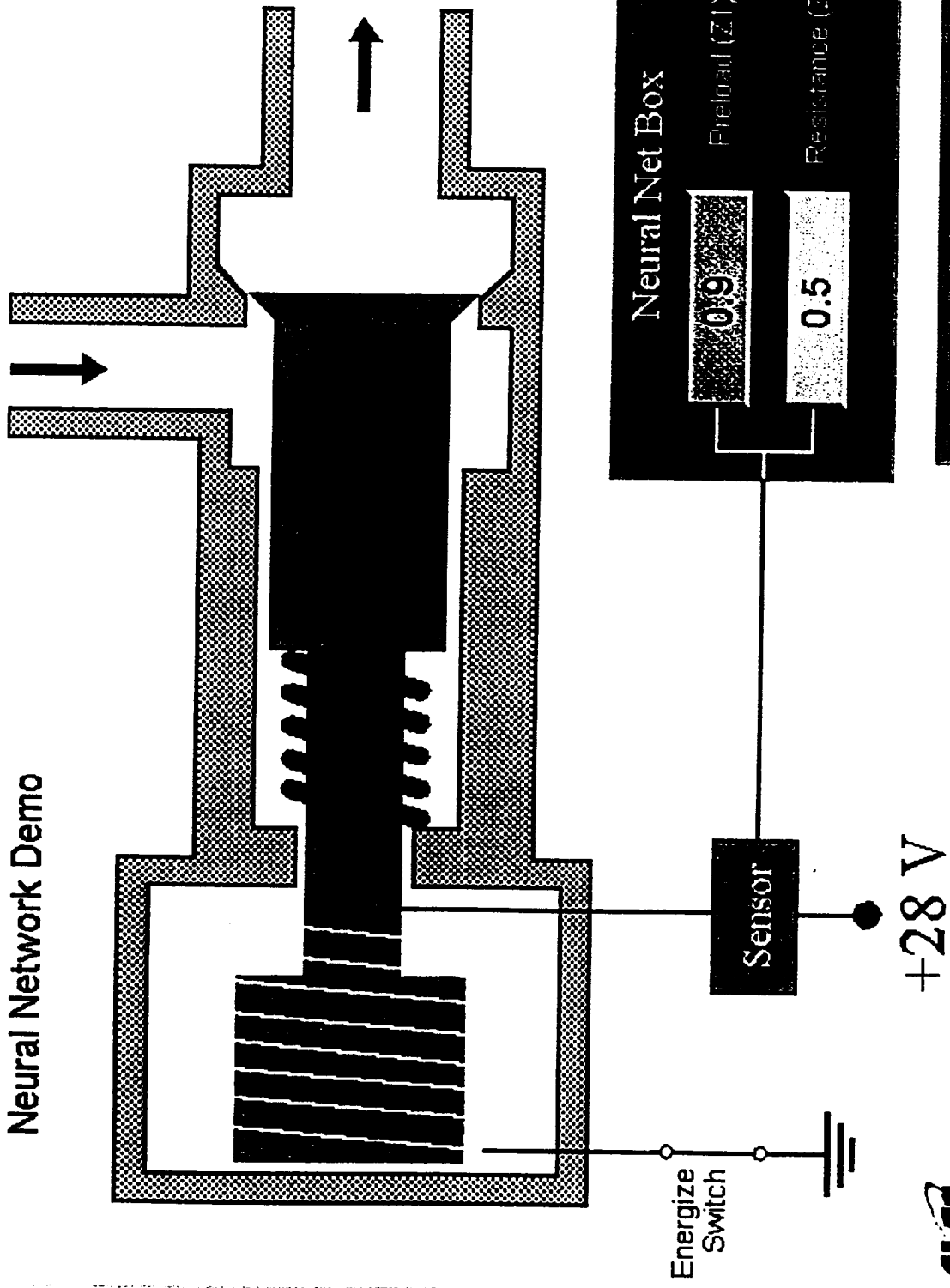


(z2) GH2FCV Resistance Related Output



# IVHM Flow Control Valve

## Neural Network Demo



1998 NASA/ASEE SUMMER FACULTY FELLOWSHIP PROGRAM

JOHN F. KENNEDY SPACE CENTER  
UNIVERSITY OF CENTRAL FLORIDA

THE ROLE OF DIVERSITY IN CONFERRING STABILITY AND RESISTANCE TO  
INVASION TO MICROBIAL COMMUNITIES: THE USE OF DILUTION TO GENERATE  
HIGH AND LOW DIVERSITY COMMUNITIES

Aaron L. Mills  
Professor  
Laboratory of Microbial Ecology  
Department of Environmental Sciences  
The University of Virginia

KSC Colleagues:  
John Sager, NASA  
Jay Garland, Dynamac Corp.

ABSTRACT

A series of dilution extinction experiments were conducted to determine if dilution could be used as a means to generate communities of differing diversity for purposes of testing hypotheses about diversity and stability of microbial communities to physical chemical perturbation and invasion by human pathogens. Domestic sewage was diluted over the range from  $10^0$  to  $10^{-8}$ , and the organisms present were allowed to regrow to the original concentration in sterile sewage from the same source as the inocula. The number of cells in the bioreactors reached and maintained levels that were approximately equivalent to the original concentrations as measured both by direct counts (acridine orange staining) and cultural counts (R2A medium). Diversity was expressed as the number of distinct colony types present on the culture plates used for enumeration of the bacteria. The number of colony types varied over the experimental period, but was always less in reactors receiving the diluted inoculum as opposed to those receiving the undiluted inoculum. Community level physiological profiles (CLPP) indicated that reducing the diversity of the microbial community resulted in no demonstrable loss of function, but distribution of the functions among the resident organisms changed in a way that was neither predicted nor understood. The undiluted inocula produced communities that were composed of specialists, whereas the communities that developed from diluted inocula were dominated by generalists. The results indicate that communities of differing diversity for experimental use in closed systems can, indeed, be produced by dilution techniques.

# THE ROLE OF DIVERSITY IN CONFERRING STABILITY AND RESISTANCE TO INVASION TO MICROBIAL COMMUNITIES: THE USE OF DILUTION TO GENERATE HIGH AND LOW DIVERSITY COMMUNITIES

Aaron L. Mills

## 1 Introduction

Bioregenerative life support systems for long-term space missions are subject to a variety of possible perturbations that can affect the ability of the system to perform its intended function, or that can make it a source of microorganisms that could be potentially pathogenic and therefore hazardous to the crew. Failure of control equipment for maintaining temperature, oxygen, agitation, etc., may lead to an alteration of the community in the bioreactor due to death of some of the strains or establishment of conditions more favorable for the growth of strains (e.g., opportunistic pathogens such as *Pseudomonas aeruginosa*) that could jeopardize the well-being of the crew or that could outcompete desirable members of the community that carry traits essential for the successful functioning of the reactor.

Most earth-surface systems are open (e.g., wastewater treatment plants), or if they are closed they are easily reinitialized from starter cultures maintained against that eventuality. On a space station or on the lunar or Martian surface, such starters will not likely be available, and all systems will be run as closed systems without the advantage of outside input. It is, therefore, essential to determine the conditions under which the microbial communities will be most stable, i.e., most resistant to physical/chemical perturbations and to invasion by alien microbes.

Bioregenerative life support systems are vulnerable to disruption due to physical or chemical perturbations. Failure of temperature control circuits could permit a temperature fluctuation outside the tolerance range of the microbes that could result in death of several important components of the community. Such a catastrophic failure without a means to "restart" the community could jeopardize the mission and place the astronauts at high risk. Thus, it is critical to know how to make the communities resistant to perturbation?

An additional problem associated with microbial communities in bioreactors involves the Potential of the system to act as a refuge for "undesirable" microbes, e.g. opportunistic pathogens. It is critical to know how to make the communities resistant to invasion.

A central theme in much of ecology is that environments with a highly diverse community are more resistant to perturbation, including invasion, than systems with low diversity (Elton, 1958). This concept has been cited so frequently (Case, 1990, Case, 1991, Huston, 1997, Robinson, et al., 1995, Robinson

**High Diversity vs. Low Diversity Community**

⇓

**Subject each to an elevated-temperature event**

⇓

**Challenge each with an invader**

and Dickerson, 1984) that it has become a paradigm of ecology. Strong experimental evidence in support of this paradigm is lacking (Robinson and Dickerson, 1984), and data in microbial systems have not examined systems of varying diversity, rather sterile systems have been compared with non-sterile ones. The non-sterile ones generally have no quantification of the diversity associated with them.

The question of diversity for bacterial communities is further complicated by the observation that microbial communities tend to

**Fig. 1** General approach for examining the effect of diversity on the stability of a microbial community



selected for use because it represents a very high diversity material which must, therefore, lead to a high diversity community. Human waste also represents material that final decisions as to its disposal will need to be made. Given the potential as a source of pathogenic organisms, sewage represents a potentially hazardous material if included in reactors housing bioregenerative processes.

## 2 Methods and Materials

Twenty one liters of sewage were obtained from the primary aeration tank at the Kennedy Space Center Wastewater Treatment Plant in a single polypropylene carboy. The sewage was allowed to settle for 1 hour, and 100 mL was withdrawn from the top of the carboy for use as an inoculum. 59 mL of sewage was placed into each of fifteen 125-mL Erlenmeyer flasks, and the flasks closed with foam stoppers. These flasks were autoclave for 20 minutes, and the remainder of the sewage was autoclaved for 1.5 h at 15 psi and 121°C. Once sterilized, the carboy of sewage was stored at 4°C until use.

Prior to inoculation of the flasks with diluted sewage, each flask was amended with a sterile solution of cycloheximide (to yield a final concentration of 25 mg L<sup>-1</sup>) to inhibit the growth of eucaryotes such as bacteriverous protozoa. Dilutions of the non-sterile sewage were then made using a portion of the sterile sewage as a diluent. The flasks were inoculated with diluted sewage at dilution levels of 0, 10<sup>-2</sup>, 10<sup>-4</sup>, 10<sup>-6</sup>, and 10<sup>-8</sup> (3 replicate flasks per level). The flasks were placed on a rotary shaker operated at 200 rpm in the laboratory (approximately 23°C).

The flasks were incubated for 3 weeks in continuous culture under fed-batch conditions. Each Monday, Wednesday, and Friday, half of the flask contents (i.e., 30 mL) was removed and replaced with fresh sterile sewage from the carboy. This practice resulted in an average retention time in the flasks of 4.7 days (1.5 volumes per 7 days). On the 10th and 17th days of the incubations, the portion of flask contents removed from each flask was partitioned and examined for several microbiological parameters as described below.

### 2.1 Total Cell Numbers

The total number of bacterial cells in each flask was determined by collecting cells from a known volume of reactor fluid on a polycarbonate filter, staining with Acridine Orange, and counting the cells under UV illumination with the epifluorescence microscope (Hobbie, et al., 1977).

### 2.2 Heterotrophic Plate Counts

Culturable heterotrophs were enumerated by spreading dilutions of the samples on the surface of R2A plates (Reasoner and Geldreich, 1985), incubation for 5 days at room temperature (ca. 23°C) and counting the resulting colonies for those plates having between 30 and 300 colonies. In the event that all dilutions fell outside the countable range, the dilution closest to the countable range was used for enumeration. Most often, this was the higher of two dilutions that surrounded the countable range. Data are reported as Colony Forming Units (CFU) per mL.

In addition to CFU, the number of different colony types was recorded for each plate within the countable range. Colony types were determined by properties outlined in Smbert and Kreig (1981), and the results were used as a measure of richness for the culturable fraction of the community in each flask.

### 2.3 Community Level Physiological Potential (CLPP)

The procedure of Garland and Mills (1991) was used to generate physiological profiles for comparison of the different dilution treatments. Physiological profiling consists of inoculating a small amount (0.15 mL) of the sample from each flask into each of the 96 wells of BIOLOG<sup>®</sup> GN microtiter plates. 95 of the wells contain a single compound that serves as a sole source of carbon and energy for the microbes; the 96th well contains no carbon compound and serves as the control for the plate. Plates were incubated at ambient temperature for 5 days. At intervals during the incubation period, the development of color in the wells (due to microbial reduction of tetrazolium violet used as an alternate terminal electron acceptor by respiring organisms) was measured in the microtiter plate reader. Profiles used for comparison among the plates were those obtained at an average well color development (AWCD) of 0.6.

CLPPs were determined for undiluted samples from each of the flasks and for dilutions of the suspensions contained in each flask. Dilutions used on day 10 were  $10^{-1}$ ,  $10^{-3}$ ,  $10^{-4}$ , and  $10^{-5}$ , and on day 17 were  $10^{-1}$ ,  $10^{-2}$ ,  $10^{-3}$ , and  $10^{-4}$ . Diluted samples were used to examine the change in functional richness (defined as the number of characters which gave positive responses) as strains were diluted out of the samples.

## 3 Results

### 3.1 Direct Counts

The initial concentration of cells inoculated into each of the flasks (Table 1) could only be determined on the basis of cultural counts using R2A medium. Initial AODCs included a large number of dead cells from the autoclaved sewage that were impossible to distinguish from the cells added in the inoculum. Dilutions resulted in inoculations of very few organisms in the highest dilutions ( $10^{-6}$  and  $10^{-8}$ ).

**Table 1.** Inocula added to each dilution series for the incubations.

Dilution	mL of original sample added to 19 mL sterile sewage	Total microbes added to each flask (viable counts on R2A)	Initial cell concentration in flask
$10^0$	1	$1.2 \times 10^7$	$6 \times 10^5$
$10^{-2}$	0.01	$1.2 \times 10^5$	$6 \times 10^3$
$10^{-4}$	0.0001	$1.2 \times 10^3$	$6 \times 10^1$
$10^{-6}$	0.000001	$1.2 \times 10^1$	$6 \times 10^{-1}$
$10^{-8}$	0.00000001	$1.2 \times 10^{-1}$	$6 \times 10^{-3}$

\*Number calculated on the basis of HPC using R2A medium.

After 10 days of incubation, cell numbers in all flasks had risen to levels which approximated the initial cell concentrations within a factor of 4 (Table 2). Furthermore, the cell concentrations were reasonably constant over the incubation period. Although the numbers varied over the range from  $0.8 \times 10^7$  to  $3.1 \times 10^7$  cells mL<sup>-1</sup>, there were no statistically significant differences in the various dilutions present. At both sampling times, the numbers of cells in the highest dilutions ( $10^{-6}$  and  $10^{-8}$ ) exceeded the numbers in the lowest dilutions ( $10^0$  and  $10^{-2}$ ) with the intermediate dilution having numbers of total cells intermediate between the highest and lowest dilutions

**Table 2.** Cell numbers (AODC) after incubation of reactors for 10 and 17 days. Initial numbers (day 0) are based on cultural counts, and are not directly comparable with those at later dates.

Dilution	HPCs (CFU mL <sup>-1</sup> )		10 <sup>7</sup> cells mL <sup>-1</sup> ± s.d.	
	Day 0 <sup>a</sup>	Day 10	Day 10	Day 17
0	6 × 10 <sup>5</sup>		1.1 ± 0.18	1.2 ± 0.13
10 <sup>-2</sup>	6 × 10 <sup>3</sup>		1.6 ± 1.3	0.81 ± 0.53
10 <sup>-4</sup>	6 × 10 <sup>1</sup>		1.3 ± 0.67	2.0 ± 1.7
10 <sup>-6</sup>	6 × 10 <sup>-1</sup>		3.7 ± 0.30	3.1 ± 0.45
10 <sup>-8</sup>	6 × 10 <sup>-3</sup>		2.3 ± 1.8	2.4 ± 0.16

Microscopic examination of microbes in the reactors showed a marked difference in the community among the various dilutions, with higher dilutions appearing less diverse than undiluted treatments (Fig. 3). The large chains of long rods evident in the low dilutions were rarely encountered in the higher dilutions, and the overall appearance of the cells was much more uniform in the diluted samples than in the undiluted ones.

### 3.2 Heterotrophic Plate Counts

The general pattern of bacterial abundance in the reactors as determined by plating on R2A medium was similar to that observed by AODC (Table 3). Numbers of organisms were relatively constant among dilutions at both days. The most apparent departure from the observed constancy was for the 10<sup>-6</sup> dilution on day 10. The maximum abundance determined by AODC was also observed in that dilution at that time (see Table 2).

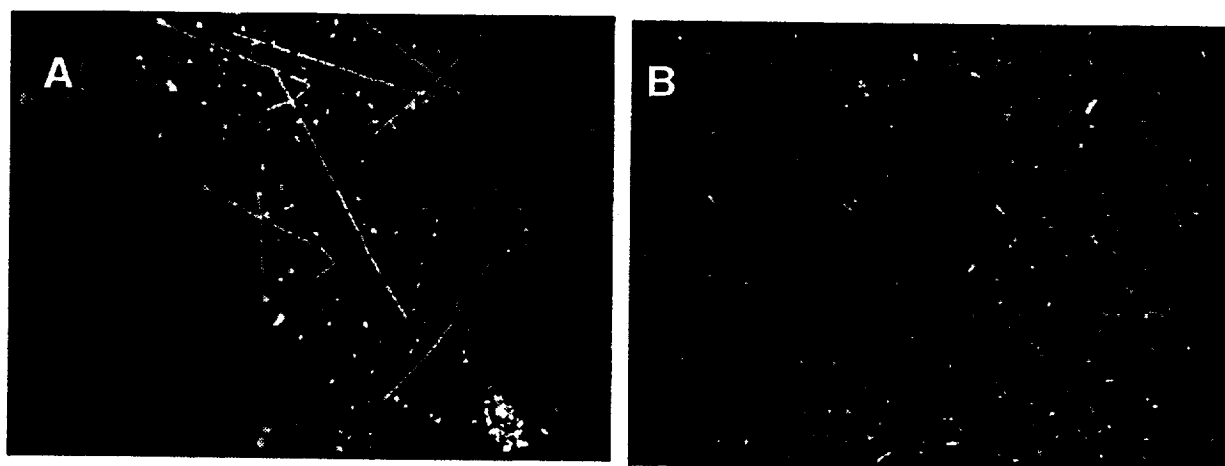


**Fig. 3.** Typical microscope fields at 1000 × magnification. Panel A represents the undiluted sample and Panel B represents a typical field from the 10<sup>-4</sup> dilution. Despite the apparent higher density in the diluted (and regrown) sample, the variety of cell types is lower, indicating reduced diversity.

**Table 3.** Numbers of bacteria recoverable in each dilution at each sampling time by plating on R2A medium

Day	Dilution				
	$10^0$	$10^{-2}$	$10^{-4}$	$10^{-6}$	$10^{-8}$
0	$1.2 \times 10^7$	$1.2 \times 10^5$	$1.2 \times 10^3$	$1.2 \times 10^1$	$1.2 \times 10^{-1}$
10	$1.3 \times 10^6$	$3.8 \times 10^6$	$1.7 \times 10^7$	$4.7 \times 10^7$	$9.6 \times 10^6$
17	$1.0 \times 10^6$	$1.6 \times 10^6$	$2.4 \times 10^6$	$5.2 \times 10^6$	$3.8 \times 10^6$

While the trends in abundance observed with the two enumeration methods were similar, the ratio of culturable to total organisms was somewhat different among the dilutions and times (Table 4). In general, the culturability (counts on R2A/AODC) was between 0.1 and 0.2 with the exception of the higher dilutions on day 10. Because a very high number of cells was recovered in the higher dilutions ( $\geq 1000$  cells per counting field), the ability of the counting system was likely compromised (due to saturation of the counting program), resulting in an underestimate of the AODC for the 3 highest dilutions on day 10. Although the counts for those days were the highest recorded, they are still thought to be underestimates; the observation that cultural counts exceeded the direct counts (culturability  $> 1$ ) in the  $10^{-4}$  and  $10^{-6}$  dilutions (and was at 0.4 for the  $10^{-8}$  dilution) supports the idea of an underestimate of direct counts. The observed values of 10% to 20% of the total cells being culturable exceed the typically quoted values of  $< 1\%$  to  $5\%$  of total bacteria being culturable in most samples.

### 3.3 Colony diversity

The number of colony types observed on the R2A plates tended to decrease with the amount of dilution as expected (Table 5). The reported values represent the total number of types observed on the plates at the countable dilution. Every colony on each of the plates was examined for morphology, no effort was made to normalize for differences in numbers of organisms since the CFUs recovered on the plates showed no significant difference.

**Table 4.** Changes in culturability of bacteria from the bioreactors. Culturability is the average number of CFU (R2A medium) at each dilution level divided by the average AODC for that dilution level. No AODC were obtained on Day 0.

Day	Dilution				
	0	2	4	6	8
0	nd	nd	nd	nd	nd
10	0.12	0.23	1.33	1.26	0.41
17	0.09	0.20	0.12	0.17	0.16

**Table 5.** Bacterial diversity in bioreactors at different dilutions as indicated by differences in numbers of types of colonies appearing on R2A medium. Values listed are averages for all plates in the countable range.

Dilution	Number of different colony types	
	Day 10	Day 17
0	8.4	7.3
2	6.6	3.7
4	6.5	3.9
6	5.5	4.8
8	1.5	3.5

### 3.4 Community Level Physiological Profiles

Because the origin of the communities in the reactors was initially the same, comparisons of the profiles showed no difference among the communities.

Examination of the functional richness (defined as the number of substrates showing positive utilization) showed a surprising result. A community that is highly diluted prior to inoculation into the BIOLOG plates would be expected to lose some functions due to the loss

of strains. More dilute samples should have fewer positive tests. The shape of the curve relating the number of positive tests to the number of organisms in each test well can be used to make inferences about the community. If tests are lost immediately upon (even a small) dilution, the community in the BIOLOG plates consists of specialists, i.e., organisms that have a narrow range of functions that are expressed in this approach. Conversely, communities from which functions are lost only at high dilution should either be composed of generalists or the community is highly redundant with respect to the functions tested (i.e., numerous organisms carry out each function present).

**Table 6.** Design of dilution-extinction experiment for the bioreactors. Bioreactor dilutions refer to the original sewage dilutions. BIOLOG dilutions refer to dilutions made from the bioreactor dilutions and inoculated into the BIOLOG plates.

BIOLOG Dilution	Bioreactor Dilution				
	$10^0$	$10^{-2}$	$10^{-4}$	$10^{-6}$	$10^{-8}$
$10^{-1}$					
$10^{-2}$					
$10^{-3}$					
$10^{-4}$					
$10^{-5}$					

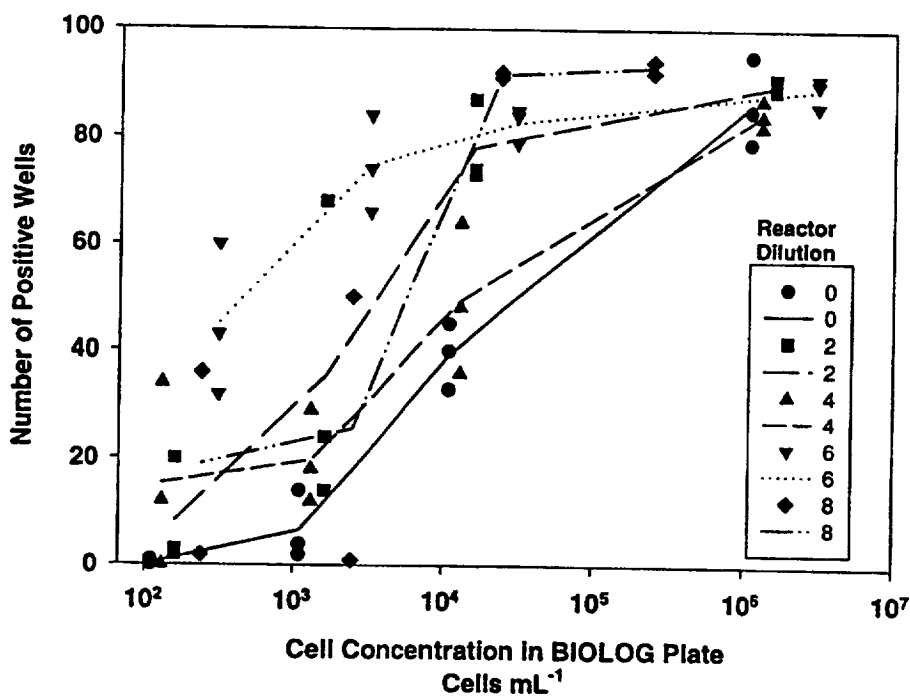


**Fig. 4.** Response of functional richness to dilution in bioreactors incubated for 10 days.

To examine the behavior of functional richness in the sewage bioreactors, a series of dilutions were inoculated into BIOLOG plates for each bioreactor dilution treatment (Table 6). The number of cells inoculated into the plates was determined by multiplying the AODC for each bioreactor dilution by the dilution made for the BIOLOG inoculation.

For the day 10 samples, the response of functional richness displayed two basic patterns of behavior (Fig. 4). In two of the reactor dilution series, the community lost functions immediately upon even a small dilution of the innocuous placed in the BIOLOG plates, whereas the richness of characters in the rest of the dilutions persisted until the inoculum had been diluted by a factor of  $10^3$  to  $10^4$ . On day 17, the same patterns persisted, but were segregated into two groups more distinctly different than on day 10 (Fig. 5.). The low reactor dilutions lost characters immediately upon slight dilution into the BIOLOG plates, whereas the higher reactor dilutions retained nearly all the characters until the samples had been diluted by a factor of  $10^4$ .

A diluted inoculum resulted in a minimal disruption of function in the reactors- probably because there were few strains present and they were evenly distributed (strains were not lost until extreme dilutions, Dilution caused a rapid disruption of function - strains were removed even at low dilutions

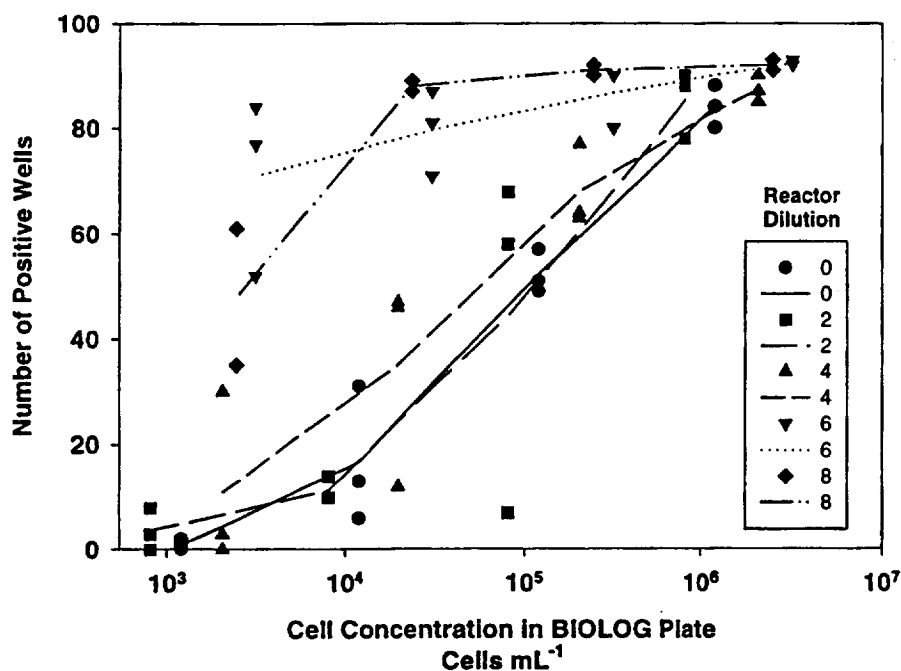


Fig. 5 Response of functional richness to dilution in bioreactors incubated for 17 days.

## 4 Discussion

The effect of dilution on a homogeneous lead distributed microbial community was presented in figure 2. In such a community, the suite of organisms present in the diluted assemblage should be a subset of being strains present in the original community, and should be represented by the most common strains present in the original community. Dilution should remove most of the rare strains, although, as seen in Figure 2, it is possible for some of the rare strains to be present in the diluted community. Given

the further assumption that there is no periodic selection for strains that would differ from that of the original community, the final community in the diluted condition should comprise the dominant strains found in the original sample.

The results of this study indicate that, indeed, dilution can work to produce communities of variable diversity, and that regrowth of the diluted suspension can produce communities with a relatively constant cell abundance. We can conclude, therefore, that dilution techniques produce communities of reduced diversity, and that such communities can provide reasonable treatments for testing physical perturbation of the community and for testing the community's resistance to invasion by "undesirable" organisms. Measurement of that diversity, however, will require the use of combined physiological and genetic techniques that are beyond the scope of this project.

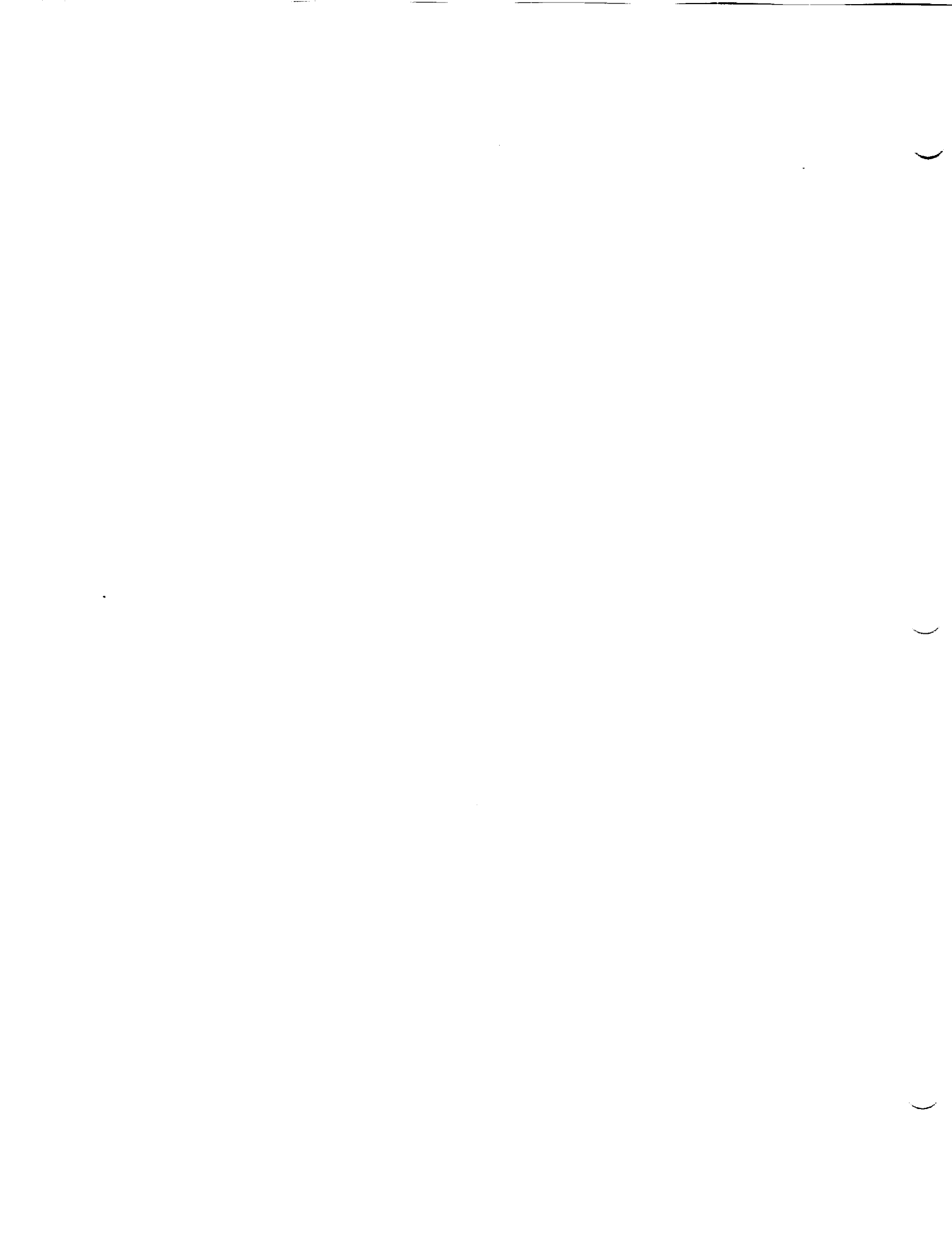
An interesting, unexplained, and potentially significant observation was that the functional richness patterns of the diluted and undiluted samples inoculated into BIOLOG plates were not similar across the dilution treatments. The change in functional richness with dilution of the samples prior to inoculation into the plates provides some evidence of the types of organisms present in the community with respect to whether or those organisms are specialists or generalists. Generalists are organisms with a wide range of functional potential; they are able to metabolize many different compounds, often under a variety of environmental conditions. Specialists are organisms that have a narrow range of functions. Using the BIOLOG approach to physiological profiling, generalists would be organisms which yield positive results for a large number of the substrates included, whereas specialists would be expected to metabolize only a few of the substrates.

Communities with few "kinds" (i.e., low diversity) have fewer niches, but those niches must be wider in order to accommodate the functions required by the ecosystem. Organisms there should be generalists. Communities in which generalists dominate are often limited by physical or chemical constraints (Mills and Mallory, 1987) as opposed to biological competition. Communities which are not under any stress from physical or chemical conditions have as their main control on populations biological competition. Communities with large numbers of "kinds" (i.e., diverse) have many narrow niches - community is characterized by specialists that survive by intergenomic competition. In such cases competition among the organisms selects for specialists - organisms that do only a few things, but that do them very well. Although dilution of strains in a community should lead to a community of reduced diversity with the dominant strains the same dominant strains as found in the undiluted samples, the reactors with a highly diluted initial inoculum developed a community of generalists as seen by the pattern of function loss when reactor samples were diluted and inoculated into BIOLOG plates. In an open system, we might expect reduced diversity to lead to reduced competition which leads to wide niches filled by generalists. At this time, it is not clear how the community (in a closed system) could be transformed from a group of specialists to a group of generalists simply by dilution.

## 5 References

1. Case, T. J. 1990. Invasion resistance arises in strongly interacting species-rich model competition communities. *Proc. Nat. Acad. Sci.* **87**:9610-9614.
2. Case, T. J. 1991. Invasion resistance, species build-up and community collapse in metapopulation models with interspecies competition. *Biological Journal of the Linnean Society.* **42**:239-266.
3. Edwards, E. A., L. E. Wells, M. Reinhard, and D. Grbic-Galic. 1992. Anaerobic degradation of toluene and xylene by aquifer microorganisms under sulfate-reducing conditions. *Appl. Environ. Microbiol.* **58**:794-800.

4. **Elton, C. S.** 1958. *The Ecology of Invasion by Animals and Plants*. Chapman & Hall, London.
5. **Garland, J. L., and A. L. Mills.** 1991. Classification and characterization of heterotrophic microbial communities on the basis of patterns of community-level-sole-carbon-source utilization. *Appl. Environ. Microbiol.* **57**:2351-2359.
6. **Hill, J., and R. G. Weigert.** 1980. Microcosms in ecological modeling, p. 138-163. *In* J. P. Giesy (ed.), *Microcosms in Ecological Research*. U. S. Department of Energy, Symp. 52. National Information Service, Springfield, VA.
7. **Hobbie, J. E., R. J. Daley, and S. Jasper.** 1977. Use of Nuclepore filters for counting bacteria by fluorescence microscopy. *Appl. Environ. Microbiol.* **33**:1225-1228.
8. **Huston, M. A.** 1997. Hidden treatments in ecological experiments: re-evaluating the exosystem function of biodiversity. *Oecologia.* **110**:449-460.
9. **Mills, A. L., and L. Mallory.** 1987. Community structure changes in epilithic bacterial communities stressed by acid mine drainage. *Microb. Ecol.* **14**:219-232.
10. **Reasoner, D. J., and E. E. Geldreich.** 1985. A new medium for the enumeration and subculture of bacteria from potable water. *Appl. Environ. Microbiol.* **49**:1-7.
11. **Robinson, G. R., G. F. Quinn, and M. L. Stanton.** 1995. Invasibility of experimental habitat islands in a California winter annual grassland. *Ecology.* **76**(3):786-794.
12. **Robinson, J. V., and J. E. Dickerson.** 1984. Testing the invulnerability of laboratory island communities to invasion. *Oecologia.* **61**:169-174.
13. **Smibert, I. M., and N. R. Krieg.** 1981. Systematics, p. 432. *In* P. Gerhardt, R. G. E. Murray, R. N. Costilow, E. W. Nester, W. A. Wood, N. R. Krieg, and G. B. e. Phillips (ed.), *Manual of methods for general bacteriology*. Washington DC, American Society for Microbiology.



## **1998 NASA/ASEE SUMMER FACULTY FELLOWSHIP PROGRAM**

**JOHN F. KENNEDY SPACE CENTER  
UNIVERSITY OF CENTRAL FLORIDA**

### **WORKFORCE ASSESSMENT AND VALIDATION EXERCISE**

**Gary P. Moynihan  
Associate Professor  
Department of Industrial Engineering  
The University of Alabama  
James Jennings AA-A**

#### **ABSTRACT**

The Kennedy Space Center workforce is undergoing a restructuring process. This process will involve organizational change, and transition to a focus on development, all while maintaining mission integrity. An overall plan for this process was developed, including consideration of KSC workforce skills, and a review of operations across the KSC organization. Methods of data collection were developed in order to support these reviews. In order to develop the plan, the application of business process reengineering (BPR) techniques was be utilized:

- 1) Understand the existing KSC environment.
- 2) Assess alternative ways of improving existing processes.
- 3) Characterize the objective KSC environment.
- 4) Compare original and objective models, and determine impact on workforce.

Additional research associated with this project addressed the determination of NASA KSC core competencies, establishment of clerical standards, and the feasibility of developing an executive information system for KSC.

## WORKFORCE ASSESSMENT AND VALIDATION EXERCISE

Gary P. Moynihan

### 1. INTRODUCTION

For the past five years, the National Aeronautics and Space Administration (NASA) has been undergoing a fundamental restructuring due to diminishing budgets. In 1993, the Agency had approximately 25,000 civil servants in its Headquarters and Field Centers [1]. Through measures such as separation incentives, hiring freezes, normal attrition, and aggressive outplacement, NASA plans to have fewer than 18,000 civil servants by the year 2000. This workforce transformation encompasses more than merely a reduction in numbers. Agency strategic planning identifies a focus on research and development, rather than operations. To accomplish this will require "reducing the infrastructure at Headquarters and the Centers; transferring operational activities to commercial contractors as appropriate, and focusing internal efforts on technology development" [1].

The John F. Kennedy Space Center (KSC) is NASA's primary launch site, and center of excellence for launch and payload processing systems. The main focus of the Center relates to the Space Shuttle. KSC is responsible for the preparation, launch, and landing of the Shuttle orbiter, crews, and payloads, as well as the subsequent recovery of the solid rocket boosters [2]. It is also NASA's primary center for expendable launch vehicles.

Consistent with NASA's strategic direction, the KSC Implementation Plan and Roadmap were developed in 1998. These identify the Center's primary goals as it transitions from an operational work environment to one of development [3]:

- Assure that sound, safe, and efficient practices and processes are in place for privatized/commercialized launch site processing.
- Increase the use of KSC's operations expertise to contribute to the design and development of new payloads and launch vehicles.
- Utilize KSC's operations expertise in partnership with other entities (Centers, industry, academia) to develop new technologies for future space initiatives.
- Continually enhance core capabilities (people, facilities, equipment, and systems) to meet Agency objectives, and customer needs for faster, better, cheaper development and operations of space systems.

With regard to the fourth goal, a zero-based review of the KSC workforce was conducted in 1997. A zero-based review implies analyzing the need for each organizational function "from the ground up, since it starts with the assumption that the activity does not exist" [4]. The review identified yearly staffing levels through the Year 2000, consistent with the Agency strategic plan. However, concern was expressed regarding the identification and correction of skill mix imbalances [1]. The objective of this research is to develop a plan for an independent assessment of the Center's current work activities in order to support the decisions necessary to transition KSC toward a development work environment. The intent of the plan is to ensure that all employees are engaged in work linked with, and supportive of, the KSC Roadmap. Further, the plan would lead to the identification of skill gaps between present and future states, for retraining/redeployment efforts.

### 2. APPROACH

The concept of Business Process Reengineering (BPR) was originated by Hammer and Champy in their 1993 book, Reengineering the Corporation [5]. They define reengineering as "the fundamental rethinking and radical redesign of business processes to achieve dramatic improvements in critical contemporary measures of performance, such as cost, quality, service and speed". BPR infers a basic restructuring of essential business functions and processes, and not merely their modification, enhancement or improvement.

As the name implies, BPR is based on the concept of analyzing processes. According to classical BPR techniques [6], processes are composed of three primary types of activities: value-adding activities (i.e., activities important to the customer); transport activities (which move work across organizational

boundaries); and control activities (which audit or control the other types of activities). Normally, a process may wind its way through many boundaries and controls within an organization. Each organizational boundary creates a transport activity and at least one control. Therefore, the more organizational boundaries that a process must transverse, the more non-value-adding activities that are present within the processes. It is this workflow path that BPR seeks to analyze and make more efficient.

Further, BPR focuses on strategic, value-added business processes, and the associated systems, policies, and organizational structures that support them. Strategic processes are those of essential importance to a company's business objectives. Value-added processes "are processes that are essential to a customer's wants and needs and that a customer is willing to pay for; they deliver or produce something that he or she cares about as part of the product or service offered" [6]. Certainly in order to achieve the maximum return on investment in a reengineering project, it is logical to begin by focusing on the most important processes in the organization. According to the literature, most corporations can be functionally decomposed into twelve to twenty-four processes, and usually no more than six of these are both strategic and value-adding [6].

Reengineering attempts to optimize the workflow and productivity in an organization. This optimization is measured in terms of performance indicators. For business corporations, these performance indicators may include reduction in cost, and increases in revenue and profitability. An important component of BPR is the deliberate and explicit mapping of these performance indicators with the processes to which they apply. Improving process workflow via BPR is merely the means to the goal of improving organizational performance as measured by these performance indicators.

The competitive pressures of the 1990's, and the associated desire to provide increased levels of value both to existing and future customers, have lead many companies to utilize this methodology. Successful BPR case studies cited in the literature include McDonnell Douglas [7], BellSouth [8], and Corning [9]. BPR has also been successfully applied to such U.S. government agencies as the Patent and Trademark Office [10].

### 3. APPLICATION OF BPR TO KSC REQUIREMENTS

The Zero-Based Review was completed in 1997, however expected resource requirements have exceeded the scope of the ZBR. In addition, KSC core capabilities are not completely understood. As a result, effective workforce management and development are limited in meeting the future requirements of the Center. The Workforce Assessment and Validation Exercise (WAVE) was initiated as a follow-on to the ZBR, in order to conduct an independent assessment of the Center's current, and future, work activities and skills. This is required to support senior management's decisions toward transitioning from an operational work environment to one of development. Further, this project will identify skill gaps between these present and future states, and make recommendations for improved skills utilization. These recommendations may include retraining, redeployment, and reorganization.

By utilizing the techniques and principles of Business Process Reengineering, the following plan was developed to meet these objectives. The plan consists of four primary stages: organization and preparation; identification of the existing baseline; determination of specific areas for transformation; and transformation of the target areas into the objective baseline. KSC management recommended that the organization and preparation stage be conducted in two phases, in order to better focus on the existing and objective baselines, respectively. The complete plan is both extensive and detailed, and is presented here in a work breakdown structure in order to provide a concise format for this report:

#### **MAJOR TASKS IN THE WORKFORCE ASSESSMENT AND VALIDATION EXERCISE**

##### 1.0 ORGANIZATION & PREPARATION (PHASE A)

###### 1.1 Recognize Need for Restructuring

###### 1.2 Establish Executive Consensus

###### 1.2.1 Secure Support for Project

###### 1.2.2 Identify Scope of Project & Issues to be Addressed

###### 1.2.3 Identify Stakeholders in Status Quo

###### 1.2.4 Set Goals and Priorities for Project

- Includes prioritizing KSC roadmap Goals & Objectives
  - Linkage to Business Objectives and Agreements (BOAs)
  - This prioritization should consider Critical Success Factors for KSC
- 1.2.5 Establish Project Charter
- 1.2.6 Establish Strategic Plan/Schedule
- 1.3 Organize Reengineering Team
- 1.3.1 Define the Approach
- Functional Decomposition (Major Functions & Supporting Activities)
  - Linkage to Supporting Matrices
- 1.3.2 Identify Team Members and Responsibilities
- Core Team
  - Functional Teams
- 1.3.3 Convey Management Expectations
- 1.3.4 Allocation of Sufficient Resources
- Manpower
  - Time
  - Budget
  - Technology
  - Training & Consultants
- 1.4 Plan for Change Management
- 1.4.1 Plan for Means of Communications with Employees
- 1.4.2 Obtain Buy-in by Current Stakeholders
- 1.4.3 Establish Detailed Plan/Schedule for Next Phase

## 2.0 IDENTIFICATION (of Existing or As-Is Baseline)

- 2.1 Identify Primary Functions /Categories
- 2.2 Identify Supporting Activities & Steps
- Utilize ISO 9000 Process Flows as initial baseline (ref. Business World on KSC homepage)
  - Individual blocks within the Process Flows would be considered as Steps
  - Each Function, Activity & Step would be assigned a unique numerical identifier for use in the supporting matrices (See 2.4)
- 2.3 Interview KSC Personnel
- Confirm Functional Decomposition (Go to 2.4)
  - Revise Functional Decomposition (Return to 2.2)
- 2.4 Develop Supporting Matrices (X to Y)
- 2.4.1 Activity/Steps to Function
- Matrix constructed as part of 2.2
- 2.4.2 Roles & Missions
- Rows along Y axis: Function, Activity, Step
  - Columns along X axis: Organization Responsible. KSC Goal/Objective, External Customer, Internal Customer, External Supplier, Internal Supplier, Performance Criteria, Executive Priority
  - Organizational Responsibility:
    - ISO 9000 Process Flows indicate initial view of responsible organizations
    - Need to identify type of involvement on matrix, e.g. "responsible for", "provides information", "receives notification"
    - If necessary, this could be broken down to individual jobs within the Organization, and their relation to Activities and Steps
  - Use KSC Roadmap for Goals & Objectives
  - Performance Indicators on KSC webpage (under Business World directory) already mapped to Goals & Objectives
  - Variety of Performance Indicators identified; Question of which are considered Critical Success Factors to KSC

- Executive Priorities set in 1.2.4

#### 2.4.3 Time Matrix

- Rows along Y axis: Activity usually, may occasionally be Step
- Columns along X axis: Frequency, Volume, Duration, and Activity Type (Value Adding, Control, Other)
- Matrix could be used to derive \$ values, if necessary, by combining with other matrices and CFO databases.
- Time Matrix only required if process modeling software used in 5.2

#### 2.4.4 Organizational Charts (Existing)

- Employees to Organization
- Also identifies organizational resources (e.g. headcount)

#### 2.4.5 Skills Assessment

- Employees to Skills
- Completed by individual KSC employees, rather than management
- Use LeRC software and approach as basis
- Skills Inventory must not only identify existing job-related skills but those that will be needed in the future (i.e. when KSC achieves a development orientation)
- Linkage of Skills to specific Activities/Steps
  - GPES system
  - Part of data validation by supervisor

### 3.0 ORGANIZATION & PREPARATION (PHASE B)

- Repeat steps in Phase A (1.0)
- Emphasis here is on identification and obtaining objective environment.

### 4.0 DETERMINATION (of Specific Areas for Transformation)

- Need to clearly identify specific areas for analysis and restructuring.
- Cannot restructure everything at once. According to BPR literature, this is a prescription for project failure.

#### 4.1 Identify set of new Customers and their requirements.

- Survey Directorates/Project Offices.
- Add new activities or modify existing activities in order to support new Customers.

#### 4.2 Identify set of existing customers whose method of support will change.

- Implied linkage (external & internal suppliers/internal customer/external customer)
- Modify Activities to reflect change in method of support upon shift to development.

#### 4.3 Highlight any Activities in this linkage that will not support 4.1 or 4.2.

#### 4.4 Focus on "Core Capabilities".

- Defined in literature as those that are both strategic and value-added.
- Considered the most vital in the organization
- Linked to KSC Core Competencies
- At KSC, activities that directly affect stated Roadmap Goals and Objectives (1.2.4).

#### 4.5 Schedule efforts in next phase.

##### 4.5.1 Near-term opportunities (over next 6 months).

- Core Process activities used currently and in the future upon transition.
- Sequenced by Executive Priority (1.2.4) as well as probability of success.
- Provide early demonstrated benefits of project.

##### 4.5.2 Longer-term opportunities.

- Focus on Core Process activities, then on other high-value Activities.
- Ignore any Activities highlighted in 4.3.
- Sequence according to Executive Priority (1.2.4)
- Develop phased transformation plan.
  - Each phase addresses 1 or more "Activity Clusters" (i.e. linked Activities).
  - Linkage implied by chain of suppliers and customers (see 4.2).
  - Avoids creating "Islands of Efficiency" among process bottlenecks.

- Better leverages project efforts.

## 5.0 TRANSFORMATION (of Target Areas Into Objective Baseline).

### 5.1 Analysis of Scheduled Activities (4.5)

#### 5.1.1 Reexamine Linkages to improve performance.

- Steps within Activity.
  - Resequence?
  - Change in Organizational Responsibility?
- Activities within Clusters.
  - Better coordination between Activities?
- Identify Redundancies.

#### 5.1.2 Define Alternatives

- Eliminate redundancies.
- Simplify Activities/Reduce Steps.
- Relocate and Retime Controls (2.4.3).
- Methods Improvement.
- Application of Technology.

### 5.2 Evaluation of Alternatives

#### 5.2.1 Evaluate each Alternative based on resulting change in Performance Indicator (2.4.2).

#### 5.2.2 Recommend use of Process Modeling Software.

- Input original:
  - Activity Flows (2.2).
  - Time Matrix Values (2.4.3).
  - Organizational resources based on Organizational Responsibility (2.4.4).
- Simulate Existing Baseline.
- Modify Activity Flow and supporting matrices to reflect Alternative.
- Simulate Alternative Activity Flow to determine:
  - Delta of time requirements.
  - Delta of manpower requirements.

#### 5.2.3 Review of Alternative by Blue Ribbon Panel

#### 5.2.4 Accept/Revise Alternative (return to 5.1.2) based on delta of Performance Indicator.

- Particularly delta of Critical Success Factors (2.4.2).

### 5.3 Comparison of Accepted Alternatives to Original Baseline.

#### 5.3.1 Determination of Impact on Workforce.

- Compare Accepted Alternate Activity Flow (5.2.4) to Original (2.2).
- Update subordinate matrices:
  - Roles and Missions (2.4.2).
  - Time Matrix (2.4.3).
- Determine delta of Skills (2.4.5) and headcount (2.4.5) for Alternative.
- Consideration of Core Competencies/Core Capabilities provides priority.

#### 5.3.2 Organizational Change.

- Specify Management Structure.
  - Obtain KSC personnel's vision of the future.
    - Ideas for reorganization.
    - Willingness to reorganize.
  - Benchmark other organizations.
  - Possible alternative structures for consideration.
  - Evaluation of Alternatives and Recommendation.
- Redraw Organizational Boundaries.
  - Use recommended management structure as summary framework.
  - Organize around Functions/Activities.
    - Consolidate resources.
    - Avoid duplication.
    - Streamline processing.

- Specify Retraining/Redeployment.
  - Identify specific available candidates.
    - Employees associated with activities no longer required in objective environment (4.3)
  - Review candidates' skills in terms of type and level.
  - Compare to organizational skill needs (5.3.1)
  - Plan redeployment if match.
  - Plan retraining as necessary to provide match.
    - Weighted change in acquisition of skill level.

#### 5.4 Implementation.

- Determine Method for System Validation.
  - Parallel test
  - Pilot test
- Determine Methods for Conversion & Transition.
  - Systems
  - Procedures
  - Documentation
  - Data conversion
- Develop Time-Phased Deployment Plan.
- Pilot New Process.
- Refine & Transition.
- Continuous Improvement.

## 4. ASSOCIATED RESEARCH

### 4.1 CORE COMPETENCIES

The subject of core competencies has received considerable attention in the management literature [11, 12]. As defined by Gallon et al. [13], "core competencies are those things that some companies know how to do uniquely well". Examples frequently cited in the literature include:

- 3M, in developing coating products.
- Sharp, in producing high-volume liquid crystal displays.
- Kodak, in developing and applying silver halide imaging materials.

As indicated, core competency statements are normally at a very summary level. They exist at the top of a hierarchy. Organizations encompass a variety of discrete activities, skills and disciplines that Gallon et al. [13] refer to as primary capabilities. These primary capabilities are the responsibility of individual departments within the organization. They provide the foundation for the core competencies.

A subset of these primary capabilities have a direct and significant impact on the organization's success. This subset is referred to as core (or critical) capabilities. In commercial business organizations, these core capabilities are responsible for improved products or service, reduced costs, improved speed to market, and competitive advantage. Core competencies may be considered to be aggregates of these core capabilities. For example, core capabilities in surface coating formulation and continuous coating processes provide the basis for 3M corporation's core competency [13].

Kennedy Space Center's core competencies in launch and payload processing are clearly defined in the KSC Implementation Plan and accompanying Roadmap [3]. Separate initiatives are underway in order to identify the underlying core capabilities and primary capabilities, with special emphasis on identifying the skills associated with them. My specific assignment dealt with the development of a KSC competency assessment and skills inventory system.

According to Glueck [14], a skills inventory "in its simplest form is a list of the names, certain characteristics, and skills of the people working for an organization. It provides a way to acquire these data and makes them available where needed in an efficient manner." Good skills inventories enable organizations to quickly determine the types of people and skills that are available for future projects.

Investigation indicated that NASA Lewis Research Center (LeRC) developed a web-based skills mix assessment software package in order to inventory the existing skills of their personnel. The system

operates on a Windows NT 4.0 server hardware platform, and utilizes Internet Information Server 3.0 (which allows NT to perform as a web-based machine). It is then linked to Microsoft Access, which acts as the actual database repository. It is recommended that this provide the basis of the KSC skills inventory. Conversations with LeRC staff indicated that Goddard Space Flight Center was also interested in acquiring a copy of this software. It appears to be becoming the common NASA standard. Such commonality would allow skills review across different Centers for the purpose of establishing cross-functional teams.

#### 4.2 CLERICAL REVIEW

The Clerical Review effort was initiated on April 23 in order to address clerical support requirement issues at KSC; i.e. workforce reductions among civil service employees, constant turnover of clerical positions, and insufficient support from available temporary workers. The project team was directed to develop an innovative approach to meeting customer requirements in the area of clerical support, and to provide management with three to four options for fulfilling clerical support requirements. The project plan included the following steps:

- 1) Baseline clerical support workload levels.
- 2) Benchmark alternative support methods.
- 3) Recommend alternative methods.
- 4) Provide a cost-benefit analysis of proposed recommendations.

I was tasked as advisor to the Workload Analysis and Alternative Solutions sub-teams.

One goal of the KSC Clerical Review initiative is to develop a framework for meeting clerical support requirements. An initial step is to baseline clerical support workload levels. Such a baseline consists of identifying task descriptions, volumes, and durations. A survey was developed as an EXCEL spreadsheet and e-mailed to the various directorate Administrative Officers for distribution to the clerical support staff in their areas. Instructions for the completion of the surveys were provided. Hardcopy versions of the survey were also distributed for any employees that were more comfortable using this media. The survey was patterned after a similar 1996 questionnaire. (Since the 1996 survey was conducted, many things have changed at the Center, making this evaluation necessary. The clerical workers were instructed to complete the survey based on work accomplished during the week of June 15 - 19, and return them to their directorate Administrative Office no later than the close of business on Monday, June 22. The surveys were then forwarded for review and analysis.

In parallel to the workload analysis, a benchmarking exercise was conducted. The results of these analyses would be linked to provide a basis for the Clerical Review team's recommendations. It was observed that many aerospace companies had gone through this type of restructuring during the past five years. Their experience in this area would be of benefit to the study. Aerospace contractors at KSC would thus provide the primary points of contact for the benchmarking, with some other organizations (known to have been involved in clerical reviews/restructuring) also contacted. A standardized set of questions were developed. (See Figure 4-8.) Aerospace companies and NASA/federal/state agencies contacted included EG&G, Johnson Controls, Boeing, Rockwell, United Space Alliance, NASA Headquarters, NASA Lewis Research Center, NASA Goddard Space Flight Center, U.S. Army Transportation Command, and Eastern Carolina University.

Some initial broad alternatives discussed included maintaining the status quo, changes in technology used, outsourcing, organizational restructuring, and methods improvement. Probably the most viable alternatives regard the improvements in technology and methods used. Emerging information systems (e.g. electronic time cards addresses "Process Time Cards" which was identified as requiring approximately 5% of their time) are progressively allowing the individual to perform duties for themselves, that previously required clerical support. Another example is the GIDEPS system that will address the surveyed activities of "Process Training Requests" (2.5% on clerical survey) and "Schedule Training" (7%). While each of these three activities identified are relatively small, combined they required, on average, almost 15% of the clerical worker's time. Therefore, the application of improved technology can have a significant impact on leveraging the available clerical support.

The clerical workload survey also indicates that the individual directorates, and sometimes specific areas within a directorate, utilize clerical support differently. This suggests that the next phase of

analysis needs to be carried out within these individual directorates, instead of looking for solutions across the KSC organization. It is proposed that KSC industrial engineers conduct a methods improvement analysis to better leverage the available time of existing clerical workers.

#### 4.3 EXECUTIVE INFORMATION SYSTEM

An Executive Information System is a computer system designed to support the informational needs of very senior managers. It promotes a proactive, anticipatory style of management by which problem indicators are closely monitored and timely corrective action implemented prior to serious problem occurrence. This type of system may be further defined as having the following characteristics [15]:

- 1) An easy to use and maintainable graphical user interface.
- 2) Integrated capabilities for data access, security, and control.
- 3) On-request "drill-down" capability to lower levels of detail.
- 4) Depiction of organizational critical success factors.
- 5) Functionality for decision support, ad-hoc queries, and what-if analysis.
- 6) Sophisticated tools for system navigation.
- 7) Data analysis features.
- 8) Advanced report generation.
- 9) Statistical analysis.
- 10) Access to a variety of external data sources.

At KSC, there are presently a large number of Center-wide and custom software, programmed in a variety of languages, and operating on a variety of hardware platforms. Customized interfaces exist between individual software applications, however there is no application that bridges these individual systems, in order to meet the needs of Center senior management. Hence, the requirement for an Executive Information System at KSC. There are currently two "supersystems" which are currently under development at KSC, which may ease this inventorying effort. Resource Management System (RMS) and the Integrated Financial Management Project (IFMP) are independently developing their own linkages to these individual information systems and databases (or in some cases replacing them). IFMP is being developed to meet most of the agency's business requirements, and will be implemented across the NASA centers. The initial phase will focus on core financial applications (e.g., Standard General Ledger, accounts payable, accounts receivable), travel, procurement, budget, time and attendance, and asset management. Establishing an EIS linked to either, or both, IFMP and RMS would facilitate the development by limiting the number and type of subordinate interfaces.

Review of the IFMP documentation, on the KSC internal web, identified a reference to a proposed EIS. Further investigation indicated an initiative to develop an EIS which will integrate with IFMP. The proposed system will utilize the HOLOS software package on a networked DEC hardware platform. The EIS is an agency-wide effort, and will be progressively implemented at the individual centers. KSC implementation is currently scheduled for March 1, 2000. Thus, development of a Center-specific EIS is unnecessary at this time. It is recommended that the agency-wide EIS be extended, in the future, to link to RMS. This will provide senior management with more comprehensive insight into Center activities.

#### 5. CONCLUSIONS

A number of interrelated initiatives are currently underway at KSC, designed to support the Center's transition from operations to development. The research tasks conducted as part of this Summer Faculty Fellowship provide an integrated subset of these initiatives. The Workforce Assessment and Validation Exercise addresses the restructuring, retraining, and redeployment of elements of the workforce during the transition. The Core Competencies initiative regards identifying and maintaining critical skills at the Center, and maps to the WAVE project. The Clerical Review was tasked with assessing and analyzing the clerical support needs of the Center, and determining how to best leverage available clerical resources in order to meet future needs. The establishment of an executive Information

System will utilize emerging systems to support the information needs of senior management in the restructured KSC organization.

#### REFERENCES

- [1] National Aeronautics and Space Administration, "NASA Workforce Restructuring Plan", <http://www.hq.nasa.gov/office/codef/codefm/rs97plan.html>, January 1997.
- [2] Barth, T. "Industrial Engineering Lifts Off at Kennedy Space Center", IIE Solutions, Vol. 29, No. 2, February 1998, pp. 27-32.
- [3] Bridges, R.D. Kennedy Space Center Implementing NASA's Strategies, Kennedy Space Center, 1998
- [4] Tomasko, R.M. Downsizing, American Management Association, New York, 1987.
- [5] Hammer, M. and Champy, J. Reengineering the Corporation, HarperBusiness, New York, 1993.
- [6] Maganelli, R.L. and Klein, M.M. The Reengineering Handbook, American Management Association, New York, 1994.
- [7] McCloud, J. "McDonnell Douglas Saves Over \$1,000,000 per Plane with Reengineering Effort", Industrial Engineering, Vol. 23, No. 10, October 1993, pp. 27-30.
- [8] Brittain, C. "Reengineering Complements BellSouth's Major Business Strategies", Industrial Engineering, Vol. 25, No. 2, February 1994, pp. 34-36.
- [9] Bambarger, B. "Corning Asahi Video Products Co. Eliminates Cost of Errors for \$2 Million Savings, Industrial Engineering, Vol. 25, No. 7, July 1994, pp. 28-30.
- [10] Taylor, S. "Patent and Trademark Office sets the Standard for Reengineering Government", Industrial Engineering, Vol. 25, No. 4, April 1994, pp. 36-38.
- [11] Simpson, D. "How to Identify and Enhance Core Competencies", Planning Review, Vol. 22, No. 6, November/December 1994, pp. 24-26.
- [12] Steele, J. "Core Process Deployment - The Key to Results Through Alignment and Accountability", National Productivity Review, Vol. 14, No. 2, Spring 1995, pp. 67-77.
- [13] Gallon, M.R., Stillman, H.M. and Coates, D. "Putting Core Competency Thinking Into Practice", Research Technology Management, Vol. 38, No. 3, May-June 1995, pp. 20-28.
- [14] Glueck, W.F. Personnel: A Diagnostic Approach, Business Publications, Inc., Dallas, TX, 1975.
- [15] MITRE Corporation, Marshall Space Flight Center Executive Information Systems Requirements Specification, 1992, Contract No. NAS9-18057.

**1998 NASA/ASEE SUMMER FACULTY FELLOWSHIP PROGRAM**

**JOHN F. KENNEDY SPACE CENTER  
UNIVERSITY OF CENTRAL FLORIDA**

**HUMAN FACTORS APPLICATIONS ON CLCS**

Susan L. Murray, Ph.D., P.E.  
Assistant Professor  
Engineering Management Department  
University of Missouri-Rolla

KSC Colleague - Kristine Kennedy

**ABSTRACT**

This report is a summary of the research conducted by Dr. Susan Murray in conjunction with the NASA/ASEE summer faculty fellowship program during the summer of 1998. This report discusses three human factors applications on the Checkout and Launch Control System (CLCS) project. The first application is an ergonomic assessment of the work environment of CLCS personnel. Second is a study of the time requirements to convert the existing written work instructions from the current Launch Processing System (LPS) to the new CLCS. The final application is the Mission Management Team (MMT) console design for the Operational Support Room (OSR) and the Operations Management Room (OMR) in the Launch Control Center (LCC).

## 1.0 Introduction to CLCS

The Kennedy Space Center (KSC) is recognized as NASA's Center of Excellence for Launch and Payload Processing Systems. It is the world's leader in the area of manned launch and payload processing. To accomplish this, thousands and thousands of maintenance and inspection tasks are performed on the Space Shuttle before each launch. Additionally, a wide variety of preparation, test, and checkout operations are conducted on the payloads and scientific experiments that are launched into space from KSC. This requires coordinating a well-planned countdown process to assure mission safety and successful launch and landing operations. Due to the continually increasing maintenance costs, technological obsolescence problems, limited system flexibility, and desires for improved Shuttle processing efficiencies, a team was chartered in 1996 to study the present Launch Processing System (LPS) and to make recommendations for an upgraded system [1].

The recommendations of the team resulted in a five-year program called the Checkout and Launch Control System (CLCS). It will replace the current LPS supporting the Shuttle Program, which is composed primarily of 1970's technology. Over time this out-of-date technology has created reliability and obsolescence problems and has serious expansion limitations for future launch vehicles. NASA has an agency-wide goal to do things better and for less cost. By replacing dated hardware and developing new computer software to reduce operation and maintenance costs while eliminating obsolescence problems, CLCS is a prime example of this goal.

The CLCS project will require a complete review of the functional requirements of hardware, system software and end user application software. By increasing the system reliability and reducing the hardware, software code lines, and facility space, the team projects a yearly operational cost savings of 50 percent once the new system is fully deployed. In addition, the team predicts a decrease in the number of processing engineers required on site for each operation and a more efficient use of required operations/process engineering personnel [1]. The Checkout and Launch Control System will replace the current Launch Processing System with state-of-the-art technology. CLCS is expected to become a showcase for KSC's ability to answer complex problems in a cost-effective manner.

## 1.1 Introduction to Human Factors

Human factors is a specialty concerned with the well being of people in complex systems. It focuses on human beings and their interaction with products, equipment, facilities, procedures, and the environment. The discipline of human factors evolved from and still has ties to both industrial engineering and psychology. Early pioneers in human productivity and worker physiology such as Frederick Taylor, Frank and Lillian Gilbreth, and numerous others, laid the foundation for human factors. The field was further developed as a discipline during World War II when the human operator became increasingly the weakest link in sophisticated military systems. Since then the discipline has continued to grow and expand into new applications.

## 1.2 Project Overview

This report is a summary of the research conducted by Dr. Susan Murray in conjunction with the NASA/ASEE summer faculty fellowship program during the summer of 1998. This report discusses three human factors applications on the CLCS project. The first application is an ergonomic assessment of the work environments of CLCS personnel. Second is a study of the time requirements to convert the existing written work instructions from the current LPS to the new CLCS. The final project is the design of the new Mission Management Team (MMT) consoles. These will be located in the OSR and OMR in each of the firing rooms of the Launch Control Center (LCC).

## 2.0 Ergonomic Assessment

Ergonomics is a term that means the study of work. It considers how a worker interfaces with a wide variety of work components. This can include the workplace environment as a whole or individual factors such as noise, lighting, temperature, glare, vibration, and various others. It is also concerned with interactions between the human operator and machines, including manufacturing equipment and computers. Preventing cumulative trauma disorders (CTD) is a primary example of this. CTD refers to a variety of disorders of the muscles, tendons, or nerves; often these disorders can be avoided by a proper application of ergonomic

principles. Ergonomic assessments are reviews of an individual's work area and work task. They attempt to identify and correct poor body postures or motions. Highly repetitive tasks or long duration tasks are particularly important, due to their potential long-term impact on the worker's health.

## 2.1 Ergonomic Assessment Survey

An ergonomic assessment survey was developed for the CLCS project personnel. Its objective was to determine the overall working conditions on the CLCS project and identify individuals interested in receiving a personal assessment. The survey was sent electronically to the CLCS-All listserv. Participants were asked a variety of questions pertaining to demographic data, working conditions (desk, seat, computer, lighting, etc.), physical problems, and their level of ergonomic training. A total of 40 responses were received from a large cross-section of individuals including developers, technical writers, engineers, and managers.

There were some surprises in the overall results. The availability of basic ergonomic aids was low. For example, 60 percent responded that they did not have a wrist rest for their keyboard and 60 percent did not have a mouse wrist rest. Only 48 percent had adjustable keyboard trays and the vast majority of those did not provide sufficient room to place the mouse at the same level. Ratings of overall work area comfort are shown in Figure 1.

The survey asked the respondents to rate the intensity and frequency of pain or discomfort they feel in various parts of their body (neck, shoulder, forearm, wrists, fingers, lower back, and legs). Intensity level ratings included *none*, *low*, *medium*, and *high*. Pain frequency was reported as the number of occurrences per week in each body part. Intensity and frequency values were very similar on the various responses, as might be expected. Figure 2 summarizes the pain intensity reported in the survey. Zero represents a report of *none* for pain intensity. Questions left blank were also included in this group. *Low*, *medium*, and *high* were labeled 1, 2, and 3 respectively. Neck, shoulder, and lower back were the areas cited with the greatest frequency and intensity of pain among the CLCS personnel.

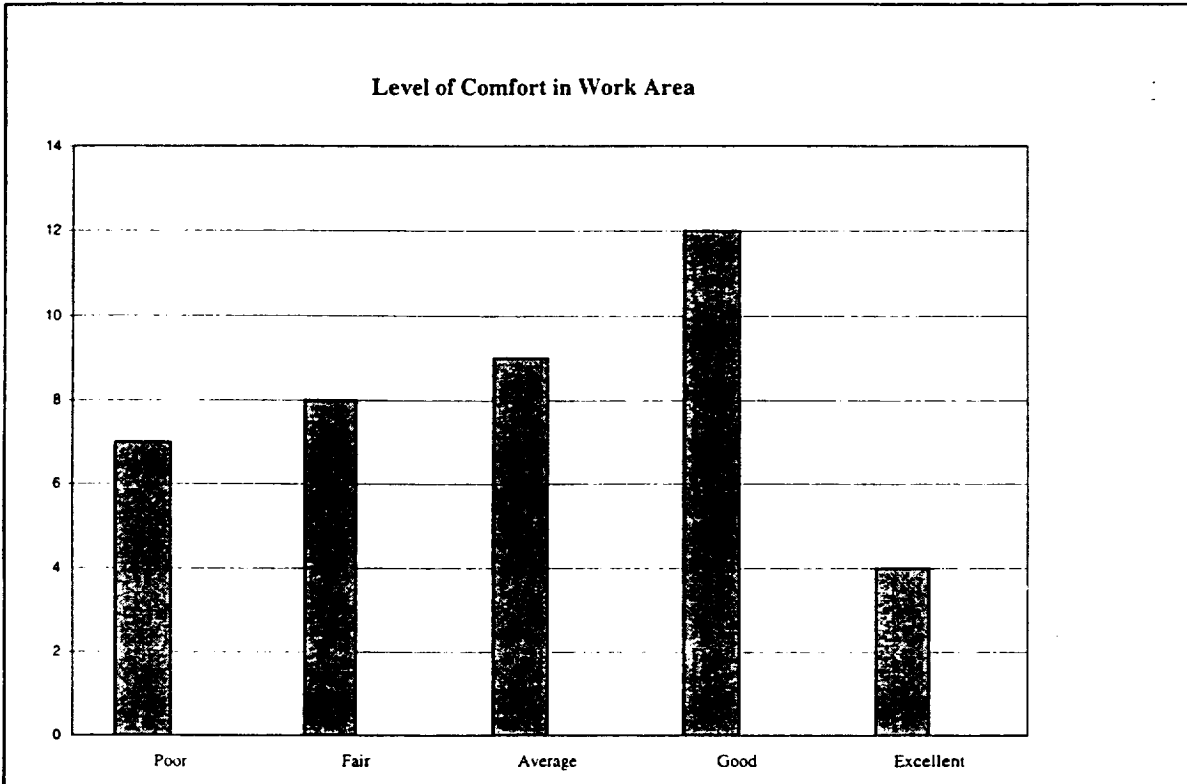


Figure 1

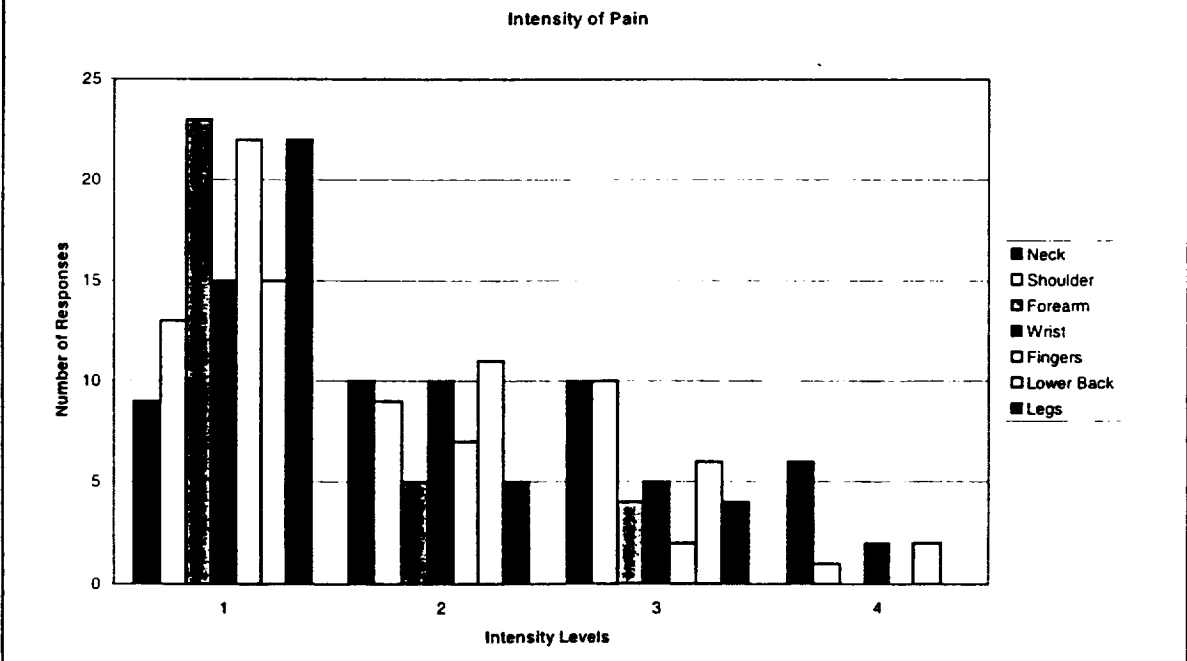


Figure 2

## 2.2 Ergonomic Assessments

Fifty percent of the participants responded that they would like a personal assessment. Everyone requesting an assessment was contacted to schedule an assessment at his or her convenience. Dr. Murray performed all of the assessments. The survey was used for background information on the subject during the assessment. The subjects sat at their workstations and described their typical work activities and any problems or concerns they might have. The worker's posture was observed and recommendations were made for changes to the workstation arrangement or worker's posture as needed.

The desired seated posture is shown in Figure 3. The feet should be flat, either on the floor or on a footrest. The joints should be at approximately 90 degrees and there should be sufficient distance between the operator and the computer monitor. If the spine, arms or legs were not in the desired position, changes to the workstation arrangement were made. Specific suggestions included raising the chair and adding a footrest, positioning the keyboard in front of the monitor, moving the mouse closer to the operator, moving the computer monitor, and adding wrist rests. The assessment was an interactive process. Subjects were encouraged to ask questions and participate in the change process.

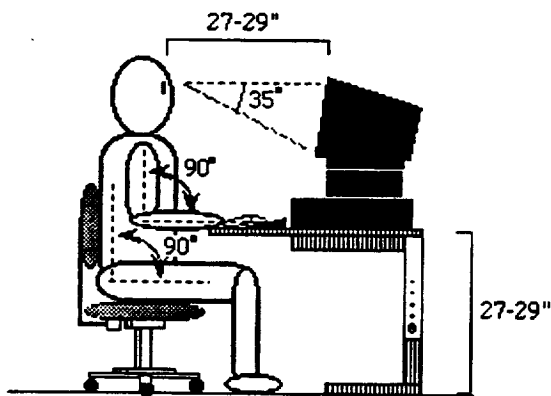


Figure 3 Reprinted from the University Computing Times, July-August 1990 [3].

Dr. Murray provided a general overview of ergonomics to everyone who received an assessment. She distributed a list of "Top Ten Ergonomic Tips" and stretching guidelines via

the CLCS newsletter and to the individuals receiving an assessment. There seems to be significant interest in ergonomic training. Each participant asked numerous questions and seemed genuinely interested in improving his or her working conditions. Detailed information on ergonomic products and/or CTD was given out as desired. It was left to the individuals to obtain ergonomic products through their own organization. Over 100 wrist rests for both keyboards and mice have recently been supplied to people on the CLCS project. These have been well received; preliminary feedback has been very positive. Overall, the suggestions were enthusiastically received and a preliminary follow-up has shown a significant reduction in the level and intensity of pain of those participating in the study.

### 3.0 OMI Conversion

Operations & Maintenance Instructions (OMI) are the written work instructions that are used to process the Shuttle and its payloads. These provide detailed step-by-step instructions for the engineers, technicians, and inspectors participating in the various operations. These books are typically hundreds of pages long and contain specifics concerning the system engineer console activities, as well as the activities performed by the shop-floor technicians. The OMIs were written for the existing LPS. As the new CLCS software is implemented, the existing work instructions will need to be modified for the new system. The CLCS project management is interested in determining an estimate for the time required for changing these work instructions. This is particularly important for scheduling purposes. The changes cannot be made until the CLCS requirements near finalization, but must be done prior to CLCS implementation. There is concern that potential bottlenecks exist that could impact the over project schedule.

A list of OMIs containing LPS activities was generated from several databases and input from system engineers. Approximately 950 OMIs from 24 Shuttle systems were reviewed for conversion requirements. The various system engineers gave their estimates for the time that would be required to redline the written documents. Operations and Maintenance Documentation (OMD) provided an estimate of the time required for making the changes in the KSC computer system. Process Planning gave a time value for the reviews required for each revised book and each new book. These numbers were summed to obtain the "most likely case" value. Due to the uncertain nature concerning these numbers, a range of time requirements was

desired for planning purposes. The assumption was made that an exponential distribution would best represent the nature of the conversion process. This was based on the fact that there are limited opportunities to improve on the estimated requirements, but numerous factors could cause the time values to be significantly increased. The 25<sup>th</sup> percentile was used as the “best case” scenario and the 75<sup>th</sup> percentile was used as the “worst case” scenario. Changes were made to the overall CLCS project plan to reflect the additional time requirements determined by this analysis.

#### 4.0 MMT Console Design

A significant portion of the CLCS project is the replacement of the existing equipment in the firing rooms. This is being done in three phases. The first two design phases are nearing completion; they are the system engineering (SE) consoles and the test conductor (TC) consoles. The mission management team (MMT) consoles are the third phase. Several console designs were considered for the system engineers and the test conductors. The analysis of the system engineering consoles was an involved process: multiple prototype consoles were built, usability tests were conducted, and numerous design revisions were made. Due to the frequent use and critical nature of these consoles, the extensive evaluation process was justified. There is a significant potential for operator errors at these consoles to cost millions of dollars and/or cause injury or loss of life.

The mission management consoles, however, are not used in a similar fashion. Typically they are only used on launch days. Unlike the system engineers, these individuals function in more of a monitoring capacity rather than a control capacity. Due to the nature of the personnel and the tasks being performed, appearance and aesthetics will be more significant than they were with the system engineering consoles. These differences dictate different design analysis procedures than those used on the systems engineering consoles.

Design requirements were identified for the MMT portion of the LCC. Each person in the OMR and the OSR requires a desktop telephone and an OIS (Operational Intercommunication System) unit. Every two people will require a computer workstation with a monitor, a power distribution chassis, a utility panel for laptop connectivity, a network hub, and sufficient desktop

space for binders. The Director of Public Affairs' work area additionally requires a video switcher to display various television networks. Size requirements were also identified for the limited space in the rooms. Additional see-over capability is required that limits the height of any console design to 42 inches.

Five ideas were developed for the MMT console designs. They are flat tabletop, split tabletop, below surface table mount, flat panel on an articulating arm, and traditional consoles. Significant advantages and disadvantages exist for each of these. The flat tabletop design would be an executive style conference table design. Placing the monitor and OIS units on top of this table design would exceed the maximum height requirement. There are also concerns that the desired aesthetics would not be achieved with this design. It was eliminated from further design considerations. The second design was a split tabletop design. In this design a rear portion of the table is lowered to reduce the overall height and to improve the see-over capability. A vendor has been contacted concerning this design and a preliminary design has been received. This design idea was deemed viable and will be included in further analysis. The final table based design placed the computer monitor under the tabletop with a glass panel for viewing from a downward angle. It was determined that the necessary viewing angle for two individuals sharing a monitor and the glare problems from the large viewing windows in the rooms would not make this a feasible alternative. It was eliminated from further consideration.

The remaining two design alternatives shifted from the tabletop approach. The first of these is mounting a flat computer monitor on an articulating arm. This would provide flexibility in positioning the monitor. Significant concerns exist about the feasibility of this design. A vendor has been contacted for specifics for this type of arrangement. Once the information has been received, a decision will be made if this is a viable alternative. There are major concerns about the function of this design. The final design alternative is a low profile console design. The OIS units and the monitors will be placed in turrets on top of the console. This angled design will satisfy the see-over requirement. Two vendors have been contacted concerning off-the-shelf designs and custom designs. This final alternative appears to meet all of the design requirements and will be included in further design analysis. This additional analysis is required to refine the

selected design alternatives and to evaluate the performance of various vendors' designs within these alternatives.

## 5.0 Conclusions

Human factors is a broad discipline with a variety of useful tools and techniques. This report details several applications on the CLCS project. In the current era of doing more for less at NASA, the Human Factors Engineering Team can provide a valuable service to improve the performance and usability of a variety of systems including equipment, computer software, and administrative procedures.

## 6.0 References:

- [1] National Aeronautics and Space Administration, *Program Management Plan Checkout and Launch Control Systems (CLCS)*, 84K00050-000, Revision A, June 19, 1997.
- [2] National Aeronautics and Space Administration, *Acronyms Checkout and Launch Control Systems (CLCS)*, 84K00240, Revision Basic, November 11, 1997.
- [3] Sheehan, Mark, *Avoiding Carpal Tunnel Syndrome: A Guide for Computer Keyboard Users*, <http://www.indiana.edu/~ucsstaff/cts.html>. (Reprinted from the University Computing Times, July-August 1990, pages 17-19.)

## 7.0 Acknowledgments

The information in this report would not have been possible without the support and assistance of numerous people. I would like to thank them for making this a very enjoyable and productive summer:

Linda Rupe and Kristine Kennedy - for their guidance, encouragement, and appreciation of sarcasm.

Mike Herold – for his assistance with a variety of challenges.

Roberta Wyrick, Greg Clements, and Rick Dawson – for their technical expertise and assistance.

Oscar Aragon and Jacqueline Bonnet – for their work on the assessment survey.

Gregg Buckingham, Jane Hodges, Ray Hosler, and Kari Stiles – for their efforts coordinating a wonderful program.

Robyn Witter and Julie Stephens – for their support and friendship.

UMR staff – for their endless legwork back in Rolla.

**1998 NASA/ASEE SUMMER FACULTY FELLOWSHIP PROGRAM**

**JOHN F. KENNEDY SPACE CENTER  
UNIVERSITY OF CENTRAL FLORIDA**

**CHARACTERIZATION OF TEST AND CHECKOUT DISTRIBUTED DATA  
PROCESSING SYSTEMS**

**Anand K. Ojha  
Associate Professor  
Department of Engineering Technology  
University of Arkansas at Little Rock  
KSC Colleague: Craig Jacobson**

**ABSTRACT**

The need for test and checkout systems to ensure safety and reliability of aircraft and related systems for space missions cannot be overemphasized. A variety of systems, developed over several years, are in use at the NASA/KSC. Most of these systems are configured as distributed data processing systems. The existence of these heterogeneous systems motivated NASA/KSC to invent some mechanism or procedure to benchmark or evaluate the performance of these diverse systems.

This paper first discusses various issues in performance evaluation of test and checkout systems. Next, it investigates four possible techniques to characterize test and checkout systems: 1) analytical method using queuing theory, 2) modeling and simulation software, 3) software emulation, and 4) monitoring tools. After discussing pros and cons of these techniques, it is determined that the monitoring tool technique would be the best choice in objectively characterizing test and checkout systems to obtain a better insight into their performance issues. Therefore, the paper finally concludes with two specific recommendations: 1) to explore the possibility of incorporating hybrid performance monitoring tools in the existing systems, and 2) to consider including such monitoring requirements while specifying new systems.

# **CHARACTERIZATION OF TEST AND CHECKOUT DISTRIBUTED DATA PROCESSING SYSTEMS**

Anand K. Ojha

## **1. INTRODUCTION**

To ensure safety and reliability, it is imperative to perform test and checkout on spacecraft and related systems. A number of systems are currently in use at the Kennedy Space Center. Some of the commonly used systems are: CITE (Cargo Interface Test Equipment), PPCU (Partial Payload Checkout Unit), TCMS, (Test, Control, and Monitor System), and CMU (Control and Monitor Unit).

The existence of a wide variety of test and checkout systems mentioned above led the NASA/KSC personnel to ask the logical question: how can these diverse test and checkout systems be benchmarked or evaluated? It should be mentioned that according to the current practice, systems to perform test and checkout are developed on as-needed basis either through custom sources or through commercial off-the-self products. In most cases, test and checkout systems are designed and updated mostly from past experience with similar or comparable systems. Often unknown safety margins are introduced to compensate for the lack of performance metric for the system. Thus the prevalent method of specifying and designing a test and checkout system is not very scientific, and to have a better understanding a logical choice will be to characterize the system. Here, characterization means a quantitative modeling of the system with the objective to obtain an insight into how the components fit and interact with each other in determining the system performance. Thus, characterization of test and checkout systems is the focus of this project. Characterization and modeling are often used interchangeably.

This paper first discusses various issues involved in the performance evaluation of test and checkout systems, lists possible strategies, and finally recommends that NASA/KSC should explore the possibility of incorporating hybrid performance monitoring in the existing system, and should also consider including such monitoring requirements while specifying new systems. The next section presents a brief overview of the test and checkout systems available at NASA/KSC. Section 3 describes the considerations in benchmarking of computer systems, and the characteristics of a test and checkout system that make benchmarking untenable. Section 4 discusses four different alternatives available to characterize test and checkout systems and presents a few analytical results from queuing theory that can be applied to such distributed systems. It finally concludes with the recommendation all test and checkout systems be incorporated with performance monitoring tools.

## **2. TEST AND CHECKOUT SYSTEMS AT KSC**

This section provides a brief synopsis of a few widely used test and checkout systems available at NASA/KSC.

### **2.1. Cargo Integration Test Equipment (CITE)**

The CITE system is used to test the mechanical fit and form of a payload to verify that its shape, electrical systems, and connectors match those of the Orbiter (Shuttle.) It provides functional simulation of orbiter avionics and power interfaces to the payload elements in the pre-launch, ascent and on-orbit configurations.

### **2.2. Partial Payload Checkout System (PPCU)**

PPCU processes the electronics systems in Spacelab and other payloads to ensure they work properly before they are put into the shuttle. The system is a modular distributed processing system based primarily on industry standard hardware/software interfaces and protocol such as, IEEE 802 network standards, TCP/IP network protocol standards, IEEE P1014 VME standards, IEEE P754 Floating-Point standards, and UNIX System V Operating systems.

### **2.3. Control and Monitor Unit (CMU)**

CMU is the latest generation processing system designed to encompass the capabilities of PPCU and Real Time Data System into one small unit ranging from a single card to a fast workstation.

### **2.4. Test Control and Monitor System (TCMS)**

TCMS has evolved from PPCU to support the activities at SSPF (Space Station Processing Facility), launch pads, SLF (Shuttle Landing Facility), and the OPF (Orbiter Processing Facility.) It is based on UNIX/X-Windows, and is built around SGI Origin 200 multi-processor computers with the functionality spread over the internal processors and Motorola's MVME167 cards linked though Ethernet. TCMS is essentially a distributed data acquisition, processing, and control system, and supports a mix of inputs including direct discrete and analog measurements and various types of serial and telemetry formats. The TCMS was originally built around Nighthawk computer system, but to benefit from the advances in the technology, the Nighthawks are being replaced by Origin 200 in the final implementation. A schematic of the TCMS is shown in Figure 1 (attached as the end of this paper.) Since several units will soon be available for experimentation, this is the system chosen for this project.

## **3. ISSUES IN BENCHMARKING COMPUTER SYSTEMS**

A benchmark suite provides a figure of merit for the system, and should be robust enough so as to provide a true reflection of the performance. This section provides a synopsis of the issues related to various benchmarks.

### **3.1. CPU Benchmarking**

The CPU has been the focus of most computer system performance evaluation, and a major concern of such studies has been the interaction between the processor and the memory, which in turn depends on the following factors [1]:

- Instruction Set

- Hardware Architecture: Caching, Pipelining, Superscaling
- Clock rate
- Compiler
- Memory Management
- Operating System

Operating system's contribution is mostly in memory management functions, and is not a dominating factor in performance consideration. The de-facto standard for CPU benchmarks is SPEC95 which consists of two suites: Cint95 and Cfp95. CInt95 is a collection of eight C programs, while Cfp95 is a collection of 10 Fortran-77 programs [2]. The output of these benchmark suites are single numbers that provides a comparison of the performance of the system with the performance of Digital Equipment Corporation's VAX-11/780 mini-computer of the late 70's.

### 3.2. I/O Benchmarking

The performance of a computer system that includes I/Os is greatly influenced by the architecture used to interface the three components: CPU, Memory, and I/O. In addition, the impact of Operating System is very pronounced. Therefore, systems containing I/O devices possess the next level of complexity in benchmarking. The confusion in this area is further compounded by the fact that depending on the system and application, there are several performance measures for systems consisting of I/O devices, and improving one measure might degrade the other. Some of the commonly used performance criteria for systems with I/O are [1]:

- Throughput (bandwidth): For supercomputer I/O, because they read large files and periodically write back updated large files to save the data from unpredictable crashes.
- Latency (response time): transaction processing, such as teller machines
- Number of transactions per second (TPS): Transaction processing, such as tax form processing. It is more important here to be able to improve the number of forms processed than the response time.

Thus, in contrast to processor performance benchmarking, the performance criterion for systems consisting of I/Os is not as unambiguous. The state of I/O benchmarking is still quite primitive compared to the processor benchmarking [1]. This is because of the widely varying schemes as a result of tradeoffs. Some of these variants are:

- cost versus performance in terms of latency and throughput
- the variety and number of I/O devices supported
- operating system and the application program that generate the I/O commands

Because of the diverse requirements, I/O benchmarks are application dependent, and examples of a few popular I/O benchmarks are provided below.

File system I/O benchmark: Unix system has an I/O benchmark suite of 70 files that take up 200 KB and run in five phases - MakeDir, Copy, ScanDir, ReadAll, Make.

Transaction System I/O benchmark: Two benchmarks, TPC-C and TPC-D, are regarded as de-facto standards for transaction processing systems [3].

TPC-C is intended for light to medium queries on a database based on an order-entry environment, and so is more appropriate for reservation systems, online transaction. The suite consists of nine types of databases, and five types of transactions. The performance is measured in Transaction Per Second (TPS) or Transaction Per Minute (TPM.)

TPC-D is targeted for complex business-oriented queries against a large database, and is suitable for decision support applications

### 3.3. Test and Checkout System Benchmarking

Now consider a test and checkout system which is a complex distributed data processing system, and in addition to the above consists of heterogeneous analog and discrete signals, multiplexers/demultiplexers, and networked systems with multiprocessors. The design of a distributed system is influenced by the following considerations:

- Response Time
- Throughput
- Utilization of Resources
- Diversity of I/O systems
- Reliability (MTBF)
- Fault Tolerance and Ability to Reconfigure
- Scalability
- Flexibility
- Ease of Use
- Portability
- Personnel Training
- Compatibility with Other Systems
- Expected Life of the System
- Cost

The first three in the above list are objective requirements; the remaining ones are quite subjective. It should nevertheless be observed from the above that, due to specific intended purpose and often competing requirements, a single generic benchmark does not seem to provide a good comparative measure to evaluate test systems. Instead, a better insight into all these issues can be obtained by quantifying the parameter that show how the components belonging to the system fit and interact with each other in determining the system performance..

## 4. SYSTEM CHARACTERIZATION CHOICES

It would appear from the discussion in the preceding section that, rather than benchmarking, a more appropriate approach to better understand test and checkout systems would be to model or characterize them. Estimating the performance of a system either by simulation or via analytical techniques requires the definition of a model that contains the

relevant features of the actual system. A model contains a definition of the set of building blocks that compose the system, a description of the functional relationships among these components, and the characterization of the workload that applies to the systems itself. Once a test and checkout system is modeled, the information can serve as a valuable pointer in planning for a new system, designing a new system, or modifying and upgrading an existing system. Since the systems being explored here are the most complex computer-based systems, the philosophy outlined here can also be applied to any computer-based system.

There are four possible approaches to performance evaluation of a distributed data processing system: 1) theoretical analysis using queuing theory, 2) modeling and simulation using a custom software, 3) software emulation of the complete system inclusive of the operating system, and 4) use of monitoring and measurement tools. The following subsections discuss these four techniques.

#### 4.1 The Queuing Network Analysis

In analytical method, results from queuing theory are used and the results are obtained through calculation of mathematical expressions. In using the queuing network model, the system, such as shown in Figure 1, can be thought of as a network of processing elements (nodes) connected through communication links. To account for parallel processing at any node, consider  $m$  to be the number of processor working in parallel at a node. For the  $i$ th node, denote  $\rho_i = \lambda_i / \mu_i$ , where,  $\lambda_i$  is the packet arrival rate and  $\mu_i$  is the service rate of each processor in packets per unit time. Then,

$$\lambda_i = \lambda_0 p_{0i} + \sum_{0 < j < i} \lambda_j p_{ji} \quad (1)$$

where,

$$p_{mn} = \text{Prob}\{\text{processor } m \text{ feeding processor } n\}.$$

For the sake of simplicity, the subscript  $i$  denoting the node number can be dropped. Now, assuming that the arrival and departure processes are Markov, it can then be shown that for the M/M/m queue the probability that there are exactly  $n$  packets at a node is [4]:

$$p_n = \begin{cases} p_0 \frac{\rho^n}{n!}, & n < m; \\ p_0 \frac{\rho^n}{m! m^{n-m}}, & n \geq m. \end{cases} \quad (2)$$

Where,

$$p_0 = \left( \sum_{j=0}^{m-1} \frac{\rho^j}{j!} + \frac{m\rho^m}{(m-\rho)m!} \right)^{-1} \quad (3)$$

The average number of packets,  $N$ , in the system can then be calculated from

$$N = \sum_j j p_j \quad (4)$$

Having obtained  $N$ , the average delay at the node can be obtained from the well known Little's formula.

Communications protocols can be treated individually. For Ethernet, the maximum value of link utilization,  $U$ , which is the ratio of the duration of useful (no collision) transmission to the total transmission duration, is given by [5]

$$U = \frac{1}{1 + 2a(1 - p_1) / p_1} \quad (5)$$

where,

$$a = \frac{\text{End-to-End Delay of the Link}}{\text{Frame Duration}} \quad (6)$$

and  $p_1$  is the probability that there is only one access during a slot duration, and can be obtained from

$$p_1 = \left(1 - \frac{1}{N}\right)^{N-1} \quad (7)$$

#### 4.2 Modeling and Simulation Software

The simulation method, based on the event-driven approach, is a description of the network structure created with the help of some readily available software which is run to obtain the performance results. TeleSim Project's SimKit from University of Calgary (<http://bungee.cpsc.ucalgary.ca/cgi-bin/download.pl>), and the SIMPACK software from the University of Florida (<http://wn.bilkent.edu.tr/prv/ftp/IEOR/Simulation/Simpack/Sim/simpack>) are some of the software tools available in the public domain for free distribution. Each of the above mentioned public domain software is just a collection of C/C++ functions that users can integrate in their own programs. Their use, however, does require some programming competency, and they do not have any graphic user interface.

Network II.5, SES Workbench, etc. are examples of commercial software, and they come with easy-to-use graphic user interface. These commercial software are expensive, and because these are based on event-driven simulation techniques, they require long execution time. In addition, they are only as good as the individuals who developed them. Nevertheless, these commercial software provide a quick way for a crude verification of concepts.

#### 4.3. Development of a Software Emulator for Test and Checkout System

The third approach requires building a complete software emulator for the test and checkout systems on the same lines as the SimOS simulation environment built for the multiprocessor system at the Stanford University [6]. This approach includes models of

hardware as well as of the operating system and emulates the complete system. The attractiveness of this strategy comes from the fact that a significant amount of verifiable work has been done in the public domain, and is available free. There are two drawbacks with this approach - first, this is manpower intensive; and second, it still gives simulated results whose validity can only be established with the help of real instrumentation discussed in the next section. However, once developed, the software emulator can serve as a useful tool in designing a new system or in modifying an existing design.

#### 4.4. Development of a Performance Monitoring System

Regardless of whether an analytical method or a modeling-software is used for characterization, each of the preceding techniques requires information about data traffic and its temporal characteristics. Therefore, it becomes necessary to first perform measurement on the system to determine the two key performance parameters: delay and resource-utilization. Thus, a logical alternative is to incorporate instrumentation in the existing system. This subsection discusses the issues related to the development of monitoring tools for test and checkout systems.

Performance monitoring techniques for distributed systems are still evolving, and efforts are underway to develop a common standard [7]. There are three approaches to designing a performance monitor: software, hardware, and hybrid. In the software approach, monitor-instructions are inserted at specific points by the programmer during development of the application program. The software approach can provide only a partial monitoring capability, because it cannot monitor events caused by external conditions, such as exceptions, interrupts, etc. Also, additional monitoring instructions degrade the performance of the system.

Events can also be monitored by external hardware in the form of a plug-in card at the processing node [8]. Every event of interest is encoded as a unique bit pattern called an *event token* that uniquely specifies *what* external event occurred and *where* it occurred. An event token is like an ID number of an event. For every event of interest, an event record is created that contains the event token and its timestamp. The event record is stored in the local memory at the processing node. Hardware monitoring is nearly non-intrusive, and in addition to interrupts, it can also monitor designated events like a logic analyzer during program-execution. The complexity of monitoring the events due to program execution increases with the complexity of architecture of the system, such as cache, virtual memory, etc.

Hybrid monitoring combines the best features of the two techniques: events caused by program-execution are logged by the software monitor, and those due to external conditions are tracked by the hardware. It is generally agreed that hardware monitoring provides a very efficient solution to the monitoring problem of distributed systems. Efforts to standardize an architecture for monitoring system have led the National Institute for Standards and Technology (NIST) to develop the MuliKron ASIC to promote standardization for hybrid monitoring. Therefore, it is all the more important that NASA/KSC explore the possibility of incorporating such hybrid monitoring tools in the distributed test and checkout systems. As explained before, the development of such monitoring tools is rather easy at the time of system development. Therefore, the inclusion of monitoring tools while developing specification of such systems

could be integrated into all future contracts. A test system without monitoring tools is like an automobile without an instrument panel.

## 5. CONCLUSION

This paper discussed the performance issues related to test and checkout systems, and the techniques available to characterize the system. From the discussions presented in the paper, it is recommended that NASA/KSC should explore the possibility of incorporating hybrid performance monitoring tools in the existing system, and should also consider including such monitoring requirements while specifying new systems. Future work requires building a small prototype monitoring system for TCMS to demonstrate the proof of concept of hybrid technique using the MultiKron ASIC developed by the NIST.

## 6. REFERENCES

- [1] D. A. Patterson and J. L. Hennessy, *Computer Organization and Design: The Hardware/Software Interface*, Fifth Edition, Morgan Kaufman, San Francisco, CA, 1998
- [2] SPEC95 Benchmark, SPEC, Santa Clara, CA. (<http://www.spec.org/osg/cpu95/>).
- [3] J Gray, and A. Reuter, *Transaction Processing: Concepts and Techniques*, Morgan Kaufmann, San Francisco, 1993.
- [4] M. A. Marsan, G. Balbo, and G. Conte, *Performance Models of Multiprocessor Systems*, MIT Press, Cambridge, MA, Second Print, 1988.
- [5] W. Stallings, *Data and Computer Communications*, Fifth Edition, Prentice Hall, New Jersey, 1998
- [6] M. Rosenblum, S. A. Herrod, E. Witchel, and A Gupta, "Complete Computer system Simulation: The SimOS Approach," *IEEE Parallel and Distributed Technology*, pp. 34-43, Winter 1995, (See also <http://simos.stanford.edu/> for updated activities.)
- [7] J. C. Harden, D. S. Reese, M. B. Evans, S. Kadambi, G. J. Henley, C. E. Hudnall, and C. Alexander, "In Search of a Standards-Based Approach to Hybrid Performance Monitoring," *IEEE Parallel and Distributed Technology*, Vol. 3, No. 4, pp. 61-71, Winter, 1995.
- [8] R. Hoffman, et al., "Distributed Performance Monitoring: Methods, Tools, and Applications," *IEEE Trans. Parallel Distributed Systems*, Vol. 5, No. 6, pp. 585-597, 1994.
- [9] A. Mink, "Operating Principles of MultiKron II Performance Instrumentation for MIMD Computers," NIST Report No. NISTIR 5571, U S Department of Commerce, Gaithersburg, MD, June 1995. (Web downloadable - <http://cmr.ncsl.nist.gov/multikron/reports.html>)

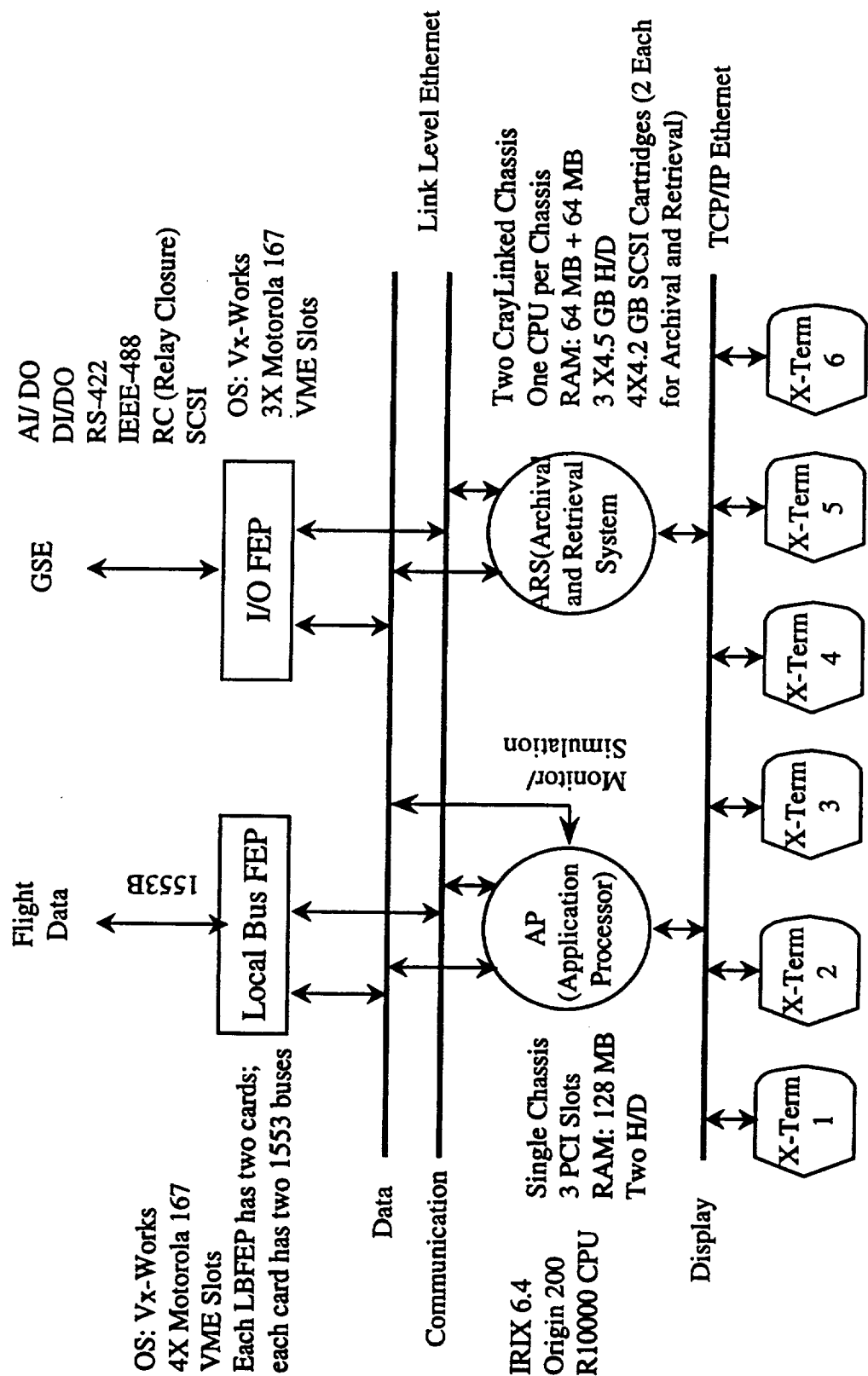


Figure 1. Schematic of TCMS

**1998 NASA/ASEE SUMMER FACULTY FELLOWSHIP PROGRAM**

**JOHN F. KENNEDY SPACE CENTER  
UNIVERSITY OF CENTRAL FLORIDA**

**APPLICATION OF STATISTICAL PROCESS CONTROL TECHNIQUES TO  
SHUTTLE PROCESSING**

Dr. Deborah M. Osborne, Associate Professor  
Department of Computing and Mathematics  
Embry-Riddle Aeronautical University  
Daytona Beach, Florida

KSC Colleagues:  
Timothy O'Brien  
Timothy Barth  
Industrial Engineering/Process Engineering

**ABSTRACT**

This report develops a series of case studies that demonstrate the application of statistical quality analysis techniques to monitor system stability and to evaluate system performance of several systems in the space shuttle program. The case studies provide examples of the use of system performance data to assist in evaluating flight readiness (CoFR) and determining need for enhancements as part of the surveillance activities of NASA Shuttle Engineering at Kennedy Space Center.

# APPLICATION OF STATISTICAL PROCESS CONTROL TECHNIQUES TO SHUTTLE PROCESSING

Deborah M. Osborne

## 1. INTRODUCTION

This report will describe an approach for implementing statistical techniques for analyzing system performance data to evaluate Certificate of Flight Readiness (CoFR), determine requirements for enhancement/upgrades, and evaluate contractor performance. A schematic depicting the application of statistical techniques to satisfy the NASA requirements of the Space Flight Operations Contract (SFOC) is provided.

Case studies included in this report focus upon the following Space Shuttle system performance data:

Orbiter System	Data and Sub-System Studied
Guidance, Navigation and Control System	ADTA/AADT Test Set Transducer Data from Air Data System
Main Propulsion System	LH2, LO2, GH2, GO2, and Helium Subsystems Data
Orbiter Maneuvering System/ Reaction Control System	OMS/RCS Helium Isolation Valve Data from Helium Pressurization Sub System
Orbiter Maneuvering System/ Reaction Control System	Primary RCS Regulator Data from Helium Pressurization Sub System
Environmental Control and Life Support System	Nickel Concentration Data from Supply and Waste Water Management System
Orbiter Mechanisms	Extension Times from the Landing Gear Sub System
Orbiter Mechanisms	Orbiter/ET Umbilical Bolt Ultrasonic Measurement Data from Orbiter/External Tank Separation System

Table 1.1. List of Case Studies Demonstrating Application of Statistical Techniques

## 2. STATISTICAL ANALYSIS OF SYSTEMS PERFORMANCE DATA

Process Engineering has surveillance responsibilities encompassing several areas: contractor performance evaluation, CoFR, enhancements, removal and replacement (R&R), and upgrades. The following diagram depicts the data collection and analysis activities for each surveillance responsibility.

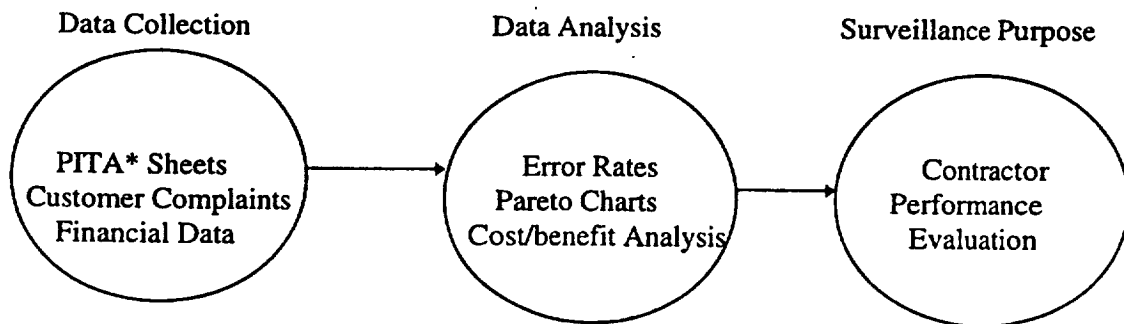


Figure 2.1a. Data Collection and Analysis Activities for Surveillance Responsibilities  
(\* Process Insight and Trend Analysis)

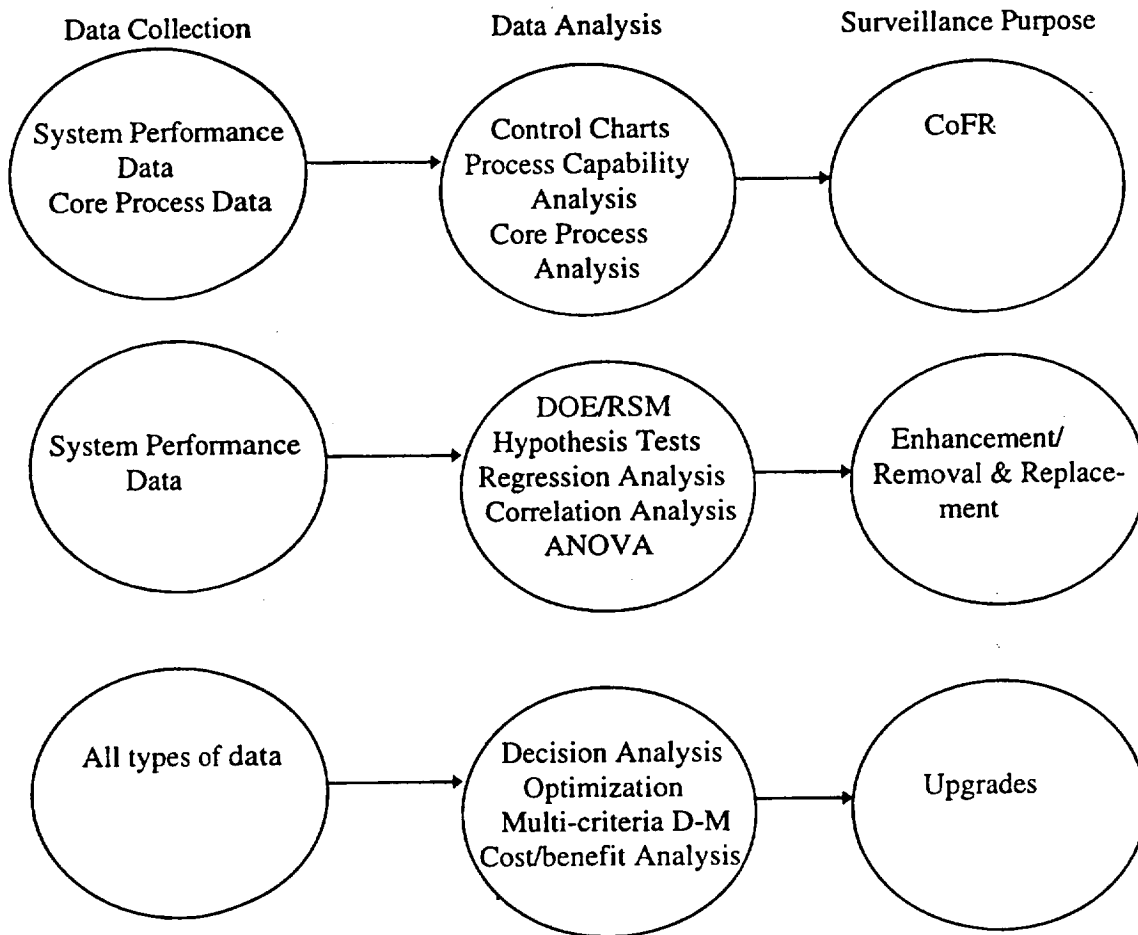


Figure 2.1b. Data Collection and Analysis Activities for Surveillance Responsibilities

The level of difficulty associated with skills that are required to use the statistical techniques can be envisioned as follows:

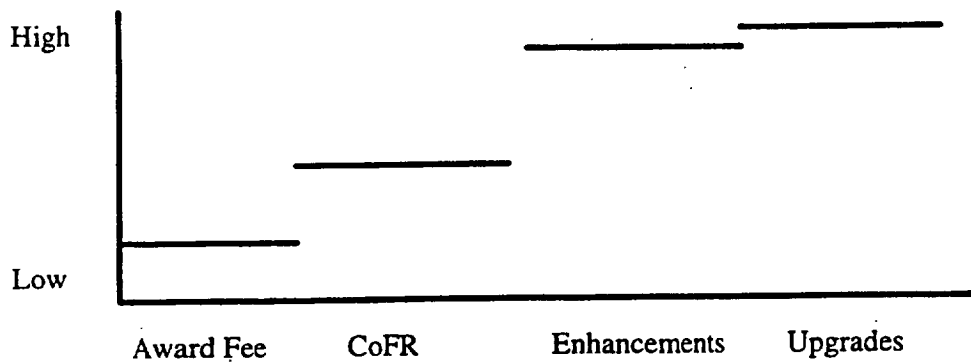


Figure 2.2. Statistical Technique Skill Level of Difficulty for Surveillance Responsibilities

The case studies included in this report support CoFR and Enhancement surveillance responsibilities.

### 3. CASE STUDIES DEMONSTRATING STATISTICAL QUALITY ANALYSIS TECHNIQUES SUPPORTING CoFR RESPONSIBILITIES

Several case studies were developed to support CoFR responsibilities. These case studies analyzed system performance data that systems engineers identified as critical variables that indicate the health of the associated system. Two case studies are highlighted in this section: main propulsion system and reaction control system. A brief description of the system is provided, followed by a review of the analysis techniques employed, and the conclusions derived from the analyses.

The Main Propulsion System (MPS) provides the necessary fuels to the Space Shuttle Main Engines (SSME) during the Shuttle's ascent from the Kennedy Space Center in Florida. These cryogenic fuels are Liquid Hydrogen (LH2, -423 °F) and Liquid Oxygen (LO2, -297 °F). The Orbiter MPS system consists of the manifolds, distribution lines and valves by which these liquid propellants pass from the external tank to the main engines. The system also provides a path that allows gaseous propellants tapped from the three SSMEs to flow back from the main engines to the external tank through two gas umbilicals to provide the ullage pressure for the hydrogen and oxygen tanks during flight. While the engines are operating, MPS also delivers Gaseous Helium (GHe) to inert and pressurize various sections of the SSME's.

During ground processing of the main propulsion system, several tests are conducted that measure the health of the system. Among these tests are five tests that collectively can be used to determine the performance of the main propulsion system. These tests include the Helium Decay Test data, LH2 Decay Test data, LO2 Decay Test data, GO2 Decay Rates data, and GH2 Decay Rates data. All analyses must be conducted for each vehicle separately. To examine the potential use of statistical quality improvement techniques for monitoring the stability of the Main Propulsion System, the data from OV-103 was used.

Before beginning the analysis to determine the stability of the helium decay test data, Pearson Product Moment correlation coefficients were computed for the eight tests included in the helium decay test process to examine the possibility that one or more of the tests were redundant. Examination of the correlations revealed that most pairs of variables were not significantly correlated, indicating that all variables should be analyzed for stability.

To determine the stability of the test results, a series of Individual X and Moving Range charts were constructed for all eight tests: Test1 Reg Out, Test1 Accum, Test2 Reg Out, Test2 Accum, Test3 Reg Out, Test3 Accum, Test4 Reg Out, and Test4 Accum. The Individual X and MR control charts are shown for the Test1 Reg Out variable:

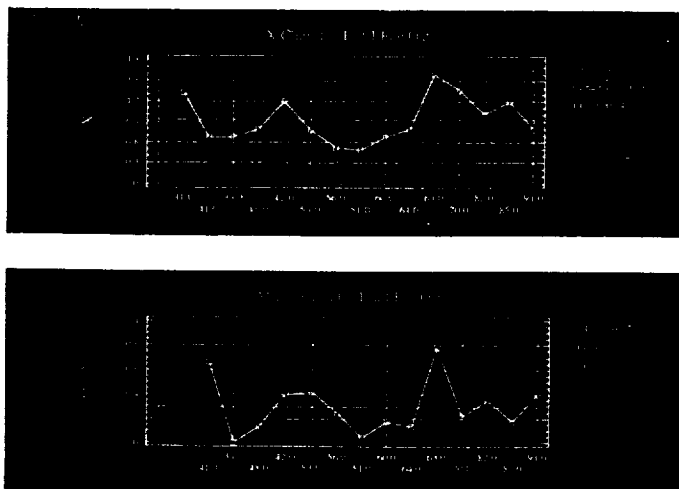


Figure 3.1. Control charts for Test 1 Reg Out

The charts are in a state of statistical control, indicating that the Test1 Reg Out process is stable. The Individual X and MR charts for the Test1 Accum variable are shown below:

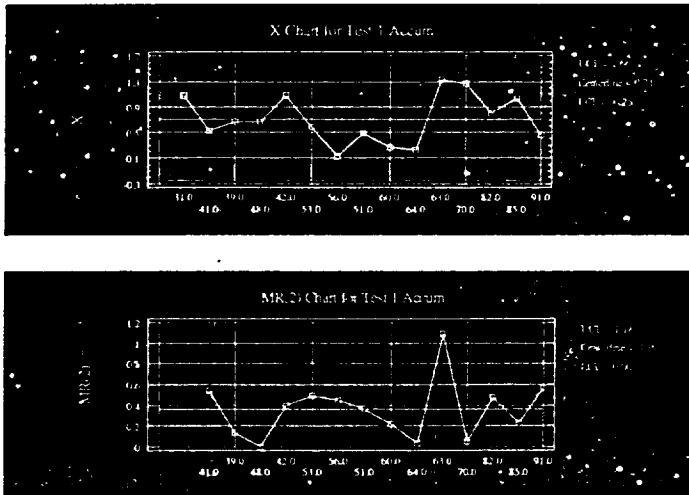


Figure 3.2. Control charts for Test 1 Accum

As was seen with the Test1 Reg Out process, the results demonstrate that the Test1 Accum process is stable. The same control charts were developed for the remaining variables, and all processes were shown to be in a state of statistical control, except the Test2 Reg Out process. The Test2 Reg Out process had a single point that was just outside the control limits for both the individual X and the MR charts. This may be explained by the small sample size included in the development of the control limits for the control charts. Hence, it is reasonable to conclude that the MPS Helium Decay Test processes are stable.

Similar techniques were used for the LH2 and LO2 Decay Test data, and these systems performance data were also stable. Insufficient data was available for analyzing the remaining two variables.

The contractor MPS group compiles a fairly extensive package each flow detailing numerous measurements taken during the ground processing flow. Since a small number of variables require monitoring to ascertain the health of the main propulsion system, much of the data collection, organization, and presentation is unnecessary. Many man-hours are expended collecting, compiling, and displaying this data. While this effort is commendable and some low level collection/tracking of that data may be necessary, it would be wiser to focus on the much smaller compilation of the critical variables of the Main Propulsion System presented in this case study, yielding an equally suitable indicator of the health of the system to management. A brief document providing the control charts and tables for the critical data should be developed for use in routine monitoring of the SFOC processes and CoFR recommendations.

While two case studies were developed using orbiter maneuvering system/reaction control system data, only the helium isolation valve case study is presented below.

The reaction control system (RCS) is a pressure-fed propulsion system utilizing storable hypergolic propellants (MMH and N2O4). It consists of three separate systems: one in the forward RCS (FRCS) module and one in each of the two aft propulsion system (APS) pods. The RCS provides attitude control and three-axis translation during external tank (ET) separation, orbit insertion, on-orbit operations, deorbit, and entry. Each RCS contains high pressure helium gas storage, pressure regulation and distribution systems for propellant tank pressurization, propellant storage and distribution systems, thrusters, electric power distribution circuitry, flight instrumentation, thermal control system, and attendant structure for component mounting. The FRCS includes 14 primary and 2 vernier thrusters. The two APS pods each

contain 12 primary and 2 vernier thrusters, which are located on each side of the aft fuselage, structurally integrated with the orbital maneuvering system (OMS).

The RCS helium isolation valves are used to isolate the high pressure gas source from the regulators and downstream components during most ground operations and certain in-flight failure modes. Two valves are arranged in a parallel fashion to maintain a level of redundancy. Each valve is bi-stable and electrically operated by the application of 24 vdc to either of two coils (open/close). Eight valves are used in the aft RCS and four are used in the forward RCS.

Ground testing is used to verify the functionality of these valves by applying high pressure helium on the upstream side and monitoring for leakage on the downstream side. A pressure rise over a specific period of time is an indication of leakage. Normally, a maximum leak rate of 600 standard cubic centimeters per hour (scch) is allowed per set of valves unless all of the associated regulators are known to be particularly robust. In this case, the combined leakage of the helium isolation valves can be as high as 1200 scch.

To monitor the stability of the helium isolation valves, each fuel and oxidizer isolation valve pair must be monitored separately. Individual X and Moving Range control charts were developed for each valve pair. As an example, Individual X and Moving Range charts were developed for the fuel and oxidizer helium isolation valves, FRC2. The fuel control charts follow:

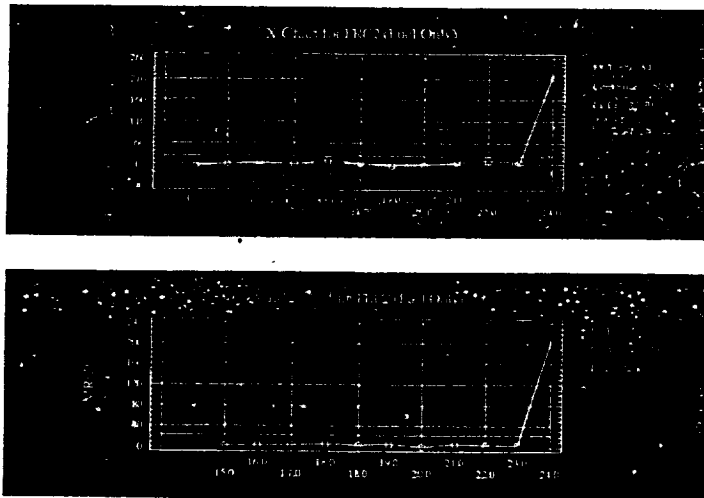
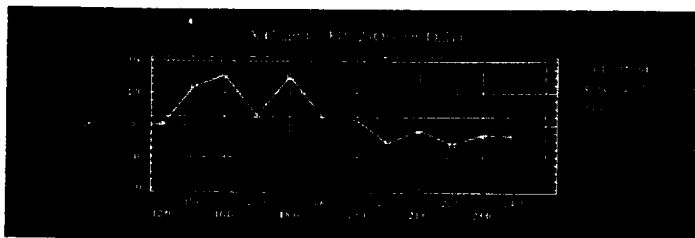


Figure 3.3. Control charts for Fuel FRC2 Helium Isolation Valve

For both the moving range and Individual X charts, the last data value is outside the control limits, indicating that there has been a significant change in the leak rate in pod flight = 24. A second set of control charts was developed to monitor the oxidizer helium isolation valve leak rate in FRC2. The corresponding Individual X and Moving Range charts follow:



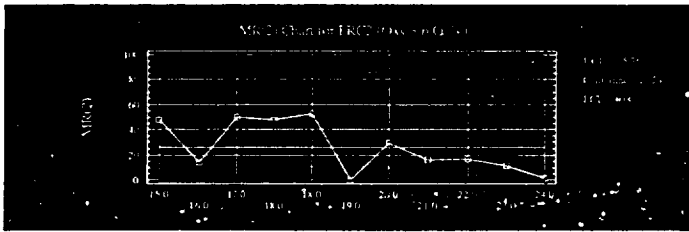


Figure 3.4. Control charts for Oxidizer FRC2 Helium Isolation Valve

For the oxidizer isolation valves, the leak rate is stable for the available pod flights. This same procedure was used to develop control charts for each fuel and oxidizer isolation valve pair for each pod/module.

Examination of the control charts associated with all helium isolation valves and research by the system engineer indicated that the control charts provided an indication of the significant changes in the performance of the helium isolation valves. However, each helium isolation valve must be monitored separately to determine the performance of the valve. Continuous monitoring and data collection over an extended period of time might reveal a pattern in valve performance which could lead to a predictive ability which does not currently exist. Prevailing test methodology centers on a pass/fail criteria with no special planning for forecast failures.

Several specific isolation valves demonstrated leakage at a stable level for several flights followed by a step-function increase to a new, higher level. Although the new level was well below the specified limits and no cause for alarm, understanding a developing pattern might be used to gain insight into overall system health.

#### 4. CASE STUDIES DEMONSTRATING STATISTICAL TECHNIQUES SUPPORTING ENHANCEMENTS

Several case studies were developed to support enhancements' responsibilities. These case studies analyzed system performance data that systems engineers identified as critical variables that indicate the health of the associated system. The analyses provided information that could be used to determine whether there is evidence to support the need for a system enhancement/modification. Two case studies are described: potable water system and air data system. A brief description of each system is provided, followed by a review of the analysis techniques employed, and the conclusions derived from the analyses.

Water is a key ingredient to a successful mission for astronauts who lift off from the Kennedy Space Center, FL (KSC) on a 2 week journey in the Space Shuttle. Storage space aboard the orbiter is very limited and each orbiter vehicle has four potable water tanks with a usable capacity of 165 pounds. This is not enough for all the water that is consumed on the extended space flight. To accommodate the additional requirement, astronauts use water which is generated as a by-product of the electrical generation system when Hydrogen and Oxygen are combined in the Orbiter's Fuel Cells to create electrical power. The water produced by the fuel cells is stored in the potable water tanks for use during the flight. It is important to ensure that the quality of the water is satisfactory for human consumption. To monitor the quality of the water, the nickel concentration, iodine level, and bacteria count are measured. In this case study, the nickel concentration was analyzed. Consideration of the nickel concentration requires monitoring the stability of the nickel concentration for each vehicle. To monitor the stability of the nickel concentration, Individual X and Moving Range charts were constructed for each vehicle at fifteen (L-15) and three (L-3) days prior to launch. Individual X and Moving Range control charts were also developed for OV-104 at L-15 days, and are presented in the following pictures:

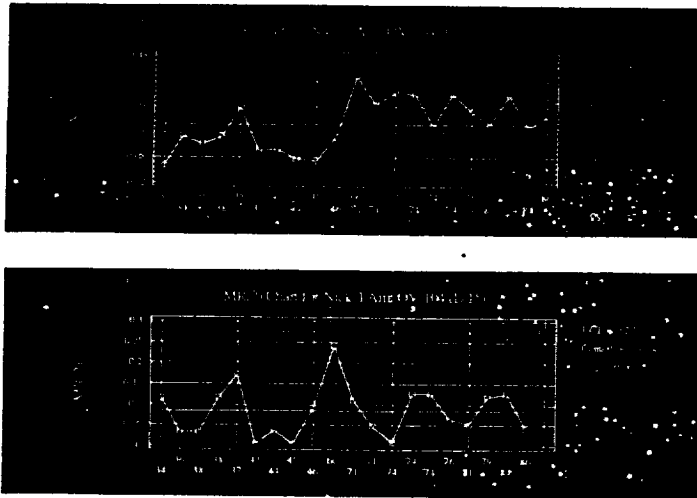


Figure 4.1. Control Charts for OV-104 Nickel Concentration at L-15

While the MR chart indicates a stable process, the Individual X chart demonstrates a statistically significant pattern, indicating that the nickel concentrations have increased significantly, beginning with STS-66. Research indicates that this is an OMDP flow.

Individual X and Moving Range charts were also developed for L-3 days for OV-104, and the same pattern that was evidenced in the L-15 days control charts is seen in the L-3 days control charts. That is, there is a significant increase in the nickel concentration from STS-66. However, the new pattern is in a state of statistical control at this higher level.

Prior to using the statistical analysis tools, the systems engineers plotted the nickel level vs. Mission. The resultant charts made it appear there may have been a worsening nickel level. This case study, however, showed the process to be stable after the initial step function increase was noticed. If statistical quality control techniques had been used, systems engineers would have reconsidered the conclusion to remove and replace (R&R) the existing chilled heat exchanger because of the "apparent" continuing increase in nickel level. Although difficult to capture at this date, the cost of resources (man-hours and material) expended would have been avoided if the R&R had not occurred.

Another case study that involved an enhancement to the orbiter vehicle is the Air Data Transducer Assembly case study. The Air Data System (ADS), a key component of the Space Shuttle's Guidance, Navigation, and Controls System (GNC), provides information to the shuttle crew for vehicle control and for monitoring vehicle movement in air mass during re-entry, especially the last ten minutes of aerodynamic flight (which includes approach and landing at the Shuttle Landing Facility). ADS is used by the navigation system to calculate: angle of attack, mach number, altitude, dynamic pressure, equivalent air speed, and true air speed. The ADS consists of the following: 2 Air Data Probes (ADP), 4 Air Data Transducer Assemblies (ADTA) containing 4 independent pressure transducers each, pneumatic titanium Dyna Tube plumbing, and flight software that processes the individual redundant pressure raw data into a single source to generate air data parameters. The ADTA outputs "drift" approximately 20-25 milli-inches per year. "Drift" is, through normal wear, a degradation of the ADTA's precision. The ADTAs are removed and calibrated about once every two years because the "drift" has caused the output error to accumulate to greater than 45 milli-inches Hg from initial installation into the orbiter. On the average, an ADTA or a component part fails and must be replaced each orbiter ground processing flow.

Because removal, off-site calibration, and replacement of ADTAs is time consuming and many replacement parts are obsolete or difficult to obtain, an advanced ADTA (known as AADTs) is being procured by NASA. These AADTs use a newer laser weld transducer with an advertised annual drift of only 0-5 milli-inches per year. AADTs are currently undergoing qualification testing. In addition to the transducer drift

improvements, this new technology has other operational advantages in that the digital electronics consumes less power, no longer requires forced air cooling, and weighs approximately 45% less (9.1 Kg/ADTA vs. 5.0 Kg/AADT). The old technology ADTA's are being phased out of the shuttle vehicles and replaced with new technology AADTs beginning in 1999.

During routine ground processing in the Orbiter Processing Facility (OPF) at Kennedy Space Center, a specialized air data test set (known as a ADTS) using seven air pressure levels (2.5, 5.228, 10.5, 15.5, 20, 25, and 29.92 inches Hg) measures the output error of the ADTAs in the shuttle for its upcoming flight. A comparison between the ADTS reference values and the ADTA transducer measurements is made, and the two values must be within 45 milli-inches Hg of one another. After several tests, a drift rate is computed to predict the out of tolerance date. In 1994, a new Air Data Test Set (ADTS) was purchased (to replace an older test set) from the same vendor currently developing the AADT. The ADTS uses the same new laser-welded transducer technology as the AADTs.

To substantiate the drift rate for the laser-welded transducers, data from the ADTS calibrations at the KSC standards lab have been collected and analyzed. In the lab, 19 levels (0.3, 0.5, 1, 2, 4, 6, 8, 10, 12, 14, 16, 18, 20, 22, 24, 26, 28, 30, and 32 inches Hg) have been used to calibrate (remove the drift bias) the ADTS. A total of eleven calibrations have been conducted on the new ADTS between 1995 and present. This analysis yielded data on the potential drift of the new AADT flight equipment to be phased into the shuttle vehicles in the near future.

Analysis of the lab data revealed that there are very high linear correlations (Pearson Product Moment Correlation Coefficients between 0.9973 and 0.9999) for all pairs of calibration data. These results indicate that a smaller number of calibration data points can be used to measure the drift associated with the AADTs and to reduce the number of calibration points the calibration lab uses to remove the bias from the ADTS transducer standard. Further analysis was conducted to predict the date when the transducer would be out of tolerance. The 26 inches of Hg level was chosen for the analysis. A scatterplot of the data revealed curvature. Thus, a quadratic and an exponential model were considered. The exponential model yielded an  $R^2$  of 0.967004. This model provides excellent prediction.

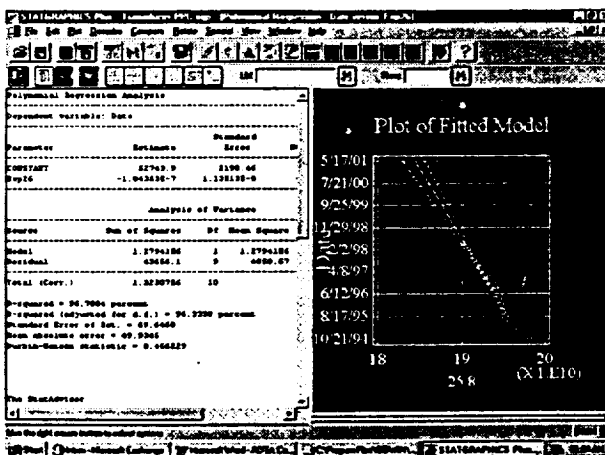


Figure 4.2. Plot of Fitted Line for 26 Inches Hg Air Pressure Data

To determine the data when the transducer would be out of tolerance, an air data pressure value of 25.955 inches Hg was used as the input. The following estimated date that the transducer will be out of tolerance was computed: 12/17/99. An analysis of the residuals indicated that the assumptions of normality and homogeneity of variance were satisfied. Hence, use of least squares regression is appropriate.

The analytical results indicate that it is not necessary to use a large number of air pressure levels to verify the calibration of the new AADT-type pressure transducers. Instead, between one and three air pressure levels are sufficient, possibly providing some redundancy to ensure that the testing equipment (ADTS) is functioning correctly when at the calibration lab. Additionally, with the use of the data collected from the 7 air pressure level OPF test using the ADTS as reference against the future AADTs, it is possible to predict the date when the AADTs will no longer be within the specification requirements. This provides engineers with useful information to plan for removal and replacement of the AADTs.

Since all data were gathered in the lab environment, it is important to collect data in the OPF and compare these data with the lab data to ensure that the actual work conditions replicate the lab conditions. This can be accomplished by using the standard 7 air pressure levels (2.5, 5.228, 10.5, 15.5, 20, 25, and 29.92 inches Hg) that have been used with the old ADTAs. Once several flows of data on the new AADTs are collected with the accompanying 7 air pressure levels for each flow, these values can be compared to the ADTS pressure transducer standard data collected at the same 7 air pressure levels. As long as there are no significant differences between the values (ADTS & AADT pressure transducers), the number of air pressure levels used for testing can be reduced to 3 or less.

## 5. CONCLUSION

Analysis of system performance data can yield information that supports the CoFR and Enhancement/Removal & Replacement responsibilities of NASA Shuttle Engineering. Control charts and process capability analyses can be used to monitor the stability and capability of space shuttle maintenance processes. Examination of these results enables NASA systems engineers to monitor the health of space shuttle systems without viewing the maintenance processes as they are worked. Other statistical techniques provide the opportunity to determine whether system components require replacement and to predict the date when replacement will be necessary. Additionally, use of statistical techniques enables systems engineers to compare the performance of competing products to determine which product provides the best value. Statistical techniques can be used to achieve cost avoidance objectives by indicating that a potential enhancement is unnecessary. Overall, there is an excellent opportunity to implement more advanced statistical techniques throughout space shuttle maintenance operations. However, to successfully implement these statistical techniques, additional skill development is required.

**1998 NASA/ASEE SUMMER FACULTY FELLOWSHIP PROGRAM**

**JOHN F. KENNEDY SPACE CENTER  
UNIVERSITY OF CENTRAL FLORIDA**

**DEVELOPMENT AND ANALYSIS OF ACCEPTANCE SAMPLING  
PLANS IN DATA VALIDATION**

Ronald F. Patterson  
Associate Professor  
Department of Mathematics & Computer Science  
Georgia State University  
Randy Tilly - KSC Colleague

**ABSTRACT**

This project, operating from the Office of Safety & Mission Assurance, will address two statistical concerns. The first concern will be to look at the statistical components that encompass the "Data Validation Project". The second concern will be to develop a introductory course in the design and analysis of experiments. This course will be developed for the "web" and will focus on the basic statistical/probabilistic principles of design and analysis of experiments (without too much detail). Emphasis will not be focused on the statistical model that generates the "analysis of variance" tables. The course will be case/example oriented and will concern itself with the interactive data platforms of some of the popular statistical software packages.

## 1. INTRODUCTION

During the summer of 1997, the Safety and Mission Assurance Directorate launch the Data Validation Project. The Data Validation Project is concerned with "performance based contracts" which involves the review of contractor provided data that will be the basis for assessing performance. This summer, the S&MA directorate has initiated a pilot project to demonstrate the concept of NASA Data Validation of contractor data. The Data Validation pilot group proceeded to demonstrate the above concepts as follows:

- They used standard audit procedures to determine process capability.
- They used sampling to assess stability once capability was determined.
- Candidate metrics was identified based on Core Process Team assessment requirements. A metric is a device that measures how well a process performs using graphs and statistical data analysis.
- They conducted research to identify potential data system requirements and contractor procedures.
- They interfaced with the United Space Alliance Program Coordination Office and reviewed generically the Contractor processes, which produced metrics.

The metric, A-GO-003, was selected by engineering for the pilot audit. The audit reviewed methods for collecting and assimilating data to produce the metric. Once the process capability was determined, a sampling plan was instituted. The sampling plan involves the identification of the population of interest, an established acceptance sampling plan, and the generation of the subsequent random samples. This report will discuss the statistical procedures that have been used by the Data Validation Pilot group. The report will also suggest some statistical procedures to be used by the contractor.

The final topic of this report will deal with the development of Web interactive training course, "Introduction to the Design and Analysis of Experiments". This course is the follow-up to two previous courses on the web. Its primary intent is to be a refresher course for persons who have taken a previous course in the design and analysis of experiments. For those persons who have never had course in the design and analysis of

Experiments, the introductory course will provide the student with the necessary background or prerequisite to pursue a more tradition course in the design and analysis of experiments.

## 2. RESULTS

**2.1. The Data Validation Project:** This report will concern itself with the sampling plan(s) associated with the pilot project mentioned in the Introduction. We would first partition the Kennedy Space Center into nine work areas. Each work area would be partitioned into sites where each site would be divided into three process areas. The first process area, Process Analysis, would contain the key or critical process; a second process area, Special Process, would contain the Special Function or "Support" Process; finally, the third process area, Area Surveillance, would contain the Quality System or "General" Process. The intent of this three-prong approach is that if the Quality System Process and the Special Function Process are in compliance, then the Key Process will ultimately be in compliance. We will deal with the Space Shuttle Main Engine (SSME) site, which resides in the Vertical Assembly Building work area. The chart below illustrates the breakdown of each process in the SSME site.

Process Analysis	Special Process	Area Surveillance	
KEY PROCESS (CRITICAL)	SPECIAL FUNCTION PROCESS (SUPPORT)	QUALITY SYSTEM PROCESS (GENERAL)	ISO 9001
1. SSME DRYING (VAB)	1. ELECTRICAL BONDING	1. DOCUMENT AND DATA CONTROL	4.5
2. HEAT EXCHANGER MASS SPEC AND PROOF PRESSURE CHECKS	2. ELECTRICAL CONNECTOR MATE	2. CONTROL OF CUSTOMER SUPPLIED PRODUCT	4.7
3. ASSEMBLY OF STRETCH JOINTS AND TORQUE JOINTS	3. MASS SPEC LEAK DETECTOR	3. IDENTIFICATION AND TRACTABILITY	4.8
4. ELECTRICAL CHECKS	4. TORQUE AND SAFETY WIRE/CABLE	4. PROCESS CONTROL	4.9
5. SSME FLIGHT READINESS TEST AND CHECKOUT	5. LIQUID PENETRATE (ROC)	5. INSPECTION AND TESTING	4.10
6. ENCAPSULATION LEAK CHECK	6. EXTENSIOMETER	6. CONTROL OF INSPECTION MEASUREMENT AND TESTING EQUIPMENT	4.11
7. TURBOPUMP FINAL TORQUE MEASURE (VAB)	7. TPS SPOT WELDING	7. INPECTION AND TEST STATUS	4.12
	8. MOLD IMPRESSION ANALYSIS	8. CONTROL OF NON-CONFORMING	4.13
	9. TOOL CONTROL	9. CORRECTIVE AND PREVENTIVE ACTION	4.14
		10. HANDLING, STORAGE, PRESERVATION AND DELIVERY	4.15
		11. CONTROL OF QUALITY RECORDS	4.16
		12. INTERNAL QUALITY AUDITS	4.17
		13. TRAINING	4.18
		14. STATISTICAL TECHNIQUES	4.20

The populations of each item in the Key Process, Special Function Process and the Quality System Process have to be determined. Once these have been determined with NASA and the contractor in common agreement, sampling can take place. This means that a sampling plan for the three processes must be developed. The sampling plan is as follows:

- The first stage consists of randomly selecting an item in each of the three processes. For example, in the pilot project, item 3 of the Key or Critical Process was selected; item 5 of the Special Function Process was selected; item 13 of the Quality System Process was selected.
- The second stage of the sampling plan consists of selecting a sample from each item selected in the first stage. The sampling scheme for each of those items are presented below:
  - For item 3 of the Key Process, the assembly of stretch joints and torque joints, the MIL STD 105E sampling plan is used to determine the sample size and acceptance number. The total number (population) of stretch and torque joints is 20 per engine. The chart below gives the letter code that determines the sample size for a given “acceptable quality level” (AQL). The pilot group chose a general inspection level III that gave a letter code of D for a lot size or population size of 20.

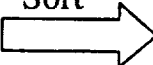
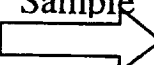
Sample Size Code Letters (MIL STD 105E)

Lot or Batch Size	Special Inspection Levels				General Inspection Levels		
	S-1	S-2	S-3	S-4	I	II	III
2 to 8	A	A	A	A	A	A	B
9 to 15	A	A	A	A	A	B	C
16 to 25	A	A	B	B	B	C	D
26 to 50	A	B	B	C	C	D	E
51 to 90	B	B	C	C	C	E	F
91 to 150	B	B	C	D	D	F	G
151 to 280	B	C	D	E	E	G	H
281 to 500	B	C	D	E	F	H	J
501 to 1200	C	C	E	F	G	J	K
1201 to 3200	C	D	E	G	H	K	L
3201 to 10000	C	D	F	G	J	L	M
10001 to 35000	C	D	F	H	K	M	N
35001 to 150000	D	E	G	J	L	N	P
150001 to 500000	D	E	G	J	M	P	Q
500001 and over	D	E	H	K	N	Q	R

The next table gives the sample size for an AQL of 1.5% and letter code D.



The above table gives the sample size for normal operations. If a fixed number of inspections exceed the acceptance number of 0, then the MIL STD 105E table for tightened sampling is used. In this case, the sample size increases to 13. If a fixed number of inspections meet the acceptance number of 0, then the MIL STD 105E for reduced sampling may be used. This is referred to as the switching rule. Going from 100% inspection to sampling allows the inspector to look at all three aspects of the above three processes. If the contractor is in compliance with the Quality System Process and the Special Function Process, then it is highly probable that the Key or Critical Process will be in control. The generation of a random sample is easily accomplished using Microsoft Excel and is described as follows:

0.757493	1		19		
0.389454	2		3		
0.040307	3		4		
0.06945	4		20		
0.282663	5		16		
0.245091	6		6	19	
0.254202	7		7	3	
0.732685	8		5		
0.911253	9		2		4
0.63025	10		17		20
0.89322	11		12		16
0.527928	12		18		6
0.9901	13		10		7
0.988267	14		8		5
0.979638	15		1		
0.235944	16		11		
0.417006	17		9		
0.623847	18		15		
0.008234	19		14		
0.073062	20		13		

The above random sample was created by generating a set of uniform random numbers equal to the size of the population. This is accomplished by using the Excel "rand" function. If we were sampling from the 20 torque and stretch joints, we would select joints 19, 3, 4, 20, 16, 6, 7, 5 in that order.

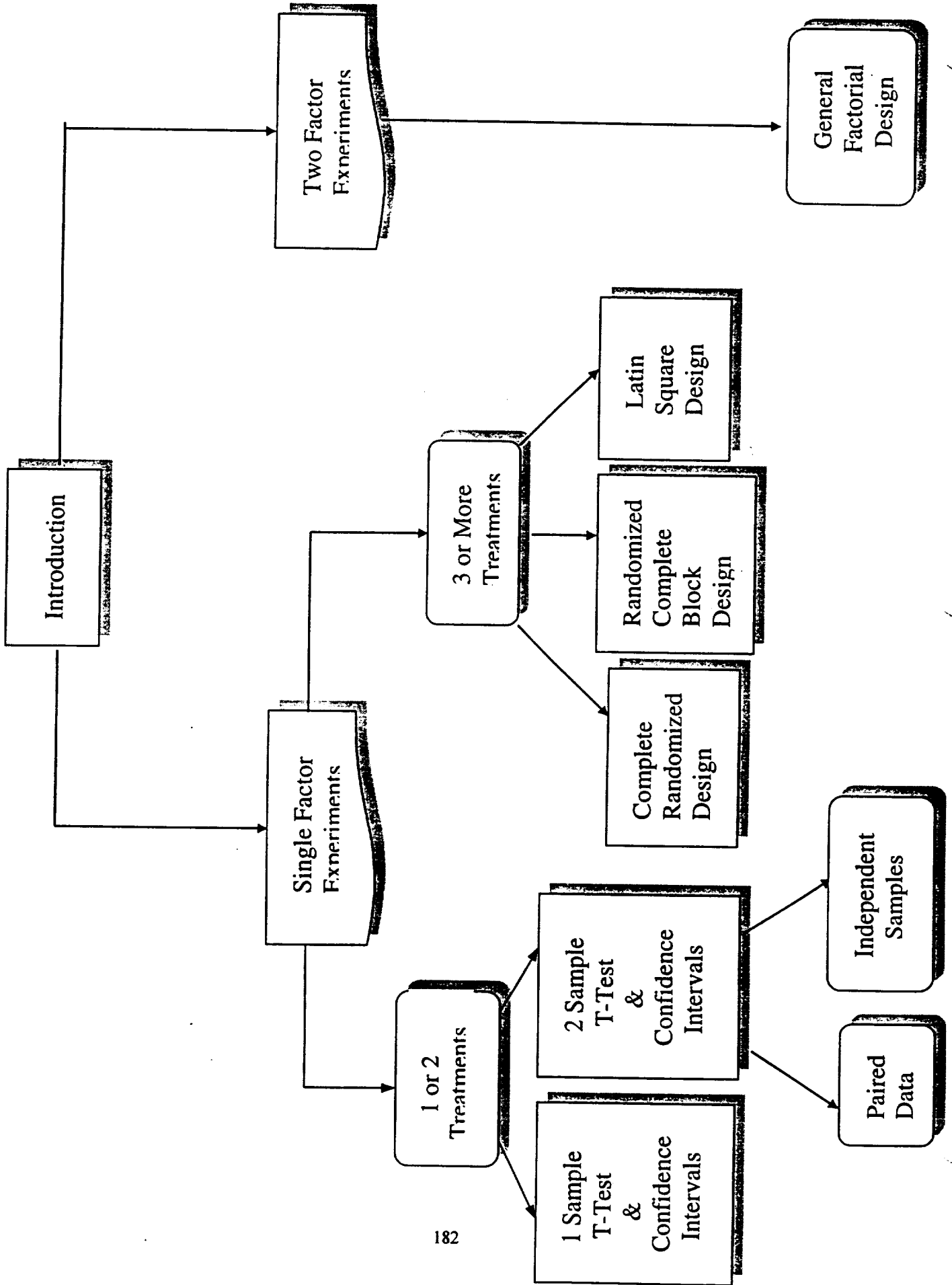
**2.2 Introduction to Design & Analysis of Experiments:** This course is part of the Web Interactive Training series of statistics courses designed for the web. The introduction to design and analysis of experiments is described as follows:

- **Audience:** NASA managers responsible for or concerned with quality assurance activities.
- **Prerequisite:** A basic course in statistical methods or statistical quality control or solid working knowledge of basis statistics, and familiarity with a statistical software package.
- **Objectives:** Upon completion of course, the student should:
  - Understand the principles of classical experimental design.
  - Understand how to design and analyze single-factor experiments.
  - Be familiar with the design and analysis of multi-factor experiments.
  - Have the necessary prerequisite to pursue a formal graduate course in experimental design.

**Approach:** Case study/example-driven. The student will begin with a simple experiment starting with hypothesis testing, confidence intervals for one and two samples, work through the basics of design and analysis for complete randomized design, randomized complete block design, the Latin square design and factorial designs using traditional analysis of variance. The student will have the opportunity to explore each of these topics in conjunction with their favorite statistical software package. Interactive data formats are provided so that the student, with a statistical software package, can simultaneously read the course material and perform the data analysis associated the examples provided in the course. Problems are provided at the end of the course to give the student the opportunity to explore the above topics in depth.

**Introduction:** Experimental design is used extensively not only in science, medicine, social science, but also in industrial process optimization and product design. An experiment is basically a test in which we apply treatments to experimental units. It could involve applying a dose of a drug to test subjects or changing the material type in batteries. Purposeful changes are made to the input variables (independent variables) of a process or system so that we may observe and identify the reasons for changes in the output response. We then attempt to draw conclusions about the population from which these samples were drawn. Careful experimental design enables us to control extraneous variables (as much as possible) and make inferences with the knowledge of risks associated with reaching a wrong conclusion. A flow chart of the course is presented below:

# Design of Experiments Web Interactive Training



### 3. Conclusion

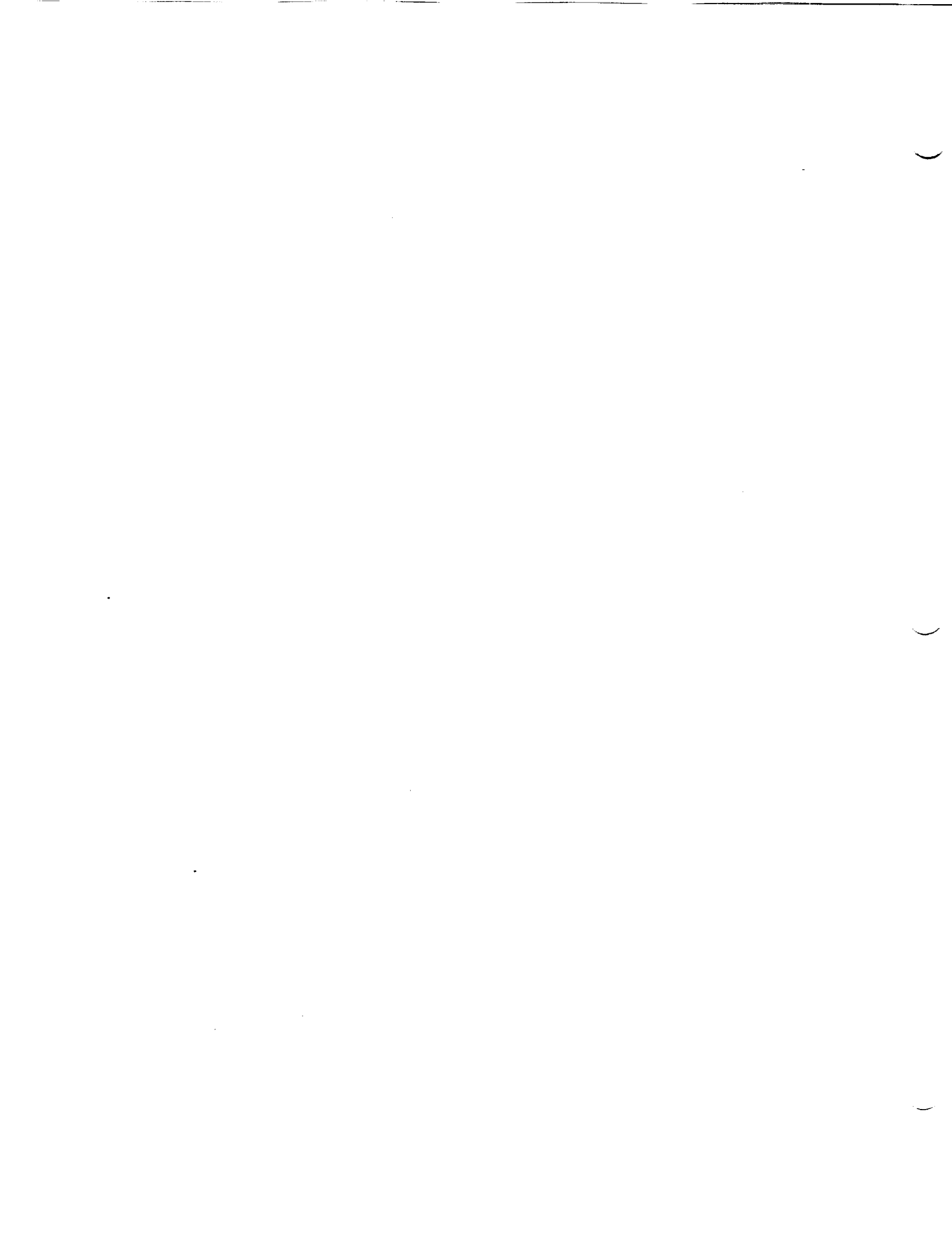
In this report, the first stage of the Data Validation Project consisted of determining if the contractor had certain ISO procedures in place. The second stage of the Validation process would be to determine if the process indicated by ISO procedures are in a state of statistical process control. The web interactive training course, introduction to design and analysis of experiments is complete. It is hoped that the course will be reviewed by an appropriate statistical organization such as the American Statistical Association.

### 4. Acknowledgements

I would like to thank the staff and management at S&MA for providing me with the opportunity to participate in the Summer Faculty Fellowship Program. In particular, I thank, Randy Tilly my KSC Colleague, Ron Dale, Fred Kohler, Bill Higgins, Sheryl Koller, Kimberly Vargas, and Nicole Scarborough. Finally, I would like to thank Gregg Buckingham, E. Ramon Hosler, and Kari L. Stiles for providing me with unique opportunities to learn about NASA and the Kennedy Space Center.

### 5. REFERENCES

- [1] Montgomery, D. C., *Introduction to Statistical Quality Control*, 1985, 3rd edition, John Wiley & Sons.
- [2] Montgomery, D. C., *Design and Analysis of Experiment*, 1985, 3rd edition, John Wiley & Sons
- [3] Statistical Analysis Systems, SAS, version 6.12.
- [4] JMP, SAS institute, version 3.1.5
- [5] Statgraphics Plus, version 3.1



**1998 NASA/ASEE SUMMER FACULTY FELLOWSHIP PROGRAM  
JOHN F. KENNEDY SPACE CENTER  
UNIVERSITY OF CENTRAL FLORIDA**

**Quantitative Infrared Thermography**

Robert E. Peale  
Associate Professor  
Department of Physics  
University of Central Florida  
KSC Colleague: Carolyn Mizell

**ABSTRACT**

Theoretical and experimental issues regarding infrared thermography are evaluated with regard to its use as a quantitative non-destructive evaluation tool for operations at KSC. Planar carbon composite on honeycomb laminates are studied as a model system.

# Quantitative Infrared Thermography

Robert E. Peale

## 1. INTRODUCTION

Infrared thermography is a non-destructive evaluation method for ceramics, metals, polymers, coatings, composites, and foam-core sandwich structures. Analysis of the thermal response to an external stimulation is performed to obtain depth profilometry and tomography. The method can reveal subsurface defects, voids, delaminations, and impact damage. Thermal response is usually characterized by infrared (IR) emission, which is imaged vs. time by an infrared camera. Flash lamp stimulation is common.

At Kennedy Space Center, flash lamp impulse stimulation has been used to gain mostly qualitative information on defect location in the surface plane. Defect detection has been demonstrated for corrosion under paint and for debonds in laminated materials. A goal of the present work is to learn to what extent *quantitative* information can be obtained. Such information might include defect thickness, depth, and composition, for example. It is hoped that this work will delineate some of the challenges in field-qualifying IR thermography for use as a routine inspection tool at KSC.

The temporal temperature distribution is key to quantitative analysis from IR imaging data. This distribution is described by the thermal diffusion equation and depends on geometry, thermal conductivity, specific heat, density, isotropy, initial and boundary conditions. Analytic solutions exist only for certain idealized situations, and numerical solutions are subject to artifacts. Fitting of theoretical curves to data requires accurate temperature measurements, but also accurate knowledge of the thermal properties of the medium and its underlying structure.

In this work, an IR imaging system is studied to reveal challenges in obtaining accurate temperature data. Thermal parameters for carbon composite and honeycomb substrate are measured, since this material is as suitable model system of importance in flight hardware. Properties of analytical solutions to the heat equation for certain simplified geometries and excitation conditions are investigated. Finally, thermographic data are compared to calculated temperature vs. time curves, and conclusions are presented.

## 2. EXPERIMENTAL DETAILS

The IR thermography system is depicted schematically in Fig. 1. A flash lamp (Speedotron 4803cx) deposits heat on the surface of a target. The lamp can be triggered manually or from the computer using a KSC-made interface box (Carl Hallberg). Mechanical, spring-loaded shutters were made at KSC by Mike Gleman to fit the flash lamp housing in an attempt to eliminate IR from the hot bulb following the flash. Shutter solenoid switches are triggered simultaneously with the flash lamp from the computer, again via the interface box. The infrared camera system (Amber 4256) is equipped with a 3-5  $\mu\text{m}$  bandpass filter and a liquid-nitrogen cooled, 256 x 256, InSb detector array. Subsequent electronics can be simply represented as consisting of integrating capacitors, transimpedance amplifiers (TIA), and an analog to digital converter. Data can be collected using the commercial software package (Ambervu) that comes with the camera. This package includes many useful image processing and analysis routines, but data acquisition routines are somewhat inflexible. In order to trigger the lamps and shutters simultaneously and to have control over the timing of frame grabs relative to the flash, special software was written at KSC by

Steve Thayer. A version modified for the present work to allow specifying the delay of the first frame after flash trigger and writing of images to disk is called "PEALE01."

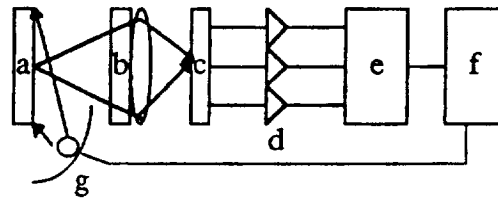


Fig. 1. Schematic of Thermography set-up. a=object. b= filter and lens. c=focal plane detector array. e=analog-to-digital converter. f=computer. g=flash lamp.

Careful calibration of the camera is required at frequent intervals because performance is a function of both shielding-vacuum quality in the pumpable detector cryostat and the length of time that liquid nitrogen has been kept in its reservoir. Goals of the calibration are to match the dynamic range to the object temperature-range of interest, to obtain uniform sensitivity over the image plane, and to correct for bad pixels. The full range of the ADC should be used without saturating it. Equally important is to adjust the system to avoid detector saturation, a problem which the system manual entirely fails to mention.

The calibration controls available are frame rate (usually 60 Hz), integration time, TLA gain and offset, and global gain and offset. The function of each is described in the user manual. The calibration procedure requires that a uniform cold and hot source be placed at different times entirely across the entrance aperture of the camera. The cold source is usually a room temperature lens cap. The hot source until now has been the operator's hand. Since the hot source is recommended to be as near as possible to the highest temperature anticipated, a broad area, resistively heated black body controlled by a diac-triac light dimmer and monitored with an LM34 IC temperature sensor was constructed by the author.

In optimizing the system for a given temperature range, images of a temperature-controlled black body, constructed by the author, were collected and analyzed. The heater was imbedded in a brass cylinder, whose end was coated in carbon soot from a candle. Images of the sooted area were averaged using the ambervu software to produce intensity vs. temperature curves.

Thermal conductivity measurements were made with the simple, home-built apparatus shown in Fig. 2. Joule heat from power resistors was assumed to flow only through the vertical stack of Al-sample-Al. Embedded temperature sensors were calibrated platinum RTDs, whose resistance was measured using the 4 point method with an HP3457A multimeter. A number of ASTM standard test methods for thermal conductivity have been described[1], and commercial versions are available from Holometrix, Inc., but measurement of a glass microscope slide using the apparatus in Fig. 2 gave results within 20% of accepted values for glass. This accuracy was considered adequate for the present, short-term study.

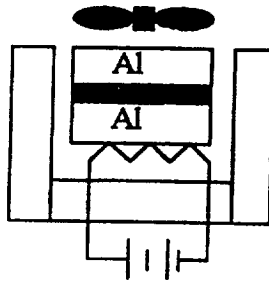


Fig. 2. Thermal conductivity apparatus. The sample is sandwiched between Al plates with imbedded temperature sensors. This block is heated resistively below and cooled by a fan above. Thermal insulation surrounds all sides but the top.

Specific heat measurements were made using a water-filled, styrofoam calorimeter, depicted in Fig. 3. A platinum RTD was used as the temperature sensor. The ASTM standard test method[2] for specific heat is similar. An accuracy of 20% was determined using known samples, which again was deemed adequate for the present study.

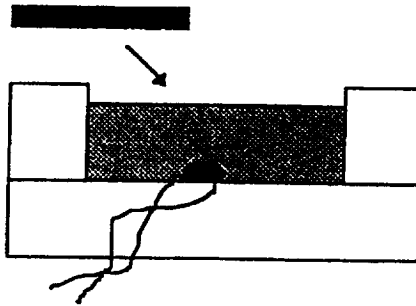


Fig. 3. Specific heat apparatus. The sample at some known elevated temperature is dropped into a styrofoam-cup calorimeter filled with a known volume of water. Initial and final water temperatures are measured with a platinum resistance thermometer.

The carbon composite material studied here consisted of carbon fibers woven into fabric and impregnated with resin. The surface of this material was the object of the IR imaging system, and it is a very good black body at 3-5  $\mu\text{m}$ , since no difference in thermal emission was observed when a portion of the surface was sooted with lamp black. The composite layer is resin bonded to a honeycomb structure consisting of resin impregnated paper.

### 3. CALCULATIONS

Theoretical emission intensity is found by integrating the Planck black body function

$$I(\lambda, T) = C_1 / (\lambda^5 (\text{Exp}[ C_2 / (\lambda T) ] - 1)) \quad (1)$$

over the 3-5  $\mu\text{m}$  wavelength range. The constants  $C_1 = 37405$  and  $C_2 = 143887.9$  when  $\lambda$  is in  $\mu\text{m}$ ,  $T$  is in K and  $I$  is in  $\text{W}/(\text{cm}^2 \mu\text{m})$ . This integral rises much faster in the

temperature range of interest than the  $T^4$  predicted by Wien's Law (integral of Eq. (1) over all wavelengths) because the peak of the black body curve shifts toward the 3-5  $\mu\text{m}$  window as temperature increases above ambient. Eq. (1) was numerically integrated using the commercial Mathematica™ package.

Analysis of the thermal conductivity data obtained using the apparatus of Fig. 2 was made using the heat flux equation[3]

$$dQ/dt = - \kappa A \text{ grad } T \quad (2)$$

The thermal conductivity  $\kappa$  is found by replacing the heat flow on the left by the electrical input power  $I \cdot V$  and grad  $T$  by the temperature difference between top and bottom divided by the sample thickness. The area of the sample  $A$  is easily measured.

The specific heat  $c_s$  of a sample is found using the apparatus of Fig. 3 by taking the heat lost by the sample to equal the heat gained by the water. This gives

$$-m_s c_s \Delta T_s = m_w c_w \Delta T_w \quad (3)$$

The subscripts  $s$  and  $w$  refer to the sample and water, respectively. The specific heat of water is 1 cal / (gram K). The mass of the water is found by measuring its volume in a graduated cylinder and using its density 1 gram / ml.

The differential equation that describes the temperature distribution vs time in the absence of mass transport is[3]

$$\rho(\bar{r})c(\bar{r}) \frac{\partial}{\partial t} T(\bar{r}, t) = \nabla \cdot [\kappa(\bar{r}) \nabla T(\bar{r}, t)] \quad (4)$$

Analytical solutions of this equation exist only for a limited range of geometries of uniform composition and for a limited range of initial and boundary conditions. Moreover, the solutions are complicated, typically involving infinite sums and error functions. For this preliminary work, we investigate simple geometries consisting of planar layers on a substrate, for which Eq. (4) reduces to an equation with one space dimension. This simplified equation is

$$\frac{\partial}{\partial t} T(x, t) = \alpha \frac{\partial^2}{\partial x^2} T(x, t) \quad (5)$$

where the thermal diffusivity  $\alpha$ , defined as  $\kappa/\rho c$ , determines the layer thermal properties. Interface properties are determined by the thermal mismatch factor[4]

$$\Gamma = \frac{e_s - e_l}{e_s + e_l} \quad (6)$$

where the thermal effusivity  $e$  is defined as  $\sqrt{c \rho \kappa}$ . The subscripts  $s$  and  $l$  refer to substrate and layer, respectively. Flash lamp excitation is usually taken as giving an instantaneous deposition of heat. In this case the solution to Eq. (5) that gives the time dependence of the surface temperature is[4]

$$T(0,t) = \frac{Q}{e_i \sqrt{\pi \alpha}} \left[ 1 + 2 \sum_{n=1}^{\infty} (-\Gamma)^n \exp\left(-\frac{\tau_n}{t}\right) \right] \quad (7)$$

where the thermal transit time  $\tau_n$  is defined as  $n^2 L^2 / \alpha$  (with  $L$  the layer thickness), and  $Q$  is the heat deposited.

To study the possibility that the flash duration is comparable to the thermal transit time, the temperature distribution in a semi-infinite medium during constant heating at unit rate is given by [4,5]

$$T(x,t) = \frac{2}{\kappa} \left[ \sqrt{\frac{\alpha}{\pi}} \exp\left(-\frac{x^2}{4\alpha t}\right) - \frac{x}{2} \operatorname{erfc}\left(\frac{x}{\sqrt{4\alpha t}}\right) \right] \quad (8)$$

The distribution after this heating is terminated at time  $T$  is

$$T(x,t) = \frac{2}{\kappa} \left[ \sqrt{\frac{\alpha}{\pi}} \exp\left(-\frac{x^2}{4\alpha t}\right) + \frac{x}{2} \operatorname{erf}\left(\frac{x}{2\sqrt{\alpha t}}\right) - \sqrt{\frac{\alpha(t-T)}{\pi}} \exp\left(-\frac{x^2}{4\alpha(t-T)}\right) - \frac{x}{2} \operatorname{erf}\left(\frac{x}{2\sqrt{\alpha(t-T)}}\right) \right] \quad (9)$$

For a finite layer of thickness  $L$ , the surface temperature during unit constant heating is [5,6]

$$T(0,t) = \frac{L}{\kappa} \left[ \frac{\alpha}{L^2} + \frac{1}{3} - \frac{2}{\pi^2} \sum_{n=1}^{\infty} \frac{1}{n^2} \exp\left(-\frac{n^2 \pi^2 \alpha t}{L^2}\right) \right] \quad (10)$$

The surface temperature after this heating terminates at time  $T$  is

$$T(0,t) = \frac{L}{\kappa} \left[ \frac{\alpha T}{L^2} + \frac{2}{\pi^2} \sum_{n=1}^{\infty} \frac{1}{n^2} \exp\left(-\frac{n^2 \pi^2 \alpha T}{L^2}\right) \left[ \exp\left(\frac{n^2 \pi^2 \alpha (t-T)}{L^2}\right) - 1 \right] \right] \quad (11)$$

#### 4. RESULTS

Camera calibration data will be presented first. Fig. 4 plots the measured image intensity for the black body and points calculated from the 3-5  $\mu\text{m}$  integral of Eq. (1) vs temperature. The measured intensity clearly saturates, showing little intensity variation in the range 320 K to 350 K, even though thermal emission is seen to rise rapidly. Thus, the camera configuration used to collect the data in Fig. 4 is unavailable for quantitative temperature measurements above 320 K. This effect is unrelated to ADC saturation, since then the saturation level would be at 4095. It is a detector saturation effect, and for a given frame rate it is affected only by the integration time. This effect is not mentioned at all in the users manual. Fig. 5 shows that when the integration time is reduced, the camera intensity response follows calculated expectations closely. Fig. 6 gives the maximum useful integration time vs. source temperature. This curve is independent of TIA gain or offset.

If one knows in advance the maximum temperature that will be imaged, the integration time should be chosen less than or equal to the value given in the curve of Fig. 6.

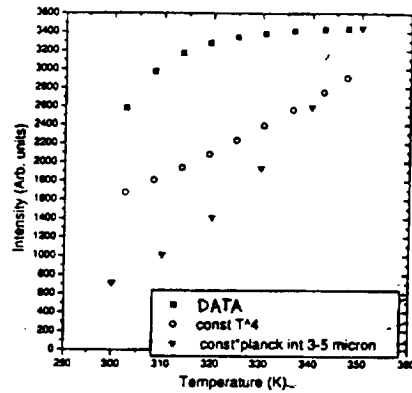


Fig. 4. Image intensity and calculated black body emission vs. source temperature.

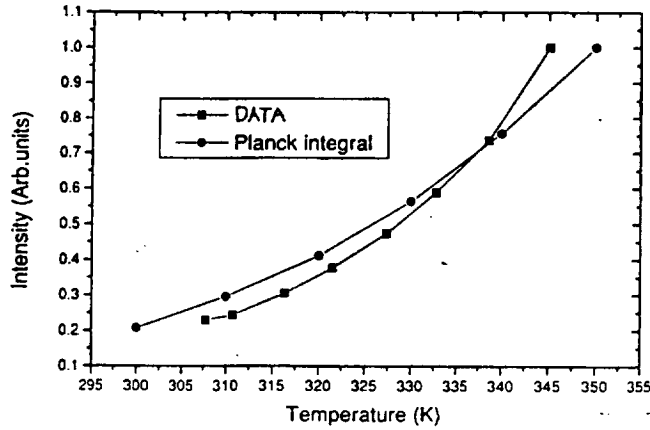


Fig. 5. Image intensity and calculated black body emission vs source temperature when the integration time has been set properly.

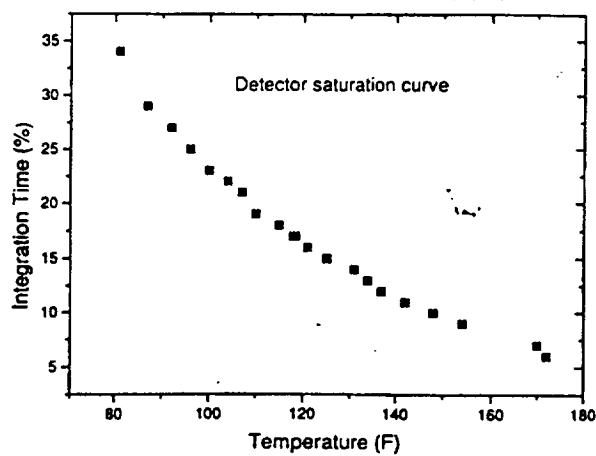


Fig. 6. Maximum useful integration time vs source temperature for 60 Hz frame rate.

The material of interest in the present work is carbon composite laminated on resin-impregnated card-board honeycomb. The measured mass densities of the component are presented in Table 1.

Table 1. Mass densities.

Material	Mass density (g/cm <sup>3</sup> )	Uncertainty
Carbon composite	1.3	7%
Honeycomb	0.05	2%

Thermal conductivity measurements gave the values given in Table 2. These values are probably all too high by about 20%. The value for honeycomb is surprisingly less than the value 0.026 W/(m K) given[7] for air, but the same reference indicates a value for styrofoam of 0.01 W/(m K). Hence, thermal diffusion in some solids may actually occur more slowly than in air.

Table 2. Thermal conductivity.

Material	Specific [cal/ (gram K)]	Uncertainty
Aluminum	0.17	20%
glass	0.24	20%
carbon composite	0.21	

Eq. (7) is formally a thermal wave interference picture with multiple reflections of thermal energy from the layer boundaries. The effect of including different numbers of terms in the sum is presented in Fig. 7 for the case where the substrate is a perfect thermal insulator ( $\Gamma = -1$ ). A finite excess temperature is expected, since the deposited heat has nowhere to go once the entire layer is equilibrated. Longer times require more terms in the sum to realize this fact. The solution with no terms kept corresponds to the semi-infinite medium.

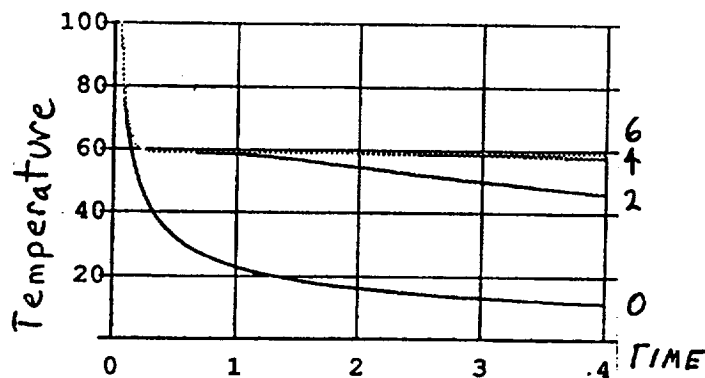


Fig. 7. Plot of calculated surface temperature vs time for different numbers of terms kept in the infinite sum.

It is important to note the thermal wave interference idea is a mathematical convenience that does not physically exist, since thermal energy cannot reflect at boundaries. Thermal energy flows opposite to existing temperature gradients. For there to be a reflection, the gradient would have to change sign, but in doing so the gradient would pass through zero, and all heat flow would stop.

The question of whether the flash is instantaneous or finite in duration is determined by comparing its actual duration to the thermal transit time. Another way is to compare the distance that heat has traveled in the layer to its thickness. To do this it is first necessary to measure the flash duration. Fig. 8 presents IR intensity vs. time with the surface temperature indicated at a few points. Two sets of data are presented with and without use of the flash lamp shutters. The precipitous drop for both data sets at 10 ms indicates that the flash duration is 10 ms and that the shutters take at least that long to close. Beyond 10 ms the slight difference between the curves indicate a slight effect of the shutters in eliminating diffusely reflected IR afterglow from the lamps. Separate time dependent imaging of a broad area hot source covered by the shutters show that they first start cutting the view at around 9 ms and are almost completely closed by 10 ms.

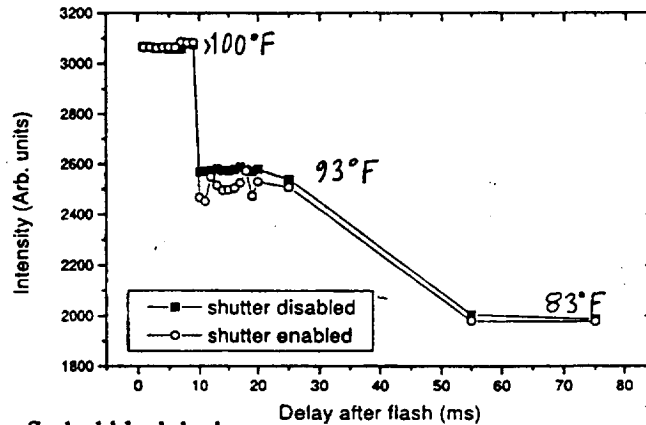


Fig. 8. IR image intensity vs time for flashed black body.

Fig. 9 shows the temperature distribution during and after a 10 ms heat pulse calculated from Eqs. (8) and (9). These curves were calculated using the thermal parameters for carbon composite. The composite layer thickness studied in this work was 0.03 cm. It is clear from Fig. 9 that by 10 ms, heat from the flash has reached the back wall. Thus the flash duration cannot be considered as short compared to thermal transit times, and Eqs. (10, 11) should be used to describe surface temperature rather than Eq. (7).

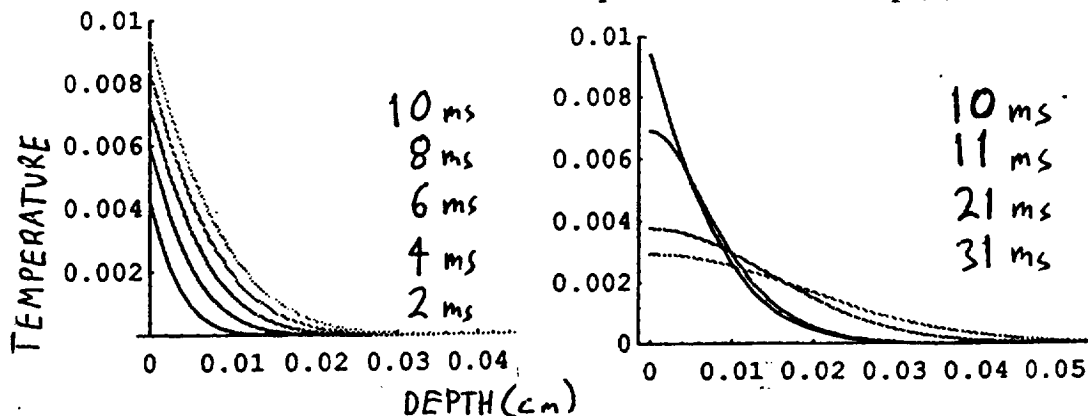


Fig. 9. Calculated heating and cooling temperature distributions in semi-infinite carbon composite for a 10 ms flash.

Fig. 10a shows the surface temperature for composite layers of 0.1, 0.2, and infinite thicknesses calculated according to Eqs. (10) and (11). Differences in the curves appear at later times, and early times are relatively insensitive. Fig. 10b shows data for a 0.3 mm composite layer on honeycomb together with the curve for semi-infinite composite. According to Fig. 10a, the data in Fig. 10b should lie slightly above the curve, but otherwise the match is not bad.

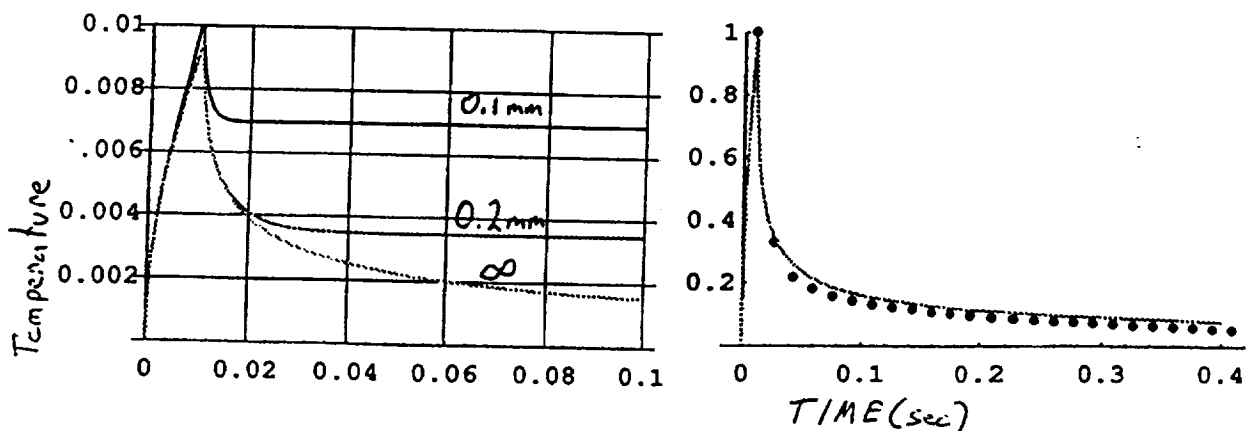


Fig. 10. Calculated surface temperature for (a) three layer thicknesses, and (b) data for  $L=0.4$  mm.

## 5. CONCLUSIONS

This work indicates that in principle IR thermography is capable of considerable quantitative materials evaluation provided proper attention is paid to a number of theoretical and experimental factors. Challenges to qualification of the technique for routine field work are numerous. Frequent camera calibration is required using known temperature-controlled radiation sources and with attention to detector saturation issues. Conversion of intensity data to temperature is necessary since physical models give temperature distributions, and the conversion algorithm is calibration dependent. Thermal parameters must be known for each of the components of the sample under study, and the geometrical arrangement must also be known. The present study dealt only with planar geometries; different geometries may pose formidable theoretical problems. Thermographic measurements produce very large, multi-dimensional data sets, and some way of automating the analysis is required. Intensity vs. time data must be fit to theoretical curves, assuming formulas for these curves can be found. Interpretation of the results will require special knowledge and experience. Additional physical effects such as convective cooling of the surface and lateral diffusion need to be considered.

To summarize, the present study evaluated a number of theoretical and experimental issues regarding IR thermography and delineated some of the questions to be addressed before IR thermography can be used as a reliable component of non-destructive evaluation for operations at KSC.

## REFERENCES

- [1] See, for example, "Standard test method for thermal conductivity of solids by means of the guarded-comparative-longitudinal heat flow technique," ASTM E1225-87.
- [2] "Standard test method for specific heat of liquids and solids," ASTM D2766-95.
- [3] L. D. Landau and E. M. Lifshitz, *Fluid Mechanics*, 2nd ed. (Pergamon, Tarrytown, NY, 1987), pp 200-207.
- [4] S. K. Lau, D. P. Almond, and P. M. Patel, "Transient thermal wave techniques for the evaluation of surface coatings," *J. Phys. D: Appl. Phys.* 24, 428 (1991).
- [5] H. S. Carslaw and J. C. Jaeger, *Conduction of Heat in Solids*, 2nd ed., (Oxford Science, Oxford, 1959).
- [6] V. Vavilov, E. Grinzato, P. G. Bison, S. Marinetti, and M. J. Bales, "Surface transient temperature inversion for hidden corrosion characterization: theory and applications," *Int. J. Heat Mass Transfer* 39, 355(1996).
- [7] F. W. Sears, M. W. Zemansky, H. D. Young, *University Physics*, 6th ed. (Addison-Wesley, Reading, MA, 1982), p. 315.

**1998 NASA/ASEE SUMMER FACULTY FELLOW PROGRAM**

**JOHN F. KENNEDY SPACE CENTER  
UNIVERSITY OF CENTRAL FLORIDA**

**Examination of PCB Clean Up Technologies in Soil**

Maria E. Pozo de Fernandez  
Assistant Professor  
Chemical Engineering Program  
Florida Institute of Technology

Jacqueline Quinn  
NASA Colleague  
KSC Environmental Program

**ABSTRACT**

Polychlorinated biphenyls (PCBs) are stable organic compounds hazardous to the environment. A series of sites heavily contaminated with PCBs have been found at the Kennedy Space Center. Current remediation techniques to treat soils contaminated with PCBs include excavation, disposal to a hazardous waste landfill and incineration. These methods are costly if large volumes are affected. The scope of this investigation is to examine alternative technologies available to clean up PCB contaminated soils on site. This report includes the description of these technologies and their potential to be implemented at the KSC sites.

# EXAMINATION OF PCB CLEAN UP TECHNOLOGIES IN SOIL

Maria E. Pozo de Fernandez

## 1. Introduction

Over the years, the nature of the operations at the Kennedy Space Center including the use and handling of hazardous propellants and toxic substances have contributed to soil and groundwater contamination. Today better knowledge in the handling of hazardous and toxic materials and stringent regulations about their use and disposal have minimized the harmful impact and the risk that these substances pose to the environment.

A series of sites heavily contaminated with polychlorinated biphenyls (PCBs) have been recently found at KSC. Although it has not been well established how these sites got contaminated with PCBs, most likely the origin of the contamination has to do with the use and handling of Aroclor<sup>®</sup> 1254 and Aroclor<sup>®</sup> 1260 which were used as dielectric fluid in electrical transformers. PCBs concentrations are as high as 11,000 ppm in some sites, which is well above the industrial limit value of 3.5 ppm established by the Environmental Protection Agency (EPA). Residential limits are 0.5 ppm. Currently the LC-37 sites, MLP rehabilitation sites and Orsino sites are under investigation.

The current methods proposed to clean the PCB contaminated soils at KSC, include excavation, disposal and treatment. Site soils containing total PCBs in excess of 1 ppm will be excavated. Soils with PCBs concentration below the Toxic Substance Control Act (TSCA) value of 50 ppm will be sent to a landfill and the ones that exceed that value will be treated. Incineration is the most common method of treatment of PCB contaminated soils, but there are other methods available that could be cost effective in treating the contaminated soils. The objective of this investigation is to obtain information about the technologies that treat PCB contaminated soils on site.

## 2. PCBs Background

Polychlorinated biphenyls (PCBs) are synthetic chlorinated organic compounds with biphenyl as the basic structural unit. Chlorination of the biphenyl molecule substituted with 1 to 10 chlorine atoms can produce 209 possible compounds referred as "congeners". These compounds are represented by the general formula  $C_{12}H_{10-n}Cl_n$ , where  $n = 1-10$ . Synthesis of these components can be accomplished through phenylation or arylation of aromatic compounds, condensation reactions, and chlorination of biphenyl in the presence of a catalyst (1).

Commercial PCB mixtures have been used as dielectric fluids in capacitors and transformers, heat transfer fluids, hydraulic fluids, lubricating and cutting oils, and as additives in pesticides, paints, copying paper, adhesives, sealants and plastics. The most common commercial mixtures used are Aroclor<sup>®</sup> 1242, 1248, 1254 and 1260. The first two digits are the number of carbon atoms in the biphenyl group and the last two digits

give the approximate %Cl content in the mixture. Composition of Aroclors<sup>®</sup> 1254 and 1260 are given in Table 2.1.

Table 2.1. Molecular Weight, %Cl and Composition of Aroclors<sup>®</sup> 1254 and 1260 (1)

Chlorobiphenyl	M.W.	%Cl	% in Aroclor <sup>®</sup>	
			1254	1260
Tetrachlorobiphenyl	291.99	48.56	11	-
Pentachlorobiphenyl	326.43	54.30	49	12
Hexachlorobiphenyl	360.88	58.93	34	38
Heptachlorobiphenyl	395.32	62.77	6	41
Octachlorobiphenyl	429.77	65.98	-	8
Nonachlorobiphenyl	464.21	68.73	-	1

PCBs are stable organic compounds. They have low dielectric constant, high heat capacity and low flammability. Solubility of PCBs in water is low and it generally decreases when the degree of chlorination increases (2). Congeners with same chlorine content have different water solubility depending on the chlorine position in the biphenyl molecule. PCBs solubility in organic solvents is high. Analysis of Aroclors and some individual congeners is done by gas chromatography, using capillary columns and electron capture detector (GC/ECD) following EPA Method 8082. This method is used to determine concentrations of PCBs in extracts from solid and aqueous matrices (3).

### 3. Soil Remediation Techniques

Remediation techniques to treat soils fall into four general treatment categories: destructive, biological, fixation and separation technologies. Destructive techniques are processes where the waste contaminant and other components of the waste are irreversibly changed. Examples of this method include incineration, in-situ vitrification, and selective chemical destruction. Biological treatment is used to biodegrade the contaminant by using bacteria or microorganisms. In this process the contaminant is destroyed using a natural process.

Fixation technologies are used to bind or encapsulate the waste and the hazardous component using mixing additives, such as, cement. The hazardous component is not destroyed, it is locked within the mixture. Separation techniques are used to separate hazardous components from the waste, reducing the volume of the hazardous waste to be further treated or destroyed. Separation technologies include solvent extraction, soil washing, and physical separation processes.

Most of these methods have been used to treat PCB contaminated soils, but not all the methods have been successful in reducing the amount of hazardous waste to an acceptable residual PCB concentration.

#### **4. PCB Soil Remediation Technologies**

Several technologies have been used to treat PCB contaminated soils. The purpose of using these technologies is to destroy or to modify the contaminants to make them non hazardous or less hazardous to the environment. Treatment technologies can be divided in two groups: Established Treatment Technologies and Innovative Treatment Technologies. Established technologies are those that have been most widely used at full scale and under different conditions. The cost of these processes are well known, and are methods already approved to treat PCBs. Incineration and Stabilization are the most widely used established technologies to treat PCBs.

Incineration is a recognized technique to destroy PCBs. This is a thermal treatment system having a destruction and removal efficiency of 99.9999% required by TSCA. In this case, the PCBs are destroyed through a combustion reaction carried out at high temperatures. The process can be used over a wide range of PCB concentrations. Stabilization or Solidification is a process used to immobilize the hazardous waste in a solid matrix using binders and additives. This method reduces the mobility of the contaminants, but does not destroy them. Permeability and wet/dry weathering tests should be performed to the solidified mass, to determine its integrity over long periods of time. The solids are sent to a landfill for disposal.

Innovative treatment technologies are new processes that have been used to treat PCBs, contaminated soils, but there is not enough information about how these processes will perform under different operating conditions. Despite this fact, many new technologies have been approved to treat PCBs contaminated soils as an alternative to land disposal and incineration (4, 5). Description of the most used innovative technologies for the treatment of PCBs will be given as follows.

**Chemical Dehalogenation.** This is a chemical process where the halogen (chlorine in the case of PCBs) is removed from the soil matrix. This is a detoxification process, where the toxic material is converted to a less toxic material by a chemical reaction. Two different processes can be used for chemical dehalogenation: the APEG method and the BCD method.

**APEG Method.** This method also known as glycolate dehalogenation, uses an alkali metal polyethylene glycolate (APEG) as the chemical reagent. Sodium hydroxide or potassium hydroxide is used with polyethylene glycol producing an alkoxide (NaPEG and KPEG reagents). It has been proved that KPEG is more effective in destroying PCBs. The alkoxide reacts with one of the chlorines on the aryl ring of the PCB to produce either potassium or sodium chloride, depending on the alkoxide used.

The APEG process consists of five steps: preparation, reaction, separation, washing and dewatering. Preparation includes soil excavation and screening to remove debris. In the reaction step, the contaminated waste and the APEG reagent are well mixed and heated between 100 to 180 °C. The vapors produced during the reaction are separated into water and gaseous contaminants in a condenser. The water can be collected for further

treatment or recycled. The treated material goes from the reactor to the separator, where the APEG reagent is removed from the soil and recycled for future use. The treated soil is neutralized by adding acid and then dewatered before disposal. The APEG technology has been used to treat PCB contaminated soils with concentrations as high as 45,000 ppm reducing it to less than 2 ppm. This process is transportable to the site. The safety considerations while using this process are the high temperatures involved, the production of compounds that are potentially explosive, the formation of flammable volatile organics, noxious fumes, and the use of alkaline reactive materials (6).

**BCD Method.** The base-catalyzed decomposition process is another method used for the dehalogenation of PCBs. In this case, sodium bicarbonate and sodium hydroxide are the chemicals used. In this process the contaminated soil is excavated and screened to remove debris, then crushed and mixed with sodium bicarbonate. The mixture is heated in a reactor at 600-800 °F, where the halogenated compounds are separated from the soil by evaporation. The treated soil is removed from the reactor and depending on its PCB concentration can be returned to the site. The contaminated gases are condensed and sent to a liquid-phase reactor, where the dehalogenation reaction takes place. From the reactor, the treated liquid mixture can be incinerated or treated using a different technology. The advantage of this method over the APEG technology is that there is no need to separate the reactants from the treated soil (7).

**Solvent Extraction.** This technology uses a solvent to separate or remove hazardous organic contaminants from sludges, sediments or soils. Solvent extraction does not destroy the contaminants, but concentrate them, reducing the volume of the hazardous waste to be chemically or thermally destroyed. This technology can be brought to the site, and has the advantage to operate without air emissions. This process makes use of organics preferential solubility in oils and various solvents over water. Generally, the contaminated soil is mixed in a countercurrent soil washer with the appropriate solvent, where the soil is separated into three main fractions or phases: solvent with dissolved contaminants, solids and water. Each fraction can be individually treated or disposed.

PCB is separated from the soil and concentrated in the solvent phase during the extraction process. The PCB rich solvent phase is then decanted and the soil phase is dried. The soil phase can be returned to the site or disposed to a landfill, depending on its final PCB concentration. The organics (PCBs) and the solvent are separated from the PCB-solvent rich phase, where the solvent can be recovered and recycled for future use (8).

**Terra-Kleen Method.** This is a solvent extraction method that has been used to treat contaminated soils at the FT-17 site at the Cape Canaveral Air Station. The contaminated soil had a PCB concentration from 2-800 ppm. This is a batch process that uses an isopropyl alcohol based solvent. The contaminated soil was excavated and piled up near the extraction unit. The soil to be decontaminated is placed in a roll off container where the extraction process takes place. The solvent is added to the contaminated soil until the container is filled up. PCB is separated from the soil and concentrated in the solvent phase during the extraction process. The solvent is left in place for 6-8 hours. The used

solvent is then decanted and analyzed for PCB content. Depending on the PCB concentration obtained, the extraction process is repeated.

On average six extraction cycles were used to clean the soil to PCB concentrations up to 1 ppm or lower. Once the extraction process is completed, the soil is air dried at 200 °F in the same container, where vapors are collected and sent to a treatment unit. The solvent content in the dried soil is usually less than 1%. The treated soil is sent back to the site. The used solvent containing water, PCBs and oil, is sent to a solvent recovery unit, where the water, the solvent and an oil-PCBs rich phase are separated.

The cleaning of the FC-17 site started in September 1997 and up to July 1998 8,000 yards have been treated recovering 200 gallons of waste containing oil and PCBs. The waste will be sent to an incineration unit for final disposal. This method proved to be cost effective for this particular application (\$99/ton), but for contaminated soils with PCB concentrations higher than 1,000 ppm the method is not cost effective compared with other technologies.

**B.E.S.T. Method.** The Basic Extractive Sludge Treatment method is a solvent extraction process, where triethylamine (TEA) is used as the solvent. In this process the contaminated soil is mixed with the solvent in an extraction vessel. Initially the mixture is heated to 40 °F. At this temperature the solvent is soluble in both the organics and water, avoiding the formation of oil-water emulsions, which are difficult to separate. The effluent (water/solvent/organics) is sent to a separator where two distinct phases are formed: a solvent/organic rich phase, and a water phase. Once the water phase is removed, subsequent extraction stages can be conducted at higher temperatures to improve extraction efficiencies. This process has been used to treat contaminated soils with PCB concentrations up to 1,500 ppm. Extraction efficiencies are usually in the order of 99%. The extraction efficiency depends on several parameters, such as, the type of soil matrix, the solvent to feed ratio, and the number of extraction stages (9).

**SCF Extraction.** Supercritical Fluid Extraction is a promising technology for the treatment of contaminated soils. The solvent used is a supercritical fluid (SCF), which is a fluid that has been heated beyond its critical temperature and pressure. The main advantage of this process is that there is little or no solvent residue in the treated soil, but the main disadvantage of the process is the higher equipment cost due to the high pressures involved. The use of SCFs to treat PCB contaminated soils has been demonstrated in a laboratory scale unit using real and spiked samples. Still this technology is in a developing stage and more work needs to be done in the field to prove the feasibility of this method (10, 11).

**Soil Washing.** This technology uses water combined with chemical additives (detergents) and a mechanical process to scrub soils. Hazardous contaminants tend to bind to silt and clay (fine soil) and these tend to bind to sand and gravel particles (coarse soil). The soil washing process separates the contaminated fine soil from the coarse soil, reducing the amount of soil that needs to be treated by other methods. This is a volume

reducing technique in which the contaminants are concentrated in a relatively small mass of material. This technology is recommended for soils with large percentage of coarse sand and gravel to be cost effective.

In this process the contaminated soil is sifted to remove rocks and debris. The remaining material enter a soil scrubbing unit, where the soil is mixed with the washing solution and agitated for few hours. The washwater is drained out from the scrubbing unit and the processed soil is rinse out with clean water. The sand and the gravel particles settle out and depending on the contamination levels, it can be returned to the site or sent to a landfill. The contaminated silt and clay settle out and are separated from the washwater. The silt and clay are tested for contaminants and sent to further treatment. The washwater is treated using wastewater treatment processes to be recycled back to the unit. This technology can be transported to the site (12).

**Thermal Desorption.** In this method the soil is heated at medium to high temperatures to vaporize the contaminants. The vapors are captured and removed for further treatment or destruction. Maxymillian Technologies, Inc. developed an indirectly heated thermal desorption system to treat soils contaminated with PCBs. This method can reduce PCB concentration in soils to 2 ppm at a rate of 10 to 20 tons per hour. Preliminary studies demonstrated that this method can successfully treat contaminated soils with PCB concentrations as high as 88,000 ppm. This technology can be transported to the site.

The process consists of an indirect-fired rotary desorber, with collection of organics in the off-gas by condensation and adsorption. In this process the soil is indirectly heated in an enclosed rotary drum, where the contaminants are desorbed from the soil by vaporization. The system can be operated in the temperature range 250 to 1000 °F. The gas stream containing volatilized contaminants, vaporized water and particles exits the desorber to enter a high temperature filter system to remove the particles from the gas. The particle-free gas is condensed. Condensed contaminants and water are sent to a wastewater system, where the contaminants are removed, concentrated and collected. The treated soil is tested to verify decontamination and can be returned to the site or sent to a landfill. The concentrated PCB waste is sent to an incinerator for final disposal (13).

**In Situ Soil Flushing.** This technology uses water or other suitable aqueous solutions to extract contaminants from soil. Soil flushing is accomplished by passing the extraction fluid through the soil using an injection or infiltration process. The flushing fluid percolates through the contaminated soil, removing contaminants as it proceeds. Contaminated flushing fluid mixes with groundwater and is collected for treatment. The contaminants are separated and the flushing fluid can be recovered and recycled. This method is most effective when is used in permeable soils. To prevent migration of contaminants to uncontaminated areas, a good collection system is required. Containment structures may be needed to ensure capture of contaminants and flushing fluids. Removal efficiencies depend on the type of soil. Extraction of PCBs can be accomplished by using a surfactant (14).

**Surfactant Washing Method.** This method was used to treat in situ soil contaminated with PCBs and oils. The test plot was 10 ft diameter and 5 ft deep with PCB average concentrations to 4,200 ppm. Witconol SN70 a nonionic alcohol ethoxylate type surfactant was used. The aqueous surfactant solution was applied on the surface of the contaminated zone, to capture the leachate at the water table by pumping from a recovery well installed at the center of the test plot. An average of 77 gal/day of the 0.75% aqueous surfactant solution was sprinkled to the surface and the washing process lasted 70 days. During the process the PCB concentration in the leachate fluctuated from 65 mg/l to 3.5 mg/l. The leachate pumped to the surface was biotreated to remove the surfactant and the oil. PCBs were removed from the leachate by an activated carbon system. A total of 85% of PCBs was removed by this method (15, 16).

**In Situ Thermal Desorption.** This method has been developed by TerraTerm Environmental Services, Inc. It is a fast method that does not require soil excavation and is used for surficial contamination to a depth of about three feet. The main component of the process is the use of "Thermal Blankets". These are electrically heated, impermeable blankets with a vapor collection system. The blanket is placed directly on the contaminated soil, and can heat the surface up to 1,100 °C. At this high temperatures the PCBs, other organics and water in the soil vaporize. The vapors are collected through the blanket's vacuum system. Most of the contaminants are oxidized near the soil surface. Remaining vapors are treated using a vapor treatment system, emitting only carbon dioxide and water into the atmosphere. This technology was used to clean a site contaminated with PCB with an average concentration over 500 ppm. The PCBs were found at the top six inches of soil across the site. The thermal blankets were operated at 900 °C. The treated soil reached a PCB concentrations level of 2 ppm, which was the cleanup target value.

A different site was treated using thermal wells instead of thermal blankets, which is a related technology. The thermal wells have heating elements placed in vacuum wellbores drilled into the soil. The heat from the well vaporizes the soil contaminants, which are drawn out of the ground by a vacuum system. In this case the thermal wells were operated at 980 °C, reducing PCBs concentrations as high as 10,000 ppm to 2 ppm. The thermal wells can be used up to a depth of 20 feet below the surface (17).

**In Situ Vitrification.** This is a process which melts the inorganic soil for the purpose of thermally destroying its organic component. Electrodes are placed in the soil to the desired treatment depth, while the treatment area is covered by an off-gas collection hood. The heat generated by the electrodes melts the soil causing the organics to volatilize and pyrolyze. The resultant gases can dissolve in the melt or move to the surface where they combust on contact with air. The products of pyrolyzation and combustion are collected by the off-gas system and are treated before being released to the atmosphere. One major concern is the potential emissions of products derived from incomplete combustion. In this process a volume reduction of 20-40% is typical. As the soil cools down, it vitrifies into a monolith resembling volcanic glass. The treated vitrified waste are left in place. PCB destruction and removal efficiency is in the order of 99.99% by this method (5).

**Bioremediation.** This method uses bacteria or microorganisms to detoxify or degrade organic contaminants. Native species may be used or specially adapted microorganisms may be introduced into the contaminated soil. Microbial degradation of PCBs depends on the degree of chlorination and the position of the chlorine atom on the biphenyl molecule. Lower chlorinated biphenyls are easier to biodegrade than the higher chlorinated compounds. Although several studies have identified some microorganisms with the ability to degrade specific PCB congeners, there is no evidence that just one microorganism will degrade all the PCB congeners. Limited data on field applications using this technique, makes it difficult to evaluate the cost, applicability and detoxification levels that will be obtained in real conditions (1).

## **5. Conclusions**

Several innovative technologies have been found in the literature that have been successfully used to clean PCB contaminated soils. Some techniques can be used over a wide range of PCB concentrations, while other techniques are limited to certain levels of PCB contamination. Many of the techniques found, such as, solvent extraction, soil washing and thermal desorption are used to separate the contaminant (PCB) from the soil, reducing the volume of the hazardous waste to be further treated or destroyed. Other techniques are based on a chemical reaction to convert the PCBs to a less toxic material. In most of the studies the target clean up PCB concentration was 2 ppm, although lower concentrations were reported in some studies.

The clean up target for PCB contaminated soils at KSC is 1 ppm for existing projects, but for future projects it is estimated to be 0.5 ppm. The Terra-Kleen Method based on the solvent extraction technique seems like a viable alternative method to landfill disposal and incineration. The advantages of using this technology is that it is already in place, it has been already used and proved effective to clean the type of soil typical of the area, the contaminated soil could be treated to the target value of 0.5 ppm, the treated soil can be returned to the site, and the amount of hazardous waste to be disposed or destroyed will be considerably reduced.

There are many parameters to be considered before selecting a soil remediation technique. Important factors that should be taken into account are the total volume of soil to be treated, the PCBs concentration and distribution (PCBs concentration varies within the site), the cost of implementing the selected technology, and the time it would take to reach the clean up target. Using the Terra-Kleen method will be economically attractive if the average PCB concentration in the contaminated soil is within 200 to 1,000 ppm and if the total volume of soil to be treated is not too large. For contaminated soils with average PCB concentration lower than 200 ppm, this method is not cost effective compared with landfill disposal and incineration.

## 6. Acknowledgments

I wish to express my appreciation to my NASA colleague Jackie Quinn for providing me with this research opportunity. Appreciation is extended to John Adkisson, Mark Ashton, Janice Everett, Harry Plaza, Rosaly Santos-Ebaugh, Joe Voor and Harold Williams from the Environmental Program and to Orlando Melendez from the Materials Lab., for providing a friendly and warm working atmosphere. I would like to thank Deda Johansen from the Jacobs Engineering Group for the tour to the CCAS solvent extraction facility. Thanks to Gregg Buckingham and Jane Hodge from NASA, Ramon Hosler and Kari Stiles from UCF for making the Summer Faculty Program a rewarding experience.

## 8. References

1. Waid, J. S.; *PCBs and the Environment*, Vol. 1, CRC Press, Inc, Boca Raton, FL (1986)
2. Erickson, M. D.; *Analytical Chemistry of PCBs*, Lewis Publishers, Inc., Ann Arbor, MI (1991)
3. EPA Method 8082. U. S. Environmental Protection Agency (1996)
4. EPA 542-F-96-001. U. S. Environmental Protection Agency (1996)
5. Amend, L. J. and P. B. Lederman, "Critical Evaluation of PCB Remediation Technologies", *Env. Progress*, 11, 3, pp. 173-177 (1992)
6. EPA 540-2-90-015. U. S. Environmental Protection Agency (1990)
7. EPA 542-F-96-004. U. S. Environmental Protection Agency (1996)
8. EPA 542-F-96-003. U. S. Environmental Protection Agency (1996)
9. Jones, G. R.; The BEST Solvent Extraction Process Treatment of Soil, Sediment and Sludges, *Env. Progress*, 11, 3, pp. 223-227 (1992)
10. Brady, B. O., C. C. Kao, K. M. Dooley, F. C. Knopf, and R. P. Gambrell, "Supercritical Extraction of Toxic Organics from Soils" *Ind. Eng. Chem. Res.*, 26, pp. 261-268 (1987)
11. Chen, P.; W. Zhou and L. L. Tavlarides, "Remediation of Polychlorinated Biphenyl Contaminated Soils/Sediments by Supercritical Fluid Extraction" *Environ. Prog.*, 16, 3, pp. 227-234 (1997)
12. EPA 542-F-96-002. U. S. Environmental Protection Agency (1996)
13. Pisanelly, A.; W. P. McCauley and A. C. Uchida, "Indirectly Heated Thermal Desorption of PCB Contaminated Soil", Proceedings of the Air & Waste Management Association 89<sup>th</sup> Annual Meeting & Exhibition, June 23-28, Nashville, TN (1996)
14. EPA 540-2-91-021. U. S. Environmental Protection Agency (1991)
15. Abdul, A. S.; T. L. Gibson, C. C. Ang, J. C. Smith and R. E. Sobczynski, "In Situ Surfactant Washing of Polychlorinated Biphenyls and Oils from a Contaminated Site", *Ground Water*, 30, 2, pp. 219-231 (1992)
16. Abdul, A. S. and C. C. Ang, "In Situ Surfactant Washing of Polychlorinated Biphenyls and Oils from a Contaminated Field Site: Phase II Pilot Study", *Ground Water*, 32, 5, pp. 727-734 (1994)
17. Attaway, M., "Destroying PCBs in Soil at a Dragstrip - In Situ", *Environ. Tech.*, 7, 5, pp. 66-68 (1997)

1998 NASA/ASEE SUMMER FACULTY FELLOWSHIP PROGRAM

JOHN F. KENNEDY SPACE CENTER  
UNIVERSITY OF CENTRAL FLORIDA

MODELING METHODOLOGIES TO ASSES SPACEPORT OPERATIONS

Alex J. Ruiz-Torres

Assistant Professor  
Department of Decision Sciences  
Florida Gulf Coast University  
Carey McCleskey

**ABSTRACT**

This paper presents a methodology by which vehicle concept architectures are mapped to spaceport operational requirements. In addition, this paper describes a prototype strategic level tool which estimates required operations and costs based on a concept vehicle architecture.

# MODELING METHODOLOGIES TO ASSES SPACEPORT OPERATIONS

## 1. INTRODUCTION

With a current emphasis on highly reusable vehicles (HRV's), a major and often ignored component of the cost of conducting space transportation business is that of ground operations: processes of controlling landing and take-off functions, the processing of people and cargo, the performance of checks, fluid servicing, on-line troubleshooting and repair, off-line logistics, and overhaul maintenance. The ground processes for space transportation systems include these and several others processes that relate to a specific vehicle design, as for example assembly/integration processes (i.e., assembly of the fuel tanks and vehicle for the shuttle system).

As space transportation evolves toward a vision of commercially viable space travel—that one day may even encompass public space travel—several challenges arise. First is the realistic estimation of the potential flight rate and vehicle utilization for a space transportation concept. The flight rate and vehicle utilization are measures that the designer cannot input, but outputs can be derived from several factors including the concepts' reliability and operational requirements. Realizing a concept's operational requirements is the second challenge that commercial space transportation systems developers now face. Information is practically non-existent at this early evolutionary stage to construct operations models that can derive accurate flight rates and infrastructure estimates (labor, facilities, etc.).

The objective of this paper is to describe the methodology of a prototype top level assessment tool which was developed to provide reusable vehicle developers (the *users*) with a *map* of the operational requirements for a vehicle concept. These operations requirements will determine ground systems investment and operational costs given a planned demand, for example the number of launch pads that must be constructed and the number of times they must be operated given 40 flights per year. The costs and performance of the ground systems is added to other costs (i.e. per vehicle cost) to provide a designer with an estimated cost to orbit vs. demand curve. This curve is then matched against market graphs, providing the user with a picture of the potentiality of the proposed vehicle concept.

## 2. SPACE TRANSPORTATION SYSTEM ELEMENTS AND COSTS

In this paper we define a Space Transportation System (STRS) as the combination of the vehicle (s) that physically moves people and objects to space with the supporting ground operating systems. In both cases, vehicle designers develop and specify the scheme by which the elements of the vehicle will be arranged into a single integrated system; the form and shapes, the propulsion systems, the number of major systems, the production processes for manufacturing and integration, and the detailed geometries of parts and subassemblies. This activity will specify manufacturing and other costs related to acquiring the first component of the STRS: the vehicle (s). The vehicle design will also specify the operational systems required to test, process, maintain, and repair the vehicle systems. For example, a single stage to orbit system does not require a mating process (union of the stages i.e. the shuttle system were the orbiter is attached to a fuel tank and two external reusable rockets). The primary modules of the supporting operating systems - the spaceport were defined in a report from the *Highly Reusable Space Transportation* project [1]. The architectural elements defined in this report were:

- *Passenger/Cargo Processing (Terminal)*: Facilities and systems required for the handling of passengers and cargo after landing, and prior to launch. Could be separated into two facilities.
- *Traffic/Flight Control*: Oversight of landing, launch, and flight operations.
- *Launch*: Vehicle departure facilities and systems.
- *Landing*: Vehicle arrival facilities and systems.
- *Vehicle Maintenance and turnaround*: Facilities and systems required to repair, inspect, and prepare the vehicle for the next launch. One such facility may be needed for each reusable stage of the vehicle.
- *Vehicle Assembly/Integration*: Facilities and systems required to combine multiple stages. Could be part of the Maintenance and Turnaround facility.
- *Vehicle Depot Maintenance*: Facilities required for the off-line repair of vehicle subsystems.
- *Expendable Elements*: Facilities required to inspect and prepare expendable items for launch.
- *Operations Management and Support*: Facilities and systems for management and engineering support.
- *Logistics*: Facilities and systems for materials acquisition, transport, storage, and disposal.
- *Spaceport Support Infrastructure*: Facilities required to support all other facilities.

- *Community Infrastructure:* Housing, medical, and other miscellaneous facilities required to sustain a community.

Several possible vehicle flows within a spaceport's basic components are illustrated in Figure 1. An airplane like vehicle that does not require major maintenance after each flight and has a single stage will move directly from landing to the terminal, and then to launch (1). If the vehicle does not require maintenance after each flight but has multiple stages then an integration function is required which can be performed at another facility or at the terminal (2). Vehicles that require major maintenance and tests procedures after each flight must flow to a turnaround facility and then proceed to integration (3) or directly to the terminal functions (4). The vehicle design specifies which of these flows will be required between landing and launch and the time required in each of these processes.

The combination of different processing times and flows is an issue that takes us to the first fundamental relationship between the vehicle and the ground operations systems: *cycle time*. The *cycle time* of a vehicle can be defined as the expected interval of time between a vehicle's landing and launch. While a typical airplane *cycle time* can be measured in hours, the *cycle time* for our current reusable STRS (the Space Shuttle) is measured in months. Finally, the expected time in orbit must be established in order to fully determine the vehicle utilization - the expected number of flights per vehicle per year.

From the estimated processes and types of ground operations systems required, investment costs, operating costs, the flight rate for a single vehicle are estimated. The costs of a STRS can then be divided as follows:

- *Fixed Operational Costs:* These are the baseline operational costs required for a single flight per year. For example management, engineering, and technical staff.
- *Variable Costs:* These are flight dependent operational costs. For example fuel, replacement parts, additional staff and insurance.
- *Development Costs:* Initial costs required to develop the STRS technologies required.
- *Facilities and Infrastructure Costs:* Initial costs required to build and equip the ground systems that will support the STRS.
- *Vehicle Acquisition Costs:* Purchase of the vehicles.

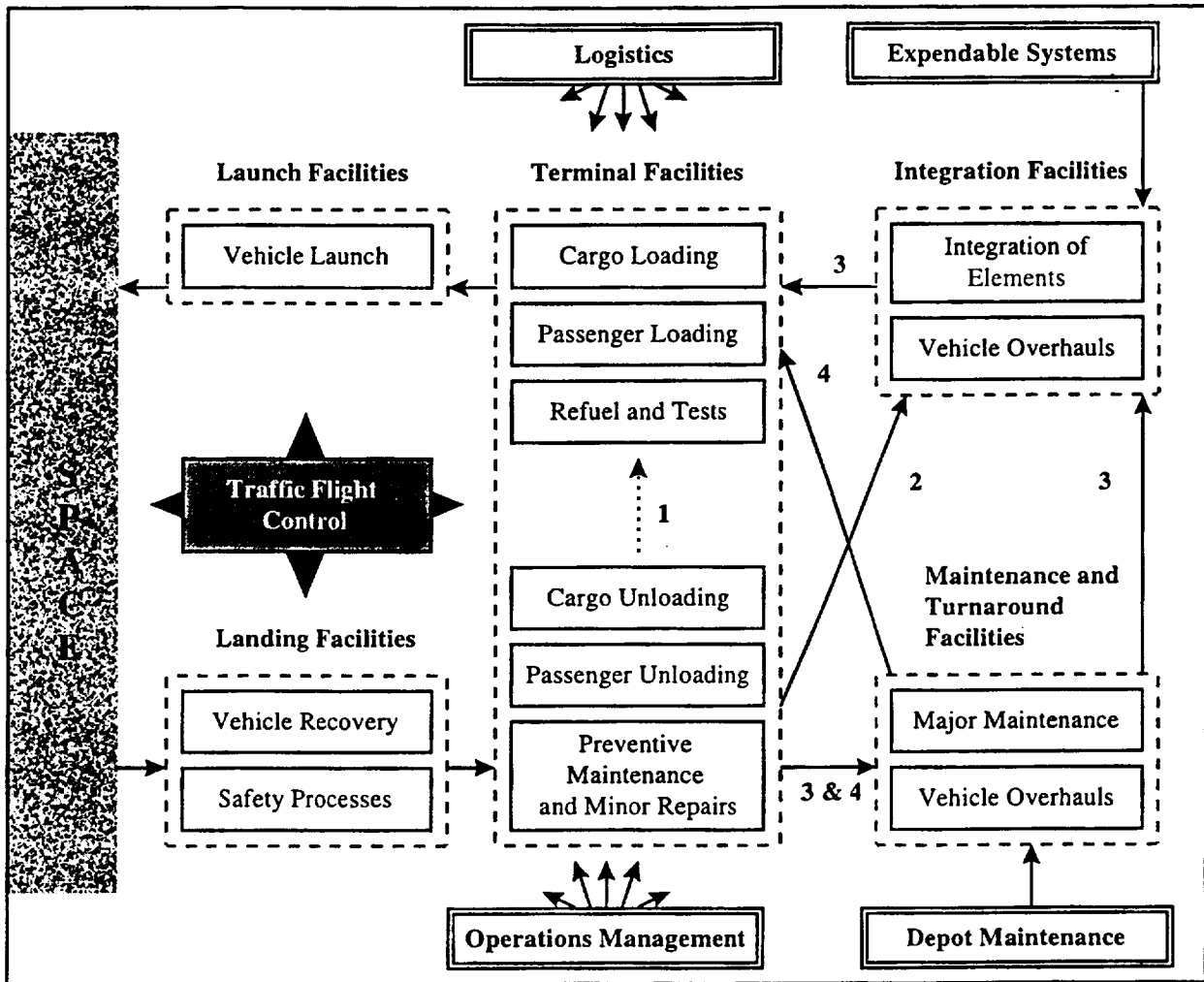


Figure 1. Spaceport functions and flows

A total cost assessment can be made for a vehicle concept by rolling up investment and operational costs, the expected life of the vehicle, and a demand for service. The demand for service (pounds per year) will determine the number of flights needed per year, and therefore the number of vehicles. As the size of the fleet grows so does the fixed operating costs (need more base staff). As the number of flights increase, the variable cost per flight may be reduced as a result of economies of scale, or increase as a result of increased complexity. The total facilities and infrastructure costs increase with fleet size and the number of flights (i.e. number of launch pads, number of maintenance hangars), but the per flight cost will eventually decrease with an increase in the number of flights given economies of scale.

### 3. PROTOTYPE TOOL

The assessment of a vehicle design's required ground operation systems and costs is a complex problem. First, space transportation is still an "adolescent" industry with a limited knowledge base, particularly for reusable systems. Second, space vehicles are one of the most complex devices created by humans, therefore assigning an operational infrastructure to a nonexistent system can only be an educated guess. The objective of the tool is to make top-level estimates by capturing existing knowledge from a team of NASA and aerospace industry experts in order to help better define concepts prior to commitment. Therefore, the developed prototype is a strategic- decision-making tool which aims to help in the early vehicle development process. A suite of tools for detailed modeling is also being developed concurrently.

The prototype was developed in Microsoft Excel ® with a Visual Basic ® front end. A menu provides access to input dialogs and to output reports. An example of the user interface is shown in Figure 2. The output reports can be on screen during the input process allowing the user to get instant feedback. The user must answer 18 questions about the most critical component of the STRS: the vehicle (1). These questions were developed by the Space Propulsion Synergy Team [2] and implemented in the current's prototype precursor, the Architecture Assessment Tool (AAT) [3]. The questions for the AAT were derived from a *Design Guide for Highly Reusable Space Transportation Systems* also developed by the Space Propulsion Synergy Team [4]. The questions relate to several top level areas: number of stages, propulsion systems, propellants, complexity, reliability, maintainability, and support systems. For each question there are 3-10 design options in a multiple choice fashion. While there could be many possibilities, even an infinite number, limiting the number of options simplified the formulation and knowledge acquisition process. Other queries in the prototype which were not in the original AAT include the payload capacity of the vehicle, the vehicle's expected life, the expected development and per vehicle acquisition costs.

Figure 2 illustrates the modeling process. As the vehicle information is entered (1), the data is fed to the knowledge engine (2). The knowledge engine is a series of models and functions that combine relevant design options to the appropriate ground system modules. The models/functions define the characteristics of the ground systems at a module level for the concept vehicle (3). For example, the cargo processing module has a function that combines all inputs relevant to the type of cargo and passengers, the technologies used to load cargo and passengers, the level of standardization of cargo

shapes, the vehicle cargo bay technologies and position, etc. Inputs related to avionics and propulsion for example, have little or no bearing in what type of cargo processing facility is needed, therefore are not included in that module's function.

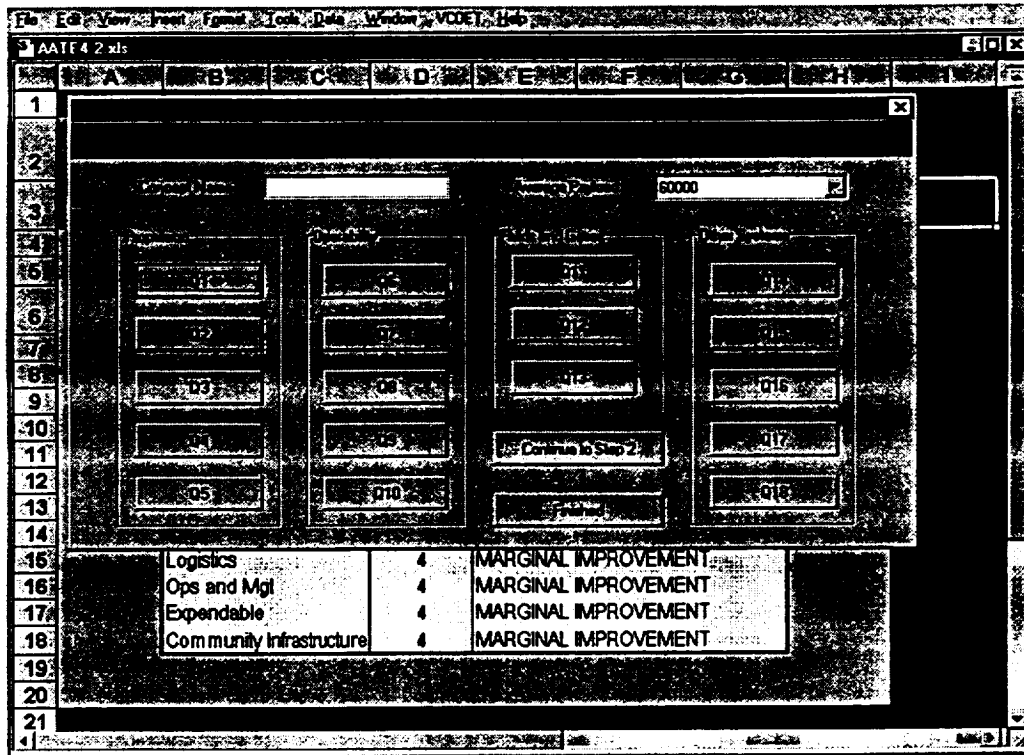


Figure 2. User Interface

For each of the 12 modules 4-8 facility types were defined based on a worldwide benchmark of ground operating systems (NASA, European Space Agency, China Space Agency). The definition at this level includes a simple description of the facilities, the cycle time (if applicable), the investment costs (facility and equipment), the fixed operational costs (materials and labor) for a single flight, and the variable operational costs (materials and labor) -for each additional flight. While the benchmarks defined existing operating systems, optimistic extrapolations were developed to generate the low cost-fast turnaround facility types. In all cases, there was a large range between the low cost, fast turnaround facilities, airport like, and the shuttle like facilities, very expensive and long turn-around with about two orders of magnitude separating them in terms of costs and cycle times.

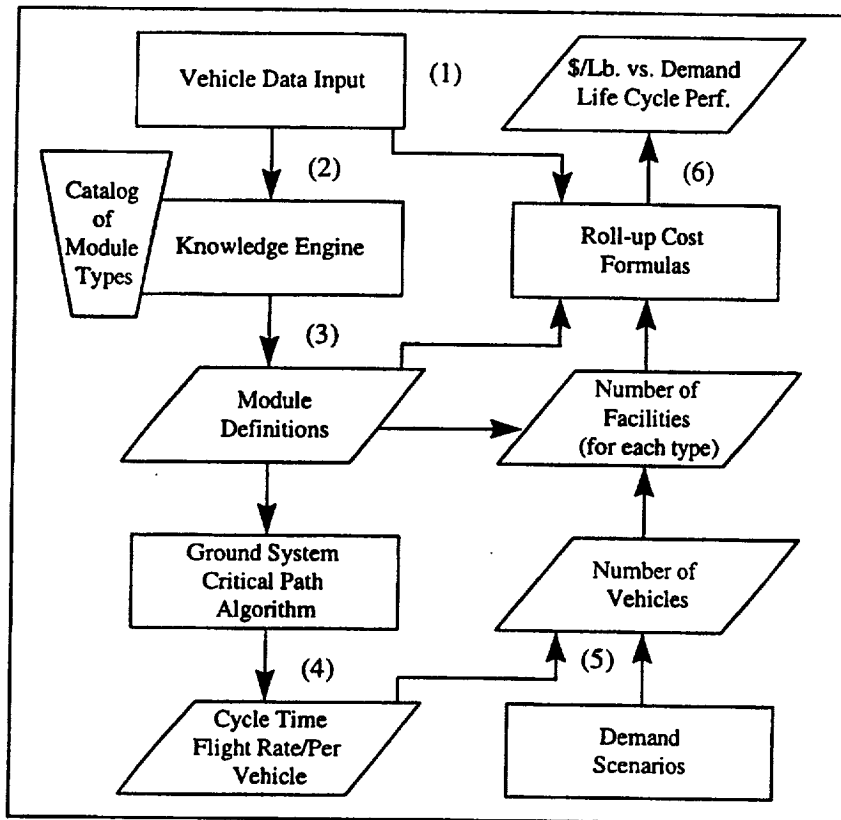


Figure 3. Process behind the developed prototype

The modules types defined by the knowledge engine are then used to determine the ground systems' critical path and a ground system cycle time (4). The vehicle cycle time combined with the expected time in orbit are used to generate the flight rate for a single vehicle. If a vehicle concept required a type V maintenance facility, its operation time in that facility was estimated at 65 days (shuttle like). Even if all other processes were instantaneous (including orbit), the lower bound estimate for this concept's flight rate would be 5.6 flights per year.

Two demand functions given a payload capacity range of 30 to 60 thousand pounds to orbit were established out of the data from the CST study [4]. The first demand function is based on realistic markets, primarily communication satellites and scientific payloads while the second provided a logarithmic demand curve and included 'far fetched' possibilities as ultra fast intercontinental travel and delivery services, space tourism, health care, and manufacturing. For each demand scenario a lower

bound number of flights and vehicles is calculated by combining the vehicle's flight rate, the capacity of the vehicle, and a demand level; number of vehicles = demand / [vehicle capacity \* flight rate] (5).

The number of vehicles is then used to determine the capacity required for each module type (6), i.e. number of launching facilities. This information is then integrated to roll-up formulas that calculate the measure of performance of interest: dollars per pound. The multiple demand level points and cost to orbit per pound values are plotted against the demand curves derived from the CST study (can also include plots from other saved vehicles). Figure 4 illustrates the output report from this process. The graph provides insights on the feasibility of the vehicle when compared to other vehicles across the two described demand scenarios.

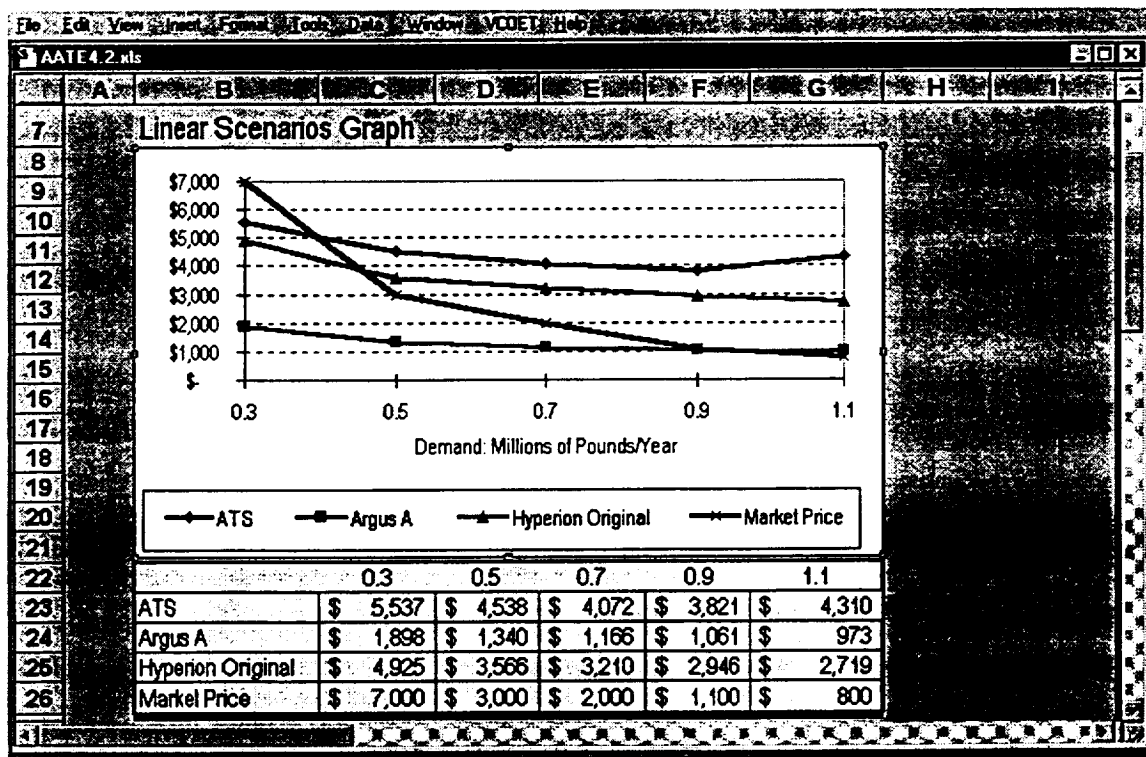


Figure 4. Vehicle Performance vs. Demand Curve

The tool can save the current vehicle configuration and two vehicles can be plotted in a single graph for easy comparison. The user can at any point change one or several design options and see the effect on the operational requirements and on the performance curve. Also an output report is generated after

each analysis which lists the number of vehicles/facilities required and a cost breakdown for each demand point.

#### 4. CONCLUSIONS

The commercialization of space transportation is the next stage on the evolution of this service. History is full of examples where the government role has changed from service provider to enabler and regulator. To make this transition a reality, we need better understanding of the total costs and financial possibilities of new systems before they are developed. Total costs of a future space transportation system can only be determined if there is an understanding of its operational requirements and flight rate. By combining operational requirements and market data, the proposed tool is able to provide a performance *map* to vehicle designers.

The prototype presented in this paper is one in a suit of tools being developed. Current work includes the use of the methodology developed for the described tool on a more 'detailed level' tool which has more than 150 inputs from the user and will provide additional insights on the operational requirements for the concept vehicle. A third tool is also being developed which combines details from the vehicle input side with spaceport architecture design considerations, for example the level of automation on spaceport operations and a description of existing facilities.

#### REFERENCES

- [1] *Highly Reusable Space Transportation* (1997) . A Catalog of Architectural Elements. Unpublished NASA Document.
- [2] *Space Propulsion Synergy Team* (1997). A Guide for the Design of Highly Reusable Space Transportation. Unpublished NASA Document.
- [3] *Space Propulsion Synergy Team* (1997). Architectural Assessment Tool. Unpublished NASA Document.
- [4] *Commercial Space Transportation Study* (1994). Final Report. Unpublished NASA Document.

1998 NASA/ASEE SUMMER FACULTY FELLOWSHIP PROGRAM

JOHN F. KENNEDY SPACE CENTER  
UNIVERSITY OF CENTRAL FLORIDA

A VISUAL EDITOR IN JAVA FOR JVIEWS

Ryan Stansifer  
Associate Professor  
Computer Science  
Florida Institute of Technology

KSC Colleague: Steve Beltz (Dynacs)

ABSTRACT

In this project we developed a visual editor in the Java programming language to create screens on which to display real-time data. The data comes from the numerous systems monitoring the operation of the space shuttle while on the ground and in space, and from the many tests of subsystems. The data can be displayed on any computer platform running a Java-enabled World Wide Web (WWW) browser and connected to the Internet. Previously a special-purpose program had been written to display data on emulations of PC GOAL screens. A new program to display data on the screens created by the new visual editor was written. The data viewer can be used in a WWW browser or as a stand alone program. It can connect directly to the data source, or it can connect indirectly through a proxy server.

Our project shows the great flexibility of the approach. The unique relation between Java and the Internet makes our system easy to administer, update, and efficient. The good graphical user interface (GUI) library and networking library in Java make it easy to develop applications. Also, Java introspection was used to good advantage in the design of the visual editor. New components can be made available to the display designer without any modification to the editor.

# 1 Introduction

During the operation of the space shuttle, sensors are monitoring many of the subsystems. This data goes to special hardware at the Launch Control Center (LCC) known as the Common Data Buffer (CDBF). Lots of data is collected, approximately 30,000 measurements. These measurements are continually changing—some of them can change rapidly at certain times. The data is used in monitoring the operation of the shuttle and in analyzing subsystems for safety, performance, technological improvements, etc. Each individual measurement is given a short tag called a function designator (FD). The list below is a sampling of the FDs as well as a short description (called the nomenclature), a value during a recent query of the data, and the units.

Func Desig	Nomenclature	Value	Units
SOIADATAV	128 OI FEP ACTIVE DATA VALID		ON ON/OFF
KMTHA001A	WIND DIRECTION CAMERA SITE 6	444.95996	DEG
KMTLA001A	WIND SPEED CAMERA SITE 6	6.719999	KT
KMTPA001A	BAROMETRIC PRESSURE CAMERA SITE 3	30.099995	INHG
KMTTA001A	AMBIENT TEMPERATURE CAMERA SITE 3	85.59999	DEGF
V61Q2551A1	CABIN HUMIDITY	12.4	PCT
V61P2405A1	CABIN PRESS	14.719997	PSIA
V61T2552A1	CABIN TEMPERATURE	79.15999	DEGF

Real-time data is monitored on system engineering consoles of then the Control Checkout and Monitor System (CCMS) in the Launch Control Center (LCC). The command and control software is written in the Ground Operations Aerospace Language (GOAL).

The PC GOAL system presents the same data to a wider audience in a format closely resembling the consoles of the CCMS. The CCP (CDBF Communications Processor) scans the memory of the CDMF every 2 seconds and broadcasts the data on the LPS Operations Net (LON). This data (and other data, e.g., FIFO) is relayed to the PC GOAL stations. The PC GOAL stations are PCs with network hardware running DOS and the PC GOAL software.

The PC GOAL system presents shuttle data on schematic-like screens described by character-oriented files known as DSP files. Figure 1 shows one of the hundreds of PC GOAL display screens (no data is been displayed, the slash character is filling the character positions that would be occupied by numerals). Each shuttle mission requires substantial effort to organize the CDBF, distribute the DSP files, etc.

```

QWB08  GNC ASCENT/RTLS MON  QDBGD
ASCENT GUIDANCE DATA  SRB SEP  STS-11111
RTLS ABORT  XXX  STAGE 1 GUID  XXX  PC 50  XXX  FLT-11111
TAL ABORT  XXX  PTL  PASS NAV INIT  XXX  INIT  XXX  00-11111
ATO ABORT  XXX  TRNAROUNDXXX  IMU REFSRDY  XXX  CMD  XXX  FMT 11111 111
MECC CMD  XXX  PWR P DN  XXX  BFS ASC OPS 101  XXX  SUBPH  XXX
MECC CONF  XXX  PREP SSME LNCH  XXX  FRZCMDXXX
ET SEP CMD  XXX  FINE CTDNXXX  AEROSUP SLW CMP  XXX  STEER  XXX
PSLS HOLD FLAG  XXX  G RDY  XXX
LAUNCH SEQ ABCRTXXX

DONS  OMB  POS  ORPOS  DONS  OMB  POS  ORPOS  DONS  OMB  POS  ORPOS  DONS  OMB  POS  ORPOS
PA  XXX  XXX  XXX  XXX  PA  XXX  XXX  XXX  XXX  PA  XXX  XXX  XXX  XXX  PA  XXX  XXX  XXX  XXX
PS  XXX  XXX  XXX  XXX  PS  XXX  XXX  XXX  XXX  PS  XXX  XXX  XXX  XXX  PS  XXX  XXX  XXX  XXX
TA  XXX  XXX  XXX  XXX  TA  XXX  XXX  XXX  XXX  TA  XXX  XXX  XXX  XXX  TA  XXX  XXX  XXX  XXX
YS  XXX  XXX  XXX  XXX  YS  XXX  XXX  XXX  XXX  YS  XXX  XXX  XXX  XXX  YS  XXX  XXX  XXX  XXX

CALIBR  ORPOS  ORPOS  SSME POS  ORPOS  SRH ORPOS  SRH ORPOS
IMU FAIL  1P  XXX  LR  XXX
RGA/AA  1Y  XXX  LT  XXX
NAV SENSOR  2P  XXX  CP  XXX
RCS  2Y  XXX  RP  XXX
RHC LEFT  RIGHT  2Y  XXX  RT  XXX
GENER  ORP  ORP  3P  XXX  CP  XXX
RHC R  3Y  XXX
P  XXX
U  XXX
SBTC
T/G
THC X+111 -111  VERT ACCEL 111.11  MACH/VEL 11111
Y+111 -111  AVVI ALT 11111  ACCEL 111.11
Z+111 -111  AVVI ALPHA 111.11  AIRSPEED 11111
AVVI SEL HG 111.11  AVVI HDG 111.11

```

Figure 1: One of PC GOAL's display screen

## 2 Jview

The Jview project is motivated by the PC GOAL system to display real-time shuttle data as conveniently and efficiently as possible. The programming language Java was chosen because of the ease of writing both graphical user interface (GUI) code and distributed programs. The Internet is the obvious mechanism to transport the data. The wide-spread availability of browsers for the World Wide Web suggests an obvious user interface for any information system large or small.

Java code can be transmitted as part of the WWW protocol, just like pictures, sound and other data. The extreme interest in Java is caused by the ability of browsers to execute the Java code. These Java programs transported across the Internet and executed locally by a WWW browser are called applets. Applets add interaction to otherwise static WWW documents. The Jview project uses applets to form a connection to a Java data manager that relays the real-time data to the applet.

### 2.1 Java applets

The key advantage with using Java applets is that after the applet makes a connection to a data server only the data is transmitted across the network. The following steps summarize the establishment of a direct connection to the data using the WWW.

1. Get document. Local machine makes a request for a document.
2. Return document. A WWW server finds the document and returns it.
3. Get applet. The WWW browser begins to display the document, requests the Java applet, and leaves space for the applet in the document.
4. Applet running. The WWW server returns the applet, the browser runs the applet which controls the space in the document.
5. Socket connection. The applet makes a socket connection to a data server on the remote machine.
6. Data pipeline. The data server exchanges UDP packets with the real-time data source, and sends the data on to the applet.

The advantages in using Java are even greater than the technical merits suggest. Administratively, the operation of a real-time data service using Java is much better. The Java

applet is written once and executed remotely; no porting has to be done. Also, the latest version of the applet is always distributed to the user; there is no version control problem. Finally, the operation of the service is easy as browsers are ubiquitous; no training is required.

The Jview system has been in operation for about a year. Since it emulates the existing PC GOAL display screens it has been easy for users to use the new system. But advances in computer systems makes it reasonable to expect more sophisticated displays. It is possible to display the data more realistically with dynamic, bitmapped components: tanks can appear to be filling, analog gauges can be simulated, sound can be incorporated, etc. Schematic diagrams can be more detailed.

To create these more sophisticated displays we have designed a visual editor. From an extensible palette of components the user composes a new graphical display for the data. Pictures and schematics (perhaps made from other tools like Adobe's PhotoShop) can be imported. Once a screen has been created, the data viewer displays it as well as updates the components with the individual data values as the data comes in. We discuss these programs in more detail after the next section on related work.

## 2.2 Related Work

There are other mechanisms that are being used to display real-time shuttle data on the Internet. We discuss two of them here.

The Exodus project displays its data on WWW documents using common gateway interface (CGI) programs. Periodically another document is produced with the data on it and sent to the WWW browser. This requires a lot of redundant network traffic when only a few numbers have changed. Also graphics are hard to produce on an HTML document without resorting to graphic images that would have to be transmitted each time to the browser.

Another direct approach is server-push. In this approach the server periodically resends the HTML document. In the meantime another program can write a new and updated version of the document. An example of this approach is the Shuttle WWW site [6] which displays real-time data about the current shuttle (and has lots of other information). This works best with text, as again an entire HTML document is transported across the Internet with each update.

An important feature of the visual editor that we have developed is that it uses any components. The components do not have to be specifically designed for the visual editor and the editor does not have to have any advanced knowledge of them. Several commercial enterprises are developing relevant components. ErgoTech Systems, Inc. [3] of Los Alamos, New Mexico has released a set of Java components for building displays used in factory automation.

### 3 Format

The project hinges on a screen format (which we call the SDO format) that the visual editor produces and that the data viewer uses to display the data. In this section we describe the format we have developed.

The essence of the screen format is given by the (simplified) version of the Java class `ScreenDisplayFormat`. The format is basically a color and size (for a plain background) or an array of bytes representing an image. Overlaying the background is an array of Java GUI components.

The GUI components of an SDO object are any Java GUI components at all. Since Java components are serializable (which means they can be written automatically out as a persistent object), then so can any object of class `ScreenDisplayFormat`. An SDO object is a serialized and compressed object of class `ScreenDisplayFormat`.

```
public class ScreenDisplayFormat {
    private String info;
    private Dimension size;
    private Color color;
    private byte [] image;
    private Component [] elements;
    private Point [] locations;
}
```

The image is stored as an array of bytes, not as a Java object of class `Image`. An object of class `Image` cannot be serialized because it depends on the platform which renders the device (the resolution and color model of the display). So to serialize the background image we use the GIF or JPG image. This can be transmitted across the network and then the internal Java image can be correctly generated on any platform.

The location of all the GUI components is kept as part of the SDO format. This appears to be unnecessary as each component has  $x$ ,  $y$  fields for this purpose. However, the visual editor must reparent all the subcomponents in order to provide the ability to move and resize them. Then the  $x$ ,  $y$  values are not the expected once. Hence, it was simpler just to keep track of the location of the components of the SDO explicitly.

### 4 Visual Editor

The screen shot of the visual editor is shown in Figure 2. The list of available components appears on the left side of the workspace. In the workspace are four components: a

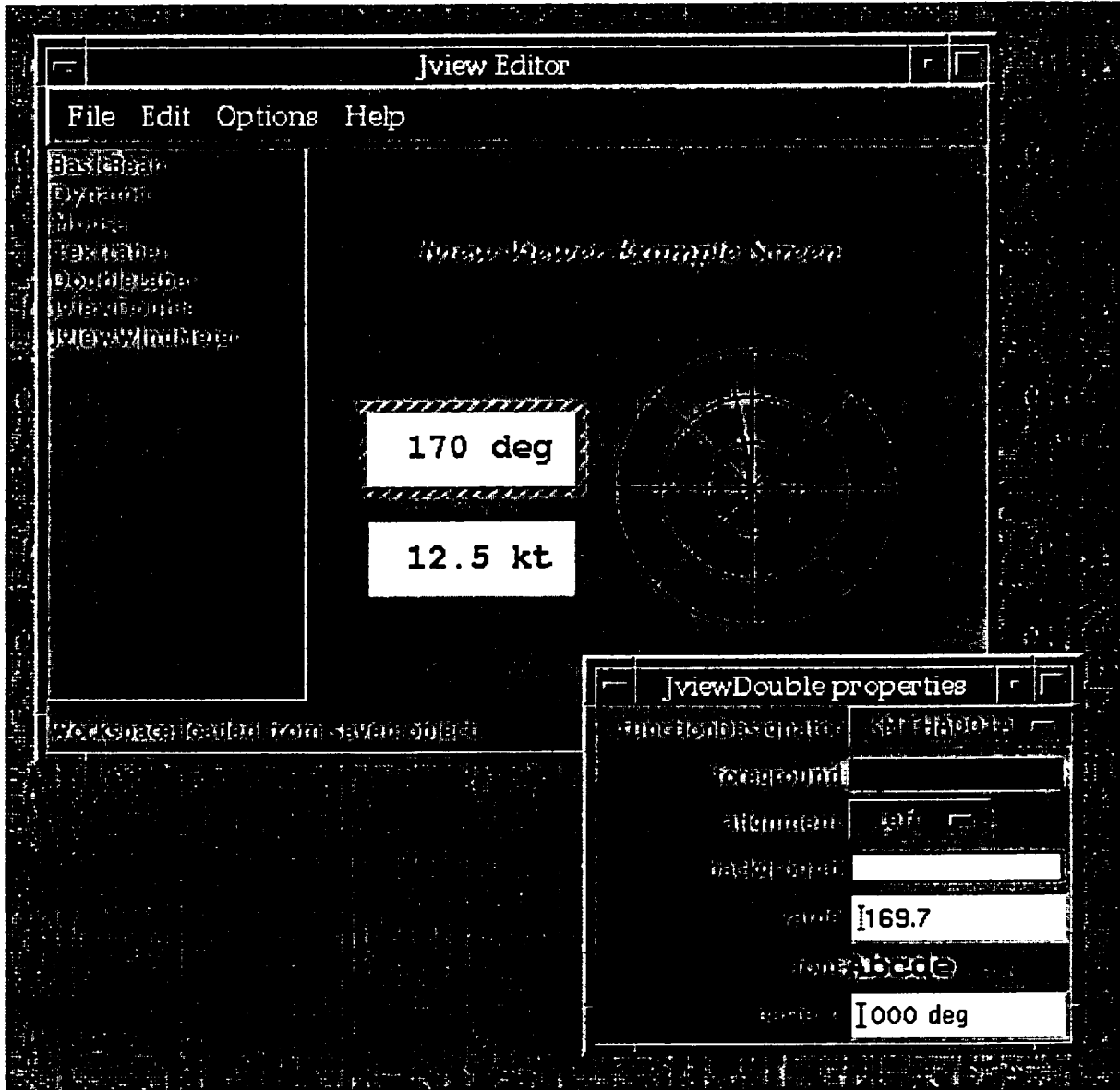


Figure 2: View of the editor

TextLabel component for the title, two JviewDouble components for the wind direction and speed, and a JviewWindMeter. The JviewDouble component for wind direction is the component currently edited. It has the hashed border around it. The current component always has a property editor in a separate little window. In this window the individual values for each property of the component can be set. For example, the JviewDouble the function designator for the current component is set from among a list of function designators to be KMTHA001A. The foreground color is set by a color editor, the font by a font editor. The data value 169.7 has been set by the user. No real data is reaching the component in the editor. But the display designer may want to see how the component reacts to some particular data value. In this case we see that the component rounds the value to the nearest degree. Other components might turn a different color for some values, etc.

## 5 Data Viewer

The display created by the editor in Figure 2 is now shown in Figure 3 as it appears in the viewer. Naturally it look very much the same, though, of course, will actual live data being constantly displayed. The view does have some parts specific to its specific function. The choice box at the top allows the users to choose the data stream desired from among those available. At the bottom of the application is the time (GMT) and the countdown time as customarily represented at NASA.

One feature of the viewer is the capacity to interrogate a component and determine what FD or FDs it is monitoring. In Figure 3 a right mouse click in the wind meter has caused a popup menu to display the two FDs that it is displaying.

The viewer can run as a stand-alone application, in a WWW document as an applet, or without an HTTP server using appletviewer. The connection to the data can be made directly if the program is run at location receiving the data. Or, the connection can be made though a proxy server that relays the data. This is especially important as the usual security policy for applets does not permit arbitrary network connection. In this case the proxy server must run on the same machine as the HTTP server that sends the applet.

## 6 Acknowledgments

I gratefully acknowledge the support of the DAP group of CLCS headed by Coleman Dugger (NASA) especially the Jview team: Steve Beltz (Dynacs), and Mark Long (Dynacs). A special thanks is due to Ray Hosler (University of Central Florida) and Greg Buckingham (NASA) who ran the NASA/ASEE Summer Faculty Fellowship Program with efficiency and

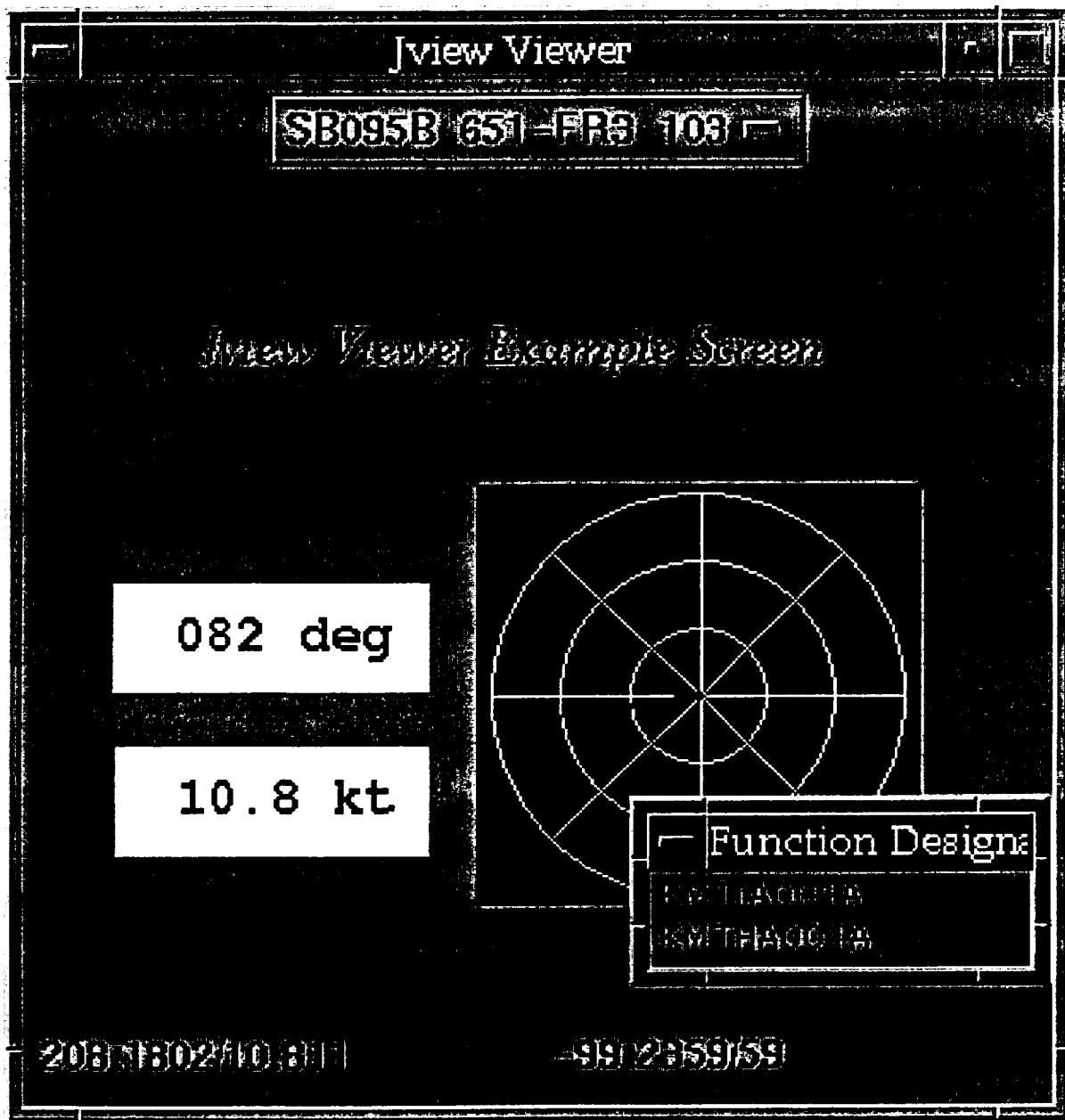


Figure 3: View of the editor

enthusiasm. The original impetus of this project in 1996 grew out of collaboration with Peter Engrand (NASA) and Charlie Goodrich (Dynacs).

## References

- [1] Patrick Chan and Rosanna Lee. *The Java Class Libraries: Second Edition, Volume 2*. Addison-Wesley, Reading, Massachusetts, 1998.
- [2] Patrick Chan, Rosanna Lee, and Douglas Kramer. *The Java Class Libraries: Second Edition, Volume 1*. Addison-Wesley, Reading, Massachusetts, 1998.
- [3] ErgoTech Systems, Inc. Ergotech web site. WWW site at <http://www.ergotech.com>.
- [4] Merlin Hughes, Conrad Hughes, Michael Shoffner, and Maria Winslow. *Java Network Programming*. Manning, Greenwich, Connecticut, 1997.
- [5] Henri Jubin. *JavaBeans by Example*. Prentice Hall, Upper Saddle River, New Jersey, 1997.
- [6] NASA, Johnson Space Center. Nasa shuttle web. WWW site at <http://suttle.nasa.gov>.
- [7] NASA, Kennedy Space Center, Checkout and Launch Control System. CLCS project home page. WWW site at <http://clcs.ksc.nasa.gov/>.
- [8] NASA, Kennedy Space Center, Launch Processing System. Lps system software pc goal home page. WWW site at <http://lpsweb.ksc.nasa.gov/SDC/PCGOAL/>.
- [9] NASA, Kennedy Space Center, Launch Processing System. Lpsweb. WWW site at <http://lpsweb.ksc.nasa.gov>.
- [10] Sun Microsystems, Inc. Javabeans. WWW site at <http://java.sun.com/beans>.

**1998 NASA/ASEE SUMMER FACULTY FELLOWSHIP PROGRAM**

**JOHN F. KENNEDY SPACE CENTER  
UNIVERSITY OF CENTRAL FLORIDA**

**SOFTWARE DEVELOPMENT FOR AUTONOMOUS CONTROL  
OF AN ISPP PLANT ON MARS**

Jonathan E. Whitlow  
Associate Professor  
Chemical Engineering Program  
Florida Institute of Technology

KSC Colleagues - Tom Lippitt-NASA & Charlie Goodrich-Dynacs

**ABSTRACT**

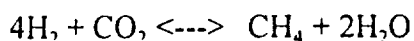
This work has focused on modeling the carbon dioxide sorption pump which is to be used in the In situ Propellant Production (ISPP) project. Using conservation principles and several simplifying assumptions led to dynamic models in three separate programming environments, specifically Simulink, Matlab and Common LISP. Results of the simulations compared well with other simulations in the literature.



## ISPP PROCESS DESCRIPTION & ANALYSIS OF COMPONENTS

The ISPP process begins with the acquisition of CO<sub>2</sub> from the atmosphere. A sorption pump which uses zeolite as the adsorbent is being evaluated for this component since it contains no moving parts and thus may prove to be more reliable than a traditional compressor. The objective of the pump is to acquire the CO<sub>2</sub> and subsequently deliver it to the downstream processes at a constant pressure and mass flow rate. The majority of the work performed this summer focused on the sorption pump and thus it is described in greater detail later in the report.

From the discharge of the sorption pump, the flow is split and a majority fed to the Sabatier reactor. The Sabatier is a fixed bed ruthenium on alumina support catalytic reactor. Prior to entering the reactor, the hydrogen and carbon dioxide will be mixed and passed through a heat exchanger where they will be preheated using the reactor effluent gases as a result of the heat generated from the exothermic reaction. The stoichiometry of the reaction is:



Although the reaction is reversible, if the reactor is operated at a sufficiently high temperature (> 570 K), the equilibrium constant is very large (~ 10<sup>6</sup>) and yields in excess of 99% can be achieved.<sup>1</sup>

After the reaction products leave the Sabatier reactor, any hydrogen is separated and returned to the reactor feed stream while the methane and water and any remaining carbon dioxide are separated. The methane is then sent to storage, the carbon dioxide is recycled or vented and the water is fed to an electrolysis unit. The electrolysis unit uses electrical energy to split the water into elemental oxygen and hydrogen. The hydrogen is then dried and recycled back to the Sabatier, while the oxygen is chilled and sent to storage.

In order to have a Mars sample return mission a propulsion mixture of 1.75 moles of oxygen per mole of methane is required. The Sabatier electrolysis process however produces a 1 to 1 mole ratio, resulting in the need for additional processing. The method shown in Figure 1 shows a Zirconia cell stack which takes additional CO<sub>2</sub> and converts it into CO and O<sub>2</sub>. The additional oxygen can then be used to insure the proper combustion ratio. Another alternative which is being examined that is not shown involves using CO<sub>2</sub> to convert excess CH<sub>4</sub> to CO and H<sub>2</sub> with the hydrogen being recycled back to the Sabatier process.

## SORPTION PUMP OPERATION

The modeling efforts for the sorption pump were based on the information and data taken from a 1997 JPL design report.<sup>2</sup> The sorption pump goes through an operating cycle which has four distinct phases as shown in Figure 2. The four operating phases are:

*Heating at Constant Volume:* In the early morning the zeolite will be fully saturated with CO<sub>2</sub> which for the Zeolite 13x which is being investigated for use, translates into 0.14 gram of CO<sub>2</sub> per gram of zeolite. At that point the valves to the pump are closed and the adsorbent bed is heated at a constant volume. This phase corresponds to the transition from point A to point B in Figure 2.

*Heating at Constant Pressure:* Once the bed of zeolite has been sufficiently pressurized to operate the Sabatier reactor, the valve to the reactor is opened and CO<sub>2</sub> begins flowing into the reactor. During the operation of this phase, the mass flow of CO<sub>2</sub> will be regulated by a mass flow controller and the pressure will be controlled by manipulating the heating rate to the bed. During this phase, which corresponds to the transition from point B to point C in Figure 2, most of the CO<sub>2</sub> adsorbed on the zeolite will be depleted.

*Cooling at Constant Volume:* Once the CO<sub>2</sub> adsorbed on the zeolite has been desorbed, the outlet valve to the Sabatier reactor is closed, the heater is turned off and the cooling phase will begin. This corresponds from point C to point D in Figure 2. Two options are being examined for cooling, a cooling jacket encasing the sorbent pump is the option which will be used during ground testing. Another option which could be utilized during actual employment on Mars is the use of a radiator coupled to a heat conductive strap.

*Cooling at Constant Pressure:* The final phase of the sorption pump completes the operating cycle by returning to point A. This phase begins when the pressure in the pump reaches the Martian atmospheric pressure. At this point, valves are opened to the atmosphere and the adsorption process begins as the CO<sub>2</sub> rich atmosphere flows into the chamber.

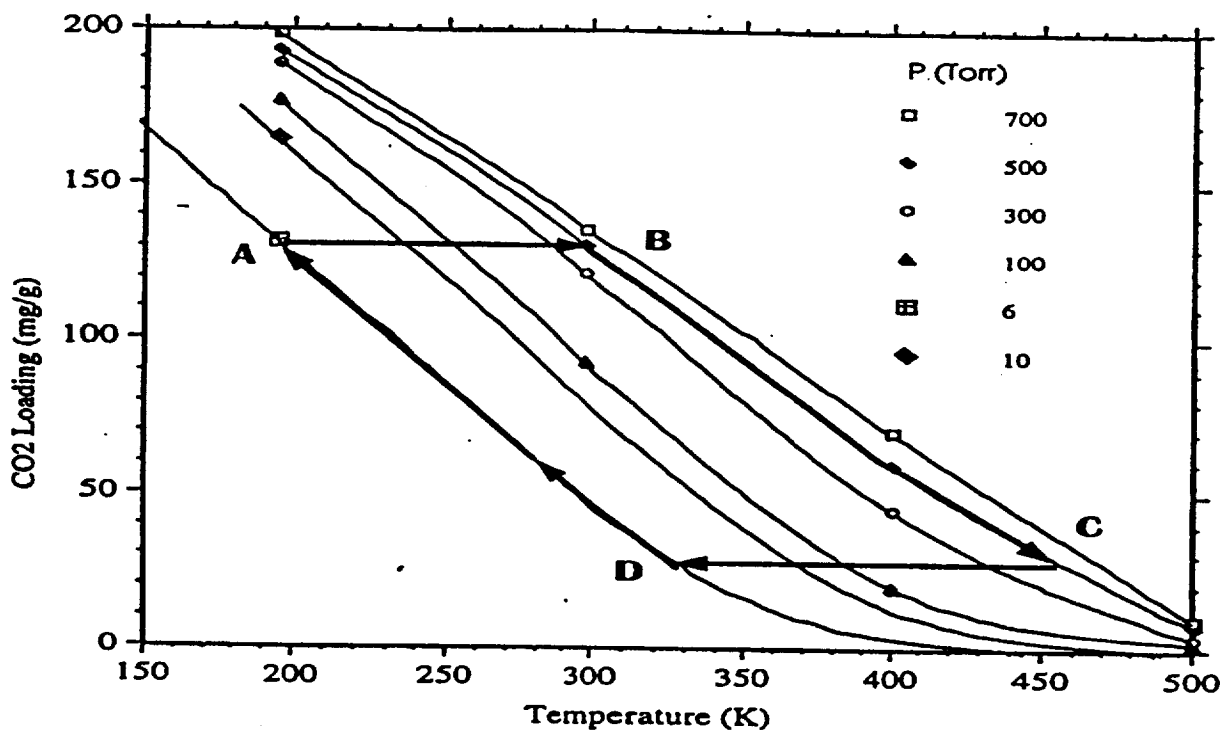


Figure 2 Sorption Pump Operating Cycle for 13X Zeolite <sup>2</sup>

## SORPTION PUMP MODELING

To accurately model and subsequently simulate the operation of the sorption pump would require considerable effort and the models would be difficult to validate. There are three phases which need to be accounted for in the conservation of energy equations, the solid zeolite, the solid aluminum casing and the vapor  $\text{CO}_2$ . In addition, since the sorption pump is a fixed bed, partial differential equations would have to be written for each phase, since the variables of interest are changing over time as well spatially. Boundary conditions would have to be established for these equations and then they would have to be coupled with the conservation of  $\text{CO}_2$  equations in the zeolite and vapor phases, as well as an equation of state and a  $\text{CO}_2$  / zeolite equilibrium relationship. To simplify the problem several assumptions were made for the system as follows:

1. The Gas Phase is 100%  $\text{CO}_2$ .
2. The Gas Phase is Uniform & Well Mixed and no thermal gradients exist in the phase.
3. The Aluminum Enclosure is Uniform and no thermal gradients exist.
4. No Thermal gradients exist between the Different Materials (ie  $T_Z = T_{\text{CO}_2} = T_{\text{Al}}$ ).
5. The Volume of the Gas Phase is equal to the Void Volume of the Zeolite Bed.

With regard to the first assumption, this should be close to the actual situation since the atmosphere is ~ 95%  $\text{CO}_2$ , and due to the fact that zeolite is preferentially adsorbed on the zeolite. While assumptions 2 through 4 reduce the accuracy of the modeling effort, the magnitude of the error can not be determined until experimental data is obtained for model verification. If the error is substantial, either a finite element approach could be taken or a compartmental model could be employed. The final assumption assumes that the bed is completely packed with zeolite and no free space exists except what is contributed by the porosity of the material.

The simplified equations used for modeling the system are as follows:

Energy Balance on the Sorption Pump:

$$Cp_Z m_Z \frac{dT_Z}{dt} = Q_{\text{Heating}} - Q_{\text{Adsorption}} - Q_{\text{Gas Phase}} - Q_{\text{Aluminum Shell}} - F_{\text{out}} H_{\text{Reactor}} - Q_{\text{Cooling}}$$

where:

$Cp_Z$  = Heat Capacity of the Zeolite (J/g-K)

$m_Z$  = Mass of Zeolite (g)

$T_Z$  = Temperature of the Zeolite (K)

$Q_{\text{Heating}}$  = Heat Input of the Electrical Heater (J/s)

$Q_{\text{Adsorption}}$  = Heat of Adsorption of  $\text{CO}_2$  (J/s)

$Q_{\text{Gas Phase}}$  = Heat Transferred into the Gas Phase (J/s) =  $Cp_{\text{CO}_2} m_{\text{CO}_2} \frac{dT_{\text{CO}_2}}{dt} = Cp_{\text{CO}_2} m_{\text{CO}_2} \frac{dT_Z}{dt}$

$Q_{\text{Aluminum Shell}}$  = Heat Transferred into the Aluminum Enclosure (J/s) =  $Cp_{\text{Al}} m_{\text{Al}} \frac{dT_{\text{Al}}}{dt} = Cp_{\text{Al}} m_{\text{Al}} \frac{dT_Z}{dt}$

$F_{\text{out}}$  = Flow of Mass Out of the Pump (g/s)

$H$  = Enthalpy of the Mass Flowing out of the Pump (J/g) [  $T_{\text{ref}} = 190$  (K) ]

Mass Balance on the Sorption Pump:

$$\frac{dm_{CO_2}}{dt} = \Delta m_{Adsorption} - F_{out}$$

where:

$m_{CO_2}$  = Mass Transferred into the Gas Phase (g)

$\Delta m_{Adsorption}$  = Rate of Mass Desorbed off of the Zeolite (g/s)

$F_{out}$  = Mass Flowing into the reactor (g/s)

Equation of State:

$$PV = nRT$$

Adsorption Equilibrium:

$$\Delta m_{Adsorption} = f(T, P)$$

The Initial modeling of the sorption pump was modeled was done in Simulink, which is a block diagram type language that runs on top of MATLAB. Simulink has built in equation solvers for both ordinary differential equations as well as algebraic equations. While the solutions of the equations were generated, the need to port them to other languages for implementation required the development of a solution algorithm. The algorithm developed for numerical solution of the sorption pump model is given in Figure 3.

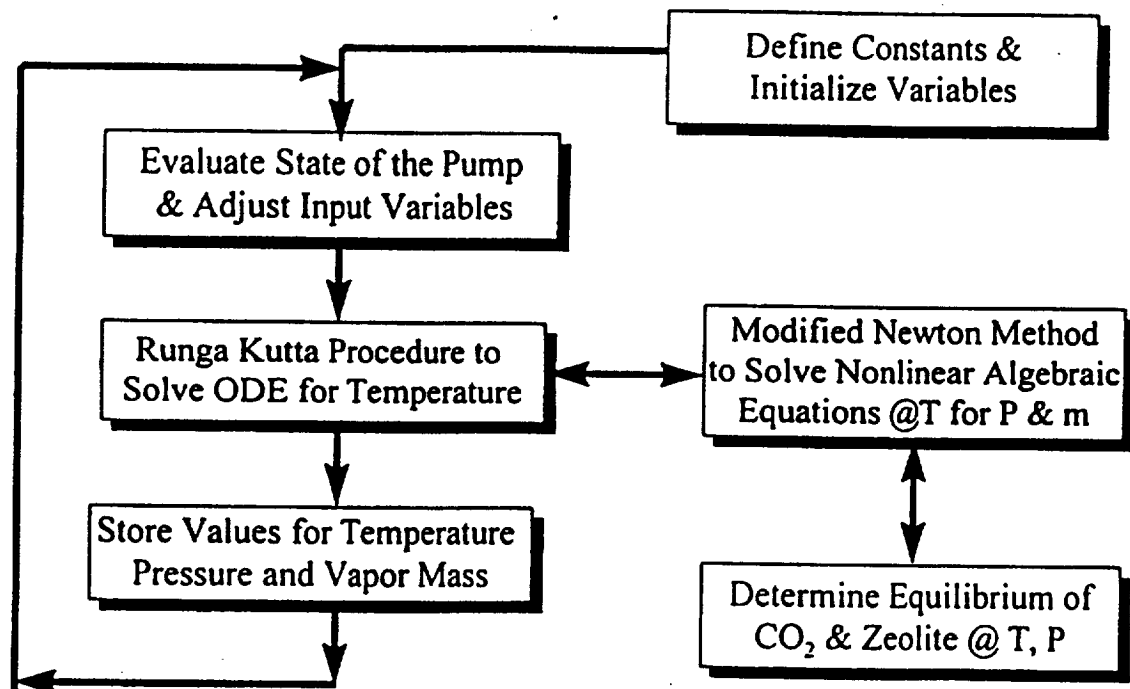


Figure 3 Algorithm for Solution of the Sorption Pump Modeling Equations

After defining the constants and initializing the variables for the system, the primary loop is entered. Since there are four possible operating phases of the pump, upon entry into the loop, the state of the pump is evaluated. Depending on the pump's state, some of the variables given in the energy balance are adjusted. For example, during heating at constant volume, the heater input is set to a maximum value, whereas a PID algorithm takes over and sets this input once the heating at constant pressure phase is entered. The next part of the algorithm uses a 4th order Runge Kutta procedure to solve the ordinary differential equation for temperature. The Runge Kutta algorithm uses an approximation of the derivative on the left hand side of the energy balance, by taking a weighted average of 4 successive approximations. Within each evaluation of the derivative, two nonlinear algebraic equations must be solved for pressure and the mass of  $\text{CO}_2$  in the vapor. The two equations used are the ideal gas law and the mass balance on the  $\text{CO}_2$ . The solution of the mass balance requires that equilibrium data is used to interpolate the adsorbed mass of  $\text{CO}_2$  on the zeolite.

The solution of the nonlinear algebraic equations at each step of the Runge Kutta procedure is obtained from a modified Newton method. This method solves for the roots of the equations by iterating with the use of derivatives of the functions approximated by the use of a first order finite difference approximation. Details of this and the Runge Kutta method can be found in the literature.<sup>3</sup> The last step of the algorithm is to store the values for the variables of interest and go back to the top of the loop. Once the models had been rewritten successfully in Matlab, the software development effort then moved to Allegro Common LISP. This effort which was also successful, utilized the Matlab simulations to aid as a debugging tool. To give a feel for the similarities and differences of the two environments, a sample of code from each is shown in Figure 4.

---

```
function [Tdot, gas_mass, P, adsorbed_mass] = Temp_dot (Temp, P, gas_mass_old, MW_CO2,
mass_zeolite, R, initial_adsorbed_mass, heat_of_sorption, delt, flow_to_reactor,
Tref, volume_gas, heat_capacity_zeolite, heat_capacity_aluminum, initial_gas_mass,
Q_heater, total_flow_to_reactor, T_coolant, coolant_flow, UA_cool)
    tol = .0001;    gas_mass = gas_mass_old;    delP = .01 * P;    delgm = .01 * gas_mass;
    for n = 1:1000    if n == 100        disp('NO Convergence');        end
    xP = P + delP;    xgas_mass = gas_mass + delgm;
    J(1,1) = (f_P(xP, gas_mass, MW_CO2, R, Temp, volume_gas) -
              f_P(P, gas_mass, MW_CO2, R, Temp, volume_gas)) / delP;
    J(1,2) = (f_P(P, xgas_mass, MW_CO2, R, Temp, volume_gas) -
              f_P(P, gas_mass, MW_CO2, R, Temp, volume_gas)) / delgm;
    J(2,1) = (f_gas(xP, Temp, gas_mass, initial_adsorbed_mass, mass_zeolite,
initial_gas_mass, total_flow_to_reactor) - f_gas(P, Temp, gas_mass,
initial_adsorbed_mass, mass_zeolite, initial_gas_mass, total_flow_to_reactor)) / delP;
    J(2,2) = (f_gas(P, Temp, xgas_mass, initial_adsorbed_mass, mass_zeolite, initial_gas_mass,
total_flow_to_reactor) - f_gas(P, Temp, gas_mass, initial_adsorbed_mass, mass_zeolite,
initial_gas_mass, total_flow_to_reactor)) / delgm;
```

Matlab Code

---

```
(defun Temp_dot ((Temp IP gas_mass_old total_flow_to_reactor)
  (setq gas_mass gas_mass_old)
  (setq delP (* .01 IP))
  (setq delgm (* .01 gas_mass))
  (do ((n 1 (+ n 1)))
      ((= n 100) n)
      (cond ((= n 100) (print '(No Convergence)))
            (< n 100)
            (setq xP (+ IP delP))
            (setq xgas_mass (+ gas_mass delgm))
            (setq J11 (/ (- (f_P xP gas_mass ITemp) (f_P IP gas_mass ITemp)) delP))
            (setq J12 (/ (- (f_P IP xgas_mass ITemp) (f_P IP gas_mass ITemp)) delgm))
            (setq J21 (/ (- (f_gas xP gas_mass ITemp total_flow_to_reactor) (f_gas IP gas_mass ITemp
total_flow_to_reactor)) delP))
            (setq J22 (/ (- (f_gas IP xgas_mass ITemp total_flow_to_reactor) (f_gas IP gas_mass ITemp
total_flow_to_reactor)) delgm)))
```

LISP Code

Figure 4 Comparison of Matlab and Common LISP Code

## SIMULATION RESULTS

Figures 5 - 7 show the results of a Matlab simulation and all are labeled A through D to correspond with the different phases of the sorption pump discussed above. Figure 5 shows how the loading changes as a function of temperature very similar to that cycle shown in Figure 2. Figure 6 gives how the bed pressure changes with time. From point A to Point B the pressure rises in an exponential fashion. Just before the valve to the Sabatier is opened at point B, a PID algorithm is used to adjust the heating rate to regulate the pressure. Once point C is reached the pressure drops quickly as the cooling begins, thus dropping the pressure back to the Martian atmospheric pressure, at which time (point D) the valves are opened.

Figure 7 shows how the bed temperature changes over time and is characterized by a steep slope from A to B and then a decreasing slope from B to C which corresponds to the bed pressure being controlled by manipulating the heater input and flow to the Sabatier reactor. At point C the heater is turned off and the valves closed causing a rapid drop in temperature. In the final phase the temperature continues to drop, but the rate of cooling is less since the cooling is based on a linear driving force between the bed temperature and the coolant temperature which is constant.

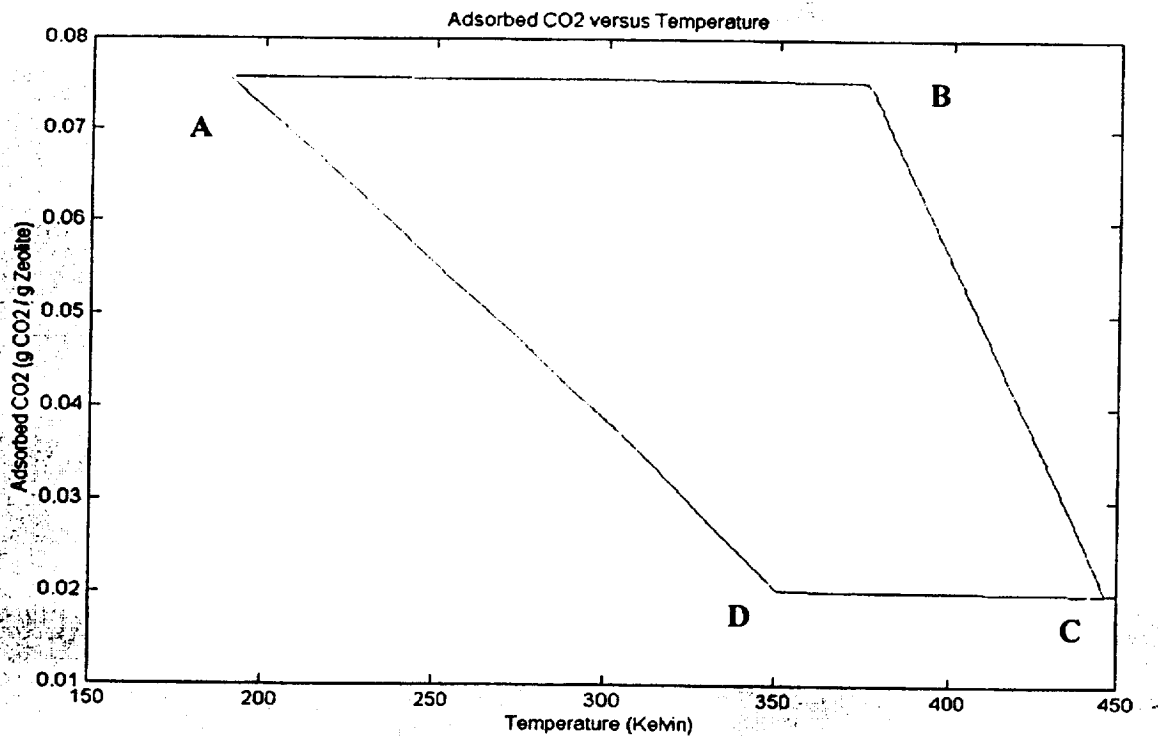


Figure 5 Simulated Sorption Pump Operating Cycle

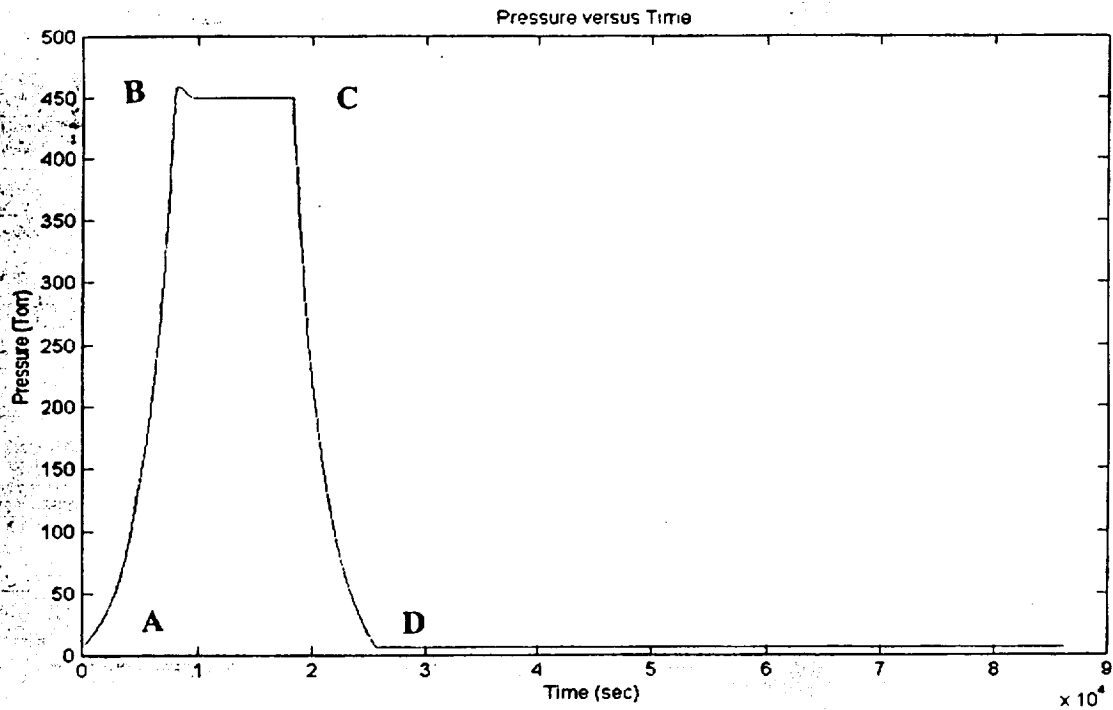


Figure 6 Bed Pressure Simulated During the Sorption Pump Operating Cycle

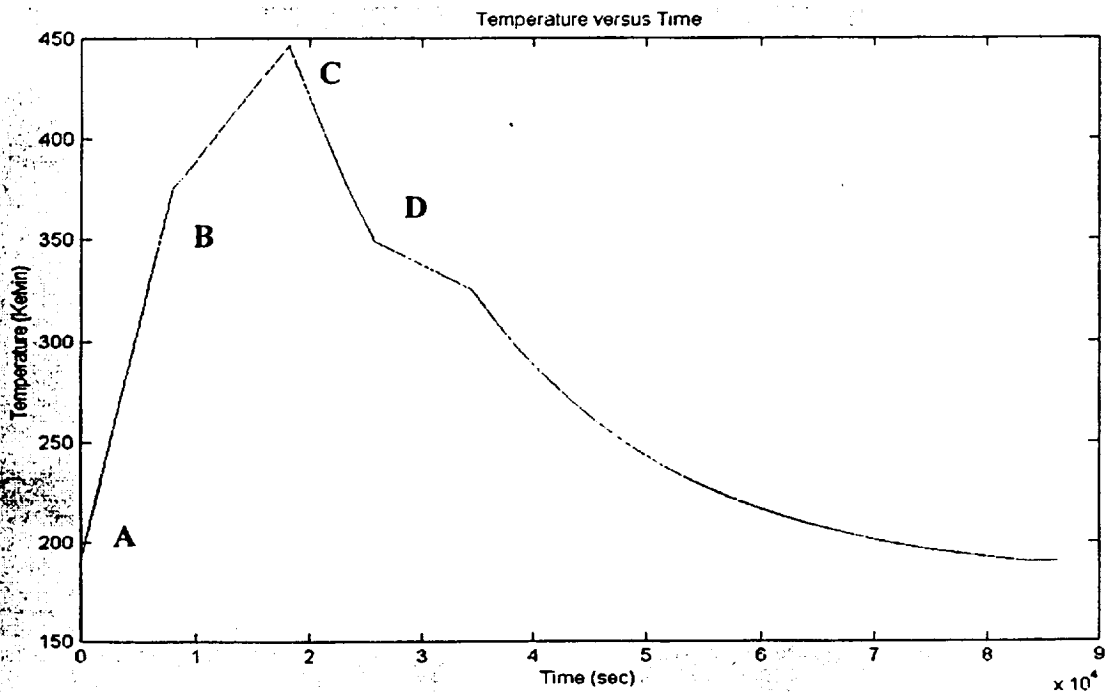


Figure 7 Bed Temperature Simulated During the Sorption Pump Operating Cycle

## CONCLUSIONS

The development of simplified dynamic models was done for a sorption pump based on the requirements for the ISPP project. The results of the simulations when compared to data obtained in the literature proved that the models were reasonable. To truly validate the models data will be needed. It is anticipated that when actual data is obtained on the sorption pump from JSC, that some modifications of the model parameters will be needed. It is not anticipated however that major changes will need to be made to the numerical algorithms.

## REFERENCES

- [1]. Zubrin R. And S. Price, "Mars Sample Return Mission Utilizing In-Situ Propellant Production", Final Report, Lockheed Martin, JSC Contract NAS9-19359, March 31, 1995.
- [2]. Rapp, D., P. Karlmann, D. L. Clark and C.M. Carr, "Adsorption Pump for Acquisition and Compression of Atmospheric CO<sub>2</sub> on Mars", Preliminary Design Report V. 18, Jet Propulsion Laboratory, JPL D-14483, April 30, 1997.
- [3]. Riggs, J. B., An Introduction to Numerical Methods for Chemical Engineers, 2nd edition, Texas Tech University Press, 1994.



# REPORT DOCUMENTATION PAGE

Form Approved  
OMB No. 0704-0188

Public reporting burden for this collection of information is estimated to average 1 hour per response, including the time for reviewing instructions, searching existing data sources, gathering and maintaining the data needed, and completing and reviewing the collection of information. Send comments regarding this burden estimate or any other aspect of this collection of information, including suggestions for reducing this burden, to Washington Headquarters Services, Directorate for Information Operations and Reports, 1215 Jefferson Davis Highway, Suite 1204, Arlington, VA 22202-4302, and to the Office of Management and Budget, Paperwork Reduction Project (0704-0188), Washington, DC 20503.

<b>1. AGENCY USE ONLY (Leave blank)</b>	<b>2. REPORT DATE</b> March 1999	<b>3. REPORT TYPE AND DATES COVERED</b> Contractor Report - Summer 1998	
<b>4. TITLE AND SUBTITLE</b>  1998 Research Reports NASA/ASEE Summer Faculty Fellowship Program		<b>5. FUNDING NUMBERS</b>  NASA Grant NAG10-244	
<b>6. AUTHOR(S)</b>  See attached list		<b>8. PERFORMING ORGANIZATION REPORT NUMBER</b>  NASA CR-1999-208546	
<b>7. PERFORMING ORGANIZATION NAME(S) AND ADDRESS(ES)</b> University of Central Florida Orlando, Florida 32816-2450 John F. Kennedy Space Center Kennedy Space Center, Florida 32899			
<b>9. SPONSORING/MONITORING AGENCY NAME(S) AND ADDRESS(ES)</b> National Aeronautics and Space Administration Washington, D.C. 20546		<b>10. SPONSORING/MONITORING AGENCY REPORT NUMBER</b>	
<b>11. SUPPLEMENTARY NOTES</b>			
<b>12a. DISTRIBUTION/AVAILABILITY STATEMENT</b> Unclassified - Unlimited Subject Category 99		<b>12b. DISTRIBUTION CODE</b>	
<b>13. ABSTRACT (Maximum 200 words)</b> This document is a collection of technical reports on research conducted by the participants in the 1998 NASA/ASEE Summer Faculty Fellowship Program at the Kennedy Space Center (KSC). This was the 14th year that a NASA/ASEE program has been conducted at KSC. The 1998 program was administered by the University of Central Florida in cooperation with KSC. The program was operated under the auspices of the American Society for Engineering Education (ASEE) with sponsorship and funding from the Education Division, NASA Headquarters, Washington, D.C., and KSC. The KSC Program was one of nine such Aeronautics and Space Research Programs funded by NASA in 1998. The NASA/ASEE Program is intended to be a two-year program to allow in-depth research by the university faculty member. The editors of this document were responsible for selecting appropriately qualified faculty to address some of the many problems of current interest to NASA/KSC.			
<b>14. SUBJECT TERMS</b>  Research and technology		<b>15. NUMBER OF PAGES</b> 234	
		<b>16. PRICE CODE</b>	
<b>17. SECURITY CLASSIFICATION OF REPORT</b>  Unclassified	<b>18. SECURITY CLASSIFICATION OF THIS PAGE</b>  Unclassified	<b>19. SECURITY CLASSIFICATION OF ABSTRACT</b>  Unclassified	<b>20. LIMITATION OF ABSTRACT</b>  III

0

3

)

)

)

